Physics Lib.

VOLUME 35 SECOND SERIES NUMBER 4

FEB 28 1930

THE PHYSICAL REVIEW

A JOURNAL OF EXPERIMENTAL AND THEORETICAL PHYSICS

CONDUCTED BY

THE

AMERICAN PHYSICAL SOCIETY

BOARD OF EDITORS

Managing Editor JOHN T. TATE, University of Minnesota, Minneapolis

I. S. BOWEN, R. S. MULLIKEN, H. D. SMYTH, E. U. CONDON, C. J. DAVISSON, F. K. RICHTMYER, K. F. HERZFELD, A. W. HULL, F. W. LOOMIS

FEBRUARY 15, 1930

Sodium and Magnesium Spark Lines in the Far Ultra-Violet, and the Quantitative Application of the Irregular Doublet Law to Isoelectronic Sequences — J. E. MACK AND R. A. SAWYER — 305

New Measurements in the Fourth Positive CO Bands — ROGER S. ESTEY — 309

Fine Structure of the Beryllium Fluoride Bands — F. A. JENKINS — 323

Relativity and Aether Drift — W. F. G. SWANN — 325

Spatial Distribution of Photoelectrons — S. E. SHEPPARD — 347

Reflection of Beams of the Alkali Metals from Crystals — JOHN B. TAYLOR — 375

Emission of Positive Ions from Tungsten and Molybdenum — LLOYD P. SMITH — 383

On the Early Stages of Electric Sparks — ERNEST O. LAWRENCE AND FRANK G. DUNNINGTON — 396

A New Regularity in the List of Existing Nuclei — HENRY A. BARTON — 409

Black Bodies in the Extreme Infra-Red — C. HAWLEY CARTWRIGHT — 415

Peltier and Thomson Effects for Bismuth Crystals — H. D. FARAN AND T. R. D. COLLINS — 422

Shatter Oscillations, Their Nature and Theory — E. H. KENNARD — 428

Letters to the Editor — 439

PUBLISHED BY THE AMERICAN PHYSICAL SOCIETY

PUBLICATION OFFICE: 450-454 AHNAIP STREET, MENASHA, WIS.

EDITORIAL OFFICE: MINNEAPOLIS, MINN.

THE AMERICAN PHYSICAL SOCIETY

OFFICERS OF THE SOCIETY

President:	HENRY G. GALE	University of Chicago, Chicago, Ill.
Vice-President:	W. F. G. SWANN	Bartol Research Foundation, Philadelphia, Pa.
Secretary:	W. L. SEVERINGHAUS	Columbia University, New York City
Treasurer:	G. B. PEGRAM	Columbia University, New York City
Editor:	JOHN T. TATE	University of Minnesota, Minneapolis, Minn.
Local Secretary for the Pacific Coast:	L. B. LOEB	University of California, Berkeley, Calif.

THE PHYSICAL REVIEW

Published by the American Physical Society at 450 Ahnaip St., Menasha, Wis. Executive office: University of Minnesota, Minneapolis, Minn. Two volumes annually, twelve issues per volume.

First series. From July 1, 1893, to January 1, 1913, the REVIEW was conducted by Edward L. Nichols, Ernest Merritt and Frederick Bedell, with the financial support of Cornell University. The first four volumes were issued annually; subsequent volumes, semi-annually; thirty-five volumes in all.

Second series. On January 1, 1913, the REVIEW was transferred to the American Physical Society as announced on the first page of the new series which was then begun. Since then it has been conducted by a Board of Editors elected by the Society. Semi-annual volumes begin in January and July. Since July 1, 1929, the REVIEW has been issued twice a month.

Contributors are referred to page 2 of the advertisements for further information.

Annual Subscription, throughout the Postal Union, $10.00 in advance.

Single copies of current volume, $.60.

General index, 1893-1920, $4.00, in advance.

Back Volumes, $6.00 per volume; Back Numbers, $1.00 per copy for issues prior to July 1, 1929 (Vols. 1-33), $.60 per copy for issues subsequent thereto. Postage is free if remittance accompanies order; otherwise postage is extra. No bound volumes can be supplied. The REVIEW offers to purchase a limited number of First Series, Vol. 1, No. 1 (at $2.00 each); Second Series, Vol. 7, No. 1, January 1916; Vol. 7, No. 2, February 1916; Vol. 7, No. 4, April 1916; and Vol. 7, No. 5, May 1916 (at $2.00 each).

Advertisements. Rates will be supplied by the Editor on request. Copy for each number must be received at Minneapolis two weeks prior to the dates of issue; old copy is used until new copy is received. Send electrotypes direct to the printers, George Banta Publishing Co., Menasha, Wis.

Discount of ten percent is allowed subscription agencies and members of the American Physical Society.

Changes of address and Complaints of failure to receive the REVIEW, in the case of members of the Physical Society, should be addressed to the Treasurer; in the case of other subscribers to 450 Ahnaip St., Menasha, Wis.; or to the Editor. New copies can be sent free in response to complaint of non-delivery only if notice of non-delivery is received within three months of date of issue.

Editorial Correspondence should be addressed to the PHYSICAL REVIEW, University of Minnesota, Minneapolis, Minn.

Entered at the postoffice at Menasha, Wis., as second class matter.
Acceptance for mailing at special rate of postage provided for in section 1103, Act of October 3, 1917, authorized September 6, 1926.

Second Series *February 15, 1930* *Vol. 35, No. 4*

THE

PHYSICAL REVIEW

SODIUM AND MAGNESIUM SPARK LINES IN THE FAR ULTRA-VIOLET, AND THE QUANTITATIVE APPLICATION OF THE IRREGULAR DOUBLET LAW TO ISOELECTRONIC SEQUENCES

By J. E. Mack[1] and R. A. Sawyer
University of Minnesota and University of Michigan

(Received January 13, 1930)

Abstract

New levels in Na III, Mg IV, and Mg V are identified through the transition $2s \leftarrow 2p$. The value of the negative term $2s2p^5\ {}^3P$ of O I is predicted.

The relativistic screening number $\sigma_2(L_{21}L_{22})$, is 3.19 for $Z=10$, 11 compared with the value 3.49 for heavier atoms, usually considered independent of Z. The difference is probably due to outer screening.

Wentzel's result $\sigma_1(n,l+1)-\sigma_1(n,l)=0.58\cdot 2^l n$ for the first order screening number σ_1 in x-rays is applied instead of the usual qualitative form of the irregular doublet law to determine the rate of dependence of the transition energy $2s^22p^5 \leftarrow 2s2p^6$ upon Z in the fluorine-like isoelectronic sequence. The extremely high result, $49\cdot 10^3 \text{cm}^{-1}$, is verified by the new Na III and Mg IV data. Certain regularities in the curves showing the rates of dependence of the irregular doublet transition frequencies upon the atomic number in isoelectronic sequences, as functions of the number of electrons present, may be used for interpolation of these rates.

SEVERAL new lines and some old ones, due to the transition $2s \leftarrow 2p$ in the spark spectra of sodium and magnesium, have been photographed with the University of Michigan's one meter vacuum spectrograph and classified.[2]

Due to the necessity of breaking down the rare gas shell $2p^6$, the several times ionized atoms in this part of the periodic table require more energy for excitation than any others of the same stage of ionization except those isoelectronic with helium and hydrogen. Attempts to obtain the lines of Na IV and Al IV and extend the scheme of Mg III have been thus far unsuccessful. The failure to obtain the PP° group of Na IV expected at $244\cdot 10^3$ cm^{-1}, in the face of the success with Mg V, may be attributed to the inconvenient physical properties of sodium. We had to insert the sodium as a

[1] National Research Fellow.

[2] We are indebted to Messrs. R. F. Bacher and G. R. Miller for aid in the photographic work.

TABLE I. *Lines and new levels in sodium and magnesium.*

SODIUM

Lines (Bowen) Int	λ	Int	λ	$\nu(\cdot 10\ \mathrm{cm}^{-1})$	Assignment		*New Levels* ($\cdot 10\ \mathrm{cm}^{-1}$)		
2	372.04	3	372.16	26870	II	$2s^22p^6\ {}^1S_0 - 2s^22p^53s\ {}^1P_1^\circ$	Na III	$2s^22p^5\ {}^2P_{1\frac{1}{2}}^\circ$	0
1	376.34	2	376.63	26551		${}^1S_0 -\ {}^3P_1^\circ$		$\frac{1}{2}$	138
		1	378.34	26431	III	$2s^22p^5\ {}^2P_{1\frac{1}{2}}^\circ - 2s2p^6\ {}^2S_{\frac{1}{2}}$		$2s2p^6\ {}^2S_{\frac{1}{2}}$	26431
		1	380.33	26293		${}^2P_{1\frac{1}{2}}^\circ -\ {}^2S_{\frac{1}{2}}$			

MAGNESIUM

Lines (Mil. Bow.) Int	λ	Int	λ	$\nu(\cdot 10\ \mathrm{cm}^{-1})$	Assignment		*New Levels* ($\cdot 10\ \mathrm{cm}^{-1}$)		
2	231.6	2	231.71	43157	III	$2s^22p^6\ {}^1S_0 - 2s^22p^53s\ {}^1P_1^\circ$	Mg IV	$2s^22p^5\ {}^2P_{1\frac{1}{2}}^\circ$	0
		1	234.25	42689		${}^1S_0 -\ {}^3P_1^\circ$		$\frac{1}{2}$	221
		1	276.28	36195	?			$2s2p^6\ {}^2S_{\frac{1}{2}}$	31162
5	320.9	1	320.90	31162	IV	$2s^22p^5\ {}^2P_{1\frac{1}{2}}^\circ - 2s2p^6\ {}^2S_{\frac{1}{2}}$			
4	323.2	2	323.20	30941		${}^2P_{\frac{1}{2}}^\circ -\ {}^2S_{\frac{1}{2}}$	Mg V	$2s^22p^4\ {}^3P_2$	0
		0	338.48	29544	?			1	161
		1	349.07	28648	?			0	254
		1	351.03	28487	V	$2s^22p^4\ {}^3P_2 - 2s2p^5\ {}^3P_1^\circ$		$2s2p^5\ {}^3P_2^\circ$	28326
		1	352.13	28399		${}^3P_1 -\ {}^3P_0^\circ$		1	28507
0	352.9	2	353.03	28326		${}^3P_{1,2} -\ {}^3P_{1,2}^\circ$		0	28580
		1	354.19	28233		${}^3P_0 -\ {}^3P_1^\circ$			
0	355.3	1	355.31	28145		${}^3P_1 -\ {}^3P_2^\circ$			

core in a hollow aluminum electrode, whereas whole electrodes were easily made of magnesium.

Table I shows all the lines, $\lambda < 380$ of Na, and $\lambda < 360$ of Mg, that have ever been detected. The already classified Na II and Mg III lines are included for completeness.[3] The present assignment of Mg $\lambda\lambda 320, 323$ has been suggested among other possibilities by Turner.[4] Now the quantitative applicability of the irregular doublet law (Part III, below), and the relative unlikelihood of the strong occurrence of such x-ray transitions as $s^2p^5s^2 \leftarrow sp^6s^2$ in magnesium alone, make this assignment certain. The intensity relations, especially when examined in connection with those given in Millikan and Bowen's first paper on far ultra-violet spectra, (Table I, Mg, first column) are most satisfactory.

Table II gives the relativistic screening numbers $\sigma_2(2s^22p^4$ or $2s2p^5)$ for oxygen-like systems and $\sigma_2(2s^22p^5)$ for fluorine-like systems, respectively, as functions of the atomic number Z. The number σ_2 is calculated from the Sommerfeld formula $\Delta\nu = \alpha^2R(Z-\sigma_2)^4/n^3l(l+1)$, which applies in these cases if $\Delta\nu$ is the doublet separation or the overall separation of the triplet.[5] The frequency of the transition $2s \leftarrow 2p$, is given in the next to last column, while the last column shows the differences in the frequency of the transitions $2s \leftarrow 2p$ for successive members of each isoelectronic sequence. The extraordinarily high values of these differences will be discussed below (Part III). The numbers in parentheses are interpolated. Backward extrapolation of the next to last column to the arc spectra shows that O I $sp^5\ ^3P$ lies about $15 \cdot 10^3$ cm^{-1} above the lowest state $s^2p^3\ ^4S$ of O II, and F I $sp^6\ ^2S$ about $16 \cdot 10^3$ cm^{-1} above the lowest state $s^2p^4\ ^3P$ of F II. Neither of these negative levels has been observed.

The mean error in wave-length separations is about 0.03A, which at 300A amounts to 30 cm^{-1}. Thus the screening numbers at the bottom of each sequence in Table II are uncertain by about 0.03, while those at the top are perhaps ten times as accurate. Only in F II is it possible to distinguish, with the available measurements, between the values of the s^2p^4 and the sp^5 screening.

[3] Detailed references to sources of spectroscopic data are omitted. The x-ray references may be found in Handbuch der Physik **21,** 338; optical spectra, in the forthcoming University of Michigan term tables. Of special importance for this paper are the following:

F I: (the tentative assignment of $s^2p^5 \leftarrow sp^6$ is wrong). H. Dingle, Roy. Soc. Proc. **A 117,** 40 (1928).

F I, F II: I. S. Bowen, Phys. Rev. **29,** 231 (1927).

Ne II: H. N. Russell, K. T. Compton, and J. C. Boyce, Nat. Acad. Sci. Proc. **14,** 280 (1928).

Ne III: J. C. Boyce and K. T. Compton, Nat. Acad. Sci. Proc. **15,** 656 (1929).

Na II: I. S. Bowen, Phys. Rev. **31,** 967 (1928).

Mg III: J. E. Mack and R. A. Sawyer, Science **68,** 1761 (1928).

Mg lines: R. A. Millikan and I. S. Bowen, Phys. Rev. **23,** 1 (1924).

[4] L. A. Turner, Phys. Rev. **32,** 727 (1928).

[5] S. Goudsmit, Phys. Rev. **31,** 946 (1928).

TABLE II. *Application of the doublet laws to oxygen- and flourine-like spectra.*

Oxygen-like isoelectronic sequence.

Z		$s^2p^4\ {}^3P$ $\Delta\nu(\mathrm{cm}^{-1})$	$sp^5\ {}^3P$ $\Delta\nu(\mathrm{cm}^{-1})$	$\sigma_2(s^2p^4)$	$\sigma_2(sp^5)$	$s^2p^4\ {}^3P_2$—$sp^5\ {}^3P_2$ $\nu(\cdot 10\ \mathrm{cm}^{-1})$	diff.
8	O I	226		3.010		...	
9	F II	492	486	2.976	2.957	16480	3950
10	Ne III	904		2.94		20430	
11	Na IV	(1560)		(2.90)		(24378)	mean 3948
12	Mg V	2540		2.85		28326	

Flourine-like isoelectronic sequence.

Z		$s^2p^5\ {}^2P$ $\Delta\nu(\mathrm{cm}^{-1})$	$\sigma_2(s^2p^5)$	$s^2p^5\ {}^2P_{1\frac{1}{2}}$—$sp^6\ {}^2S_{\frac{1}{2}}$ $\nu(\cdot 10\ \mathrm{cm}^{-1})$	diff.
9	F I	408	3.216	...	
10	Ne II	782	3.194	21627	4804
11	Na III	1380	3.15	26431	4731
12	Mg IV	2210	3.17	31162	

II. On the Regular Doublet Law

Fig. 1 shows the screening numbers from Table II, with the other relativistic $2p$-screening numbers, calculated with the aid of the Goudsmit separation factors.[5] The assumption of normal coupling, where necessary for calculating the screening, is well justified.[6] The fourth power formula is applied throughout, for it is a good approximation to call the $2p$-electrons non-penetrating. All principal quantum numbers omitted in the notation are 2. The $1s^2$ shell is present in each configuration. Within the limits of experimental error, all the values decrease smoothly toward horizontal asymptotes.[7] The p^2 and sp^2 curves are considerably flatter than their neighbors.

The addition of an s-electron to s^2p^5 makes a change only on the order of 0.01 in the $2p$-screening, quite in contrast with the case where less than five $2p$-electrons are present, as in N I, for instance, where the presence of a $3s$-electron alters the screening by half a unit. This often-noted constancy

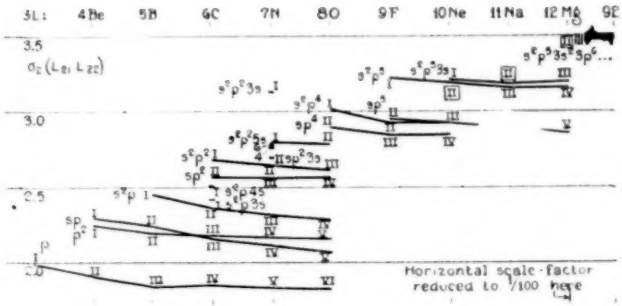

Fig. 1. Values of $\sigma_2(2p)$.

now extends from neon to magnesium. The study of the neon spectum has been exceedingly fruitful, but this sharp distinction between five and less than five equivalent p-electrons seems still to need a special explanation.

The square boxed II's in Fig. 1 mark the real x-ray screening numbers. The difference of 0.30 in the value of σ_2 between the lower and the higher atomic numbers is probably due to the influence of the outer electrons $3s^23p^6 \cdots$, which is also noticeable[8] in the slopes of the first order screening number curves. In some cases among the σ_2's for electrons of higher principal quantum number, the difference is in the other direction: e.g., for Ni II $3d^9$, $\sigma_2 = 13.70$, whereas for the x-rays of the heavier elements, $\sigma_2(M_{32}M_{33}) = 13.0$; but in these cases disturbances arising from interaction with the fields

[6] This is not true for He I, Li II $(1s)p$, which are consequently omitted from the figure. For the hydrogen-like sequence, which is also omitted, of course $\sigma_2 = 0$ for all Z.

[7] Except for N I $sp^4\ {}^4P\Delta\nu = 63.5$, $\sigma_2 = 3.37$, which has been omitted from the figure. This anomaly is well verified experimentally (S. B. Ingram, Phys. Rev. **34**, 421 (1929)).

[8] J. E. Mack, O. Laporte and R. J. Lang, Phys. Rev. **31**, 748 (1928).

of the many closed shells, are probably sufficient to account for the discrepancy.[9]

III. On the Irregular Doublet Law

Heretofore the irregular doublet law has been applied to optical spectra only in the following qualitative rule: In an isoelectronic sequence, the transition frequency $\nu(n,l)-\nu(n,l+1)$ is approximately a linear function of the atomic number Z.

The irregular doublet law for x-rays can be stated, following Wentzel, in a refined form[10] as

$$\sigma_1(n,l+1)-\sigma_1(n,l)=0.58\cdot 2^l n \tag{1}$$

for inner electrons; where n and l have their usual spectroscopic meaning, R is Rydberg's energy constant, and $\sigma_1=Z-n\,(\nu_{\text{red}}/R)^{1/2}$. If $5\cdot 10^{-5}(Z-\sigma_2)^4$ may be neglected compared with ν/R, as it may be for our purposes among the light elements with which we are concerned,[11] then ν_{red} is the same as ν, the energy required to remove the electron.

From Eq. (1) and the definition of σ_1, we have

$$\nu_{\text{red}}(n,l)-\nu_{\text{red}}(n,l+1)=0.58\cdot 2^l R\left[0.58\cdot 2^l+2(Z-\sigma_1(n,l+1))/n\right] \tag{2}$$

$$\frac{\Delta}{\Delta Z}\left[\nu_{\text{red}}(n,l)-\nu_{\text{red}}(n,l+1)\right]=\frac{0.58\cdot 2^{l+1}R}{n}\left[1-\frac{\Delta}{\Delta Z}\sigma_1(n,l+1)\right] \tag{3}$$

for inner electrons.

With the aid of the newly found data we can study (Table III and Fig. 2) the frequency of the irregular doublet transition $2s\leftarrow 2p$ as a function of the atomic number (Z) and the net charge (indicated by a roman numeral), for systems of one to nine electrons. The rows labeled "upper config." and "lower config." in Table III show the electron configurations between which the transition takes place. All omitted principal quantum numbers are 2. The $1s^2$ shell is present except in the configurations marked ( ) or ($1s$). The row $(Z+1)$ II gives the transition frequency[12] (in terms of the Rydberg constant) for the first spark spectrum isoelectronic with the arc spectrum of atomic number Z. The row $(Z+1)\text{II}-Z\text{II}$ (row A) gives the rate at which the transition frequency for first spark spectra depends upon Z, while the row $(Z+1)\text{II}-Z\text{I}$ (row B) gives the rate at which the transition frequency depends upon Z in each isoelectronic sequence. The organization

[9] The importance of such disturbances is shown, for instance, by the fact that the separations for some of the one-electron doublets among the heavier atoms actually have negative values. The case of Hg II $5f\,^2F\ \Delta\nu=-257$ (F. Paschen, Preus, Akad. Sitzungsber. p. 536 (1928)) is especially striking.

[10] G. Wentzel, Zeits. f. Physik **16**, 41 (1926); A. Sommerfeld, "Atombau" 4th ed. p. 459.

[11] At $Z=10$, Ne II, "reduction" decreases the $-2s$ term (L_{11}) from $3.563R$ to $3.509R$, and the $-2p$ term (L_{21}) from $1.592R$ to $1.585R$.

[12] In the optical part, the frequency given is the difference between the lowest level in the lower configuration and the lowest level of the same multiplicity in the upper configuration.

TABLE III. *Transition frequencies 2s←2p. (Unit-Rydberg constant).*

Upper config.	( )p	(1s)p	p	sp	sp^2	sp^3	sp^4	sp^5	sp^6	$1s^2sp^63s^23p^6$ etc.(L_{11})		
Lower config.	( )s	(1s)s	s	s^2	s^2p	s^2p^2	s^2p^3	s^2p^4	s^2p^5	$1s^2s^2p^63s^23p^6$ etc.(L_{21})		
Z	1	2	3	4	5	6	7	8	9	41	73	91
$(Z+1)$II	0	0.17	0.29	0.67	0.68	0.84	1.10	1.50	1.971	... 18.4	..... 42.4	..... 60.4
Same, reduced									1.924	... 16.9	..... 32.5	 42
A $(Z+1)$II–ZII		0.17	0.12	0.38	0.01	0.16	0.26	0.40	.47	mean .47	mean .49	mean .53
B $(Z+1)$II–ZI	0	0.08	0.16	0.28	0.25	0.26	0.29	0.36[a]	.44[a]	"	"	"
$(Z+1)$II$\sigma_1(2p)$									7.48	14.2	19.9	22.4
$\Delta\sigma_1/\Delta Z$										mean 0.23	mean 0.16	mean 0.14

[a] $(Z+2)$III$-(Z+1)$II is used here because the configurations sp^5, sp^6 are unknown in the arc spectra.

of Table III will be made clear by a comparison of columns 8 and 9 with the last two columns of Table II (e.g. 216270 $cm^{-1} = 1.971R$, and 48040 $cm^{-1} = 0.44R$). Table III is divided by vertical lines into an optical part (left) and an x-ray part (right); column 9 must be included in both parts because of the double role of the L levels of Ne II. Elements 42 Mo, 74 W, and 92 U are chosen as samples for the x-ray part.

No modification of the meaning of any quantity is needed in putting the x-ray data in row $(Z+1)$II. But for clearness the "reduced" values are used in the rest of the x-ray part of the table, which means simply that the complicating effects of the relativity and spin corrections are eliminated.

There are no direct data on isoelectronic sequences of x-ray spectra, such as would be required to fill the spaces ditto-marked in the table. But all the difference between the quantity that belongs in such a space, and the quantity recorded just above it, is due to the influence of an outer electron. The presence of such an electron can have but little influence on an x-ray energy level, and clearly the subtraction of one L-level from another to determine the transition frequency, would tend to cancel out this little influence. So we can confidently conclude that the numbers in the spaces marked with ditto marks in row B should be very nearly the same as those above them in row A.

The ordinary $L_{21}L_{22}$ first order x-ray screening number, and its rate of dependence on Z (e.g. $(14.8-7.48)/(41-9) = 0.23$) are given in the last two rows.

We shall now show that the values of the numbers in italic type, column 9, are in quite close agreement with values that may be calculated for them simply by the use of the x-ray data to the right of the lines in Table III, the irregular doublet law, and the ionizing potential[13] of Ne I.

The quantities appearing in the row $(Z+1)$II reduced and row A of Table III are simply the $\nu_{red}(2, 0) - \nu_{red}(2, 1)$ in Eq. (2) and its derivative in Eq. (3), respectively. So as long as we confine ourselves to inner electrons (i.e. to x-ray levels) the quantities in row A are given by Eq. (3). And so are the quantities in row B, from our discussion of the ditto marks. Thus, using the average slope of σ_1 from the last row of the table, we have directly from Eq. (3):

$$\begin{aligned}(\text{italic numbers, Table III}) &= 0.58R\ (1-0.23)\\ &= 0.45R\\ &= 49 \cdot 10^3\ cm^{-1}\end{aligned}$$

an extraordinarily high value for the rate of dependence of an irregular doublet transition upon Z in an isoelectronic sequence, but in good agreement with the experimental data.

Fig. 2 shows the rate of dependence of the transition frequency $2s \leftarrow 2p$ upon the number of electrons present, for the cases we have been considering: Table III, row A, (first spark spectra)[14] and row B (isoelectronic sequences)

[13] Or any other data that gives the σ_1's of Ne.

[14] The abscissae for this curve are shifted by half a unit, since it is a first difference curve.

The change in scale factor masks the fact that the curve for the x-ray part of the figure, is almost horizontal. Three facts readable from Fig. 2 are worth pointing out here:

1). The extrapolability of the x-ray curve to $0.45R$ for the fluorine-like sequence, which has been discussed above.

2). The uselessness of attempts to apply Wentzel's regularity to outer electrons.[15]

3). The smoothness of the isoelectronic sequences curve, compared with the successive first spark spectra curve, from $Z=1$ to $Z=9$. Wide irregularities occur in the optical part of row A curve, superimposed upon the general upward trend with increasing Z that might be expected due to the increasing differences in screening between $2s$ and $2p$, as the K and L shells are being added. It is often pointed out that such irregularities can be explained

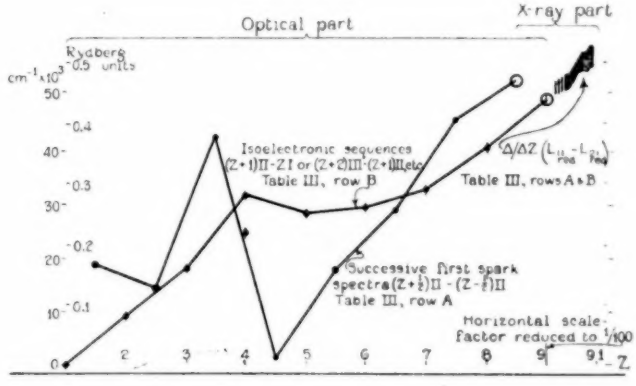

Fig. 2. Rates of dependence of the transition frequency $2s \leftarrow 2p$ upon the atomic number, in successive first spark spectra (A) and in isoelectronic sequences (B).

qualitatively by considerations based on the discrete changes in the number of electrons present: such as the formation of stable configurations at 2 and 4 and the neglect of higher multiplicities at 4, 5, and 6. To the first degree of approximation these irregularities are absent in the row B curve, because the differences in an isoelectronic sequence involve identical electron structures. Quite generally it appears that isoelectronic sequence irregular doublet transition curves such as the row B curve, depart from linearity only by a slight upward curvature, with a peak wherever the lower configuration is a Pauli shell.[16] (See the $4s \leftarrow 4p$ data, below).

The irregular doublet we have been considering ($2s$, $2p$) is uniquely favored for the quantitative application of the law to isoelectronic sequences,

[15] E.g., B. C. Mukherjee and B. B. Ray, Zeits. f. Physik **57,** 345 (1929).

[16] If we used $sp \leftarrow p^2$ in the beryllium-like sequence (the isolated point at 4, $0.22R$ in Fig. 2) we would eliminate the peak at 4. (Such a choice would also make the row A curve smoother, lowering the ordinate at 3.5 and raising that at 4.5 by $0.11R$). Similarly in the $4s \leftarrow 4p$ list below, the choice of $3d4s \leftarrow 3d4p$ instead of $4s^2 \leftarrow 4s4p$ would lower the ordinate for the 20-electron sequence to 0.110.

for only here is it possible to excite an electron from a normally closed shell (here $2s^2$) in increasingly heavy atoms even up to those wherein the next shell with the same principal quantum number (here $2p^6$) is normally closed. But we can apply the regularities we have found for $2s \leftarrow 2p$, somewhat more crudely in other sequences. For instance, the following shows (in part) the rate of dependence upon Z in isoelectronic sequences, of the frequency $4s \leftarrow 4p$, analogous to Table III, row B:

lower config.					$3p^5s$	s	s^2	$3d^2s$	$3d^8s$	$3d^9s$	$3d^{10}s$	s^2
No. electrons	1	· · · 11	12	13	· · · 18	19	20	21	· · · 27	28	29	30
rate	0	.059	.069	.074	.089	.111	.185[16]	.116	.133	.147	.161	.219

At 30 the experimental data stops, the $4s^2$ shell being so stable that there is no data on optical transitions involving $4s$ electrons for $Z > 30$; whereas the $4p$ electrons do not become inner electrons until $Z = 36$. It is not possible to calculate the rate in the sequence joining x-ray and "semi-optical" spectra (the bromine-like sequence in the case $4s \leftarrow 4p$) from Eq. (3) with the same accuracy as in the $2s \leftarrow 2p$ case, for the curvature and uncertainty in the x-ray, σ_1 curves increases with increasing principal quantum number.[17] The rate for $4s \leftarrow 4p$ in the bromine-like sequence from Eq. (3) is about $0.58 \cdot 2(1-.4)/4 = .17$.

Interpolations in such tables as this, allowing for the peaked but otherwise smooth character of the curves, should be quite reliable.

[17] A. Sommerfeld, "Atombau" p. 460.

NEW MEASUREMENTS IN THE FOURTH POSITIVE CO BANDS

By Roger S. Estey
Washington Square College, New York University

(Received October 28, 1929)

Abstract

That part of the fourth positive system of CO lying between 1970A and 2800A has been remeasured together with sixteen bands not previously observed. An equation for the band heads is given, the constants of which yield the values $D'=12.00$ volts, $D''=11.17$ volts for the heat of dissociation.

Modifications in values of frequency have been small, while those of intensity have been rather large. Some discrepancies have been removed. Revision of intensity estimates permits a far more accurate comparison than previously with Condon's theory of intensity distribution and shows the superiority of Morse's $U(r)$ function. Using this function, the distribution of intensity among the bands of the fourth positive system agrees perfectly with Snow and Rideal's value of the moment of inertia for the normal state, $I_0''=15.0\times10^{-40}$ g cm^2.

The quantum assignment of Asundi's infra-red electronic bands has been revised.

Introduction

THE fourth positive band system of CO, which extends at least from 2800A to 1300A, has never been completely measured by any one investigator. The work on this system prior to 1926 is fully described by Birge.[1] His paper analyzes data taken by Deslandres (42 bands), Bair (22 bands), Duncan (14 bands), Lyman (100 bands), and Leifson (12 bands), all under low dispersion. Subsequent to 1926 papers have appeared on the energy levels of CO,[2,3] the mode of dissociation,[4] CO in active nitrogen,[5] the isotope effect,[6] and a series of papers on the structure of the various systems.[7,8,9,10]

The initial vibrational levels of this system are the same as the final levels of the Angstrom bands and of the new bands analyzed by Herzberg,[7] and Johnson and Asundi,[8] while the final levels are the same as those of the Cameron bands and several absorption systems. These relationships are shown in Fig. 1, which diagrams the electronic energy levels for neutral CO. In addition to the bands just mentioned there are shown the third

[1] Birge, Phys. Rev. **28,** 1157 (1926).
[2] Hopfield and Birge, Phys. Rev. **29,** 922 (1927).
[3] Duffendack and Fox, Astrophys. J. **65,** 214 (1927).
[4] Hogness and Harkness, Phys. Rev. **32,** 936 (1928).
[5] Knauss, Phys. Rev. **32,** 417 (1928).
[6] Birge, Phys. Rev. **34,** 379 (1929).
[7] Herzberg, Zeits. f. Physik **52,** 815 (1929).
[8] Johnson and Asundi, Proc. Roy. Soc. **A123,** 560 (1929).
[9] Asundi, Proc. Roy. Soc. **A124,** 277 (1929).
[10] Asundi, Nature **123,** 47 (1929).

positive and the three A systems. Asundi[9] has contributed two other new systems, the five B and an unnamed system in the near infra-red. The absorption and emission systems described by Hopfield and Birge are also shown.

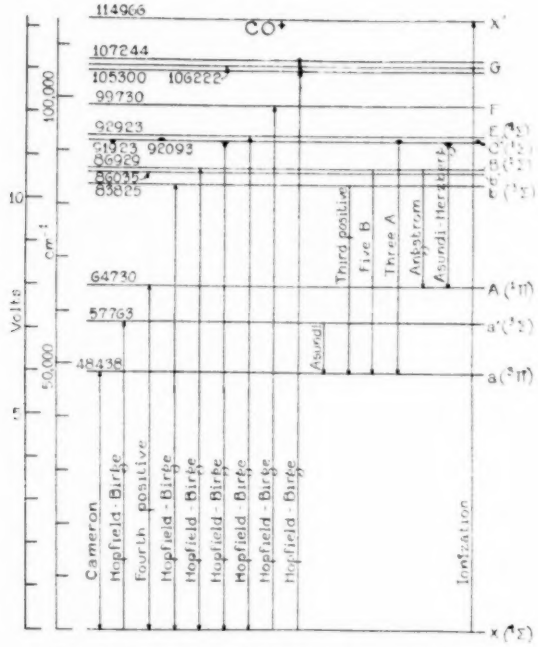

Fig. 1. Energy level diagram for neutral CO.

Asundi's vibrational analysis[11] of the infra-red system requires revision with respect to the initial state. The upper electronic level is at 57763 cm^{-1} (Birge, private communication) rather than at 58927, and the most recent value[12] for ω_0' is 1173 cm^{-1}. This yields the equation for the infra-red bands

$$\nu = 9325 + (1173n' - 9n'^2) - (1726.5n'' - 14.4n''^2).$$

Accordingly the initial quantum numbering must be increased by one unit and the band called 1, 0 by Asundi is really the 2, 0 band.

The present knowledge of the fourth positive band system is somewhat inaccurate because it has been measured under low dispersion only, and because of a lack of satisfactory wave-length standards in the region which it occupies. Therefore it seemed advisable to remeasure as many bands as could be reached with a quartz spectrograph.

Experimental Details

The CO bands were excited at 0.3 mm pressure in a water-cooled U-shaped discharge tube, the straight portion of which was viewed end on. This straight portion was 23 cm long and 6 mm in diameter. Large iron

[11] His equation is $\nu = 10489 + (1155n' - 9n'^2) - (1726.5n'' - 14.4n''^2)$.

[12] Mulliken, Phys. Rev. **32,** 186 (1928).

electrodes permitted an input of 1.2 amperes at 2200 volts from a 3 KVA power transformer. Magnesium carbonate in an electrically heated side tube served as a source of CO_2 which later broke down to CO in the discharge. The vapor pressure of CO_2 over magnesium carbonate is constant at constant temperature. In this way fresh gas was provided as rapidly as required by the clean-up of the electrodes.

The pictures were taken on Hilger Schumann plates, or oiled Eastman 40's with a Hilger E 1 quartz spectrograph. This instrument has a dispersion of 3.91A/mm at 2800A and 1.21A/mm at 1970A, the limits of the range covered in this investigation.

Copper arc and spark lines and nickel spark lines as listed by Shenstone[13,14,15] served as standards below 2500A, while in the region above this iron standards as listed in volume VII of Kayser and Konen, "Handbuch der Spektroskopie," were used. The transformations between wave-lengths and wave-numbers were made with the aid of Kayser's "Tabelle der Schwingungszahlen."

Results

The new measurements on the band heads are shown in the following table.

Table I. *Fourth positive bands of CO.*

λ(I.A.)	ν(cm⁻¹)	*I*	*n'*, *n''*	O−C	λ(I.A.)	ν(cm⁻¹)	*I*	*n'*, *n''*	O−C
2799.7	35708.2	9	9 22	+ 1.6	2356.5	42422.3	4	5 15	+1.1
2785.4	35890.3	8	4 18	− 4.8	2337.9	42760.1	7	8 17	+0.7
2742.6	36450.7	6	11 23	+14.1	2332.5	42860.0	3	4 14	+2.0
2740.0	36486.0	4	7 20	− 4.0	2311.5	43249.2	8	7 16	+0.5
2712.1	36860.5	4	6 19	− 7.7	2286.1	43728.5	7	6 15	−0.5
			10 22?	−15.8	2273.9	43963.4	3	9 17	−0.2
2698.3	37049.7	6	13 24	− 4.2	2272.3	43994.0	1	12 19	+4.4
2684.0	37247.4	3	5 18	+10.1	2261.7	44200.0	9	5 14	−0.2
2680.8	37291.5	5	9 21	+15.5	2247.2	44486.6	7	8 16	−0.8
2662.9	37541.8	4	12 23	+ 4.6	2238.3	44663.8	9	4 13	+1.3
2661.5	37561.7	4	15 25	+ 3.0	2221.5	45001.4	10	7 15	−0.8
2659.6	37587.9	4	4 17	− 9.6	2215.8	45115.9	3	3 12	+0.1
2630.0	38011.4	6	11 22	± 0.0	2196.8	45506.4	10	6 14	−1.6
2598.3	38474.8	4	10 21	− 1.8	2173.0	46004.7	9	5 13	−0.1
2594.5	38531.5	1	16 25	+10.3	2150.2	46492.6	8	4 12	±0.0
2567.8	38932.8	5	9 20	− 0.1	2137.0	46779.9	5	7 14	−1.2
2556.0	39111.7	3	12 22	− 0.3	2128.3	46971.1	8	3 11	−0.2
2538.6	39379.7	4	8 19	− 0.4	2113.1	47309.6	9	6 13	−2.9
2521.8	39642.7	3	14 23	− 7.9	2107.2	47440.3	7	2 10	−0.8
2509.9	39830.1	8	7 18	+11.8				9 15	−3.8
2492.9	40102.1	8	10 20	− 0.3	2089.9	47834.0	10	5 12	−0.8
2483.8	40248.8	3	6 17	+ 1.3	2086.9	47901.5	1	1 9	−0.4
2463.2	40584.6	10	9 19	+ 0.3	2067.6	48349.4	10	4 11	+1.3
2458.0	40671.5	2	5 16	+ 3.8	2046.3	48852.9	10	3 10	+0.5
2433.9	41057.5	9	8 18	+ 0.5	2025.8	49347.8	9	2 9	+0.1
2424.1	41239.3	5	11 20	+ 1.7	2011.8	49690.6	8	5 11	+0.2
2407.6	41552.0	7	7 17	+ 1.3	2005.8	49838.2	5	1 8	+4.2
2394.2	41754.2	3	10 19	+ 0.3	λ(vac.)				
2393.1	41773.9	4	13 21	− 4.5	1990.8	50230.9	10	4 10	+1.7
2381.6	41975.3	6	6 16	− 0.2	1970.0	50761.7	8	3 9	+2.6
2365.5	42261.9	5	9 18	+ 0.7					

[13] Shenstone, Phys. Rev. **28,** 449 (1926).
[14] Shenstone, Phys. Rev. **29,** 380 (1927).
[15] Shenstone, Phys. Rev. **30,** 255 (1927).

The assignment of vibrational quantum numbers (n', n'') is substantially that given by Birge. A few bands given by him were not measured because of overlapping by other bands. Otherwise, all bands given by Birge, as well as many new bands, have been measured and quantum numbers assigned.

The new measures on fifty-eight bands yield the equation[16]

$$\nu = 64729.60 + (1497.63\, n' - 17.262\, n'^2) - (2149.08\, n'' - 12.761\, n''^2).$$

The column headed "O−C" in Table I lists the observed minus calculated values of the band heads as calculated from this equation. Unfortunately it was possible to measure bands of relatively large quantum numbers only. For this reason the equation written above probably does not express the origin of the system and the bands near it as well as the former equation[16] does, although for the region represented by the bands of Table I the new equation is probably the better.

The plates showed clearly the presence of a single P, Q, and R branch in each band. The bands degrade to the red. Although they were unresolved at the origin and it was impossible to determine how many lines were missing, there is no reason to doubt the correctness of the assumption that these bands result from a $^1\Pi$ to $^1\Sigma$ transition.

Discussion

Accuracy in our present methods of evaluating the heat of dissociation of a molecule from data on vibrational energy levels depends on our ability to extrapolate to $\omega_n = 0$ the $\omega_n : n$ curve. Fortunately in many cases including this one the $\omega_n : n$ curve is nearly linear over the known range, which facilitates extrapolation. The data in this paper, being more accurate and extensive, yield a more reliable extrapolation and provide a more certain value of the heat of dissociation than that previously reported.[17] The heat of dissociation of a CO molecule in the normal state, as now determined, is 11.17 volts. To raise a CO molecule to the $^1\Pi$ level and dissociate it there requires 12.00 volts.

The large extent of the fourth positive system affords both opportunity and difficulty in discussing vibrational intensity relations. Table I gives, under the heading "I", simple visual estimates of intensity, allowing as well as possible for overlapping bands and for large variations in plate sensitiveness over the range considered. Fig. 2 shows in a graphical manner the intensities of the observed bands. The diameters of the circles are proportional to the intensities of the corresponding bands.

A theory has been given by Condon[18] which predicts, from a knowledge of certain band constants including the moment of inertia, which bands of a system will be the most intense. A $U(r)$ curve (potential energy as a function of r) is drawn for each of the two electronic states involved. Such a curve

[16] The next most recent equation (I.C.T. Vol. 5, p. 412) is $\nu = 64765 + (1499.0n' - 17.24n'^2) - (2154.7n'' - 12.70n''^2)$. $D = 11.2$ volts.

[17] Birge and Sponer, Phys. Rev. **28**, 259 (1926).

[18] Condon, Phys. Rev. **28**, 1182 (1926).

shows the extremes between which a molecule with a given amount of energy can vibrate. Condon's theory is based on the assumption that the molecule spends most of its time in an extreme position and that as a consequence the transitions between the extreme positions are the most probable. Since the $U(r)$ curve represents these extremes, transitions drawn between the upper and lower of two $U(r)$ curves of a molecule are according to the theory the most probable, and on an n', n'' diagram (cf. Fig. 2) they fall on a smooth curve roughly parabolic in form with the vertex near the origin of the system. If the constants and the function on which the $U(r)$ curves are based are correct, then the theoretical intensity distribution curve should pass through the most intense bands observed. The $U(r)$ function used by Condon in

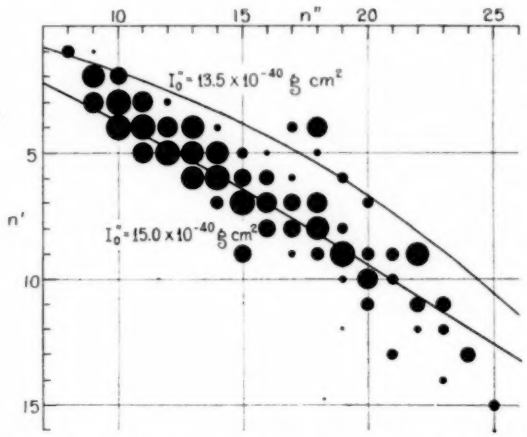

Fig. 2. Intensities of band heads. The intensity of each band as listed in Table I is proportional to the diameter of the corresponding circle on the n', n'' diagram. Intensity distribution curves based on Morse's $U(r)$ function are plotted for two values of I_0''. The observed distribution of band intensities agrees with $I_0''=15.0\times10^{-40}$ g cm².

developing his theory is a power series, and for computing purposes the polynomial composed of the first three terms is used. In the particular case of the CO molecule this polynomial is satisfactory only over a very small range of r near r_0. An intensity curve using $I_0''=14.9$ appears in Condon's paper.[18] This curve fits near the origin, but for quantum numbers higher than $n''=10$ the upper branch becomes concave upward while the trend of the bands in this region is concave downward.

Fortunately another form of $U(r)$ function is available[19] which has the following properties: (a) when r is zero, U is very large, (b) when r is r_0, U is at its only minimum, (c) when r is very large, U is asymptotic to D, the heat of dissociation, and (d) when the quantum theory is applied, the function yields the correct expression for the vibrational energy levels. This function is given by the expression

$$U=A+De^{-2a(r-r_0)}-2De^{-a(r-r_0)},$$

where A is the constant which moves the entire curve up or down on the energy scale, D is the heat of dissociation, $a=0.2454(M\omega_0 x)^{1/2}$, where M is

[19] Morse, Phys. Rev. **34**, 57 (1929).

the reduced mass in terms of the atomic weights; and r and r_0 are nuclear separations, the latter corresponding to the special case of zero vibrational energy.

Theoretical intensity curves are drawn on Fig. 2 corresponding to $U(r)$ curves computed from the following constants:

	A	D	a	r_0
Initial	97500	32500	2.67	1.24
Final	91394	91394	2.29	1.09
	91394	91394	2.29	1.15

Curves corresponding to two values of the moment of inertia ($I_0'' = 15.0 \times 10^{-40}$ g cm^2, giving $r_0'' = 1.15$A, and $I_0'' = 13.5 \times 10^{-40}$, giving $r_0'' = 1.09$) appear on Fig. 2 because at the time the figure was first drawn Snow and Rideal's paper[20] giving $I_0'' = 15.0 \times 10^{-40}$ had not appeared and it seemed probable that the lower value of I_0'' was about right.[9,21] The intensity curve corresponding to the lower value of the moment of inertia does not fit the observed bands very well, while the intensity curve corresponding to the larger value is an excellent fit, especially in the center of the diagram. For low quantum numbers the fit is really better than the figure would indicate because bands observed by others with a vacuum spectrograph are not shown since the diagram shows only the data of the author.

The intensity distribution among the bands of the fourth positive system is very distinct evidence in favor of the larger value of the moment of inertia if we assume that the $U(r)$ function given above is essentially correct. The evidence strongly favors this assumption and the intensity distribution can therefore be taken as good evidence from the electronic bands for the correctness of the infra-red value of the moment of inertia for the normal state. This represents a new and useful check on the value of this constant.

Babcock[22] has estimated the prevalence of O^{16} relative to O^{18} as 1250:1. If we assume that C^{12} has an atomic weight 12.000 and that C^{12} and C^{13} are the only factors influencing the atomic weight (12.003) of carbon,[23] then they are prevalent in the ratio of 333:1. This calculation shows, in harmony with the experimental findings of King and Birge[24] that $C^{13}O^{16}$ is much more prevalent than $C^{12}O^{18}$ or $C^{13}O^{18}$. Therefore the calculated positions of several favorably located band heads of the $C^{13}O^{16}$ molecule have been examined on a heavily exposed plate, but no isotopic heads have been found. This does not cast doubt on the isotopic heads reported by Birge on the fourth positive absorption plates taken by Hopfield, but merely goes to show that absorption spectra show these faint bands more readily than do emission spectra.

I wish to express my appreciation for the advice and assistance of Professor R. S. Mulliken.

[20] Snow and Rideal, Proc. Roy. Soc. **A125,** 462 (1929).

[21] Lowry, J.O.S.A. & R.S.I. **8,** 647 (1924). A numerical error appears in this paper (Lowry, private communication) and a recalculation of Lowry's data by the writer gives $I_0 = 13.0 \times 10^{-40}$ g cm^2.

[22] Babcock, Phys. Rev. **34,** 540 (1929).

[23] Birge, Phys. Rev. Sup. **1,** 1 (1929).

[24] King and Birge, Phys. Rev. **34,** 376 (1929).

FINE STRUCTURE OF THE BERYLLIUM FLUORIDE BANDS

By F. A. Jenkins
Department of Physics, University of California

(Received December 24, 1929)

Abstract

Wave-length measurements of BeF bands.—New wave-length measurements have been made of the rotational lines of the BeF bands in the regions λλ3009.5–3026.3, 2908.9–2927.8, and 3126.1–3140.8, which include all the stronger lines of the (0, 0), (1, 0) and (0, 1) bands. The source was a cored carbon arc run at atmospheric pressure. The Harvard 21-foot grating was used in the second order, giving a linear dispersion of 0.97 A per mm and an effective resolving power of nearly 100,000. The wave-numbers of the lines in the six branches of each band are tabulated for rotational quantum numbers up to about $K=50$ in the R branches, 45 in the Q branches, and 30 in the P branches. Visual intensity estimates are also included.

Term analysis of BeF bands.—The rotational structure is found to be that characteristic of a $^2\Pi \rightarrow {}^2\Sigma$ electronic transition, with a relatively small value of $\Delta E/B$, +15.667, in the Π state. The combination relations among the lines of the (1, 0), (0, 0) and (0, 1) bands are satisfied within the experimental error in every case where exact agreement is to be expected. The R-Q, Q-P relations show a small combination defect, which is referred to Λ-type doubling in the initial state. This doubling is slightly greater for the levels involved in the low-frequency sub-band, and therefore it is assumed that the $^2\Pi$ state is normal. Rotational terms having the same K in the initial state draw rapidly together as the rotation increases, due to the loose coupling of the spin with the molecular axis. Quantitative agreement is obtained between the observed term-differences, ΔF, and their values calculated by the theoretical energy formulas derived by Hill and Van Vleck for the transition from case a to case b type of spin coupling. Equations capable of representing all the lines in a given band are deduced.

Constants of BeF molecule.—The following values for the more important molecular constants are obtained: $B^{(0)\prime}=1.41060$ cm^{-1}, $B^{(0)\prime\prime}=1.47928$, $\alpha'=0.01610$ cm^{-1}, $\alpha''=0.01685$, $D^{(0)\prime}=-8.301\times10^{-6}$ cm^{-1}, $D^{(0)\prime\prime}=-8.209\times10^{-6}$, $\beta'=1.060\times10^{-8}$ cm^{-1}, $\beta''=2.903\times10^{-8}$, $I_e'=(19.50\pm0.03)10^{-40}$ g cm^2, $I_e''=(18.59\pm0.03)10^{-40}$, $r_e'=1.390\times10^{-8}$ cm, $r_e''=1.357\times10^{-8}$, $\omega_e'=1172.56$ cm^{-1}, $\omega_e''=1265.62$, $x_e'=0.007488$, $x_e''=0.007206$, $\nu_e=33{,}233.61$ cm^{-1}, $\Delta E=22.10\pm0.1$ cm^{-1}.

Introduction

BAND spectra are known for a large number of diatomic alkaline earth halides,[1] the most familiar being those of the fluorides, such as CaF. In general, the rotational structure of these bands is so finely spaced that there seems to be little hope of carrying out a detailed fine structure analysis, even

[1] For the experimental material on the alkaline earth halides, other than BeF, see H. Kayser, "Handbuch der Spectroscopie," Vols. 5, and 6, and S. Datta, Proc. Roy. Soc. **99A** 436 (1921). General treatments of the relations between the electronic states, molecular constants, etc., have been given by R. Mecke, Zeits. f. Physik **42,** 390 (1927) and by R. C. Johnson, Proc. Roy. Soc. **122A,** 161, 189 (1929).

with spectrographs of the highest resolving power. The most favorable case for analysis is the lightest molecule of this class, BeF, for which, owing to its small moment of inertia, the spacing of the lines in a band should be great enough to permit almost complete resolution. A band system due to this molecule was first reported by Datta[2] in 1922. Its bands are shaded toward the red and lie completely in the ultra-violet, the head of the strongest occurring at λ3009.6. Datta undertook a study of the fine structure of this band, and was able to identify three fairly regular series of lines. It is obvious, however, from an examination of his reproduction, and of the curves obtained, that the resolving power he used (third order of a 10-foot grating) was insufficient for a satisfactory quantum analysis of the band structure. Each of his series, as will appear in the present work, represents the blending of two or more true series. For the analysis to be reported here, new plates were taken, having a dispersion and actual resolution from 2 to 3 times greater than those attained by Datta. This comparatively small advantage has made possible a complete and satisfactory interpretation of the rotational structure.

The BeF bands were first considered from the standpoint of the quantum theory by Mulliken.[3] Vibrational quantum numbers were assigned, and an equation derived for the frequencies of the heads, as measured by Datta. The molecule BeF was classed with a number of one-valence-electron emitters of band spectra, such as BO, CN, CO^+, N_2^+, the spectra of which appeared to be qualitatively similar. From such considerations, it was concluded that the ultra-violet BeF system represents a $^2\Pi \rightarrow {}^2\Sigma$ electron jump, analogous to the α bands of BO, the red CN bands, etc. The latter are of the double double-headed type, the first head in each pair being formed by an R, and the second by a Q branch.[4] Each of the BeF bands has only 3 heads, the first two forming a close pair of nearly equal intensity, and the third being somewhat weaker. It has therefore been assumed that the second and third heads are those of the Q branches, the second R head being too faint to be observed. On this view, the two Q heads should represent approximately the double origin of the band and from these $\Delta E \leqq 35$ cm^{-1} for the $^2\Pi$ state. A revised interpretation of the formation of the heads has recently been given by Jevons.[5] From a critical study of Datta's measurements, especially with regard to the variation of the mutual separations of the heads with vibrational quantum number, he concluded that the first pair of heads is formed by two closely parallel R branches and the third by one of two Q branches. Evidence for a second Q head was found on the writer's spectrograms early in the present work, but it appeared later during the analysis that this apparent head is merely a fortuitous accumulation of lines at the point in question.

In beginning the analysis of a band of complex structure, it is very desirable to have as a starting point an approximate idea of the type of band

[2] S. Datta, Proc. Roy. Soc. **101A,** 187 (1922). An excellent reproduction of the band system as a whole is given.

[3] R. S. Mulliken, Phys. Rev. **26,** 561 (1925).

[4] F. A. Jenkins, Proc. Nat. Acad. **13,** 496 (1927).

[5] W. Jevons, Proc. Roy. Soc. **122A,** 216 (1929).

structure, i.e. number of branches, approximate electronic separation, etc. According to the revised interpretation by Jevons, the rotational structure of the BeF bands should resemble that of the green MgH bands, where the electronic doublet separation is relatively small, and the corresponding branches of the two sub-bands draw rapidly together with increasing rotational quantum number. Bands showing this type of "rotational distortion" are fairly numerous[6] and, as in BeF, three heads are usually observed, one of the Q branches not forming a head due to the distortion effect. Such a structure is characteristic of a $^2\Pi \rightarrow {}^2\Sigma$ or $^2\Sigma \rightarrow {}^2\Pi$ transition, in which the ratio of the doublet energy difference, ΔE, to the constant B, is small (i.e. less than about 20). A point strongly opposed to the previous interpretation, with $\Delta E/B$ large, appeared in the fact that, although the bands are closely grouped in sequences the distance from the R head to the origin would be extremely small (3 cm^{-1}). This would violate the rule of Birge and Mecke, according to which a small change in the vibration frequency during the transition is always accompanied by a small change in the moment of inertia. It therefore seemed probable that in BeF the $\Delta E/B$ is small. By postulating that the bands are of the MgH type, preliminary investigations of the structure[7] showed that Jevons' scheme is essentially correct.

Experimental Procedure

The spectrograms were obtained in the second order of the 21-foot grating at Harvard University, giving a dispersion of 0.97A per mm in the region investigated. An arc in air between carbon poles, both cored with a mixture of $BeKF_3$ and powdered carbon, gives not only the BeF, but also the BeO band system with considerable intensity in the flame surrounding the poles.[8] Therefore, the BeO bands were also obtained on these plates. The rotational quantum analysis of the latter system has been given by Miss J. E. Rosenthal and the writer,[9] and also independently by Bengtsson.[10] In the former article will be found a brief description of the experimental details pertaining to the spectrograms used in the present investigation, since the BeF and BeO spectra were photographed simultaneously. Two sets of plates were of use for our purpose, one showing the stronger sequence $\Delta v = 0$[11] with the best possible resolution (slow, fine-grained plates) and another on which the 0 sequence is considerably over-exposed, but the sequences $+1$ and -1 are of satisfactory

[6] R. S. Mulliken, Phys. Rev. **32,** 388 (1928).

[7] The main results embodied in the present article were given in a paper before the American Physical Society, Washington Meeting, April, 1929. Cf. Phys. Rev. **33,** 1090 (1929) (Abstract).

[8] Jevons, ref. 5, finds that the oxide bands are relatively stronger in the outer part of the flame.

[9] J. E. Rosenthal and F. A. Jenkins, Phys. Rev. **31,** 705 (Apr. 1928) (Abstract), Phys. Rev. **33,** 163 (1929).

[10] E. Bengtsson, Arkiv. för Mat. Astro. och Fysik, **20A,** No. 21, p. 1, June 1928.

[11] The nomenclature used here conforms with the revised system recently proposed (Mulliken, private communication). In this v represents the vibrational quantum number, formerly n.

intensity. The first heads of the three sequences are, according to Mulliken's assignment: λ3009.582 (0), λ2908.994 (−1) and λ3126.116 (+1). Doublets with a separation of 0.04A are resolved on these plates. The iron arc comparison spectrum shows no relative displacement on the two sets. An enlargement of part of the 0 sequence from the first set is shown in Fig. 1, accompanied by a Fortrat diagram of the (0, 0) band, according to our complete analysis.

In order to take full advantage of the combination principle, it was necessary to study bands which would yield agreements in the term-differences of

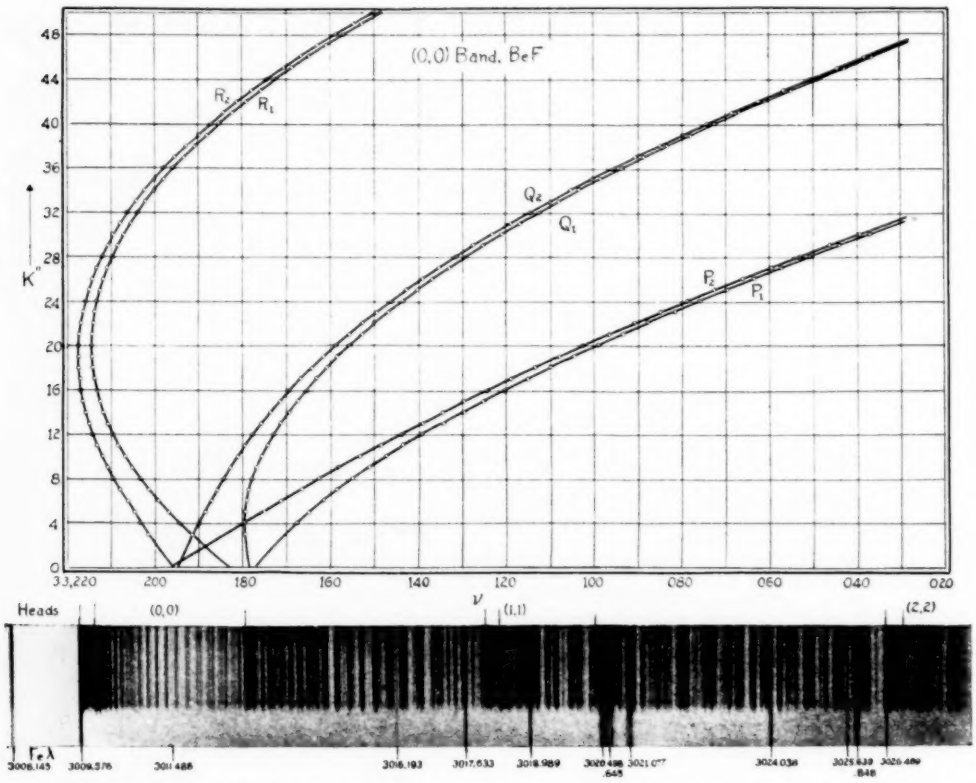

Fig. 1. (0, 0) *band of BeF.* The spectrum has been enlarged to practically the same scale as the diagram, but the correspondence of the lines with points on the diagram is not exact throughout, because the latter is on a scale of frequencies.

both the initial and the final states. Accordingly, wave-length measurements were made of the lines in the first band of each of the three above-mentioned sequences, i.e. in the (0, 0), (1, 0) and (0, 1) bands. The secondary Fe wave-length standards given by Fabry[12] were used throughout. The measurements included every line in each sequence as far as the first head of the third band in that sequence. This was necessary because, as will be apparent in Fig. 1, many lines of the first band are intermingled with those of the second. In

[12] Ch. Fabry, Int. Crit. Tables, Vol. V, p. 275.

general, our wave-lengths agree well with those of Datta.[2] Table I gives the wave-numbers in vacuum of all lines assigned to the above three bands. A large number of measured lines belonging to the second bands of the sequences are not given, because they represent only certain parts of these bands and would be of little value for the present purpose. Although there is an element

TABLE I. *Wave-number and intensity data for BeF bands.*

	R_2 *head*, $\lambda_{air}=3009.582$		(0, 0) band R_1 *head*, λ3009.873		Q_1 *head*, λ3013.011	
K''	R_2	R_1	Q_2	Q_1	P_2	P_1
3	33,201.42²1	33,191.43¹0	33,190.66²3	——	——	——
4	203.21²2	194.24¹1	189.85²4	33,179.45³4*d*	33,179.76²2	33,167.42²3*d*
5	205.06²0	196.73¹1*d*	188.44¹1	179.45³4*d*	174.92¹0	164.92²3
6	206.71²1	199.14¹1	187.03²4	178.97²1	171.26³4	161.41³4
7	207.84²3	201.42²1	185.74¹2	178.59¹1	166.59³4	158.30²5
8	209.47³4*d*	203.21²2	184.14²4*d*	177.64²5	161.41³4	154.82¹1
9	210.71³4	205.06²0	182.74¹3	176.76¹2	156.87²2	151.03¹2
10	211.77³3*d*	206.71²1	180.96²4*d*	175.65²5	153.18¹1	147.13¹0–
11	213.11³3	208.38²3	179.45³4*d*	174.17²3	148.42²2*d*	143.36²3*d*
12	214.18²5*d*	209.47³4*d*	177.64²5	172.82¹2	143.89²2	138.93³4*d*
13	214.95²2	210.71³4	175.65²5	171.26³4	138.93³4*d*	134.32³3
14	215.69²2	211.77³3*d*	173.53¹2	169.30²4*d*	134.32³3	129.57²3*d*
15	216.36²1	212.44²2	171.26³4	167.42²3*d*	129.57²3*d*	125.00²3
16	216.65¹1	213.11³3	169.30²4*d*	165.33¹3	124.22¹2	120.13¹1*d*
17	216.94²1	213.75²2	166.59³4	163.08¹3	118.78²4*d*	115.02²2*d*
18	217.41⁴5*d*	214.18²5*d*	164.05¹3	160.77²4	113.51¹2	109.75²3
19	217.41⁴5*d*	214.18²5*d*	161.41³4	158.30²5	107.81²4	104.48¹2
20	217.41⁴5*d*	214.18²5*d*	158.56²5	155.58²5	102.36¹2	099.04¹2
21	217.41⁴5*d*	214.18²5*d*	155.58²5	152.59³5	096.54¹3*d*	093.44²3
22	216.94²1	214.18²5*d*	152.59³5	149.87²4*d*	090.71¹0*d*	087.67¹1*d*
23	216.36²1	213.75²2	149.28¹4	146.61¹3	084.82²4	081.83¹2*d*
24	215.69²2	213.11³3	145.93¹3	143.36²3*d*	078.58¹3*d*	075.89¹1
25	214.95²2	212.44²2	142.48¹4	139.96¹3	072.37²4	069.49¹2*d*
26	214.18²5*d*	211.77³3*d*	138.93³4*d*	136.47¹3	065.89¹3	063.30¹2*d*
27	213.11³3	210.71³4	135.10¹3	132.77¹3	059.46¹2	057.09¹3
28	211.77³3*d*	209.47³4*d*	131.19²4	128.94¹5	052.86¹2	050.52²5*d*
29	210.71³4	208.38²3	127.20¹3	125.00²3	046.12¹4*d*	043.70¹2
30	209.47³4*d*	207.02¹2	123.01¹4	120.82²4	039.08¹4	036.84¹4
31	207.84²3	205.44¹2	118.78²4*d*	116.72¹2	——	——
32	205.98¹2	203.98²3*d*	114.28¹3	112.38¹3*d*		
33	203.98²3*d*	202.14²4	109.75²3	107.81²4		
34	202.14²4	200.03²5	105.07¹3	103.14¹3		
35	200.03²5	197.79²4*d*	100.22¹3	098.30¹3*d*		
36	197.79²4*d*	195.66¹4	095.27¹3*d*	093.44²3		
37	195.27¹4	193.23¹3	090.20¹2*d*	088.41¹2*d*		
38	192.58¹3	190.66¹3	084.82²4	083.17¹2		
39	189.85²4	187.93¹3	079.49¹3	077.82¹3		
40	187.03²4	185.10¹3	073.91¹4	072.37²4		
41	184.14²4*d*	182.08¹3	068.20¹4	066.69¹3		
42	180.96²4*d*	178.97²1	062.44¹4	060.96¹3		
43	177.64²5	175.65²5	056.61¹4	054.98¹3		
44	174.17²3	172.10¹2	050.52²5*d*	048.97¹3		
45	170.39¹3	168.60¹2	044.20¹3*d*	042.72¹3*d*		
46	166.59³4	164.92²3	037.90¹2	036.43¹5		
47	162.74¹2	160.77²4	——	——		
48	158.56²5	156.87²2				
49	154.50¹1	152.59³5				
50	149.87²4*d*	148.42²2*d*				
51	145.58¹2	143.89²2				
52	140.85¹2	138.93⁴4*d*				
53	136.12¹1	134.32³3				
54	131.19²4	129.57²3*d*				
55	125.94¹1	——				

TABLE I. (Continued)

			(0, 1) band			
	R_2 head, λ3126.116		R_1 head, λ3126.366		Q_1 head, λ3130.369	
K''	R_2	R_1	Q_2	Q_1	P_2	P_1
5			31,941.19[1]1			
6			940.39[2]4			
7	——	——	939.28[2]4	31,932.20[1]1		
8	31,963.42[4]5*d*	31,957.34[2]2*d*	938.24[1]2*d*	931.45[2]3*d*		
9	964.92[3]3	959.12[1]2	937.37[1]3	930.95[1]2*d*		
10	966.43[3]3	961.64[4]5*d*	935.89[1]2	929.89[2]3*d*		
11	967.96[3]3	963.42[4]5*d*	934.40[1]3*d*	929.01[1]2*d*	——	——
12	969.38[3]3	964.92[3]3	932.99[1]3*d*	928.60[2]5*d*	31,899.20[1]1	31,894.22[1]1
13	970.72[3]3	966.43[3]3	931.45[2]3*d*	927.06[1]2	894.72[1]1	889.94[2]4
14	971.81[2]4*d*	967.96[3]3	929.89[2]3*d*	925.60[1]1	890.60[1]0	886.24[2]2
15	972.78[4]4	969.38[3]3	928.60[2]5*d*	924.48[2]5*d*	886.24[2]2	881.65[2]0*d*
16	974.32[3]3*d*	970.72[3]3	926.47[1]2	922.73[2]5	881.65[2]0*d*	877.37[1]0
17	975.02[4]4	971.43[2]3*d*	924.48[2]5*d*	921.14[1]4	876.74[2]2	873.22[2]4
18	975.66[4]4*d*	972.78[4]4	922.73[2]5	919.36[1]3	872.42[1]4	868.52[1]0
19	976.64[4]5*d*	973.75[3]3*d*	920.70[1]4	917.44[1]5	867.65[2]1*d*	863.70[2]2*d*
20	977.28[2]2*d*	974.32[3]3*d*	918.65[1]3	915.54[1]3*d*	862.18[2]3*d*	859.12[1]1
21	977.95[2]2	975.02[4]4	916.39[1]3	913.50[1]4	857.32[1]1	853.83[2]4*d*
22	978.55[2]0	975.66[4]4*d*	914.09[1]3	911.24[1]4*d*	851.95[1]0	849.12[1]0
23	979.10[4]5*d*	976.08[2]4*d*	911.77[1]4*d*	909.07[2]5*d*	846.99[2]2	844.11[1]1
24	979.10[4]5*d*	976.64[4]5*d*	909.07[2]5*d*	906.64[2]5	841.86[1]1	839.08[1]1
25	979.34[2]2	976.78[4]3	906.64[2]5	904.16[2]3	836.50[2]1	833.46[2]1*d*
26	979.34[2]2	976.78[4]3	904.16[2]5	901.47[2]5	831.07[1]0	——
27	979.34[2]2	976.78[4]3	901.47[2]5	898.80[2]2*d*	——	
28	979.10[4]5*d*	976.78[4]3	898.40[1]2*d*	895.98[1]0		
29	979.10[4]5*d*	976.64[4]5*d*	895.41[1]5	893.02[1]5*d*		
30	978.55[2]0	976.08[2]4*d*	892.12[1]1	889.94[2]4		
31	977.95[2]2	975.66[4]4*d*	888.94[1]1	886.79[1]1		
32	977.28[2]2*d*	975.02[4]4	885.60[1]1*d*	883.61[1]1		
33	976.64[4]5*d*	974.32[3]3*d*	882.24[1]4*d*	880.31[1]3		
34	975.66[4]4*d*	973.75[3]3*d*	878.70[1]1	876.74[2]2		
35	975.02[4]4	972.78[4]4	875.05[1]1	873.22[2]4		
36	973.75[3]3*d*	971.81[2]4*d*	871.40[1]1	869.50[1]5		
37	972.78[4]4	970.72[3]3	867.65[2]1*d*	865.84[1]2		
38	971.43[2]3*d*	969.38[3]3	863.70[2]2*d*	862.18[2]3*d*		
39	970.06[1]1	967.96[3]3	859.71[1]2	858.14[1]3*d*		
40	968.64[1]1	966.43[3]3	855.57[1]2*d*	853.83[2]4*d*		
41	966.95[1]3*d*	964.92[3]3	851.26[1]1	849.92[1]2*d*		
42	965.31[1]4	963.42[4]5*d*	846.99[2]2	845.49[1]1		
43	963.42[4]5*d*	961.64[4]5	842.52[1]0	841.07[1]2		
44	961.64[4]5	959.79[2]4*d*	838.04[1]1*d*	836.50[2]1*d*		
45	959.79[2]4*d*	957.80[1]2*d*	833.45[2]1	831.97[1]3		
46	957.34[2]2*d*	955.62[1]2	——	——		
47	954.84[1]3*d*	953.43[1]2				
48	952.79[1]3	951.07[1]3				
49	950.39[1]3	948.56[1]3				
50	947.63[1]3	945.97[1]2				
51	945.03[1]3	943.32[1]2				
52	942.13[1]2	940.39[2]4				
53	939.28[2]4	——				

of arbitrariness in reporting the data in this way, that is in giving only lines assigned to the P, Q and R branches, it should be emphasized that every line of measurable intensity up to the head of the second band is accounted for and included in Table I. It is true that, due to the complexity of the structure blends of two or more lines are frequent, and the same wave-number often occurs several times in the table. It will be shown below, however, that this

TABLE I. (Continued)

	R_2 *head*, λ2908.994		(1, 0) band R_1 *head*, λ2909.300		Q_1 *head*, λ2911.700	
K''	R_2	R_1	Q_2	Q_1	P_2	P_1
4			——	34,334.17^{1}2		
5			——	333.80^{2}3		
6			34,341.22^{2}2	333.05^{2}3		
7			339.19^{2}3	332.22^{1}1		
8			337.60^{1}2*d*	331.55^{2}4		
9			336.01^{2}3*d*	329.87^{2}2	——	——
10			333.80^{2}3	328.20^{2}2	34,306.27^{2}5	34,300.19^{1}1
11			331.55^{2}4	326.50^{1}3	301.07^{2}2	295.61^{2}5*d*
12			329.53^{2}4*d*	324.63^{2}4	296.22^{2}3*d*	291.08^{2}3
13			327.03^{1}3	322.53^{2}3*d*	291.08^{2}3	286.38^{1}1
14			324.63^{1}4	320.35^{2}5	285.68^{2}4	281.21^{2}4*d*
15	——		321.58^{1}2	317.95^{2}3*d*	280.69^{2}1	276.61^{2}4*d*
16	34,365.95^{2}5*d*	——	318.79^{1}3	315.24^{1}2	274.37^{2}4	270.55^{1}1
17	365.95^{2}5*d*	34,362.28^{2}5*d*	315.99^{1}3*d*	312.63^{2}5*d*	268.66^{1}1	265.24^{2}3*d*
18	365.28^{1}2*d*	362.28^{2}5*d*	312.63^{2}5*d*	309.33^{2}4	262.67^{1}0	259.39^{2}5*d*
19	364.71^{1}2	361.75^{2}2	309.33^{2}4	306.27^{2}5	256.56^{1}1	253.19^{1}2
20	363.87^{1}2	360.98^{1}2	305.76^{2}5	302.81^{2}3	250.38^{2}3	247.19^{1}3
21	363.09^{1}2	360.00^{1}3	302.07^{1}2	299.34^{1}2	244.12^{1}0	240.76^{1}3
22	361.75^{2}2	359.14^{2}4	298.27^{2}3*d*	295.61^{2}5*d*	237.27^{2}2	233.94^{1}1*d*
23	360.54^{1}1	357.94^{1}3	294.39^{1}2	291.68^{1}3	230.55^{1}3	227.55^{1}3
24	359.14^{2}4	356.50^{1}2	290.14^{1}2	287.66^{2}4*d*	223.56^{1}2	220.88^{2}3*d*
25	357.40^{1}3	354.95^{1}2*d*	285.68^{2}4	283.40^{1}3	216.56^{1}3	213.84^{2}3
26	355.71^{1}2	353.28^{1}3	281.21^{2}4*d*	278.83^{1}3	209.54^{1}1	207.11^{2}0
27	353.90^{1}2*d*	351.53^{2}3*d*	276.61^{2}4*d*	274.37^{2}4	202.56^{1}3*d*	199.42^{1}4
28	351.53^{2}3*d*	349.31^{2}4*d*	271.90^{1}3*d*	269.55^{2}4	194.40^{1}1*d*	192.13^{1}3
29	349.31^{2}4*d*	346.97^{2}4*d*	266.74^{1}3	264.60^{1}3	186.47^{1}2	184.38^{2}5
30	346.97^{2}4*d*	344.63^{1}3	261.49^{1}3	259.39^{2}5*d*	178.55^{2}2	176.55^{1}2*d*
31	344.16^{1}3	341.95^{1}2*d*	256.07^{1}2	254.15^{1}3	170.40^{1}0	168.30^{1}0
32	341.22^{2}2	339.19^{2}3	250.38^{2}3	248.57^{1}4	161.97^{2}3*d*	159.95^{1}1
33	338.27^{1}2	336.01^{2}3*d*	244.87^{1}3	243.04^{1}3	153.93^{2}1	151.83^{1}2
34	335.00^{1}2	333.05^{2}3	239.08^{1}1	237.27^{2}2	——	——
35	331.55^{2}4	329.53^{2}4*d*	233.09^{1}3*d*	231.26^{1}4		
36	328.20^{2}2	326.03^{1}2	226.88^{1}3	225.23^{1}2		
37	324.32^{2}4	322.53^{2}3*d*	220.88^{2}3*d*	218.89^{1}4*d*		
38	320.35^{2}5	317.95^{2}3*d*	213.84^{2}3	212.32^{1}3*d*		
39	316.30^{1}2	314.30^{1}2	207.11^{2}0	205.57^{1}5*d*		
40	311.79^{1}1	310.05^{1}2	200.24^{1}1	198.64^{1}2		
41	307.48^{1}2	305.76^{2}5	193.07^{1}3	191.70^{1}3		
42	302.81^{2}3	301.07^{2}2	185.77^{1}4	184.38^{2}5		
43	298.27^{2}3*d*	296.22^{2}3*d*	178.55^{2}2	177.13^{1}1		
44	293.03^{1}1	291.08^{2}3	170.90^{1}0	169.31^{1}3		
45	287.66^{2}4*d*	286.16^{1}3	163.17^{1}1	161.97^{2}3*d*		
46	282.46^{1}1	280.69^{2}1	155.40^{1}3	153.93^{2}1		
47	277.16^{1}0	275.06^{1}1	147.21^{1}0	145.97^{1}0		
48	270.96^{1}1	269.55^{2}4	——	——		
49	265.24^{2}3*d*	263.54^{1}1				
50	259.39^{2}5*d*	257.53^{1}1*d*				

does not materially detract from the certainty of our interpretation of the band structure. Following each wave-number in Table I, a superscript gives the number of times a given value appears, or in other words the number of lines of the band coinciding so closely as to be unresolved and measured as a single line. The last number gives a rough measure of the intensity, on a scale 0 to 5, from eye estimates made during the measurements. These are only strictly comparable for lines near together. The letter *d* indicates a particularly wide or diffuse line. Thus, for example, the line $R_1(26)$ in the (0, 0) band

is given as 33,211.77[4] $3d$, since it is a diffuse line formed by the near coincidence of $R_1(26)$, $R_2(28)$, $R_1(14)$, $R_2(10)$, and is of intensity 3 on the scale employed. Regularities in the intensities, as well as the significance of the designations R_2, R_1, K, etc., will be discussed below in connection with the quantum analysis.

Interpretation of the Data

Solution of band structure. In attacking the problem of sorting out the various branches, it was noticed from the outset that a short series of very strong lines appears in the region between the second and third heads of each band, and another at some distance beyond the third head (See Fig. 1). These lines are sharp only for a few members, becoming diffuse and soon separating into doublets at each end. Since the separation of adjacent lines in the first of these series is slightly less than that of the close double head, which is that formed by the branches R_2 and R_1 according to the provisional interpretation, it appeared that these strong lines must have about the separation of the so-called "natural" doublets of the R branch. These doublets are formed by pairs of lines with the same value of K[13] in the $^2\Pi$ state, and the components approach each other as the rotation increases to the point where the spin axis becomes coupled nearly as in Hund's case b.[6] With the doublets spaced so that the second component of one falls on the first component of the next, the above-mentioned series show exactly the aspect they should. This is the strongest of the series identified by Datta. Similarly, the second series is formed by an analogous coincidence in the doublets of the Q branch. With this opening, it was a simple matter to identify two series of doublets, those of the R and Q branches. The approximate assignment of rotational quantum numbers to these lines in the (0,0) band was then obtained in the following way. The first differences of the *mean* wave-numbers for the Q doublets were plotted against an arbitrary numbering, and extrapolated to zero spacing. This gives roughly the position of the band origin, ν_0, and a revised numbering of the Q lines, (starting with 1 at the point of convergence) which is correct to one or two units. The slope of the line is $2(B'-B'')$. Next, taking the mean values of the R doublets, we use the formula for the distance II from the (mean) R head to the origin.

$$II = B' - \frac{(B')^2}{B'-B''} .$$

One thus obtains approximate values of both B' and B'', and also an idea of the assignment of quantum numbers to the R lines, from the relation $K_{head} = B'/(B'-B'')$, to the nearest whole number. The method of working with mean values of the natural doublets recommends itself for such preliminary work, since these follow very nearly the simple relations in a band with singlet R, Q and P branches.

[13] K is used here for the resultant of Λ and N, where Λ measures the effective component of the resultant orbital angular momentum along the nuclear axis, and N the angular momentum of the nuclei (K formerly j_k, Λ formerly σ_k, N formerly m). Also J will here replace the former j (quantum number of the total angular momentum).

To be certain of the true K assignment, recourse must be had to the combination principle. To this end, the above process was repeated for the (1,0) band, and the R and Q series identified, with their approximate numbering. By suitably shifting the relative numbering in these series, both in the (0, 0) and (1, 0) bands, two sets of $R-Q$ differences were found which agreed throughout the observed range. These represent the combination differences $R_m(K)-Q_m(K+1) \cong \Delta_1 F''(K)$, of the final state $v''=0$. In a $^2\Sigma$ state, one has[14]

$$\Delta_1 F''(K) = 2B''(K+1) + 4D''(K+1)^3 + \cdots, \qquad (1)$$

where D can be approximated by the theoretical relations given on p. 327. Correcting for the cubic term, which is small, there results a series of quantities practically linear in K, which may be used to determine the final true assignment of K values. In agreement with the theoretical requirement for an odd molecule, the K values appeared definitely to be whole numbers. These $R-Q$ combination agreements obtained between the (0, 0) and (1, 0) bands were afterwards proved to be unique by the method of Pomeroy.[15] This is a systematic procedure for trying all possible relative numberings for the four branches,[16] which eliminates the possibility of a fortuitous agreement yielding false combination differences. Three other possible assignments were indeed found, with the short range of lines then available, but all of these gave a relative numbering far outside the range of possible error in the preliminary assignment reached by the method first described. Considering finally the (0, 1) band, it was found that with but a slight shift in the preliminary numbering, satisfactory equality could be obtained with the differences $R_m(K)-Q_m(K) = \Delta_1 F'_m(K)$ from the (0, 0) band.

In identifying the remaining lines of the bands, a convenient procedure described by Loomis and Wood[17] was followed. Having the lines of a portion of a given branch, one derives an empirical formula in K to fit the wave-numbers of these members, using again the mean value of each doublet. The deviations of all observed lines from this equation are then plotted; at least of all which lie within a few cm^{-1} on either side of each calculated value. Such a diagram is shown in Fig. 2 for the Q lines of the (0, 0) band. The series stand out clearly among the extraneous lines, and the proper line to choose in each case is apparent. The method has the added advantage that any other series with approximately the same spacing as those used, such as the so-called "satellite" series, will reveal their presence. By this means, the Q branches were extended to small values of K, the low-frequency components converging in the third head, and the high-frequency components extending into the comparatively simple portion beyond this head. The low K lines of the R branches could then be found by adding the appropriate combination

[14] This expression for $\Delta_1 F''$, the difference between adjacent rotational terms of the lower state, is derived directly from the term formula, Eq. (3) below.

[15] W. C. Pomeroy, Phys. Rev. **29**, 59 (1927).

[16] I am indebted to Mr. S. W. Nile, New York University, for performing this lengthy calculation.

[17] F. W. Loomis and R. W. Wood, Phys, Rev. **32**, 223 (1928).

differences $\Delta_1 F''(K)$, computed from Eq. (1), to the mean values $Q_m(K+1)$. Adding and subtracting half the doublet separation for $Q(K+1)$, the R lines going up to the head were identified as a series of weak lines not previously assigned. The location of this series was clearly not that to be expected if the doubling of $R(K)$ was assumed to be the same as that of $Q(K)$. This is a proof that the large doubling is in the initial state, and that the transition is $^2\Pi \rightarrow {}^2\Sigma$, and not $^2\Sigma \rightarrow {}^2\Pi$. This statement will be evident if one refers to the energy level diagram of Fig. 3.

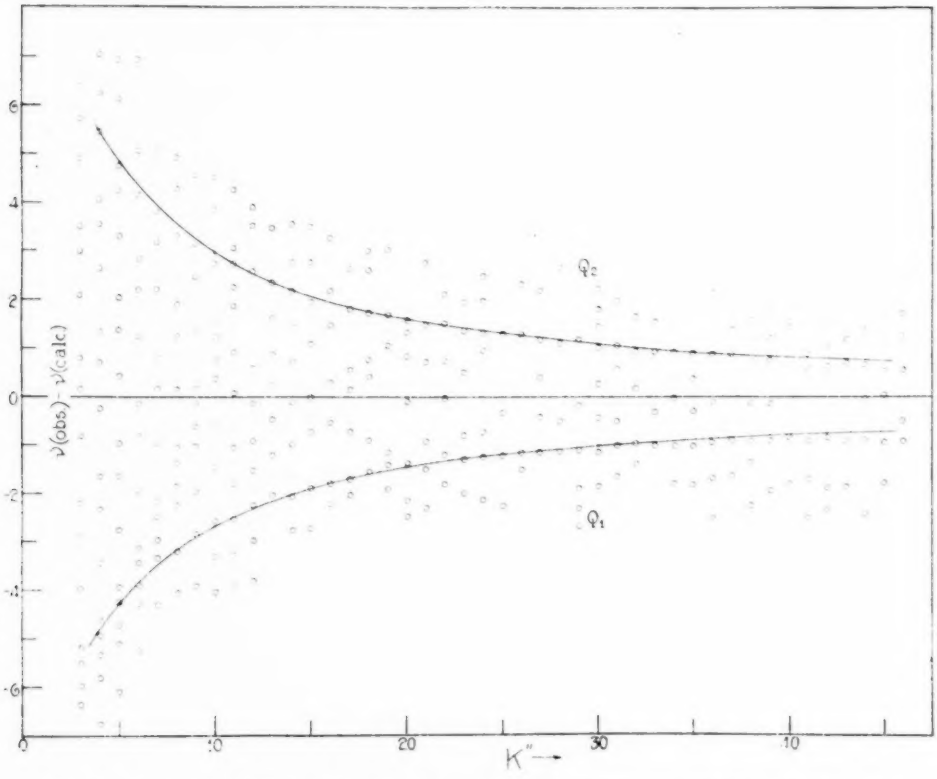

Fig. 2. Deviations of lines in the (0, 0) band from the approximate formula for the mean wave-numbers of the Q doublets: $Q_m(K) = \nu_0 - B' + (B' - B'')\ (K+\frac{1}{2})^2 + (D' - D'')\ (K+\frac{1}{2})^4 = 33{,}185.80 - 0.0685(K+\frac{1}{2})^2 - 0.0920 \times 10^{-6}\ (K+\frac{1}{2})^4$. The curves give the deviations of the theoretical values of $Q(K)$, calculated by Eq. (11).

The R branches are comparatively free from overlapping by extraneous lines, but their extension to values of K lower than that of the head could not be satisfactorily done in the weaker bands (0, 1) and (1, 0), especially the latter, where the value of K_{head} is smallest. Graphs of the type shown in Fig. 2 were used to identify the Q and P branches in all three bands. The preliminary equation for finding the P branches was based on the aproximate relation

$$P_m(K) = Q_m(K-1) - [R_m(K-1) - Q_m(K)]. \qquad (2)$$

This is strictly true only in the absence of the well-known Λ-type doubling associated with $^2\Pi$ states. A systematic deviation from the predicted positions of the P lines was in fact found, of nearly the same magnitude for the components P_2 and P_1. The observed lines were slightly displaced toward lower frequencies from the values calculated by Eq. (2).

Analysis of rotational terms. The lines given in Table I comprise six branches for each band, three of which, R_1, Q_1 and P_1, are to be correlated with terms of the initial and final states in which the spin vector, $S=1/2$, when completely uncoupled from the nuclear axis, stands parallel to the resultant vector K of the orbital and nuclear angular momenta. Similarly, for R_2, Q_2 and P_2, S is anti-parallel to K in both states. In the lower state, $^2\Sigma$, there is no component, Λ, of the orbital angular momentum along the molecular axis, and hence no interaction of the spin with this axis, even at very low values of K. The rotational terms may then be represented by

$$F_i(J)=BK(K+1)+D[K(K+1)]^2+\cdots. \tag{3}$$

In this case each level is a degenerate pair, $F_2(K-1/2)$ coinciding with $F_1(K+1/2)$, where F_1 and F_2 designate terms having S parallel and antiparallel to K, respectively. If this degeneracy is removed by the rotation, we have ρ-type doubling, but in the present case no evidence for this doubling was found, as explained below, under *Intensities*.

In the initial state, $^2\Pi$, the situation is more complicated. At high speeds of rotation, the condition is almost the same as in the $^2\Sigma$ case, levels of the same K coming close together. In Fig. 3, the tendency of these levels to approach each other is evident, even when K is relatively small. With decreasing K, the corresponding levels diverge more and more, as the interaction of the spin with the molecular axis beomes stronger. In the limit of no rotation if the doublet is normal, S is anti-parallel to Λ for F_1 terms ($^2\Pi_{1/2}$), and parallel for $F_2(^2\Pi_{3/2})$. If it is inverted, S is parallel to Λ for F_1 terms ($^2\Pi_{3/2}$) and antiparallel for $F_2(^2\Pi_{1/2})$. In either case the set of lower energy is designated F_1. Two methods are available for distinguishing a normal from an inverted doublet. There should be more missing lines in the $^2\Pi_{3/2}$ than in the $^2\Pi_{1/2}$ sub-band. In the present case these could not be determined, due partly to the numerous cases of superposition, and partly to the faintness of the first few lines in a branch. An alternative criterion is available in the magnitude of the Λ-type doubling. In case a, this is always much larger for $^2\Pi_{1/2}$ than for $^2\Pi_{3/2}$.[18] It was impossible in our case to detect this doubling for low values of K, and at larger values the type of coupling approaches case b rapidly. Van Vleck has shown[18] that in the strict case b the Λ-type doubling should be equal for $^2\Pi_{1/2}$ and $^2\Pi_{3/2}$. That this is not exactly true in the BeF bands, even for very large K, can be most directly shown by comparing the natural doublet separation for $Q(K)$ with that for $R(K-1)$and $P(K+1)$. The Q branch separations are noticeably smaller, which shows that the Λ-type doubling is greater in the F_1' states (see Fig. 3). The difference is not great, however, and is only

[18] J. H. Van Vleck, Phys. Rev. **33**, 467 (1929). R. S. Mulliken, Phys. Rev. **33**, 507 (1929).

considerable for high K values, as will be seen in Fig. 4, which represents graphically the course of these natural doublet separations. In the absence of confirmatory evidence from the missing lines, it seemed best to assume that the $^2\Pi$ state is normal.

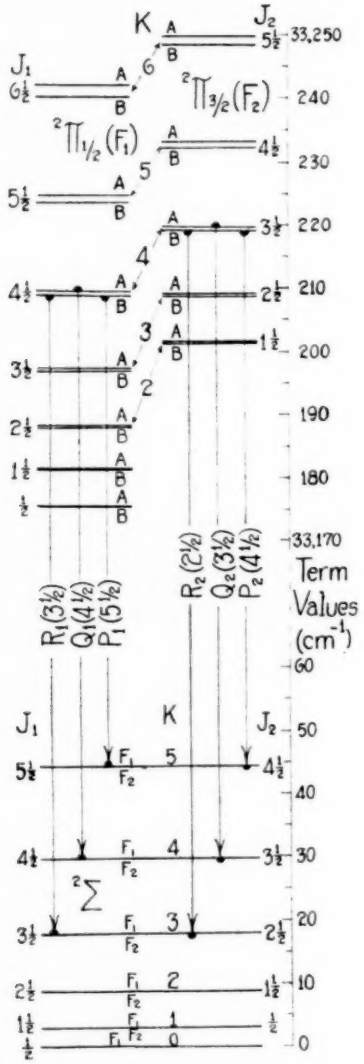

Fig. 3. First few rotational terms in the initial and final states $v=0$, drawn to scale according to Eqs. (3) and (4). The transitions shown by the vertical arrows give the natural doublets $R(K-1)$, $Q(K)$ and $P(K+1)$, (here $K=4$) which have the same doublet separation, except for slight differences in the Λ-type doubling for $F_1'(K)$ and $F_2'(K)$. The latter doubling, to be visible, is magnified 100-fold.

The effect of the transition from case a at low rotational speeds to case b at high speeds upon the energy formula for doublet states was first studied quantitatively by Kemble.[19] The resulting equations were tested with the OH

[19] E. C. Kemble, Phys. Rev. **30**, 387 (1927).

bands, and gave excellent agreement except at the lowest values of K. Slight discrepancies were to be expected, because the formulas were based on the old quantum theory. More recently, Hill and Van Vleck,[20] using the new mechanics, have obtained a convenient closed formula for the energy throughout the transition from case a to case b, applicable to both normal and inverted doublets. Aside from their statement that somewhat better agreement with experiment is obtained in the case of OH than found by Kemble, this formula appears not to have been applied in any specific case. It is therefore desirable to see how well it is capable of giving the observed rotational terms in Be F. Denoting by λ the ratio $\Delta E/B\Lambda$, and introducing the term in $D[K(K+1)]^2$ appropriate to case b (since this is appreciable only at higher values of K) the equations of Hill and Van Vleck may be written

$$\begin{aligned} F_2(J) &= B(K^2-\Lambda^2)+\frac{B}{2}\left[4K^2+\lambda(\lambda-4)\Lambda^2\right]^{1/2}+D\left[K(K+1)\right]^2+\cdots \\ F_1(J-1) &= B(K^2-\Lambda^2)-\frac{B}{2}\left[4K^2+\lambda(\lambda-4)\Lambda^2\right]^{1/2}+D\left[K(K-1)\right]^2+\cdots . \end{aligned} \tag{4}$$

The J in each case is that appropriate to the value of K in the same equation, that is, $J_2=K-1/2$, $J_1=K+1/2$. For a $^2\Pi$ state, $\Lambda=1$ always. The constant $B=h/8\pi^2Ic$ is best determined from the initial state combination differences at relatively high K, where case b is approximated. Thus, one has

$$\Delta_1F_m'(K)=2B'(K+1)+4D'(K+1)^3+\cdots . \tag{5}$$

Taking $\Delta_1F'_m(K)$ as the mean of the combination differences $R_m(K)-Q_m(K)$ and $Q_m(K+1)-P_m(K+1)$, to eliminate the effect of Λ-type doubling, the constants[21] $B^{(0)\prime}$ and $B^{(1)\prime}$, were evaluated by least squares from the ΔF's between $K=20$ and 30. For this purpose, the effect of the term in $(K+1)^3$ was first allowed for by using the accurate values of $D^{(0)\prime}$ and $D^{(1)\prime}$ obtained from the theoretical relations[22]

$$\begin{aligned} D^{(v)} &= D_e+\beta(v+\tfrac{1}{2}) \\ D_e &= -4B_e^3/\omega_e^2 \\ \beta &= \frac{\alpha^2}{6\omega_e}+\frac{20\alpha B_e^2-32x_eB_e^3}{\omega_e^2} . \end{aligned} \tag{6}$$

The equation for β is taken from Kemble's work,[23] and is in a more convenient form than that given by Pomeroy.[15] The ω_e and x_e were taken from Jevons' work,[5] and α was approximated from preliminary results. An analogous com-

[20] E. L. Hill and J. H. Van Vleck, Phys. Rev. **32**, 250 (1928).

[21] The vibrational quantum number v to which a constant refers will be indicated as a superscript, in parentheses.

[22] The subscript e indicates that the constant refers to the *equilibrium* position of the nuclei ($v=-\frac{1}{2}$).

[23] E. C. Kemble, Jour. Opt. Soc. Am. **12**, 1 (1926). The possibility of getting this convenient expression for β was kindly called to my attention by Prof. R. T. Birge.

putation with $\Delta_1 F''$, using Eq. (1), gave the constants $B^{(0)''}$ and $B^{(1)''}$ of the final state.

Since it was impossible to obtain observed values of the separations of the lowest levels, it was necessary to choose a value for λ such that Eqs. (4) fit the

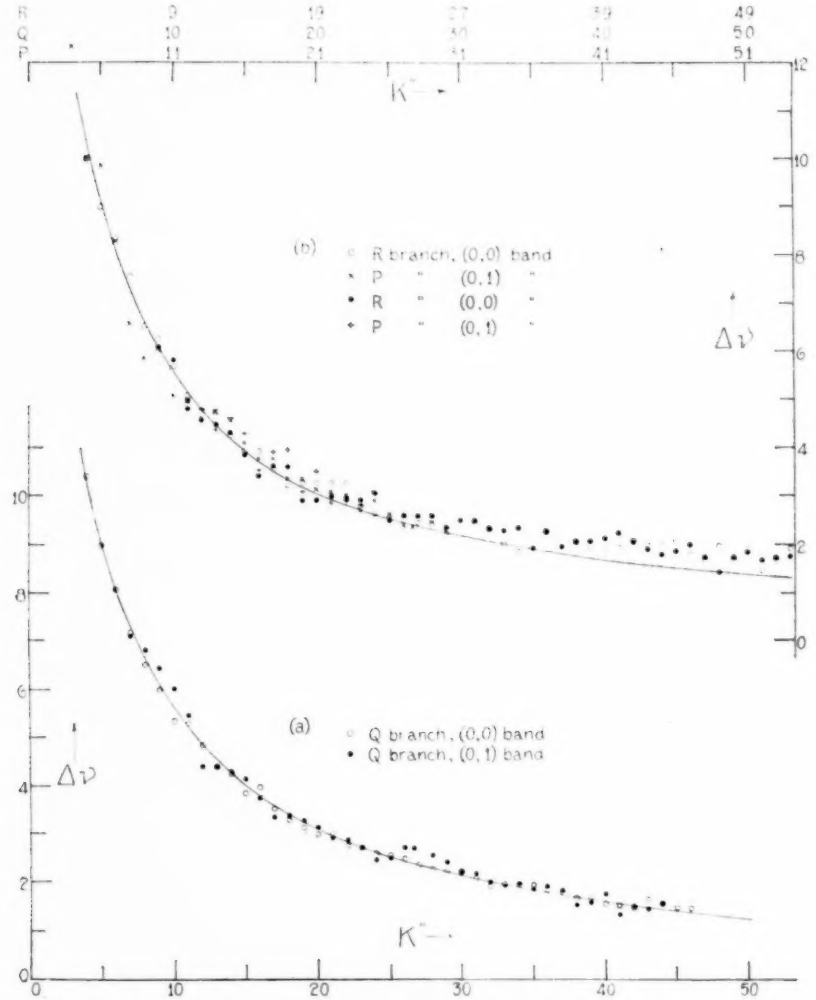

Fig. 4. Separation of the natural doublets as a function of rotational quantum number. In (a) the curve gives the theoretical separations from Eq. (7). The curve in (b) gives the best representation of the empirical separations in the Q branches, to show their divergence from those in the R and P branches at high values of K.

data for higher K most exactly. If this can be done, we have the electronic difference in the upper state for zero rotation, ΔE, since by definition $\lambda = \Delta E/B$. Instead of calculating the actual $F(J)$ values, it is more convenient to use the expression derived from Eqs. (4) for the natural doublet separation:[21]

[21] The equation for Δ given by Hill and Van Vleck applies not to the actual doublets, but to a mean value of the separation for two adjacent ones.

$$\Delta = F_1'(K) - F_2'(K) = B'\left[\tfrac{1}{2}\left\{4K^2+\lambda(\lambda-4)\right\}^{1/2}+\tfrac{1}{2}\left\{4(K+1)^2+\lambda(\lambda-4)\right\}^{1/2} - 2(K+\tfrac{1}{2})\right] \cong B'\left[\left\{4(K+\tfrac{1}{2})^2+\lambda(\lambda-4)\right\}^{1/2}-2(K+\tfrac{1}{2})\right]. \quad (7)$$

The best representation of Δ from the Q branches, shown graphically in Fig. 4(a) is obtained with $\lambda = +15.667$, assuming a normal doublet. If the doublet is taken as inverted, an equally good fit is obtained with $\lambda = -11.667$. With $B' = 1.4108$ (see p. —), this gives for the electronic separation in the $^2\Pi$ state $\Delta E = +22.10$ cm^{-1} if it is normal, -16.46 if inverted. A change of ± 0.1 cm^{-1} in these quantities makes the agreement with the observed Δ curves definitely less exact.

The rotational terms, $F(J)$ are not found directly from the spectrum, but only their differences, ΔF. Table II contains these quantities for all cases in which agreements between different sets are to be expected. Strict equality should only be found for corresponding differences in two bands with a common vibrational state, for example $R_2(K) - Q_2(K)$ in the (0, 0) and (0, 1) bands. The agreement of the differences $R - Q$ with $Q - P$ is only approximate, due to the Λ-type doubling in the initial state. It seemed best, for purposes of comparison with the theory, to eliminate the effect of this

TABLE II. *Agreements in the combination differences.*

K	$R_2(K)-Q_2(K)$ $=\Delta_1F_2'-\delta F_2(K+\frac{1}{2})$		$R_1(K)-Q_1(K)$ $=\Delta_1F_1'-\delta F_1(K+\frac{1}{2})$		$R_2(K)-Q_2(K+1)$ $=\Delta_1F_2''-\delta F_2(K+1)$		$R_1(K)-Q_1(K+1)$ $=\Delta_1F_1''-\delta F_1(K+1)$	
	(0,0)	(0,1)	(0,0)	(0,1)	(0,0)	(1,0)	(0,0)	(1,0)
17	50.4	50.5	50.7	50.3	52.9	53.3	53.0	53.0
18	53.4	53.0	53.4	53.4	56.0	56.0	55.9	56.0
19	56.0	56.0	55.9	56.3	58.9	58.9	58.6	58.9
20	58.8	58.6	58.6	59.2	61.8	61.8	61.6	61.6
21	61.8	61.6	61.6	61.5	64.8	64.8	64.3	64.4
22	64.4	64.5	64.3	64.4	67.7	67.4	67.6	67.5
23	67.1	67.3	67.1	67.0	70.4	70.4	70.4	70.3
24	69.8	70.0	69.8	70.0	73.2	73.5	73.2	73.1
25	72.5	72.7	72.5	72.6	76.0	76.3	76.0	76.1
26	75.2	75.2	75.3	75.3	79.1	79.1	79.0	78.9
27	78.0	77.9	77.9	78.0	81.9	82.0	81.8	81.9
28	80.6	80.7	80.5	80.8	84.6	84.8	84.5	84.7
29	83.5	83.7	83.4	83.6	87.7	87.8	87.6	87.6
30	86.5	86.4	86.2	86.1	90.7	90.9	90.3	90.5
31	89.1	89.0	88.7	88.9	93.6	93.8	93.1	93.4
32	91.7	91.7	91.6	91.4	96.2	96.3	96.2	96.2
33	94.2	94.4	94.3	94.0	98.9	99.2	99.0	98.7
34	97.1	97.0	96.9	97.0	101.9	101.9	101.7	101.8
35	99.8	100.0	99.5	99.6	104.8	104.7	104.3	104.3
36	102.5	102.4	102.2	102.3	107.6	107.3	107.2	107.1
37	105.1	105.1	104.8	104.9	110.5	110.8	110.1	110.2
38	107.8	107.7	107.5	107.2	113.1	113.2	112.8	112.4
39	110.4	110.4	110.1	109.8	115.9	116.1	115.6	115.7
40	113.1	113.0	112.7	112.6	118.8	118.7	118.4	118.4
41	115.9	115.7	115.4	115.0	121.7	121.7	121.1	121.4
42	118.5	118.3	118.0	117.9	124.3	124.3	124.0	123.9
43	121.0	120.9	120.7	120.6	127.1	127.4	126.7	126.9
44	123.6	123.6	123.1	123.3	130.0	129.9	129.4	129.1

TABLE II. (Continued)

K	$Q_2(K+1)-P_2(K+1)$ $=\Delta_1F_2'+\delta F_2(K+\frac{1}{2})$		$Q_1(K+1)-P_1(K+1)$ $=\Delta_1F_1'+\delta F_1(K+\frac{1}{2})$		$Q_2(K)-P_2(K+1)$ $=\Delta_1F_2''+\delta F_2(K+1)$		$Q_1(K)-P_1(K+1)$ $=\Delta_1F_2''+\delta F_1(K+1)$	
	(0,0)	(0,1)	(0,0)	(0,1)	(0,0)	(1,0)	(0,0)	(1,0)
9	27.8	....	28.5	....	29.6	29.7	29.6	29.7
10	31.0	....	30.8	....	32.5	32.7	32.3	32.7
11	33.8	33.8	33.9	34.4	35.6	35.3	35.2	35.4
12	36.7	36.7	36.9	37.1	38.7	38.5	38.5	38.3
13	39.2	39.3	39.7	39.4	41.3	41.4	41.7	41.3
14	41.7	42.4	42.4	42.8	44.0	43.6	44.3	43.7
15	45.1	44.8	45.2	45.4	47.0	47.2	47.3	47.4
16	47.8	47.7	48.1	47.9	50.5	50.1	50.3	50.0
17	50.5	50.3	51.0	50.8	53.1	53.3	53.3	53.2
18	53.6	53.1	53.8	53.7	56.2	56.1	56.3	56.1
19	56.2	56.5	56.5	56.4	59.0	59.0	59.3	59.1
20	59.0	59.1	59.2	59.7	62.0	61.6	62.1	62.1
21	61.9	62.1	62.2	62.1	64.9	64.8	64.9	65.4
22	64.5	64.8	64.8	65.0	67.8	67.7	68.0	68.1
23	67.4	67.2	67.5	67.6	70.7	70.8	70.8	70.8
24	70.1	70.1	70.5	70.7	73.6	73.6	73.9	73.8
25	73.0	73.1	73.2	....	76.6	76.1	76.7	76.3
26	75.6	....	75.7	....	79.5	78.7	79.4	79.4
27	78.3	....	78.4	....	82.5	82.2	82.2	82.2
28	81.1	....	81.3	....	85.1	85.4	85.2	85.2
29	83.9	....	84.0	....	88.1	88.2	88.2	88.1

TABLE II. (Continued)

K	$R_2(K)-P_2(K)$ $=\Delta_2F'_{2B}$		$R_1(K)-P_1(K)$ $=\Delta_2F'_{1B}$		$R_2(K-1)-P_2(K+1)$ $=\Delta_2F_2''$		$R_1(K-1)-P_1(K+1)$ $=\Delta_2F_1''$	
	(0,0)	(0,1)	(0,0)	(0,1)	(0,0)	(1,0)	(0,0)	(1,0)
12	70.3	70.2	70.5	70.7	74.2	....	74.1	....
13	76.0	76.0	76.4	76.5	79.9	....	79.9	....
14	81.4	81.2	82.2	81.7	85.4	....	85.7	....
15	86.8	86.5	87.4	87.7	91.5	....	91.6	....
16	92.4	92.7	93.0	93.3	97.6	97.3	97.4	....
17	98.2	98.3	98.7	98.2	103.1	103.3	103.4	102.9
18	103.9	103.2	104.4	104.3	109.1	109.4	109.3	109.1
19	109.6	109.0	109.7	110.0	115.0	114.9	115.1	115.1
20	115.1	115.1	115.1	115.6	120.9	120.6	120.7	121.0
21	120.9	120.6	120.7	121.2	126.7	126.6	126.5	127.0
22	126.2	126.6	126.5	126.5	132.6	132.5	132.4	132.4
23	131.5	132.1	131.9	132.0	138.4	138.2	138.3	138.3
24	137.1	137.2	137.2	137.6	144.0	144.0	144.3	144.1
25	142.6	142.8	143.0	143.3	149.8	149.6	149.8	149.4
26	148.3	148.3	148.5	....	155.5	154.9	155.4	155.5
27	153.6	....	153.6	....	161.3	161.3	161.2	161.2
28	158.9	....	158.9	....	167.0	167.4	167.0	167.1
29	164.6	....	164.7	....	172.7	173.0	172.6	172.8

doubling by defining the ΔF's in terms of the centers of the doublet levels. Reference to Fig. 3 will show that to obtain these ΔF's, the differences between actual lines must be corrected by an amount proportional to the

combination defect $[R(K)-Q(K+1)]-[Q(K)-P(K+1)]$, which we will call $2\delta F$. According to the theory,[18] the Λ-type doubling, and hence the combination defect, should be proportional to $(J+\frac{1}{2})^2$. Graphs of $2\delta F$ against J for F_1' and F_2' states gave curves similar to that obtained by Loomis and Wood[17] for the Na_2 bands, in which the defect could be satisfactorily represented as proportional to $(J+\frac{1}{2})^2$. Hence a simple method of taking the Λ-type doubling into account in the energy formulas is to give slightly different values of B to the F_A and F_B levels. Their difference can be found from the combination defect by the relation[17]

$$2\delta F=[F_A'(J+1)-F_B'(J+1)]+[F_A'(J)-F_B'(J)]$$
$$\cong 2[F_A'(J+\tfrac{1}{2})-F_B'(J+\tfrac{1}{2})]=2(B_A'-B_B')(J+\tfrac{1}{2})^2. \tag{8}$$

The values of $B_A'-B_B'$ obtained in this way were, for F_1' states, $+0.00046$, and for F_2', $+0.00028$. The corrections, δF_1 and δF_2, to be applied to the

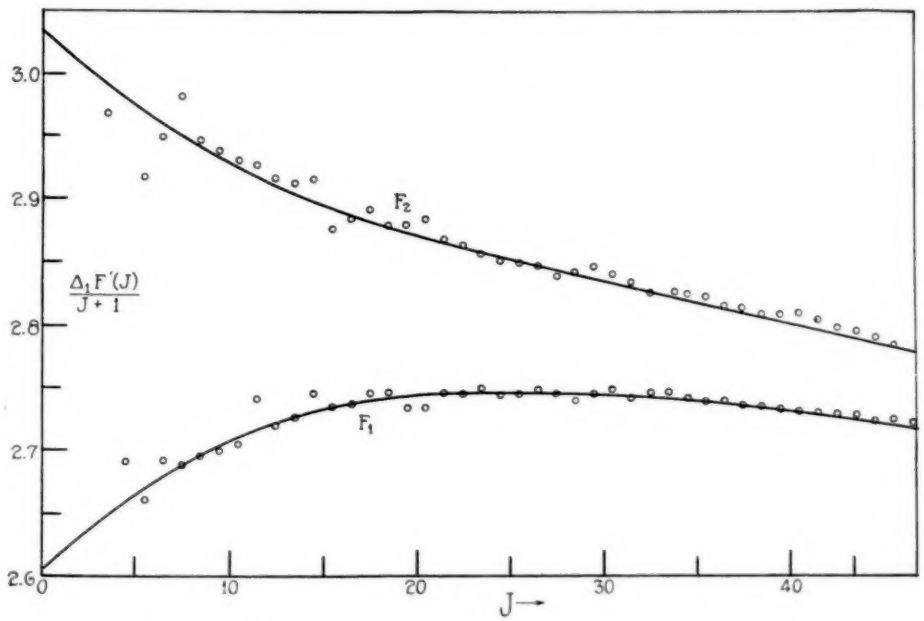

Fig. 5. Comparison of $\Delta_1F'(J)/(J+1)$ with the theoretical curves (Eq. (10)). Data from the (0, 0) band.

combination differences to obtain the quantities Δ_1F' are indicated above each column in Table II.

The formula for Δ_1F' may be found from Eqs. (4) as follows:

$$\frac{dF_i(J)}{dJ}=\Delta_1F_i(J-\tfrac{1}{2})=2B'(J+\tfrac{1}{2})\left[1\pm(4(J+\tfrac{1}{2})^2+\lambda(\lambda-4))^{-1/2}\right]$$
$$+4D'(J+\tfrac{1}{2}\pm\tfrac{1}{2})^3+\cdots. \tag{9}$$

The upper sign applies to F_2 and the lower to F_1. This formula was tested in several cases, and agreed with the observed ΔF's within a few hundredths cm^{-1}. For a graphical comparison of the theory with the empirical results, it is more convenient to divide the ΔF's throughout by $(J+\frac{1}{2})$. Thus, to a close approximation

$$[\Delta_1 F_i'(J-\tfrac{1}{2})]/(J+\tfrac{1}{2}) = 2B'\left[1 \pm \left\{4(J+\tfrac{1}{2})^2+\lambda(\lambda-4)\right\}^{-1/2}\right]+4D'(J+\tfrac{1}{2}\pm\tfrac{1}{2})^2. \quad (10)$$

In Fig. 5 are plotted the observed quantities $\Delta F/(J+1)$ against J, and the curve represents the theoretical values from Eq. (10). Although systematic discrepancies are evident, especially at high J, it is probable that these could be somewhat reduced by slight adjustments of the constants. This was not attempted, but it is clear that the theory accounts remarkably well for the rather complicated variation of the ΔF's. Not only do the two sets draw together in the proper way, but they show the expected downward trend at large J values due to the term in D'.

The term-formulas (4) are surprisingly simple, considering the complexity of the uncoupling phenomenon involved. They permit the representation of all the lines of a complex band of this kind by comparatively compact and convenient formulas. Taking Eqs. (3) for the terms of the lower state, and Eqs. (4) for those of the upper, and forming the appropriate differences for the several branches, one obtains expressions of the form:

$$\nu = a+bK+c/2\left[4K^2+\lambda(\lambda-4)\right]^{1/2}+dK^2+eK^3+fK^4. \quad (11)$$

TABLE III. *Values of coefficients for each branch.*

Lines	a	b	c	d	e	f
$R_2(K-1)$	ν_0-B_{2B}'	B''	B_{2B}'	$B_{2B}'-B''$	$2(D'+D'')$	$D'-D''$
$R_1(K-2)$	$\nu_0-B_{1B}'-2B''$	$3B''$	$-B_{1B}'$	$B_{1B}'-B''$	$-2(D'-3D'')$	$D'-D''$
$Q_2(K)$	ν_0-B_{2A}'	$-B''$	B_{2A}'	$B_{2A}'-B''$	0	$D'-D''$
$Q_1(K-1)$	ν_0-B_{1A}'	B''	$-B_{1A}'$	$B_{1A}'-B''$	0	$D'-D''$
$P_2(K+1)$	$\nu_0-B_{2B}'-2B''$	$-3B''$	B_{2B}'	$B_{2B}'-B''$	$2(D'-3D'')$	$D'-D''$
$P_1(K)$	ν_0-B_{1B}'	$-B''$	$-B_{1B}'$	$B_{1B}'-B''$	$-2(D'+D'')$	$D'-D''$

The coefficients to be used for each branch are given in Table III. The origin, ν_{00} of the (0, 0) band was found by applying these equations to several lines of each branch, the average of a number of consistent values being 33,187.21 cm^{-1}. Eq. (11), taken in connection with our final values of the constants, listed below, represents all the lines of the (0, 0) band quite accurately, the largest consistent deviation being about 0.2 cm^{-1}. Errors of this size would not be noticeable in a diagram on the scale of that in Fig. 1. Small systematic trends are apparent, however, when the lines are represented graphically by the method illustrated in Fig. 2. Nevertheless, the formulas reproduce the observed lines to the same order of accuracy as do the more familiar ones applicable to bands of simpler structure.

The molecular constants resulting from the present study of the band structure are given in Table IV. All are expressed in cm^{-1} units.

TABLE IV. *Molecular constants.*

Initial state, $^2\Pi$ (normal)	Final state, $^2\Sigma$
$\Delta E = 22.10$	
$B_{1A}^{(0)} = 1.41083$	
$B_{1B}^{(0)} = 1.41037$	$B^{(0)} = 1.47928$
$B_{2A}^{(0)} = 1.41074$	
$B_{2B}^{(0)} = 1.41046$	
$\alpha = B^{(0)} - B^{(1)} = 0.01610$	0.01685
$D^{(0)} = -8.301 \times 10^{-6}$	-8.209×10^{-6}
$\beta = D^{(1)} - D^{(0)} = 1.060 \times 10^{-8}$	2.903×10^{-8}

Defining B_e as the value of $h/8\pi^2 I_e c$ for the non-vibrating molecule, we have $B^{(v)} = B_e - \alpha(v+\frac{1}{2})$, whence $B_e = B^{(0)} + \alpha/2 = 1.48770$ in the lower state. Using the relation $I_e = 27.66/B_e$ given by Birge,[25] the equilibrium value of the moment of inertia in the less excited state becomes $(18.59 \pm 0.03)\ 10^{-40}$ g cm^2, and the corresponding internuclear distance 1.357A. In the more excited state, these quantities are, respectively, $(19.50 \pm 0.03)\ 10^{-40}$ g cm^2 and 1.390A.

Intensities. The intensity in each branch rises to a maximum at about $K = 20$, and then falls off slowly in the usual way. On our plates, the first few lines were too faint to be observed. The two components of each natural doublet are, as far as can be judged, of equal intensity. Because of the great amount of overlapping in the P branches and the outer part of the Q branches it is difficult to compare the relative intensities of the various branches. By considering only the weaker lines in the regions where blends are frequent, an approximation can be made, however. The P branches have about the same intensity as the R—perhaps slightly less. The Q lines are much stronger, with about twice the intensity of the R lines of the same rotational quantum number.

Mulliken's scheme[6] for $^2\Pi \rightarrow {}^2\Sigma$ transitions predicts certain satellites of the strong branches, and two further branches, for which $\Delta K = \pm 2$. All of these should be relatively weak when $\Delta E/B$ is small. In the absence of ρ-type doubling in the final state, his satellites ${}^RQ_{21}$ and ${}^QP_{21}$ coincide with the strong branches R_2 and Q_2 respectively. Similarly, ${}^QR_{12}$ and ${}^PQ_{12}$ coincide with Q_1 and P_1. Our failure to observe these satellites is the most important evidence for the absence of appreciable ρ-type doubling in the $^2\Sigma$ state of BeF. Of Mulliken's double R- and double P-form branches, which may be called S_{21} and O_{12}, the former is definitely absent, and therefore almost certainly the latter as well. Our graphical investigations by the method of Fig. 2 show no evidence for the presence of the satellites Q_{2B2A} and Q_{1B1A}, which violate the selection principle for Λ-type doubling, but which are, however, found in the OH bands.

Vibrational structure. Jevons[5] has derived the following equations to represent the heads of some 45 bands of this system.

[25] R. T. Birge, Phys. Rev. Supplement **1**, 62 (1929).

R_2 *heads:* $\nu = 33{,}217.3 + 1153.3v' - 5.88v'^2 - 1247.1v'' + 11.21v''^2 - 4.92v'v''$
R_1 *heads:* $\nu = 33{,}214.3 + 1153.9v' - 5.67v'^2 - 1247.1v'' + 11.50v''^2 - 5.36v'v''$
Q_1 *heads:* $\nu = 33{,}179.9 + 1163.8v' - 8.78v'^2 - 1256.5v'' + 9.12v''^2$.

The coefficients in the third equation, except the constant term, apply equally well to the band origins, since the head of the Q_1 branch occurs at a very small value of K. Assuming that the vibrational constants are the same in $^2\Pi_{3/2}$ and $^2\Pi_{1/2}$, the variation with v of the distance from the Q_1 head to the origin is probably negligible. Inserting the constant, ν_{00}, evaluated above, the equation for origins becomes

$$\nu_0 = 33{,}187.21 + 1163.8v' - 8.78v'^2 - 1256.5v'' + 9.12v''^2 \qquad (12)$$

The vibration frequency for infinitesimal amplitudes is, accordingly, $\omega_e = \omega^{(0)} + x\omega^{(0)} = 1265.62$ in the final state, and 1172.58 in the initial state. The electronic frequency, ν_e of the system-origin is obtained as the constant term when Eq. (12) is transformed to express ν_0 as a function of $(v+\frac{1}{2})$. We find $\nu_e = 33{,}233.61$.

Morse[26] has recently found an empirical relation connecting the constants $\omega^{(0)}$ and $r^{(0)}$, which is useful as a check on the correctness of our analysis. According to this rule, $\omega^{(0)} r^{(0)} = 3000 \pm 120 \text{A}^3/\text{cm}$. In the present case the product is 3159 and 3176 in the upper and lower states, respectively. Another important rule, due to Birge[27] requires that $2xB^{(0)}/\alpha = 1.4 \pm 0.2$. From our constants, this ratio for BeF is 1.32 in the upper state, and 1.27 in the lower.

Conclusions

This is the first analysis of a band structure of the contracting doublet type in a spectrum other than that of a diatomic hydride. Due to the much closer spacing of the lines (the moment of inertia is 13 times that of OH), the actual resolving power available was not far above the mimimum required for an unambiguous proof of the structure by the application of the combination principle. In view of the various agreements with the theory, and especially of the graphical proofs of the reality of the different line series, it is thought that our results are justified in all their more essential respects. Several investigators[1,5] have drawn conclusions concerning the electronic states of other alkaline earth halides from a study of the positions and intensities of the heads in the numerous band systems of these molecules. As stated above, these systems appear to be beyond the reach of our present spectrographs, as far as the rotational structure is concerned. It should be emphasized that bands due to entirely different types of electronic transitions may show an almost identical gross structure. For example, the BeF bands described here show very nearly the same relative spacing and intensity of the three heads in each band as do the blue-green TiO bands recently analysed by Christy,[28] although the states involved are even of a different mul-

[26] P. M. Morse, Phys. Rev. **34,** 57 (1929).
[27] R. T. Birge, Phys. Rev. **31,** 919 (1927) (Abstract).
[28] A Christy, Phys. Rev. **33,** 701 (1929).

tiplicity; the transition is $^3\Pi \rightarrow {}^3\Pi$. Therefore, unless one brings every available type of evidence to bear, it seems that conclusions based on a study of the band heads alone must be regarded as highly speculative.

The $^2\Pi \rightarrow {}^2\Sigma$ system of BeF constitutes the entire known spectrum of this molecule. Although it has not as yet been obtained in absorption, it appears probable, from analogy with the iso-electronic molecule CN, that the $^2\Sigma$ state is the normal electronic configuration. The band systems in the visible region due to a number of other alkaline earth halides have been found in absorption.[29] Mulliken[30] has given a provisional assignment of quantum numbers to the individual electrons in BeF as follows: in the $^2\Sigma$ state, $(2s\sigma)^2\,(3p\sigma)^2\,(2p\pi)^4\,(3s\sigma)$, and in the $^2\Pi_i$ state, $(2s\sigma)^2\,(3p\sigma)^2\,(2p\pi)^4\,(3p\pi)$. The assignment given for $^2\Sigma$ is identical with that for the $^2\Sigma$ state (normal state) of BO, CN and CO^+. For the $^2\Pi$ state, however, the arrangement differs from that proposed for the inverted $^2\Pi$ states of BO, etc., which are designated $(2s\sigma)^2\,(3p\sigma)^2\,(2p\pi)^3\,(3s\sigma)^2$, $^2\Pi$. This difference in interpretation is based on the fact that ΔE in the $^2\Pi$ state is much smaller for BeF than for the others ($\Delta E = 126,\ 56,\ 126$). No contradiction to Mulliken's conclusions is therefore contained in our assumption of a normal $^2\Pi$ state, with $\Delta E = 22.10$.

In conclusion, it is a pleasure to acknowledge several valuable suggestions in connection with this work from Professors R. T. Birge and R. S. Mulliken, as well as assistance in the measurements and computations from Mr. S. W. Nile and Professor F. W. Doermann.

[29] J. M. Walters and S. Barratt, Proc. Roy. Soc. **118A,** 120 (1928)
[30] R. S. Mulliken, Phys. Rev. **32,** 286 (1928).

RELATIVITY AND AETHER DRIFT[1]

By W. F. G. Swann
Bartol Research Foundation of the Franklin Institute

(Received January 10, 1930)

Abstract

While aether drift experiments originally suggested the line of thought which led to the formulation of the restricted theory of relativity, it would seem that the fundamental significance of that theory does not depend primarily upon these experiments. The most logical origin of the transformation of the restricted theory is to be found as a special case of the general theory, and the purpose of the present paper is to show how, with this in view, the fundamental working content of the restricted theory, the invariance of laws under the Lorentzian transformation, is something which has no fundamental relation to the question of whether the aether drift experiments do or do not give a positive result.

THE general belief thirty years ago that the Michelson-Morley-Miller experiment gave a "null" result lead to a formulation of the restricted theory of relativity in a form in which the actual space and time measures of observers in two relatively moving systems S and S' were considered, and in which postulates were stated and a law of transformation from one set of measures to the other was derived such as to insure that both observers would measure the same velocity c in all directions for the velocity of light. The transformations are the well-known transformations first derived by Larmor and Lorentz in electromagnetic theory, and are of the form

$$x'=\beta(x-vt)\ ;\ y'=y\ ;\ z'=z\ ;\ t'=\beta\left(t-\frac{v}{c^2}x\right) \tag{1}$$

where $$\beta=\left(1-\frac{v^2}{c^2}\right)^{-1/2}.$$

The desire to provide for the null effects in other experiments which had been attempted and which might yet be attempted to detect the earth's "absolute motion" lead to the further postulate that the same transformation of measures which served to conceal from the observers any difference as regards the propagation of light in their two systems would also serve to conceal from them any analogous difference as regards any other experiments which they might perform. The postulate was completely provided for by the more widely embracing postulate that the laws of nature[2] are invariant under the Lorentzian transformation (1), at least this is the case if the two sets of

[1] Presented at the Chicago Meeting of the American Physical Society, November 30, 1929

[2] The more detailed significance of the content of this statement will be discussed in an article "Relativity and Electrodynamics" now in process of publication in the Physical Review Supplement.

coordinates specified in (1) correspond to the actual measures of observers in the two systems. There are, in fact, two aspects to the restricted theory of relativity as usually understood. The first, which we shall call (*A*), which takes (1) as relations between the actual measures of observers in the two systems, and the second which we shall call (*B*) which concerns itself with the form of physical laws as expressed in the first instance, at any rate, in *one* system of coordinates. In its general form, aspect *B* may be said to imply that "There exists a way of assigning numbers to identifiable points in space-time (there exists a set of coordinates) such that if the laws of nature are expressed in terms of them, they will be found to be invariant under the Lorentzian transformation (1); so that if there exists one set of coordinates in which the statement is true, there exists an infinity of all others, obtainable from the first by Lorentzian transformations, in which the statement is also true." But there will also be a multifold infinity of other sets of coordinates such that if the laws be expressed in terms of these, the statement will not be true.

The test of the forms of the physical laws is the problem of a single observer, who needs for his purpose no collaboration of an obliging assistant sailing through heaven with half the velocity of light. It must be maintained most emphatically that the aspect *B* involves no implication that the different systems obtainable from each other by Lorentzian transformation have anything to do with the actual measures of observers traveling with the corresponding velocity v in relation to the first named system. The quantity v is simply an arbitrary parameter in the equations of transformation, a parameter which does its duty by enabling the transformation to say something about the laws by itself disappearing from the transformed equations. There is no v in the original equations in x, y, z, t, and although v goes into the equations when they are expressed in terms of x', y', z', t', it mysteriously disappears when everything is boiled down. Even in the case of the electromagnetic equations, where, for example the density ρ in the old equations becomes replaced by $\beta\rho(1-u_x v/c^2)$, in the transformed equations, u_x being the x component velocity of the electricity in the undashed system, and where v consequently *appears* to take part in the final equations, it actually disappears owing to the fact that the quantity $\beta\rho(1-u_x v/c^2)$ turns out to be the quantity which, in the dashed system, plays the part of ρ' the electric density in that system.

Having found the forms of the laws in one system of coordinates, the question as to whether or not they are invariant under (1) is a matter to be tested with pen and paper, and not by experiment. *Experiment does play a part in the whole procedure, but its part is played in formulating the laws in one system of coordinates only.*

One immediately commences to wonder what elements are concerned in the question of whether or not *our* system of measures is such that the laws when expressed in terms of them may be expected to be invariant. In order to bring out the essentials of some of the elements here involved, let us consider what the situation would have been if laws had been of such

a type that they were invariant under the Lorentzian transformation when written down in terms of a system of coordinates x, y, z, t, obtainable from ours which we shall call x'', y'', z'', t'', by the transformation

$$x''=x-vt;\ y''=y;\ z''=z;\ t''=t \tag{2}$$

i.e., the transformation which a mid-Victorian physicist would have made to allow for what he believed to be a motion of his system of coordinates through space with velocity v. Then, of course, if the laws were written down in the same form but in the double dashed system, they would be wrong. However, if v were of the order of 18 miles per second, which is the sort of velocity we talk about when considering aether drift experiments, it would be necessary to measure to one part in 10^8, i.e., to an accuracy of v^2/c^2 in order to find the errors in the erroneous laws. Even in our doubled dashed system of coordinates we should consequently discover these laws, although we ought not to. This statement needs some amplification.

If the laws are true when written down in terms of x, y, z, t, i.e., in the system of coordinates which we shall call S, they will also be true when written down in the same form in x', y', z', t', (the system S') as given by (1), since they are supposed invariant under that transformation. Suppose now, we write them down in the same form, but in x'', y'', z'', t'', (the system S''). What will be the situation? If we neglect quantities of the order v^2/c^2, we may write

$$\left.\begin{aligned} &x''=x'\ ;\ y''=y'\ ;\ z''=z' \\ &t''=t=t'+\frac{v}{c^2}x=t'+\frac{v}{c^2}(x''+vt'') \\ \text{i.e.,}\quad &t''=t'+\frac{v}{c^2}x''=t'+\frac{v}{c^2}x' \end{aligned}\right\} \tag{3}$$

Now let there be any experiment which involves the measurement of the differences of the coordinates of two points (denoted by subscripts 1, and 2) which difference remains constant for all values of t' and so of t''. Such a measurement we shall call a measurement of type I. Then, it is obvious that, excluding the order v^2/c^2,

$$x_2''-x_1''=x'_2-x_1'\ ;\qquad y_2''-y_1''=y_2'-y_1'\ ;\qquad z_2''-z_1''=z_2'-z_1'.$$

Again, suppose that the experiment involves the measurement of the difference between two times at a fixed value of x', y', z', and hence at a fixed value of x'', y'', z''. We shall call this a measurement of type II. It is obvious that, in this case, to the order referred to

$$t_2''-t_1''=t_2'-t_1'.$$

Now practically all accurate experiments in the field in question involve measurements included in the above types. Thus, suppose for example, we should perform an experiment on the variation of e/m with velocity; and, to fix our ideas, suppose the measurements are made by the usual

magnetic deflection experiment, followed by a compensation of the magnetic deflection by an electrostatic deflection to determine the velocity ω of the electrons. We here use ω to denote the velocity of the electron as distinct from the very much smaller velocity v associated with the transformation. *It is to be distinctly understood that it is the same experiment which is being discussed in the two systems of measures S' and S''.* The magnetic deflection involves the measurements of lengths which are constant for all time during the experiment, and it also involves the measurement of a magnetic field. The lengths in question involve measurements of the type I, and consequently they are the same excluding the order v^2/c^2 whether they are measured in S' or S''. As regards the magnetic field, we may trace its measurement according to any consistent scheme, with the same ultimate conclusions. Suppose it is measured by the time of oscillation of a magnet whose moment is subsequently determined by allowing it to vibrate in the vicinity of another similar magnet. The experiment involving the measurement of the time of vibration is one in which two times are recorded at a fixed position, and so is a measurement of type II. The moment of inertia of the magnet involves its dimensions and density. The measurements of the dimensions are of type I. The measurement of density may be regarded as the comparison of the linear dimensions (measurement of type I) of a kilogram of the material, and of the standard kilogram, the equality of the two kilograms being tested by a dynamic method.[3] For example, it may be tested by annulment of velocity at impact after traveling with equal and opposite velocities. In this test the velocity as tested in S'' is related to that tested in S' by the relation

$$\frac{dx''}{dt''}=\left(\frac{dx'}{dt'}\right)\Big/1+\left(\frac{v}{c^2}\right)\left(\frac{dx'}{dt'}\right)$$

which is easily derivable from (3). In general dx'/dt' would be much less than v, so that $dx''/dt''=dx'/dt'$ except for quantities of an order less than v^2/c^2. A similar set of arguments applies to the determination of the moment of the magnet by measuring its time of vibration in the field of a similar magnet, and the net result of all these considerations is that the magnetic field as measured by use of the system of units S' will come out the same as that obtained by using the system S'', if we neglect v^2/c^2. A similar conclusion will readily be seen to follow for measurement of the electric field utilized in the determination of ω, the electronic velocity. Hence the net result of all of these considerations is that, exclusive of the order v^2/c^2, an observer using the system S' will measure values of e/m and of ω which are the same as those obtained by using the system S''.

It is quite true that the values of ω would be different to a higher order if they could be measured directly in S' and in S''. For if $x_2'-x_1'$ is the distance travelled by the electron in the time $t_2'-t_1'$ as measured in S', the velocity ω' as measured in that system is

[3] The simple and actually used method of comparison of masses by comparison of weight involves logical complications which would require too much space to unravel here

$$\omega' = \frac{x_2' - x_1'}{t_2' - t_1'}$$

while in S'', it is

$$\omega'' = \frac{x_2'' - x_1''}{t_2'' - t_1''} = \frac{x_2' - x_1'}{t_2' - t_1' + \frac{v}{c^2}(x_2' - x_1')}$$

$$= \frac{x_1' - x_1'}{(t_2' - t_1')\left(1 + \frac{v}{c^2}\omega'\right)}$$

i. e.,

$$\omega'' = \omega' \Big/ \left(1 + \frac{v\omega'}{c^2}\right)$$

which, since ω' may be comparable with c, results in ω'' differing from ω' by quantities of the order $\omega' v/c$. However, it is never in any such way as this that velocities are measured. Even in the measurement of a velocity such as that of light, which approaches most nearly the direct measurement of a velocity, the back and forth journeys of the light are both involved, so that terms involving v/c to the first order become eliminated.

If, in a manner analogous to that adopted above for the e/m experiment we may trace through the kind of experiments whose performance leads to the formulation of the electromagnetic equations, we shall find that if the electromagnetic equations are true when expressed in the measures of S', the *experiments used to test them* will give the same results in S'' as S' exclusive of the order v^2/c^2, so that the observer in S'' will discover the equations, although, strictly speaking he ought not to. We must again emphasize that in the above it is the *same* experiments which are supposed discussed in the of S' and S'' units.

It is perhaps worth while pointing out that the electromagnetic equations, when written down in the same form in S′ and S'' are not equivalent in all respects up to but excluding v^2/c^2. Thus if the set expressed in S'' be transformed to S' it will differ from the set originally written down in S' in that in certain places the magnetic fields will have added to them or subtracted from them terms of the order vE/c, and the electric fields will experience corresponding additions or subtractions of the order vH/c. Moreover, terms of the order $\omega' v/c^2$ will make their appearance, where ω' is the velocity of the electricity in S'. All that is maintained is that all experiments so far performed to detect quantities even of the order v/c are experiments falling under classes I and II. This may not seem obvious at first sight in all cases; but if the actual calculations associated with any test be carried completely through to the point where the comparison is between quantities actually measured, it will be found to be true. There are respects in which the electro-

magnetic equations when written down in S' and S'' would differ in their conclusions to the order v/c as regards *ideal* experiments. Thus the wave equation for E is contained in the equations, and in one dimension in free space it is

$$\frac{\partial^2 E'}{\partial t'^2} = c^2 \frac{\partial^2 E'}{\partial x'^2} \tag{4}$$

in S' while, in the same form in S'' it is of course

$$\frac{\partial^2 E''}{\partial t''^2} = c^2 \frac{\partial^2 E''}{\partial x''^2}$$

where E'' refers to the quantity which is defined in S'' in the same manner as E' is defined in S'.

This equation, on transformation to S' by (3) gives

$$\frac{\partial^2 E''}{\partial t'^2} = c^2 \left(\frac{\partial}{\partial x'} - \frac{v}{c^2} \frac{\partial}{\partial t'} \right)^2 E''$$

i.e.,

$$\left(1 - \frac{v^2}{c^2}\right) \frac{\partial^2 E''}{\partial t'^2} = c^2 \left(\frac{\partial^2 E''}{\partial x'^2} - \frac{2v}{c^2} \frac{\partial^2 E''}{\partial x' \partial t'} \right)$$

the general solution of which is

$$E'' = f_1(x' + c_1 t') + f_2(x' - c_2 t')$$

where, excluding terms of the order v^2/c^2

$$c_1 = c - v$$

$$c_2 = c + v$$

and f_1 and f_2 are arbitrary functions. The general solution of (4) is of course

$$E'' = f_1(x' + ct) + f_2(x - ct).$$

Thus, anyone who measured the velocity of a wave directly in the system S', by measuring the distance travelled by the wave front in one direction in a measured time, would obtain a result differing to the order v/c from that obtained if he had measured the velocity of the same wave in S''. As already remarked, however, it is not by such procedures that accurate experiments are made.

In view of the foregoing considerations it is not remarkable that we should be led to discover a great scheme of regularity like the electromagnetic scheme lying, as it were, within one part in 10^8 of what our measurements in S'' would predict if we made them with infinite accuracy. Having discovered the scheme of equations, the discovery of its invariance under the Lorentzian transformation is a matter for pen and paper rather than for experiment.

Now, of the two aspects A and B of the restricted theory of relativity it is B which contains the whole of the usefulness of the theory as a working tool. When we study new branches of physics we examine the laws we propose, to see whether they satisfy the mathematical criterion of invariance.[4] The test, as has been stated, is one of pen and paper, and has no relation whatever to the question of what would happen to measuring apparatus if a velocity were imparted to it.

An example of a class of problem in which, at first sight, we appear to utilize the correspondence between the actual measures and the corresponding Lorentzian system of coordinates, is afforded by the problem leading to the deduction of the Fresnel coefficient on the basis of the theory of relativity. The argument normally proceeds by our taking our stand in imagination in a system of axes moving with the medium. In this system we write for the propagation of a wave along the axis of x,

$$P = P_0 \sin 2\pi\nu(t - x/V) \tag{5}$$

where V is the velocity applicable to the medium at rest. On applying the Lorentzian transformation to a system S', specified by (1), equation (5) becomes replaced by

$$P = P_0 \sin 2\pi\nu'(t' - x'/V') \tag{6}$$

where

$$\left.\begin{aligned} &\nu' = \beta\nu(1 - v/V), \quad \beta = (1 - v^2/c^2)^{-1/2} \\ \text{and} \quad &V' = V(1 - v/V)(1 - vV/c^2)^{-1} \end{aligned}\right\} \tag{7}$$

The quantity ν' gives the modification of the original frequency as a result of the Doppler effect, generalized into relativistic form, and V' gives the velocity of the wave in the moving medium when that velocity, which is $-v$ in this case, is measured relative to one who does not participate in the motion of the medium.

The foregoing argument *appears* to involve the principle that if we moved with the medium, the propagation would take place in our frame of reference as it would take place for a medium at rest. The transformation then represents the phenomenon as viewed by one who does not participate in the motion of the medium, and appears to involve something concerned with a relation between the actual measures in the two systems. This conclusion is only apparent, however. The picture of the observer moving along with the medium is one which really plays no part in what we actually do in our mathematical derivation. If we concentrate specifically on what we really do, the story assumes a different aspect as follows: Eq. (5) represents the propagation of the wave with respect to a medium at rest in our axes. We are interested in using the Lorentzian transformation to discover, if possible, the form of the law of propagation when the medium is in motion in our axes. Our criterion is that we must produce a law of propagation which is invariant under the Lorentzian transformation. Now

[4] I hold no brief for the procedure we adopt, my object here is simply to say what it is.

we may regard our transformation which resulted in (6) as representing the mathematical technique of discovering a suitable invariant law, minus v being the velocity of the medium in our S' system of axes. For we know that a further transformation of the Lorentzian type will leave (6) invariant in form. The equation will, in fact, become

$$P = P_0 \sin 2\pi\bar{\nu}(\bar{t} - \bar{x}/\bar{V})$$

where

$$\bar{\nu} = \beta_2 \nu'(1 - v_2/V'), \quad \beta_2 = (1 - v_2^2/c^2)^{-1/2}$$
$$\bar{V} = V'(1 - v_2/V')(1 - v_2 V'/c^2)^{-1}$$

and v_2 refers to the velocity associated with the second transformation. Remembering that if $-\bar{v}$ the velocity of the medium in the barred system of coordinates, is given by:

$$-\bar{v} = -\frac{v + v_2}{(1 + vv_2/c^2)}$$

and using (7) we readily find that

$$\bar{\nu} = \bar{\beta}\nu(1 - \bar{v}/V), \quad \bar{\beta} = (1 - \bar{v}^2/c^2)^{-1/2}$$
$$\bar{V} = V(1 - \bar{v}/V)(1 - \bar{v}V/c^2)^{-1}$$

showing that the second transformation leaves the form (6)–(7) unchanged. The important thing to realize is that the foregoing technique of discovering an invariant law has nothing whatever to do with the question of what would happen in the case of an observer who, with his measuring instrument, participated in the motion of the medium. All that we have said would be applicable if the said measuring instruments were rendered utterly unrelated to their former selves as a result of causing them to move with the medium. There is only *one* set of measuring instruments in mind in the whole argument the set associated with the observer who measures the velocity $-v$ for the medium.

Now the Michelson-Morley-Miller experiment is one sensitive to the order v^2/c^2; and a positive result from it invalidates conclusions drawn from the aspect A, but leaves untouched the aspect B, which is the only one of practical use, and which can stand absolutely independent of A.

The aspect B says absolutely nothing about what should happen in the Michelson-Morley-Miller experiment. It has no story to tell as to what happens to things when set in motion, except to this very limited extent: If we knew the complete laws of nature we could predict what happens to a body as a result of changing its motion in any assigned way; and, the aspect B does place upon the complete laws the requirement of invariance. Apart from this, the aspect B is perfectly content if the Michelson-Morley-Miller experiment gives a positive result.

But while one might accept all of the above arguments, he might well say "Yes, but is it not a remarkable thing that the laws of Nature should

be invariant under transformation (1) unless there is something fundamental behind the story?" The old developments of the transformation based upon the postulate of invariance of light velocity, and the relation between the measures of observers in different systems, did place *something* behind the story, even though that something itself did not rest on anything very obvious. The answer to this question is to be found in the general theory of relativity. However, even in this remark we must be careful. It is customary to say that the restricted theory is a special case of the general theory; but, it is only the aspect B which is a special case of it. Aspect A is not contained in it as a necessary consequence at all. Let us probe the matter a little more deeply.

Perhaps the most concise statement of the general theory applicable to the case in hand is to the effect that it maintains that the laws of nature take the form of differential equations involving the coordinates of things, or quantities expressible in terms of these quantities and involving in addition the derivatives of certain quantities $g_{\mu\nu}$, which satisfy equations usually written

$$G_{\mu\nu}=0 \tag{8}$$

which are invariant under any point transformation of coordinates, in the sense that if we make an arbitrary transformation, Eq. (8) come back to the same form in new $g_{\mu\nu}$'s which we shall denote by dashed quantities and which are related to the old $g_{\mu\nu}$'s, in such a way as to make

$$\sum\sum g_{\mu\nu}dx_\mu dx_\nu = \sum\sum g_{\mu\nu}'dx_\mu' dx_\nu' \tag{9}$$

ds^2 is usually written for either of the quantities occurring in (9). Moreover, the general theory of relativity demands that the laws of nature shall be invariant under an arbitrary of transformation. An example of such a set of laws is the equation of the geodesic.

$$\frac{d^2x_\mu}{ds^2}+\frac{1}{2}\sum_{\alpha=1}^{4}\sum_{\nu=1}^{4}\sum_{\lambda=1}^{4}\left\{g^{\mu\lambda}\left(\frac{\partial g_{\alpha\lambda}}{\partial x_\nu}+\frac{\partial g_{\nu\lambda}}{\partial x_\alpha}-\frac{\partial g_{\alpha\nu}}{\partial x_\lambda}\right)\right\}\frac{dx_\alpha}{ds}\frac{dx_\nu}{ds}=0 \tag{10}$$

where $g^{\mu\lambda}=\dfrac{\text{minor of } g_{\mu\lambda}}{g}$, and $g=\begin{vmatrix} g_{11} & g_{12} & g_{13} & g_{14} \\ = & = & = & = \\ g_{41} & g_{42} & g_{43} & g_{44} \end{vmatrix}$.

In the first place, I would remark that the invariance as understood in (10) is a very different kind of thing from the invariance as understood in the restricted theory. If in (10), the derivatives of the g's were inserted as functions of the coordinates, the resulting equation would not be invariant under any transformation of coordinates. It is not as invariant as all that. It would not, in general, be invariant even under the Lorentzian transformation. By the invariance of (10) we mean[5] that on an arbitrary transformation it comes back to the same form in new g's which are related to the old g's by (9).

[5] A fuller discussion of the significance of invariance in the general theory will be given in a paper "Relativity and Electrodynamics" now in process of publication in the Physical Review Supplement.

Now if there is a region of space in which the g's become

$$\left.\begin{aligned} g_{\mu\nu}&=0 \quad \text{if} \quad \mu\neq\nu \\ g_{11}&=g_{22}=g_{33}=-g_{44}/c^2=-1 \end{aligned}\right\} \tag{11}$$

so that, using x, y, z, t, instead of x_1, x_2, x_3, x_4

$$ds^2=-dx^2-dy^2-dz^2+c^2dt^2 \tag{12}$$

then, since it is a characteristic of the Lorentzian transformation that it leaves (12) invarient, i.e that it leaves the new g's as -1, -1, -1, c^2 if the old g's were -1, -1, -1, c^2, we see that in a region where the g's are of the form (11) such equations as (10) or, of course, any other equations invariant in the sense of the general theory will be invariant not only in that sense but in the more drastic sense of the restricted theory *for the Lorentzian transformation.* For the form (11), which makes all the g's constants, requires all the terms involving g's to vanish in the system of coordinates in which (11) holds, and consequently the invariance of (12) under the Lorentzian transformation insures the disappearance of the g's from equations (10) when expressed in any system of coordinates derivable from the former set by a Lorentzian transformation. We may then say that if in any set of laws we have g's such functions of the coordinates that the ds^2 as given by

$$ds^2=\sum g_{\mu\nu}dx_\mu dx_\nu$$

reverts at infinity to (12), or to something transformable to that form; then, when expressed in terms of the coordinates applicable to the form (12) the special theory will hold in the form B. This is perhaps the most logical birthplace of the special theory. The special theory will not hold however, in a system of coordinates derivable from one of the Lorentzian set by a transformation which is not a Lorentzian transformation. To illustrate the matter let us consider the problem of astronomical motion, in which it is customary to take such solutions of (8) as give a line element of the symmetrical form:

$$ds^2=-\gamma^{-1}dr^2-r^2d\theta^2-r^2\sin^2\theta d\phi^2+c^2\gamma dt^2 \tag{13}$$

where

$$\gamma=1-2m/r.$$

If we go off to infinity, γ becomes unity, and the line element assumes the ordinary polar form transformable to the form

$$ds^2=-dx^2-dy^2-dz^2+c^2dt^2 \tag{14}$$

by the ordinary transformation for polar coordinates. We should therefore conclude that in the coordinates x, y, z, t, occurring in (14) the special theory should hold for all differential equations to which the g's of (13) were in the more general case applicable.

Suppose however, that taking (13) and before proceeding to infinity we make a single transformation equivalent in Cartesian coordinates to

$$x''=x+vt, \quad y''=y\,; \quad z''=z, \quad t''=t. \tag{15}$$

The new g's appropriate to the new expression of the line element would be solutions of (8), for no transformation would rob them of this property since (8) is invariant under any transformation. In proceeding to the solution of any problem in these coordinates, we should, of course, obtain exactly the same differential equations as we obtained before[6] but transformed to the dashed system of coordinates specified by (15). We should obtain exactly the result which would be obtained by a mid-Victorian physicist who had somehow or other been led to the differential equations which he considered as applicable to the subject when referred to axes at rest and had then corrected them because he learned that the solar system was moving through space with a velocity v. When we proceed to infinity, however, with our x'', y'', z'', t'', coordinates, we no longer obtain a line element of the form (14) but one obtainable from it by the transformation (15); and the form of this line element tells us immediately that the restricted theory even in the aspect B will not hold in the coordinates in terms of which that line element is expressed.

Thus, all that the general theory predicts as regards the restricted theory, is that, if we make a transformation back from x'', y'', z'', t'', to x, y, z, t, we shall find ourselves in a set of coordinates such that at infinity the laws expressed in terms of them will be invariant under the Lorentzian transformation, so that they will also be invariant in any coordinates obtained from these coordinates by a Lorentzian transformation. They will not, however, be invariant when expressed in the double dashed coordinates. Further, the general theory, at least without further hypothesis, has no story to tell as to the relation between different Lorentzian systems of coordinates and the corresponding measuring rods, etc. I am perfectly aware of the fact that the equivalence of the line element ds and the ds of experimental measurements is frequently stressed. I merely wish to point out that such equivalence amounts to an extra postulate, and a postulate not essential to the main content of the general or restricted theories—a postulate moreover which leads to such dangerous conclusions as are involved in the "red shift" of the spectrum lines of the sun, and which appears to place upon the theory a burden of prediction greater than it need bear.

[6] We here refer to the differential equations typified in the astronomical problem by the equations obtained from (10) by substituting the appropriate values of the g's.

THE SPATIAL DISTRIBUTION OF PHOTOELECTRONS

By S. E. Szczeniowski*
Ryerson Physical Laboratory, University of Chicago

(Received December 6, 1929)

Abstract

The perturbation of a hydrogen-like atom by a plane polarized electromagnetic wave is considered on the basis of Dirac's equation, and perturbed wave functions are obtained. These functions lead by a method similar to that used by Sommerfeld in his "Wellenmechanisches Ergänzungsband" to a formula for the spatial distribution of the photoelectrons. To the first approximation this formula differs from that given by a factor 5/9 in the second term. The angle between the average direction of the emission of the photoelectrons and the electric vector of the incident wave appears therefore to be equal to $h\nu/cmv$ instead of the value $(9/5)(h\nu/cmv)$ given. The factor 5/9 follows from the consideration of the normalizing factors for the spherical harmonics, which were not introduced by Sommerfeld. A second approximation has also been obtained showing the influence of electron spin. This approximation differs from that obtained by Carrelli in that the spin and some other terms not considered by Carrelli and also the factor 5/9 appear.

THE photoelectric effect has been treated theoretically on the basis of the wave mechanics by G. Wentzel,[1] G. Beck[2] and by A. Sommerfeld,[3] who gave a better approximation than the first two authors. However, all these authors have started either from the ordinary form of the Schrödinger equation (Wentzel, Beck) or from the form which takes into account the magnetic field but does not consider the relativity and spin effects. It is therefore of some interest to make the corresponding calculations on the basis of the wave equation given by Dirac. By means of this equation the relativity corrections and the spin influence can be found.

The computations in the present paper will proceed in a manner closely similar to the one used by Sommerfeld in his book.

I. Perturbation of a Hydrogen-Like Atom by an Electromagnetic Wave

Dirac has shown[4] that the Hamiltonian expression for one electron can be written in the form

$$H=(p_0+eA_0/c)+\rho_1(\sigma,p+eA/c)+\rho_3 mc. \tag{1}$$

In this expression ρ_1, ρ_3 are four-row matrices, σ is a vector four-row matrix, whose components σ_1, σ_2, σ_3 are ordinary four-row matrices which satisfy the following relations

* Fellow of the International Education Board.

[1] G. Wentzel, Zeits. f. Physik **40**, 574 (1926); **41**, 828 (1926).

[2] G. Beck, Zeits. f. Physik **41**, 443 (1927).

[3] A. Sommerfeld, Atombau und Spektrallinien, Wellenmechanisches Ergänzungsband, p. 207.

[4] P. A. M. Dirac, Proc. Roy. Soc. **A117**, 610 (1928); **118**, 351 (1928).

$$\sigma_1\sigma_2 = i\sigma_3 = -\sigma_2\sigma_1$$
$$\sigma_2\sigma_3 = i\sigma_1 = -\sigma_3\sigma_2 \tag{2}$$
$$\sigma_3\sigma_1 = i\sigma_2 = -\sigma_1\sigma_3$$

$$\sigma_1^2 = 1\ ;\quad \sigma_2^2 = 1\ ;\quad \sigma_3^2 = 1. \tag{3}$$

Similar relations are valid for ρ_1, ρ_3; moreover all σ's are commutable with all ρ's.

The parenthesis $(\sigma,\ p+eA/c)$ stands for a scalar product of the two vectors σ and $p+eA/c$. A is the vector potential, A_0 the scalar potential.

To the Hamiltonian (1) correspond two mutually adjoint functions, ψ and ϕ, each of which has four components.

To obtain Dirac's equations it is to be assumed that

$$p_0 = \frac{ih}{2\pi c}\frac{\partial}{\partial t} \tag{4}$$

and p is to be interpreted as a vector operator, whose components are given by the relations

$$p_x = -\frac{ih}{2\pi}\frac{\partial}{\partial x}\ ;\qquad p_y = -\frac{ih}{2\pi}\frac{\partial}{\partial y}\ ;\qquad p_z = -\frac{ih}{2\pi}\frac{\partial}{\partial z}\ . \tag{5}$$

Then simultaneously

$$(p_0+eA_0/c)\psi+\rho_1(\sigma, p+eA/c)\psi+\rho_3 mc\psi = 0 \tag{6}$$

$$\phi(-p_0+eA_0/c)+\phi\rho_1(\sigma, -p+eA/c)+\phi\rho_3 mc = 0. \tag{7}$$

In the Eqs. (6) and (7) the following notation has been used. If μ is a four rowed matrix, then

$$\mu\psi = \sum_{k=1}^{4}\mu_{ik}\psi_k \qquad (i=1,2,3,4) \tag{8}$$

$$\phi\mu = \sum_{k=1}^{4}\phi_k\mu_{ki} \qquad (i=1,2,3,4) \tag{9}$$

If the matrices ρ and σ are hermitian, as, for instance, those given by Dirac,[4] ϕ is the conjugate complex function to ψ. This will be the case in the present paper. The operators p_0 and p in Eq. (7) operate backwards.

Dirac has shown, also, that the electric charge and current densities are given by

$$\rho = -e\phi\psi \tag{10}$$

and

$$J = ec\phi\rho_1\sigma\psi. \tag{11}$$

In these expressions $\phi\psi$ stands for $\sum_{k=1}^{4}\phi_k\psi_k$ and $\phi\mu\psi$ for $\sum_{i,k=1}^{4}\phi_i\mu_{ik}\psi_k$.

It will be convenient to use the equations of second order, which correspond to the Eqs. (6) and (7) and in the present case will be equivalent to

them. These equations were also derived by Dirac and can be written in the form

$$\left\{-\left(\frac{ih}{2\pi c}\frac{\partial}{\partial t}+\frac{eV}{c}\right)^2+\left(-\frac{ih}{2\pi}\nabla+\frac{eA}{c}\right)^2+m^2c^2\right\}\psi$$
$$+\frac{eh}{2\pi c}(\sigma,H)\psi+\frac{ieh}{2\pi c}\rho_1(\sigma,E)\psi=0 \quad (12)$$

$$\left\{-\left(-\frac{ih}{2\pi c}\frac{\partial}{\partial t}+\frac{eV}{c}\right)^2+\left(\frac{ih}{2\pi}\nabla+\frac{eA}{c}\right)^2+m^2c^2\right\}\phi$$
$$+\frac{eh\phi}{2\pi c}(\sigma,H)-\frac{ieh}{2\pi c}\phi\rho_1(\sigma,E)=0 \quad (13)$$

In these equations ∇ stands for a vector operator with components $\partial/\partial x$, $\partial/\partial y$, $\partial/\partial z$; H and E are the magnetic and electric field intensities which correspond to the scalar potential $V=A_0$ and the vector potential A, whereas (σ, H) and (σ, E) are scalar products of vectors σ and H or σ and E respectively.

The point of departure for the following considerations will be an undisturbed hydrogen-like atom in the k-th quantum state, consequently V will be equal to Ze/r, where Ze is the charge of the nucleus. The corresponding initial proper functions will be denoted by ψ_k and ϕ_k. As in the present case ϕ_k is always the conjugate complex function to ψ_k it will be sufficient to consider only the functions ψ.

Accordingly the initial conditions are described by the equations

$$\left\{-\left(\frac{ih}{2\pi c}\frac{\partial}{\partial t}+\frac{eV}{c}\right)^2+\left(-\frac{ih}{2\pi}\nabla\right)^2+m^2c^2\right\}\psi_k+\frac{ieh}{2\pi c}\rho_1(\sigma,E_0)\psi_k=0 \quad (14)$$

where E_0 designates the intensity of the electrostatic field of the nucleus.

Eq. (14) can be written in the form

$$\frac{1}{c^2}\frac{\partial^2\psi_k}{\partial t^2}-\Delta\psi_k-\frac{4\pi ieV}{hc^2}\frac{\partial\psi_k}{\partial t}-\frac{4\pi^2e^2V^2}{h^2c^2}\psi_k+\frac{4\pi^2m^2c^2}{h^2}\psi_k+\frac{2\pi ie}{hc}\rho_1(\sigma,E_0)\psi_k=0 \quad (15)$$

It will be now supposed that the atom is disturbed by a plane polarized electromagnetic wave, whose field can be derived from the vector potential

$$A=A_x=a\cos 2\pi\nu\left(t-\frac{z}{c}\right)$$

It is known that

$$H=\operatorname{curl} A\ ;\quad E=-\operatorname{grad} A_0-\dot{A}/c \quad (16)$$

and therefore

$$\begin{aligned} &H_x=H_z=0\ ;\quad H_y=a\cdot(2\pi\nu/c)\sin 2\pi\nu(t-z/c)\\ &E_y=E_z=0\ ;\quad E_x=a\cdot(2\pi\nu/c)\sin 2\pi\nu(t-z/c)\,. \end{aligned} \quad (17)$$

Eqs. (17) correpond to an electromagnetic wave, which proceeds in the direction of the z axis and is polarized in the yz plane.

If the values (17) are applied to Eq. (12) it assumes the form

$$\frac{1}{c^2}\frac{\partial^2\psi}{\partial t^2}-\frac{4\pi^2e^2V^2}{h^2c^2}\psi-\frac{4\pi ieV}{hc^2}\frac{\partial\psi}{\partial t}-\Delta\psi-\frac{4\pi iea}{hc}\cos 2\pi\nu\left(t-\frac{z}{c}\right)\frac{\partial\psi}{\partial x}$$
$$+\frac{4\pi^2e^2a^2}{h^2c^2}\psi\cos^2 2\pi\nu\left(t-\frac{z}{c}\right)+\frac{4\pi^2m^2c^2}{h^2}\psi+\frac{4\pi^2\nu ea}{hc^2}\sin 2\pi\nu\left(t-\frac{z}{c}\right)\sigma_2\psi \qquad (18)$$
$$+\frac{2\pi ie}{hc}\rho_1(\sigma,E_0)\psi+\frac{4\pi^2 iea\nu}{hc^2}\rho_1\sigma_1\psi\sin 2\pi\nu\left(t-\frac{z}{c}\right)=0.$$

It is convenient to introduce exponentials instead of sines and cosines in Eq. (18). Moreover the term with a^2 as a factor can be neglected, since usually the amplitude a of the disturbing wave is very small. Then

$$\frac{1}{c^2}\frac{\partial^2\psi}{\partial t^2}-\frac{4\pi^2e^2V^2}{h^2c^2}\psi-\frac{4\pi ieV}{hc^2}\frac{\partial\psi}{\partial t}-\Delta\psi+\frac{4\pi^2m^2c^2}{h^2}\psi+\frac{2\pi ie}{hc}\rho_1(\sigma,E_0)\psi$$
$$-\frac{2\pi iea}{hc}\frac{\partial\psi}{\partial x}\left[e^{2\pi i\nu(t-z/c)}+e^{-2\pi i\nu(t-z/c)}\right]-\frac{2\pi^2\nu iea}{hc^2}\left[e^{2\pi i\nu(t-z/c)}\right. \qquad (19)$$
$$\left.-e^{-2\pi i\nu(t-z/c)}\right]\sigma_2\psi+\frac{2\pi^2 e\nu a}{hc^2}\left[e^{2\pi i\nu(t-z/c)}-e^{-2\pi i\nu(t-z/c)}\right]\rho_1\sigma_1\psi=0.$$

Eq. (19) can be simplified by the introduction of a perturbation parameter $\chi=-2\pi iea/hc$. On account of the factor a this parameter is a small quantity, so that all the terms, which have a power of a larger than unity as a factor can be neglected. Therefore it can be assumed that

$$\psi=\psi_k+\chi v+\cdots. \qquad (20)$$

In the expression above ψ_k denotes the proper function for the initial state of the atom and therefore

$$\psi_k=\bar{\psi}_k e^{-2\pi iE_kt/h} \qquad (21)$$

where E_k is the proper energy of the atom in the initial state and $\bar{\psi}_k$ is a function of the spatial coordinates only. On account of Eq. (20) the substitution of (21) into Eq. (19) leads to

$$\frac{1}{c^2}\frac{\partial^2 v}{\partial t^2}-\frac{4\pi^2e^2V^2}{h^2c^2}v-\frac{4\pi ieV}{hc^2}\frac{\partial v}{\partial t}-\Delta v+\frac{4\pi^2m^2c^2}{h^2}v+\frac{2\pi ie}{hc}\rho_1(\sigma,E_0)v$$
$$+\frac{\partial\bar{\psi}_k}{\partial x}\left\{\exp\left[-\frac{2\pi i}{h}(E_k+h\nu)t+2\pi i\nu\frac{z}{c}\right]\right.$$
$$\left.+\exp\left[-\frac{2\pi i}{h}(E_k-h\nu)t-2\pi i\nu\frac{z}{c}\right]\right\} \qquad (22)$$
$$+\frac{\pi\nu}{c}\left\{\exp\left[-\frac{2\pi i}{h}(E_k-h\nu)t-2\pi i\nu\frac{z}{c}\right]\right.$$

$$-\exp\left[-\frac{2\pi i}{h}(E_k+h\nu)t+2\pi i\nu\frac{z}{c}\right]\Bigg\}\sigma_2\psi$$

$$+\frac{i\pi\nu}{c}\Bigg\{\exp\left[-\frac{2\pi i}{h}(E_k-h\nu)t-2\pi i\nu\frac{z}{c}\right]$$

$$-\exp\left[-\frac{2\pi i}{h}(E_k+h\nu)t+2\pi i\nu\frac{z}{c}\right]\Bigg\}\rho_1\sigma_1\bar{\psi}=0$$

The terms with the squares of χ were omitted, according to the former assumption.

The form of Eq. (22) suggests that

$$v=v_+e^{-(2\pi i/h)(E_k+h\nu)t}+v_-e^{-(2\pi i/h)(E_k-h\nu)t}. \tag{23}$$

If z/λ is written instead of $\nu z/c$ then, on account of (23) Eq. (22) takes the form

$$-\frac{4\pi^2}{h^2c^2}(E_k\pm h\nu)^2v_\pm-\frac{4\pi^2e^2V^2}{h^2c^2}v_\pm-\frac{8\pi^2eV}{h^2c^2}(E_k\pm h\nu)v_\pm-\Delta v_\pm$$

$$+\frac{4\pi^2m^2c^2}{h^2}v_\pm+\frac{2\pi ie}{hc}\rho_1(\sigma,E_0)v_\pm+\frac{\partial\bar{\psi}_k}{\partial x}e^{\pm 2\pi iz/\lambda} \tag{24}$$

$$\mp\frac{\pi\nu}{c}e^{\pm 2\pi iz/\lambda}\sigma_2\bar{\psi}_k\mp\frac{i\pi\nu}{c}e^{\pm 2\pi iz/\lambda}\rho_1\sigma_1\bar{\psi}_k=0.$$

All upper signs in this equation belong together; the same applies to the lower signs.

Eq. (24) can be written in the form

$$\Delta v_\pm+\frac{4\pi^2}{h^2c^2}[(E_k\pm h\nu+eV)^2-m^2c^4]v_\pm-\frac{2\pi ie}{hc}\rho_1(\sigma,E_0)v_\pm$$

$$=\frac{\partial\bar{\psi}_k}{\partial x}e^{\pm 2\pi iz/\lambda}\mp\frac{\pi}{\lambda}e^{\pm 2\pi iz/\lambda}\sigma_2\bar{\psi}_k\mp\frac{i\pi}{\lambda}e^{\pm 2\pi iz/\lambda}\rho_1\sigma_1\bar{\psi}_k. \tag{25}$$

Since

$$(E_k\pm h\nu+eV)^2-m^2c^4=(E_k\pm h\nu+eV+mc^2)(E_k\mp h\nu+eV-mc^2) \tag{26}$$

and, except for very great values of ν, the expression $E_k\pm h\nu+eV$ is nearly equal to mc^2, it follows that the Eq. (25) differs from that given by Sommerfeld[5] only by the terms connected with the electron spin.

However, it is to be remembered that in Eq. (25) the functions v_+ and v_- stand for four components each. Furthermore in Sommerefeld's equations e is the electron charge, whereas in the present paper e denotes the absolute value of the electron charge. This explains the difference of signs, since eV stands for Sommerfeld's $-U$.

The solution of the Eq. (25) can be assumed in the form of an infinite series of the proper solutions of the undisturbed problem. However it is to

[5] A. Sommerfeld, reference 3, p. 195, Eq. (8).

be taken into account, that the hydrogen atom has a continuum of proper functions for electron energies greater than mc^2 in addition to a discrete set of proper functions for electron energies less than mc^2. Accordingly

$$v_{\pm} = \sum_j B_j^{\pm} \bar{\psi}_j + \int B^{\pm}(E') \bar{\psi}(E') dE'. \tag{27}$$

However, the expansion of the right side of the Eq. (25) into a corresponding series of proper functions meets a difficulty pointed out by Darwin.[6] Darwin has shown that the proper functions of the hydrogen atom form an incomplete set of orthogonal functions and that therefore it is not possible to develop an arbitrary four component function into a series of these proper functions. To do this the number of orthogonal solutions must be doubled. It means that in order to go through the calculations the existence of the solutions which correspond to the negative proper energies of the electron must be admitted. These solutions are obtained if the sign of the electron charge in Dirac's equation is changed from negative to positive and it is clear that they have no physical meaning. Therefore it is to be remembered that only those terms of the above mentioned series expansion which correspond to positive proper energies are to be taken into account in further considerations.

According to these considerations the series expansion can be written in the following form

$$\frac{\partial \bar{\psi}_k}{\partial x} e^{\pm 2\pi i z/\lambda} \mp \frac{\pi}{\lambda} e^{\pm 2\pi i z/\lambda} \sigma_2 \bar{\psi}_k \mp \frac{i\pi}{\lambda} e^{\pm 2\pi i z/\lambda} \rho_1 \sigma_1 \bar{\psi}_k = \sum_j A_j^{\pm} \bar{\psi}_j + \int A^{\pm}(E') \bar{\psi}(E') dE'. \tag{28}$$

The integrals in the equation above are to be extended from $E' = mc^2$ to $E' \to \infty$ and from $E' = -mc^2$ to $E' \to -\infty$, but only the integrals within positive limits have a physical meaning.

The functions $\bar{\psi}_j$, $\bar{\psi}(E')$ are sclutions of the undisturbed Eq. (14) and therefore

$$-\frac{4\pi^2}{h^2c^2} E_j^2 \bar{\psi}_j - \Delta\bar{\psi}_j - \frac{8\pi^2}{h^2c^2} E_j e V \bar{\psi}_j - \frac{4\pi^2 e^2 V^2}{h^2c^2} \bar{\psi}_j + \frac{4\pi^2 m^2 c^2}{h^2} \bar{\psi}_j + \frac{2\pi i e}{hc} \rho_1(\sigma, E_0) \bar{\psi}_j = 0. \tag{29}$$

Similar equation is valid for $\bar{\psi}(E')$

The Eq. (29) leads to

$$\Delta\bar{\psi}_j - \frac{2\pi i e}{hc} \rho_1(\sigma, E_0) \bar{\psi}_j = -\frac{4\pi^2}{h^2c^2} [(E_j + eV)^2 - m^2c^4] \bar{\psi}_j. \tag{30}$$

[6] G. Darwin, Proc. Roy. Soc. **A118**, 654 (1928).

If Eqs. (27), (28) and (30) are substituted into (26), then it is found that

$$B_j^{\pm}=\frac{h^2c^2}{4\pi^2}\,\frac{A_j^{\pm}}{(E_k\pm h\nu+eV)^2-m^2c^4}$$
$$B^{\pm}(E')=\frac{h^2c^2}{4\pi^2}\,\frac{A^{\pm}(E')}{(E_k\pm h\nu+eV)^2-(E'+eV)^2}\,. \tag{31}$$

On account of these relations Eqs. (20) leads to

$$\begin{aligned}\psi=\bar{\psi}_k e^{-2\pi i E_k t/h}-\frac{hc\,i\,e\,a}{2\pi}\Bigg\{&\Bigg[\sum_j\frac{A_j^{+}\bar{\psi}_j}{(E_k+h\nu+eV)^2-(E_j+eV)^2}\\&+\int\frac{A^{+}(E')\bar{\psi}(E')dE'}{(E_k+h\nu+eV)^2-(E'+eV)^2}\Bigg]e^{-2\pi i(E_k+h\nu)\,t/h}\\&+\Bigg[\sum_j\frac{A_j^{-}\bar{\psi}_j}{(E_k-h\nu+eV)^2-(E_j+eV)^2}\\&+\int\frac{A^{-}(E')\bar{\psi}(E')dE'}{(E_k-h\nu+eV)^2-(E'+eV)^2}\Bigg]e^{-2\pi i(E_k-h\nu)\,t/h}\Bigg\}\,.\end{aligned} \tag{32}$$

From Eq. (10) the electric charge density is

$$\begin{aligned}\rho=-e\bar{\phi}_k\bar{\psi}_k+\frac{hc\,i\,e\,a}{2\pi}\Bigg\{&e^{2\pi i\nu t}\Bigg[\sum_j\frac{A_j^{+*}\bar{\phi}_j\bar{\psi}_k}{(E_k+h\nu+eV)^2-(E_j+eV)^2}\\&-\sum_j\frac{A_j^{-}\bar{\phi}_k\bar{\psi}_j}{(E_k-h\nu+eV)^2-(E_j+eV)^2}\Bigg]+e^{-2\pi i\nu t}\Bigg[\sum_j\frac{A^{-*}\bar{\phi}_j\bar{\psi}_k}{(E_k-h\nu+eV)^2-(E_j+eV)^2}\\&-\sum_j\frac{A_j^{+}\bar{\phi}_k\bar{\psi}_j}{(E_k+h\nu+eV)^2-(E_j+eV)^2}\Bigg]\Bigg\}\,.\end{aligned} \tag{33}$$

According to the former assumptions the terms whose coefficients are proportional to a^2 were neglected, furthermore the integrals, which correspond to the continuous spectrum are not written out.

From Eq. (33), which is very similar to the one given by Sommerfeld[7] the dispersion formulas could be obtained in the usual way.

As long as $h\nu \ll mc^2$

$$(E_k\pm h\nu+eV)^2-(E_j+eV)^2\leqq 2mc^2(E_k-E_j\pm h\nu) \tag{34}$$

because the energy values include the energy mc^2, so that on the one hand eV is negligibly small with regard to E_k or E_j (except for the K-levels of the heavy elements) and on the other hand each of these terms differs only negligibly (with the same exception) from mc^2 (the energy mc^2 in electron-volts is of the order of $5\cdot 10^5 v$.

With that simplification the Eq. (33) leads to the usual dispersion formula. Only when $h\nu$ begins to be comparable with mc^2 and especially for the

[7] A. Sommerfeld, reference 3, p. 197.

heaviest elements does Eq. (33) give results differing appreciably from the usual dispersion formula. As $h\nu$ is equal to mc^2 for $\lambda \leqq 24XU$ it follows that the difference begins to be appreciable for X-rays of the order of 0.1A.

According to Eq. (28) the value of $Aj^{\pm}$ is given by

$$A_j^{\pm} = \frac{1}{C_j}\left\{ \int \bar{\phi}_j \frac{\partial \bar{\psi}_k}{\partial x} e^{\pm 2\pi i z/\lambda} d\tau \mp \frac{\pi}{\lambda} \int e^{\pm 2\pi i z/\lambda} \bar{\phi}_j \sigma_2 \bar{\psi}_k d\tau \right. \\ \left. \mp \frac{i\pi}{\lambda} \int e^{\pm 2\pi i z/\lambda} \bar{\phi}_j \rho_1 \sigma_1 \bar{\psi}_k d\tau \right\}. \tag{35}$$

Eq. (35) is obtained if Eq. (28) is multiplied by $\bar{\phi}_j$ on the left-hand side and integrated over the whole space. Furthermore the normalizing integrals

$$\int \bar{\phi}_j \bar{\psi}_j d\tau = C_j \tag{36}$$

are to be used. The integrations in the expressions (36) extend over the whole space.

II. The Photoelectric Current

The photoelectric current excited in a given direction by an electromagnetic wave incident on a hydrogen like atom can now be found on the basis of Eq. (32). Only the photoelectric emission from a single atom will be considered here. To calculate this emission, those excited states of the atom which belong to the continuous spectrum are to be considered. Therefore in the present case the sums in Eq. (32) can be omitted as irrelevant. The values of the coefficients $A^{\pm}(E')$ are given by the formulas

$$A^{\pm}(E') = \frac{1}{C(E')}\left\{ \int \bar{\phi}(E') \frac{\partial \bar{\psi}_k}{\partial x} e^{\pm 2\pi i z/\lambda} d\tau \mp \frac{\pi}{\lambda} \int \bar{\phi}(E') \sigma_2 \bar{\psi}_k e^{\pm 2\pi i z/\lambda} d\tau \right. \\ \left. \mp \frac{i\pi}{\lambda} \int \bar{\phi}(E') \rho_1 \sigma_1 \bar{\psi}_k e^{\pm 2\pi i z/\lambda} d\tau \right\} \tag{37}$$

where

$$C(E') = \lim_{\Delta_n E' \to 0} \frac{\int \Delta_n \bar{\phi}(E') \Delta_n \bar{\psi}(E') d\tau}{\Delta_n E'} \tag{38}$$

(the integral extends over the whole space) and

$$\Delta_n \bar{\phi}(E') = \int_{\Delta_n E'} \bar{\phi}(E') dE' \; ; \quad \Delta_n \bar{\psi}(E') = \int_{\Delta_n E'} \bar{\psi}(E') dE' \tag{39}$$

(see Fuess[8]).

In Eq. (32) the term $\bar{\psi}_k e^{-2\pi i E_k t/h}$ can be also omitted. This term represents the initial k-th quantum state of the atom and therefore its radial part contains an exponential of the type $e^{-\mu r}$, where μ is a real positive number.

[8] E. Fuess, Ann. d. Physik **81**, 281 (1926).

Since $\mu \sim 10^9$ this exponential vanishes very rapidly with increasing r. (The same applies to the terms of the sums in Eq. (32)). On the other hand the radial parts of the functions $\overline{\varphi}(E')$ have as a factor an exponential $e^{\mu' r}$ where μ' is purely imaginary. They vanish therefore only slowly with growing r. It follows that for the values of r great compared with the atomic dimensions (and it is these values that are to be considered for the photoelectric effect) only the integrals in Eq. (32) are to be taken into account.

According to Sommerfeld[9] the integrands of these integrals can be separated into three factors

$$a)\ \frac{A^{\pm}(E')}{(E_k \pm h\nu + eV)^2 - (E' + eV)^2}; \qquad b)\ \overline{\psi}(E') \qquad \text{and} \qquad c)\ e^{-2\pi i (E_k \pm h\nu)\, t/h}.$$

In the factor (a) only V depends upon the coordinates, but, as V is equal to $e\,Z/r$ it can be safely omitted in the computations. The factor (a) then becomes a constant, i.e. it depends only upon E'.

The factor (c) gives the dependence of $\overline{\psi}$ upon the time. The expression $E_k \pm h\nu$ in the exponent can be interpreted as the energy of the photoelectron. The kinetic energy of the photoelectron is

$$\epsilon = E_k \pm h\nu - mc^2.$$

If the $+$ sign is taken this can be written in the form $\epsilon = h\nu - J$ where $J = mc^2 - E_k$ is the ionization potential. The corresponding expression with the $-$ sign becomes negative. Hence there cannot be given a physical interpretation to the corresponding parts of ψ unless the possibility of existence of states with negative total energy is admitted. The existence of these states has already been admitted to obtain an expansion of the right side of the perturbed Eq. (25) into a series of the proper functions of the undisturbed problem. The factor $E_k - h\nu$ could then be written in the form $-(-E_k + h\nu)$ and the negative kinetic energy of the photoelectron, which evidently has no physical significance would be $\epsilon' = -(-E_k + h\nu) - (-mc^2)$ or $\epsilon' = -(h\nu - J)$. This forms an analogue to Einstein's photoelectric equation.

According to the above considerations these parts of ϕ which correspond to the $-$ sign in the expression $E_k \pm h\nu$ can be omitted, the more so, that the parts with the $+$ sign will be incomparably greater than the parts with the $-$ sign on account of the expression $(E_k + h\nu + eV)^2 - (E' + eV)^2$ in the denominator of the integrands, which tends to zero with E' tending to $E_k + h\nu$.

The factor (b) is the really interesting one for the determination of the spatial distribution of the photoelectrons. Moreover it must be added that only the radial parts of the functions ψ have the continuous spectra. The directional parts have only the discrete proper functions. Therefore on account of the foregoing considerations the following expressions are properly to be used in the subsequent calculations (because $A_j^{\pm}$ and $A(\pm E')$ should be explicity written as $A_{jkm}^{\pm}$ and $A_{km}^{\pm}(E')$)

[9] A. Sommerfeld, reference 3, p. 209.

$$\psi \leqq -\frac{hcie a}{2\pi} e^{-2\pi i(E_{k_0}+h\nu)t/h}\left\{\sum_k \sum_m \int \frac{\overset{+}{A}_{km}(E')\bar{\psi}_{km}(E')dE'}{(E_{k_0}+h\nu+eV)^2-(E'+eV)^2}\right\}. \quad (40)$$

To avoid the divergence of the integral in (40) the integration can be performed according to Wentzel[10] along a path which extends slightly around the pole $E'=E_{k_0}+h\nu$ into the positive part of the complex plane E'.

Darwin[11] has shown that the solutions of Dirac's equations for a central electrostatic field can be written in the form

$$\begin{aligned} \bar{\psi}^{(1)}_{km} &= -iF_k P^{m}_{k+1} & \bar{\psi}^{(3)}_{km} &= (k+m+1)G_k P_k{}^{m+1} \\ \bar{\psi}^{(2)}_{km} &= -iF_k P^{m-1}_{k+1} & \bar{\psi}^{(4)}_{km} &= (-k+m)G_k P_k{}^{m+1} \end{aligned} \quad (41)$$

and

$$\begin{aligned} \bar{\psi}^{(1)}_{km} &= -i(k+m)F_{-k-1}P^{m}_{k-1} & \bar{\psi}^{(3)}_{km} &= G_{-k-1}P^{m}_{k} \\ \bar{\psi}^{(2)}_{km} &= -i(-k+m+1)F_{-k-1}P^{m+1}_{k-1} & \bar{\psi}^{(4)}_{km} &= G_{-k-1}P_k{}^{m+1}. \end{aligned} \quad (42)$$

The functions $P_k{}^m$ are spherical harmonics defined in the following way

$$P_k{}^m = (k-m)!\sin^m\theta\left(\frac{d}{d\cos\theta}\right)^{k+m}\left(\frac{\cos^2\theta-1}{2^k\cdot k!}\right)\cdot e^{im\phi}. \quad (43)$$

It can be shown that

$$P_k{}^{-m} = (-1)^m P_k{}^{m*} \quad (44)$$

so that only the values of $P_k{}^m$ for positive m need to be known. Furthermore

$$\int_0^{\pi}\int_0^{2\pi} P_k{}^m P_k{}^{m*}\sin\theta d\theta d\phi = \frac{4\pi}{2k+1}(k+m)!(k-m)!. \quad (45)$$

The functions F_k and G_k depend upon the radius r only and satisfy the relations

$$\begin{aligned} &\frac{2\pi}{h}\left(\frac{E+eV}{c}+mc\right)F_k+\frac{dG_k}{dr}-\frac{k}{r}G_k=0 \\ &-\frac{2\pi}{h}\left(\frac{E+eV}{c}-mc\right)G_k+\frac{dF_k}{dr}+\left(\frac{k+2}{r}\right)\cdot F_k=0. \end{aligned} \quad (46)$$

For a hydrogen-like atom with the nuclear charge Ze the potential V is equal to eZ/r and so, if the following notation is used

$$\frac{2\pi}{h}\left(\frac{E}{c}+mc\right)=A^2;\quad \frac{2\pi}{h}\left(\frac{E}{c}-mc\right)=B^2 \qquad \frac{2\pi e^2 Z}{hc}=\gamma=Z\alpha \quad (47)$$

where α is the Sommerfeld fine structure constant, then instead of (46)

$$\begin{aligned} &\left(A^2+\frac{\gamma}{r}\right)F_k+\frac{dG_k}{dr}-\frac{k}{r}G_k=0 \\ &\left(B^2+\frac{\gamma}{r}\right)G_k-\frac{dF_k}{dr}-\frac{k+2}{r}F_k=0. \end{aligned} \quad (48)$$

[10] G. Wentzel, Zeits. f. Physik **40**, 574 (1926).
[11] C. G. Darwin, reference 6.

The solutions (41) and (42) correspond to different values of the inner quantum number j. For the solution (41) $j=k+\frac{1}{2}$, for (42) $j=k-\frac{1}{2}$. Moreover, for the solution (41) $-k-1\leq m\leq k$ which leads to $2k+2$ different solutions, whereas for the type (42) one has $-k\leq m\leq k-1$ i.e. $2k$ different solutions. In each case there are $2j+1$ solutions as it should be.

In the subsequent calculations the normalizing integrals for the proper functions (41) and (42) are used. These integrals were given by Darwin[12] For the solution (41)

$$C'_{km}=\int \bar{\phi}_{km}\bar{\psi}_{km}d\tau=4\pi(k+m+1)!(k-m)!\int_0^\infty (F_k^2+G_k^2)r^2dr \tag{49}$$

and for the solution (42)

$$C''_{km}=\int \bar{\phi}_{km}\bar{\psi}_{km}d\tau=4\pi(k+m)!(k-m-1)!\int_0^\infty (F_{-k-1}^2+G_{-k-1}^2)r^2dr\,. \tag{50}$$

It is also to be noted that the solutions (41) and (42) form an orthogonal set of functions, i. e.

$$\int \bar{\phi}_{kmj}(E)\bar{\psi}_{k'm'j'}(E')d\tau=0 \tag{51}$$

except for $E=E'$, $k=k'$, $m=m'$ and $j=j'$ (j—inner quantum number).

Darwin has also shown that for $E<mc^2$ a hydrogen-like atom has a set of discrete proper values of E, which correspond to the solutions (41) and (42). For $E>mc^2$ there are solutions for each value of E. This last condition corresponds to the existence of a continuous spectrum. It can be shown that in this latter case F_k and G_k are complex functions, which to the first approximation correspond to spherical waves diverging from the nucleus (or converging towards the nucleus).

To find the approximate forms of F_k and G_k for $r\to\infty$ all terms in Eqs. (48) with r in the denominator can be omitted in the first approximation. This leads to

$$A^2F+dG/dr=0\,;\qquad B^2G-dF/dr=0 \tag{52}$$

with both A^2 and B^2 positive. Hence

$$A^2F+\frac{1}{B^2}\frac{d^2F}{dr^2}=0\,;\qquad B^2G+\frac{1}{A^2}\frac{d^2G}{dr^2}=0 \tag{53}$$

and

$$F=ae^{iABr}\,;\quad G=be^{iABr}. \tag{54}$$

These values of F and G substituted into Eqs. (52) give

$$a=-ibB/A=-ibp \tag{55}$$

p is a small quantity and so $\bar{\psi}^{(1)}$ and $\bar{\psi}^{(2)}$ are small compared with $\bar{\psi}^{(3)}$ and $\bar{\psi}^{(4)}$.

[12] C. G. Darwin, reference 6.

In the second approximation a and b can be considered as varying slowly with r and so all terms with a/r^2, a'/r and a'' and analogous terms for b are to be omitted. If the values (53) and (54) are substituted into Eqs. (48) the above assumption leads to

$$a'+\frac{a}{r}\left[1-\frac{i\gamma}{2}\left(\frac{A}{B}+\frac{B}{A}\right)\right]=0 \tag{56}$$

and the same equation for b

If one puts

$$\frac{\gamma}{2}\left(\frac{A}{B}+\frac{B}{A}\right)=\delta \tag{57}$$

then the Eq. (56) takes the form

$$a'+\frac{a}{r}(1-i\delta)=0 \tag{58}$$

whence

$$a=Ce^{i\delta\log r}/r. \tag{59}$$

Therefore finally

$$\begin{aligned} F&=-ipCe^{i(ABr+\delta\log r)}/r \\ G&=Ce^{i(ABr+\delta\log r)}/r. \end{aligned} \tag{60}$$

On the basis of the notations (47) it can easily be found that AB is usually of the order 10^9, whereas δ is, for high speed photoelectrons and low atomic numbers, small compared with unity. As the log r varies much more slowly than r it follows that $\delta \log r=\tau$ can be considered to this approximation as a constant.

All is now prepared for the actual calculation of the coefficient $A^{+}_{km}(E')$ in Eq. (40). These coefficients are given by Eq. (37), which, written in the developed form is

$$\begin{aligned} C_{km}(E')A_{km}(E') &= \int \bar{\phi}^{(1)}_{km}(E')\frac{\partial\bar{\psi}^{(1)}_{k_0}}{\partial x}e^{2\pi iz/\lambda}d\tau \\ &+\int \bar{\phi}^{(2)}_{km}(E')\frac{\partial\bar{\psi}^{(2)}_{k_0}}{\partial x}e^{2\pi iz/\lambda}d\tau \\ &+\int \bar{\phi}^{(3)}_{km}(E')\frac{\partial\bar{\psi}^{(3)}_{k_0}}{dx}e^{2\pi iz/\lambda}d\tau+\int \bar{\phi}^{(4)}_{km}(E')\frac{\partial\bar{\psi}^{(4)}_{k_0}}{\partial x}e^{2\pi iz/\lambda}d\tau \\ &-\frac{\pi}{\lambda}\Big[-i\int \bar{\phi}^{(1)}_{km}(E')\bar{\psi}^{(2)}_{k_0}e^{2\pi iz/\lambda}d\tau+i\int \bar{\phi}^{(2)}_{km}(E')\bar{\psi}^{(1)}_{k_0}e^{2\pi iz/\lambda}d\tau \\ &-i\int \bar{\phi}^{(3)}_{km}(E')\bar{\psi}^{(4)}_{k_0}e^{2\pi iz/\lambda}d\tau+i\int \bar{\phi}^{(4)}_{km}(E')\bar{\psi}^{(3)}_{k_0}e^{2\pi iz/\lambda}d\tau\Big] \end{aligned} \tag{61}$$

$$-\frac{i\pi}{\lambda}\Big[\int \bar{\phi}^{(1)}_{km}(E')\bar{\psi}^{(4)}_{k_0}e^{2\pi iz/\lambda}d\tau+\int \bar{\phi}^{(2)}_{km}(E')\bar{\psi}^{(3)}_{k_0}e^{2\pi iz/\lambda}d\tau$$

$$+\int \bar{\phi}^{(3)}_{km}(E')\bar{\psi}^{(2)}_{k_0}e^{2\pi iz/\lambda}d\tau+\int \bar{\phi}^{(4)}_{km}(E')\bar{\psi}^{(1)}_{k_0}e^{2\pi iz/\lambda}d\tau\Big].$$

The Eq. (61) follows from (37) if it is remembered that, according to Dirac[13]

$$\sigma_2=\begin{vmatrix}0 & -i & 0 & 0\\ i & 0 & 0 & 0\\ 0 & 0 & 0 & -i\\ 0 & 0 & i & 0\end{vmatrix} \quad \text{and} \quad \rho_1\sigma_1=\begin{vmatrix}0 & 0 & 0 & 1\\ 0 & 0 & 1 & 0\\ 0 & 1 & 0 & 0\\ 1 & 0 & 0 & 0\end{vmatrix}. \tag{62}$$

To simplify the calculations it will be supposed that the hydrogen-like atom considered is initially in the normal unexcited state. According to Darwin two possibilities are then to be considered[14].

Either

$$\begin{aligned}\bar{\psi}^{(1)}_{k_0}&=\frac{-i\gamma}{1+(1-\gamma^2)^{1/2}}P_1{}^0r^\beta e^{-r/a_0} & \psi^{(3)}_{k_0}&=r^\beta e^{-r/a_0}\\ \bar{\psi}^{(2)}_{k_0}&=\frac{-i\gamma}{1+(1-\gamma^2)^{1/2}}P_1{}^1r^\beta e^{-r/a_0} & \psi^{(4)}_{k_0}&=0\end{aligned} \tag{63}$$

or

$$\begin{aligned}\bar{\psi}^{(1)}_{k_0}&=\frac{-i\gamma}{1+(1-\gamma^2)^{1/2}}P_1{}^{-1}r^\beta e^{-r/a} & \bar{\psi}^{(3)}_{k_0}&=0\\ \bar{\psi}^{(2)}_{k_0}&=\frac{-i\gamma}{1+(1-\gamma^2)^{1/2}}P_1{}^0r^\beta e^{-r/a_0} & \bar{\psi}^{(4)}_{k_0}&=-r^\beta e^{-r/a_0}\end{aligned} \tag{64}$$

In the equations above β denotes $(1-\gamma^2)^{1/2}-1$ and a_0 is equal to a/Z where a is the radius of the first Bohr orbit.

Accordingly either

$$\begin{aligned}\frac{\partial\bar{\psi}^{(1)}_{k_0}}{\partial x}&=\frac{-i\gamma}{1+(1-\gamma^2)^{1/2}}\frac{\partial}{\partial r}(r^{\beta-1}e^{-r/a_0})P_1{}^0r\sin\theta\cos\phi & (rP_1{}^0=z)\\ \frac{\partial\bar{\psi}^{(2)}_{k_0}}{\partial x}&=\frac{-i\gamma}{1+(1-\gamma^2)^{1/2}}\frac{\partial}{\partial r}(r^{\beta-1}e^{-r/a_0})P_1{}^1r\sin\theta\cos\phi-\frac{i\gamma}{1+(1-\gamma^2)^{1/2}}r^{\beta-1}e^{-r/a_0}\\ \frac{\partial\bar{\psi}^{(3)}_{k_0}}{\partial x}&=\frac{\partial}{\partial r}(r^\beta e^{-r/a_0}) & (rP_1{}^1=x+iy)\\ \frac{\partial\bar{\psi}^{(4)}_{k_0}}{\partial x}&=0\end{aligned} \tag{65}$$

[13] P. A. M. Dirac, Proc. Roy. Soc. **117,** 680 (1928).
[14] C. G. Darwin, l. c.

or

$$\frac{\partial \bar{\psi}^{(1)}_{k_0}}{\partial x} = -\frac{i\gamma}{1+(1-\gamma^2)^{1/2}} \frac{\partial}{\partial r}(r^{\beta-1}e^{-r/a_0}) P_1^{-1} r \sin\theta\cos\phi + \frac{i\gamma}{1+(1-\gamma^2)^{1/2}} r^{\beta-1}e^{-r/a_0}$$

$$\frac{\partial \bar{\psi}^{(2)}_{k_0}}{\partial x} = -\frac{i\gamma}{1+(1-\gamma^2)^{1/2}} \frac{\partial}{\partial r}(r^{\beta-1}e^{-r/a_0}) P_1^{0} r \sin\theta\cos\phi \qquad (-rP_1^{-1} = x - iy) \tag{66}$$

$$\frac{\partial \bar{\psi}^{(3)}_{k_0}}{\partial x} = 0$$

$$\frac{\partial \bar{\psi}^{(4)}_{k_0}}{\partial x} = -\frac{\partial}{\partial r}(r^{\beta}e^{-r/a_0}).$$

These two possibilities will be considered separately.

The integrals in Eq. (61) differ from zero only for certain definite values of k and m. The next step of the computations consists in determining these values.

On account of the appearance of the factor $e^{2\pi iz/\lambda}$ in the integrands there are two possible ways of performing the computations. Either as Sommerfeld has done, one can develop the function $e^{2\pi ir\cos\theta/\lambda}$ into a series of powers of $^{r\cos\theta/\lambda}$ and then can calculate the possible values of the coefficients $A_{km}(E')$ on the basis of this expansion or one can start from the function $e^{2\pi ir\cos\theta/\lambda}$ itself. This last method was used recently by Carrelli.[15] Both these methods lead to the same results on account of the absolute and uniform convergence of the series

$$1+\frac{x}{1!}+\frac{x^2}{2!}+\frac{x^3}{3!}+\cdots \tag{67}$$

for all points of the x plane. The series (67) can be therefore integrated term by term, which gives the same result as the integration of the function e^x itself. The same applies to the products of the exponential by various spherical harmonics and the products of the expansion (67) by these harmonics.

Carrelli finds the coefficients $A_{km}(E')$ in the form of the functions of a quantity R equal to

$$\lambda/2\pi\ (1/a_0+iAB)$$

and then develops these functions into series of R. Sommerfeld's method leads immediately to the power series of R as the value for $A_{km}(E')$. It is obvious that both these power series are identical.

Carrelli has computed only the coefficients $A_{11}(E')$ and $A_{21}(E')$ on the basis of the Schrödinger equation and in his calculations took into account only the first two terms of the power series expansions for each of these coefficients. These terms were of the order of $1/R^2$ and $1/R^4$ for the coefficient $A_{11}(E')$ and of the orders of $1/R^3$ and $1/R^5$ for the coefficient $A_{21}(E')$.

[15] A. Carrelli, Zeits. f. Phys. **56**, 694 (1929).

To be consistent Carrelli should also find the first term of the expansion, which corresponds to the coefficient $A_{31}(E')$, whose order is $1/R^4$ and the first term of the expansion for $A_{41}(E')$ which is of the order of $1/R^5$. These last two terms were neglected by Carrelli and this invalidates his result. To appreciate the influence of the above mentioned terms one has to consider that in Carrelli's case the perturbed wave function can be written in the form

$$\psi = A_{11}Q_1^1 \cos\phi + A_{21}Q_2^1 \cos\phi + A_{31}Q_{31}^1 \cos\phi + A_{41}Q_4^1 \cos\phi \tag{68}$$

where Q_k^m denote the spherical harmonics used by Carrelli. The values of the harmonics in (68) are

$$\begin{aligned} Q_1^1 &= \sin\theta & Q_2^1 &= 3\sin\theta\cos\theta \\ Q_3^1 &= (3/2)\sin\theta(5\cos^2\theta - 1) & Q_4^1 &= (5/2)\sin\theta\cos\theta(7\cos^2\theta - 3) \end{aligned} \tag{69}$$

whence

$$\psi = \sin\theta\cos\phi\left\{A_{11} + 3A_{21}\cos\theta + \frac{15}{2}A_{31}\cos^2\theta - \frac{3}{2}A_{31} + \frac{35}{2}\cos^3\theta A_{41} - \frac{15}{2}A_{41}\cos\theta\right\}. \tag{70}$$

It follows, that the terms omitted by Carrelli were

$$-\frac{3}{2}A_{31} \quad \text{and} \quad -\frac{15}{2}A_{41}\cos\theta.$$

In the present paper Sommerfeld's method of computation will be used. To obtain the degree of approximation comparable with that of Carrelli the exponential $e^{2\pi ir\cos\theta/\lambda}$ will be developed into a power series, whose first four terms will be retained. Thus

$$e^{2\pi ir\cos\theta/r} = 1 + \frac{2\pi ir}{\lambda}\cos\theta - \frac{2\pi^2 r^2}{\lambda^2}\cos^2\theta - \frac{4\pi^3 ir^3}{3\lambda^3}\cos^3\theta. \tag{71}$$

To find the values of k and m for which Eq. (61) differs from zero it is sufficient to take into account the orthogonality relations for the functions P_k^m, as Sommerfeld has done. Those relations are

$$\int_0^{\pi}\int_0^{2\pi} P_k^m P_l^{n*}\sin\theta d\theta d\phi = 0 \begin{pmatrix} k \neq l \\ m \neq n \end{pmatrix}. \tag{72}$$

Furthermore in Eqs. (65) and (66) $\frac{1}{2}(e^{i\phi} + e^{-i\phi})$ can be written instead of $\cos\phi$. The values of the functions P_k^m for those values of k and m which enter into consideration in this paper are given below

$$\begin{aligned} P_0^0 &= 1 & P_1^1 &= \sin\theta e^{i\phi} \\ P_1^0 &= \cos\theta & P_2^1 &= 3\sin\theta\cos\theta e^{i\phi} \\ P_2^0 &= 3\cos^2\theta - 1 & P_3^1 &= 3\sin\theta(5\cos^2\theta - 1)e^{i\phi} \end{aligned}$$

$$P_3^0 = 3(5\cos^3\theta - 3\cos\theta) \qquad P_4^1 = 15\sin\theta(7\cos^3\theta - 3\cos\theta)e^{i\phi}$$
$$P_4^0 = 3(35\cos^4\theta - 30\cos^2\theta + 3) \tag{73}$$
$$P_2^2 = 3\sin^2 e^{2i\phi}$$
$$P_3^2 = 15\sin^2\theta\cos\theta e^{2i\phi}$$
$$P_4^2 = 15\sin^2\theta(7\cos^2\theta - 1)e^{2i\phi}.$$

It will be supposed now that the initial state of the atom is given by Eqs. (63) and (65). The two types of the solutions, given by the Eqs. (41) and (42) have to be considered separately. The reasoning quite similar to that of Sommerfeld shows that for the solution (41) the coefficients $A'_{km}(E')$ (the accent is used to denote the first type of the solution) are different from zero for

$$\begin{aligned} &k=0 \quad m=-1 && k=3 \quad m=\pm 1 \\ &k=1 \quad m=\pm 1 && k=4 \quad m=\pm 1 \\ &k=2 \quad m=\pm 1 \end{aligned} \tag{74}$$

Similarly for the solution (42) the coefficients $A''_{km}(E')$ (two accents denote the second type of solution) are different from zero for

$$\begin{aligned} &k=1 \quad m=-1 && k=4 \quad m=\pm 1 \\ &k=2 \quad m=\pm 1 && k=5 \quad m=\pm 1 \\ &k=3 \quad m=\pm 1 \end{aligned} \tag{75}$$

It is to be noted that for the term $-4\pi^3 ir^3\cos^3\theta/3\lambda^3$ in the expansion (71) only the integrals in Eq. (61) with the greatest absolute value were taken into account.

For the sake of brevity the following notations are used in the subsequent calculations (κ is equal to AB).

$$\int_0^\infty \frac{\partial}{\partial r}(r^{\beta-1}e^{-r/a_0})e^{-i\kappa r}r^2dr = Q_1 \tag{76}$$

$$\int_0^\infty \frac{\partial}{\partial r}(r^{\beta-1}e^{-r/a_0})e^{-i\kappa r}r^3dr = Q_2 \tag{77}$$

$$\int_0^\infty \frac{\partial}{\partial r}(r^{\beta-1}e^{-r/a_0})e^{-i\kappa r}r^4dr = Q_3 \tag{78}$$

$$\int_0^\infty r^\beta e^{-r/a_0}e^{-i\kappa r}dr = Q_4 \tag{79}$$

$$\int_0^\infty r^\beta e^{-r/a_0}e^{-i\kappa r}rdr = Q_5 \tag{80}$$

$$\int_0^\infty r^\beta e^{-r/a_0}e^{-i\kappa r}r^2dr = Q_6 \tag{81}$$

$$\int_0^\infty \frac{\partial}{\partial r}(r^\beta e^{-r/a_0})e^{-i\kappa r}rdr = Q_7 \tag{82}$$

$$\int_0^\infty \frac{\partial}{\partial r}(r^\beta e^{-r/a_0})e^{-i\kappa r}r^2dr = Q_8 \tag{83}$$

$$\int_0^\infty \frac{\partial}{\partial r}(r^\beta e^{-r/a_0})e^{-i\kappa r}r^3dr = Q_9 \tag{84}$$

$$\int_0^\infty \frac{\partial}{\partial r}(r^\beta e^{-r/a_0})e^{-i\kappa r}r^4dr = Q_{10}. \tag{85}$$

If the values (73) of the spherical harmonics and the normalizing integrals (49) and (50) are taken into account then with regard to Eq. 61 it follows after some easy calculations that

$$A'_{0,-1}(E')=\frac{\pi}{\lambda}Q_5\left(i+\frac{\gamma p}{6}\right)+\frac{\pi^2}{3\lambda^2}Q_6(2p+i\gamma) \tag{86}$$

$$A'_{1,1}(E')=-\frac{i\gamma p}{12}Q_1+\frac{\pi^2}{30\lambda^2}i\gamma pQ_3+\frac{Q_7}{6}-\frac{\pi^2}{15\lambda^2}Q_9+\frac{i\pi^2}{15\lambda^2}\gamma pQ_6-\frac{\pi\gamma}{6\lambda}Q_5 \tag{87}$$

$$A'_{1,-1}(E')=\frac{i\gamma p}{12}Q_1-\frac{\pi^2}{30\lambda^2}i\gamma pQ_3-\frac{Q_7}{6}+\frac{\pi^2}{15\lambda^2}Q_9-\frac{2\pi^2}{3\lambda^2}Q_6+\frac{\pi\gamma}{6\lambda}Q_5 \tag{88}$$

$$A'_{2,1}(E')=\frac{\pi\gamma p}{30\lambda}Q_2+\frac{i\pi}{\lambda}Q_8-\frac{\pi^2}{15\lambda^2}i\gamma Q_6-\frac{2i\pi^3}{105\lambda^3}Q_{10} \tag{89}$$

$$A'_{3,1}(E')=\frac{\pi^2}{210\lambda^2}i\gamma pQ_3-\frac{\pi^2}{105\lambda^2}Q_9 \tag{90}$$

$$A'_{2,-1}(E')=-\frac{\pi\gamma p}{30\lambda}Q_2-\frac{i\pi}{\lambda}Q_8+\frac{\pi^2}{15\lambda^2}i\gamma Q_6+\frac{2i\pi^3}{105\lambda^3}Q_{10} \tag{91}$$

$$A'_{3,-1}(E')=-\frac{\pi^2}{210\lambda^2}i\gamma pQ_3+\frac{\pi^2}{105\lambda^2}Q_9 \tag{92}$$

$$A'_{4,1}(E')=-\frac{2i\pi^3}{2835\lambda^3}Q_{10} \tag{93}$$

$$A'_{4,-1}(E')=\frac{2i\pi^3}{2835\lambda^3}Q_{10} \tag{94}$$

$$A''_{1,-1}(E')=\frac{i\gamma p}{6}Q_1-\frac{\pi^2}{15\lambda^2}i\gamma pQ_3+\frac{i\gamma p}{2}Q_4-\frac{Q_7}{3}+\frac{2\pi^2}{15\lambda^2}Q_9+\frac{2\pi^2}{3\lambda^2}Q_6+\frac{\pi}{\lambda}Q_5\left(ip-\frac{\gamma}{6}\right) \tag{95}$$

$$A''_{2,1}(E')=\frac{\pi\gamma p}{30\lambda}Q_2+\frac{i\pi}{15\lambda}Q_8+\frac{\pi\gamma p}{6\lambda}Q_5-\frac{\pi^2}{15\lambda^2}i\gamma A_6-\frac{2i\pi^3}{105\lambda^3}Q_{10} \tag{96}$$

$$A''_{2,-1}(E')=-\frac{\pi\gamma p}{30\lambda}Q_2-\frac{\pi\gamma p}{6\lambda}Q_5-\frac{i\pi}{5\lambda}Q_8-\frac{2\pi^2}{3\lambda^2}Q_6(p+i\gamma)+\frac{2i\pi^3}{35\lambda^3}Q_{10} \tag{97}$$

$$A''_{3,1}(E')=\frac{\pi^2 i\gamma p}{105\lambda^2}Q_3-\frac{2\pi^2}{105\lambda^2}Q_9+\frac{\pi^2}{15\lambda^2}i\gamma pQ_6 \tag{98}$$

$$A''_{3,-1}(E')=-\frac{2\pi^2}{105\lambda^2}i\gamma pQ_3+\frac{4\pi^2}{105\lambda^2}Q_9 \tag{99}$$

$$A''_{4,1}(E')=-\frac{2i\pi^3}{945\lambda^3}Q_{10} \tag{100}$$

$$A''_{4,-1}(E')=\frac{2i\pi^3}{567\lambda^3}Q_{10} \tag{101}$$

$$\left.\begin{aligned}A''_{5,1}(E')&=0\\A''_{5,-1}(E')&=0\end{aligned}\right\} \tag{102}$$

If it is taken into account that

$$\frac{\partial}{\partial r}(r^{\beta}e^{-r/a_0}) = \left(\beta r^{\beta-1} - \frac{r^{\beta}}{a_0}\right)e^{-r/a_0} \tag{103}$$

and

$$\frac{\partial}{\partial r}(r^{\beta-1}e^{-r/a_0}) = \left((\beta-1)r^{\beta-2} - \frac{r^{\beta-1}}{a_0}\right)e^{-r/a_0} \tag{104}$$

then with the notation $q = 1/a_0 + i\kappa$ and

$$S = \int_0^{\infty} r^{\beta}e^{-qr}dr \tag{105}$$

it can be shown by integration by parts that

$$Q_1 = -\frac{S}{a_0 q}(1+a_0 q) \qquad (106)$$

$$Q_2 = -\frac{S}{a_0 q^2}(2+a_0 q) \qquad (107)$$

$$Q_3 = -\frac{2S}{a_0 q^3}(3+a_0 q) \qquad (108)$$

$$Q_4 = S \qquad (109)$$

$$Q_5 = \frac{S}{q} \qquad (110)$$

$$Q_6 = \frac{2S}{q^2} \qquad (111)$$

$$Q_7 = -\frac{S}{a_0 q}\left(1+\gamma^2\frac{i a_0 k}{2}\right) \qquad (112)$$

$$Q_8 = -\frac{2S}{a_0 q^2}\left[1+\frac{i\gamma^2}{2}\left(i+\frac{a_0 k}{2}\right)\right] \qquad (113)$$

$$Q_9 = -\frac{6S}{a_0 q^3} \qquad (114)$$

$$Q_{10} = -\frac{24S}{a_0 q^4} \qquad (115)$$

The expressions (106) (115) were simplified by taking into account the fact that β is equal to $(1-\gamma^2)^{1/2}-1$ or approximately to $-\gamma^2/2$ and is therefore very small. Accordingly it was put equal to zero in all the Q's with the exception of Q_7 and Q_8 whose values, on the evidence of the expressions (86)-(102) are the most important ones. Therefore in the expressions (112) and (113) β was put equal to $-\gamma^2/2$.

On the basis of Eqs. (41) and (42) together with (40) one can write if the radial parts of the functions $\psi_{km}(E')$ which are common to all terms on account of the expressions (60), are omitted

$$\begin{aligned}
\bar{\psi}_3 \sim\ & A'_{0,-1}(E')(0-1+1)P_0^{-1} + A'_{1,-1}(E')(1-1+1)P_1^{-1} \\
& + A'_{1,1}(E')(1+1+1)\cdot P_1^{1} + A_{2,1}(E')(2+1+1)P_2^{1} + A'_{2,-1}(E')(2-1+1)P_2^{-1} \\
& + A'_{3,1}(E')(3+1+1)P_3^{1} + A'_{3,-1}(E')(3-1+1)P_3^{-1} + A'_{4,1}(E')(4+1+1)\cdot P_4^{1} \\
& + A'_{4,-1}(E')(4-1+1)P_4^{-1} + A''_{1,-1}(E')P_1^{-1} + A''_{2,1}(E')P_2^{1} \\
& + A''_{2,-1}(E')P_2^{-1} + A''_{3,1}(E')P_3^{1} + A''_{3,-1}(E')P_3^{-1} + A''_{4,1}(E')P_4^{1} \\
& + A''_{4,-1}(E')P_4^{-1} = P_1^{1}\cdot 3A'_{1,1}(E') + P_1^{-1}[A'_{1,-1}(E') + A''_{1,-1}(E')] \\
& + P_2^{1}[4A'_{2,1}(E') + A''_{2,1}(E')] + P_2^{-1}[2A'_{2,-1}(E') + A''_{2,-1}(E')] \\
& + P_3^{1}[5A'_{3,1}(E') + A''_{3,1}(E')] + P_3^{-1}[3A'_{3,-1}(E') + A''_{3,-1}(E')] \\
& + P_4^{1}[6A'_{4,1}(E') + A''_{4,1}(E')] + P_4^{-1}[4A'_{4,-1}(E') + A''_{4,-1}(E')].
\end{aligned} \tag{116}$$

and

$$\begin{aligned}\psi_4 \sim & A'_{0,-1}(E')(0-1)P_0{}^0+A'_{1,1}(E')(-1+1)P_1{}^2+A'_{1,-1}(E')(-1-1)P_1{}^0\\ & +A'_{2,1}(E')(-2+1)P_2{}^2+A'_{2,-1}(E')(-2-1)\cdot P_2{}^0+A'_{3,1}(E')(-3+1)P_3{}^2\\ & +A'_{3,-1}(E')(-3-1)P_3{}^0+A'_{4,1}(E')(-4+1)P_4{}^2+A'_{4,-1}(E')(-4-1)P_4{}^0\\ & +A''_{1,-1}(E')P_1{}^0+A''_{2,1}(E')P_2{}^2+A''_{2,-1}(E')P_2{}^0+A''_{3,1}(E')P_3{}^2+A''_{3,-1}(E')P_3{}^0\\ & +A''_{4,1}(E')P_4{}^2+A''_{4,-1}(E')P_4{}^0=-P_0{}^0A'_{0,-1}(E')+P_1{}^0[A''_{1,-1}(E')\\ & -2A'_{1,-1}(E')]+P_2{}^0[A''_{2,-1}(E')-3A'_{2,-1}(E')]+P_2{}^2[A''_{2,1}(E')-A'_{2,1}(E')]\\ & +P_3{}^0[A''_{3,-1}(E')-4A'_{3,-1}(E')]+P_3{}^2[A''_{3,1}(E')-2A'_{3,1}(E')]\\ & +P_4{}^0[A''_{4,-1}(E')-5A'_{4,-1}(E')]+P_4{}^2[A''_{4,1}(E')-3A'_{4,1}(E')].\end{aligned} \tag{117}$$

With regard to $\bar{\psi}_1$ and $\bar{\psi}_2$ it is to be remembered that they are small, of the order of p, when compared with $\bar{\psi}_3$, $\bar{\psi}_4$. Therefore it is sufficient to compute for them only the terms with the greatest absolute values and hence only the terms with the coefficients $A'_{1,-1}(E')$, $A'_{1,1}(E')$ and $A''_{1,-1}(E')$ are considered. Thus

$$\begin{aligned}\bar{\psi}_1 &= -p\{P_2{}^1A'_{1,1}(E')+P_2{}^{-1}A'_{1,-1}(E')+P_0{}^{-1}(1-1)A''_{1,-1}(E')\}\\ &= -p\{P_2{}^1A'_{1,1}(E')+P_2{}^{-1}A'_{1,-1}(E')\}\end{aligned} \tag{118}$$

and

$$\begin{aligned}\bar{\psi}_2 &= -p\{P_2{}^2A'_{1,1}(E')+P_2{}^0A'_{1,-1}(E')+P_0{}^0(-1-1+1)A''_{1,-1}(E')\}\\ &= -p\{P_2{}^2A'_{1,1}(E')+P_2{}^0A'_{1,-1}(E')-P_0{}^0A''_{1,-1}(E')\}.\end{aligned} \tag{119}$$

If Eqs. (86) (102) and (106) (115) are taken into account and substituted into Eqs. (116) (119) then after some calculation

$$\bar{\psi}_1 = -p\sin\theta\cos\theta\cos\phi \tag{120}$$

$$\bar{\psi}_2 = -p\sin^2\theta\cos\phi e^{i\phi} \tag{121}$$

$$\begin{aligned}\bar{\psi}_3 = & \left(1+\gamma^2\frac{ia_0\kappa}{2}\right)\sin\theta\cos\phi-\frac{i\gamma p}{2}(1+a_0q)\sin\theta\cos\phi+\frac{i\gamma pa_0q}{2}\sin\theta e^{-i\phi}\\ & +\frac{4\pi i}{\lambda q}\sin\theta\cos\theta\cos\phi\left[1+\frac{i\gamma^2}{2}\left(i+\frac{a_0\kappa}{2}\right)\right]+\frac{\pi\gamma p}{\lambda q}(2+a_0q)\sin\theta\cos\theta\cos\phi\\ & -\frac{\pi\gamma a_0}{\lambda}\sin\theta\cos\theta\cos\phi-\frac{12\pi^2}{\lambda^2q^2}\sin\theta\cos^2\theta\cos\phi\\ & +\frac{2\pi^2}{\lambda^2q^2}(3+a_0q)i\gamma p\sin\theta\cos^2\theta\cos\phi-\frac{2\pi^2}{\lambda^2}\frac{a_0}{q}i\gamma p\sin\theta\cos^2\theta e^{i\phi}\\ & +\frac{\pi a_0}{2\lambda}\sin\theta(\gamma e^{i\phi}+2ipe^{-i\phi})-\frac{2\pi^2}{\lambda^2}\frac{a_0}{q}\sin\theta\cos\theta(2pe^{-i\phi}-i\gamma e^{i\phi})\\ & -\frac{32i\pi^3}{\lambda^3q^3}\sin\theta\cos^3\theta\cos\phi\end{aligned} \tag{122}$$

$$\psi_4=\frac{\pi i a_0}{\lambda}-\frac{i\gamma p a_0 q}{2}\cos\theta. \tag{123}$$

In the Eq. (123) only the terms with the greatest absolute values were taken into account, the rest can be safely omitted to the present approximation. Moreover in all the four Eqs. (120)-(123) the common factor $-S/a_0 q$ was omitted.

The Eqs. (120), (121), (122) and (123) represent a spherical material wave diverging from the considered atom, whose amplitude depends upon the direction in space. This can be seen at once if one takes into account the neglected common radial factors. Therefore the spatial distribution of the photoelectrons (whose kinetic energy and velocity do not depend upon the direction of emission as can be seen from the foregoing discussion) is given by the intensity of these waves or by the density of electric charge emitted in a considered direction, which is equal to

$$-e\phi\bar{\psi}=-e(\bar{\phi}_1\bar{\psi}_1+\bar{\phi}_2\bar{\psi}_2+\bar{\phi}_3\bar{\psi}_3+\bar{\phi}_4\bar{\psi}_4). \tag{10}$$

It is to be remembered that ϕ is conjugate complex with regard to ψ. According to the relations (120)-(123)

$$\begin{aligned}
\phi\psi\sim{}& p^2\sin^2\theta\cos^2\phi+\frac{\pi^2 a_0^2}{\lambda^2}+\frac{\gamma^2 p^2}{4}a_0^2 qq^*\cos^2\theta-\frac{\pi a_0^2}{2\lambda}\gamma p(q+q^*)\cos\theta\\
&+\sin^2\theta\cos^2\phi+\frac{16\pi^2}{\lambda^2 qq^*}\sin^2\theta\cos^2\theta\cos^2\phi-\frac{4\pi i}{\lambda qq^*}(q-q^*)\sin^2\theta\cos\theta\cos^2\phi\\
&+\frac{2\pi a_0 k\gamma^2}{\lambda qq^*}(q+q^*)\sin^2\theta\cos\theta\cos^2\phi+\left[\frac{2\pi i\gamma^2}{\lambda qq^*}(q-q^*)\right.\\
&\left.-\frac{\pi\gamma^2 a_0\kappa}{\lambda qq^*}(q+q^*)\right]\sin^2\theta\cos\theta\cos^2\phi-\frac{12\pi^2}{\lambda^2 q^2 q^{*2}}(q^2+q^{*2})\sin^2\theta\cos^2\theta\cos^2\phi\\
&+\frac{a_0 i\gamma p}{2}(q^*-q)\sin^2\theta\cos^2\phi+\frac{2\pi\gamma p}{\lambda}\left(a_0+\frac{q+q^*}{qq^*}\right)\sin^2\theta\cos\theta\cos^2\phi\\
&-\frac{2\pi a_0\gamma}{\lambda}\sin^2\theta\cos^2\theta\cos^2\phi+\frac{i\gamma p a_0}{2}(qe^{-i\phi}-q^*e^{i\phi})\sin^2\theta\cos\phi\\
&+\frac{\pi a_0}{\lambda}(\gamma\cos\phi+2p\sin\phi)\sin^2\theta\cos\phi+\frac{6\pi^2 i}{\lambda^2 q^2 q^{*2}}(q^{2*}-q^2)\gamma p\sin^2\theta\cos^2\theta\cos^2\phi\\
&-\frac{2\pi^2}{\lambda^2}\frac{a_0 i\gamma p}{qq^*}(q-q^*)\sin^2\theta\cos^2\theta\cos^2\phi-\frac{4\pi^2}{\lambda^2}\frac{a_0 p}{qq^*}\cdot(qe^{i\phi}+q^*e^{-i\phi})\sin^2\theta\cos^2\theta\cos\phi\\
&+\frac{2\pi^2}{\lambda^2}\frac{a_0 i\gamma}{qq^*}(q^*e^{i\phi}-qe^{-i\phi})\sin^2\theta\cos^2\theta\cos\phi\\
&+\frac{32}{\lambda^3(qq^*)^3}i\pi^3(q^3-q^{*3})\sin^2\theta\cos^3\theta\cos^2\phi
\end{aligned} \tag{124}$$

$$-\frac{2\pi^2 a_0 i\gamma p}{\lambda^2}\sin^2\theta\cos^2\theta\cos\phi(e^{-i\phi}/q-e^{-i\phi}/q^*)$$

$$+\frac{48i\pi^3}{\lambda^3 qq^*}\left(\frac{1}{q}-\frac{1}{q^*}\right)\sin^2\theta\cos^3\theta\cos^2\phi\cdot$$

If on the other hand the initial state of the atom is described by Eqs. (64) and (66) then it is found that for the solutions of the type (41) the coefficients $A'_{km}(E')$ are different from zero for

$$\begin{array}{llll} k=0 & m=0 & k=3 & m=0,\ -2 \\ k=1 & m=0,\ -2 & k=4 & m=0,\ -2 \\ k=2 & m=0,\ -2 & & \end{array} \tag{125}$$

whereas for the type (42) $A''_{km}(E')$ differ from zero for

$$\begin{array}{llll} k=1 & m=0 & k=3 & m=0,\ -2 \\ k=2 & m=0,\ -2 & k=5 & m=0,\ -2 \\ k=3 & m=0,\ -2 & & \end{array} \tag{126}$$

After some calculations quite similar to the ones given previously for the foregoing possibility it follows that in this second case

$$\bar{\psi}_1 = p\sin^2\theta\cos\phi e^{-i\phi}$$

$$\bar{\psi}_2 = -p\sin\theta\cos\theta\cos\phi \tag{127}$$

$$\bar{\psi}_3 = \frac{\pi i a_0}{\lambda}-\frac{i\gamma p a_0 q}{2}\cos\theta \tag{128}$$

$$\bar{\psi}_4 = -\left\{\left(1+\frac{\gamma^2 i a_0\kappa}{2}\right)\sin\theta\cos\phi-\frac{i\gamma p}{2}(1+a_0 q)\sin\theta\cos\phi+\frac{i\gamma p a_0 q}{2}\sin\theta e^{i\phi}\right. \tag{129}$$

$$+\frac{4\pi i}{\lambda q}\sin\theta\cos\theta\cos\phi\left[1+\frac{i\gamma^2}{2}\left(i+\frac{a_0\kappa}{2}\right)\right]+\frac{\pi\gamma p}{\lambda q}(2+a_0 q)\sin\theta\cos\theta\cos\phi$$

$$-\frac{\pi\gamma a_0}{\lambda}\sin\theta\cos\theta\cos\phi-\frac{12\pi^2}{\lambda^2 q^2}\sin\theta\cos^2\theta\cos\phi+\frac{2\pi^2}{\lambda^2 q^2}(3+a_0 q)i\gamma p\sin\theta\cos^2\theta\cos\phi$$

$$-\frac{2\pi^2}{\lambda^2}\frac{a_0}{q}i\gamma p\sin\theta\cos^2\theta e^{-i\phi}+\frac{\pi a_0}{2\lambda}\sin\theta(\gamma e^{-i\phi}+2pie^{i\phi}) \tag{130}$$

$$\left.-\frac{2\pi^2}{\lambda^2}\frac{a_0}{q}(2pe^{i\phi}-i\gamma e^{-i\phi})\sin\theta\cos\theta-\frac{32i\pi^3}{\lambda^3 q^3}\sin\theta\cos^3\theta\cos\phi.\right\}$$

Therefore in this case

$$\phi\psi = p^2\sin^2\theta\cos^2\phi+\frac{\pi^2 a_0^2}{\lambda^2}+\frac{\gamma^2 p^2 a_0^2 qq^*}{4}\cos^2\theta-\frac{\pi a_0^2\gamma p}{2\lambda}(q+q^*)\cos\theta$$

$$
\begin{aligned}
&+\sin^2\theta\cos^2\phi+\frac{16\pi^2}{\lambda^2qq^*}\sin^2\theta\cos^2\theta\cos^2\phi-\frac{4\pi i}{\lambda qq^*}(q-q^*)\sin^2\theta\cos\theta\cos^2\phi\\
&+\frac{2\pi a_0\kappa\gamma^2}{\lambda qq^*}(q+q^*)\sin^2\theta\cos\theta\cos^2\phi+\left[\frac{2\pi i\gamma^2}{\lambda qq^*}(q-q^*)\right.\\
&\left.-\frac{\pi\gamma^2a_0\kappa}{\lambda qq^*}(q+q^*)\right]\sin^2\theta\cos\theta\cos^2\phi-\frac{12\pi^2}{\lambda^2(qq^*)^2}(q^2+q^{*2})\sin^2\theta\cos^2\theta\cos^2\phi\\
&+\frac{a_0i\gamma p}{2}(q^*-q)\sin^2\theta\cos^2\phi+\frac{2\pi\gamma p}{\lambda}\left(a_0+\frac{q+q^*}{qq^*}\right)\sin^2\theta\cos\theta\cos^2\phi\\
&-\frac{2\pi\gamma a_0}{\lambda}\sin^2\theta\cos\theta\cos^2\phi+\frac{i\gamma pa_0}{2}(qe^{i\phi}-q^*e^{-i\phi})\sin^2\theta\cos\phi\\
&+\frac{\pi a_0}{\lambda}\sin^2\theta\cos\phi(\gamma\cos\phi-2p\sin\phi)+\frac{6\pi^2i}{\lambda^2(qq^*)^2}(q^{*2}-q^2)\gamma p\sin^2\theta\cos^2\theta\cos^2\phi\\
&+\frac{2\pi^2a_0i\gamma p}{\lambda^2qq^*}(q^*-q)\sin^2\theta\cos^2\theta\cos^2\phi-\frac{4\pi^2}{\lambda^2}\frac{a_0p}{qq^*}(qe^{-i\phi}+q^*e^{i\phi})\sin^2\theta\cos^2\theta\cos\phi\\
&+\frac{2\pi^2}{\lambda^2}\frac{a_0i\gamma}{qq^*}(q^*e^{-i\phi}-qe^{i\phi})\sin^2\theta\cos^2\theta\cos\phi\\
&+\frac{32i\pi^3}{\lambda^3(qq^*)^3}(q^3-q^{*3})\sin^2\theta\cos^3\theta\cos^2\phi\\
&-\frac{2\pi^2a_0i\gamma p}{\lambda^2}\sin^2\theta\cos^2\theta\cos\phi(e^{-i\phi}/q-e^{i\phi}/q^*)\\
&+\frac{48i\pi^3}{\lambda^3qq^*}\left(\frac{1}{q}-\frac{1}{q^*}\right)\sin^2\theta\cos^3\theta\cos^2\phi\cdot
\end{aligned}
\tag{131}
$$

According to G. Wentzel[16] the average of the expressions (124) and (131) is to be taken to find the real spatial distribution of the photoelectrons. Therefore this distribution is given by

$$
\begin{aligned}
\phi\psi\sim{}&p^2\sin^2\theta\cos^2\phi+\frac{\pi^2a_0^2}{\lambda^2}+\frac{\gamma^2p^2a_0^2qq^*}{4}\cos^2\theta-\frac{\pi a_0^2\gamma p}{2\lambda}(q+q^*)\cos\theta\\
&+\sin^2\theta\cos^2\phi+\frac{16\pi^2}{\lambda^2qq^*}\sin^2\theta\cos^2\theta\cos^2\phi-\frac{4\pi i}{\lambda qq^*}(q-q^*)\sin^2\theta\cos\theta\cos^2\phi\\
&+\frac{\pi a_0\kappa\gamma^2}{\lambda qq^*}(q+q^*)\sin^2\theta\cos\theta\cos^2\phi+\frac{2\pi i\gamma^2}{\lambda qq^*}(q-q^*)\sin^2\theta\cos\theta\cos^2\phi\\
&+\frac{a_0i\gamma p}{2}(q^*-q)\sin^2\theta\cos^2\phi-\frac{12\pi^2}{\lambda^2(qq^*)^2}(q^2+q^{*2})\sin^2\theta\cos^2\theta\cos^2\phi
\end{aligned}
$$

[16] G. Wentzel, l. c.

$$-\frac{2\pi\gamma a_0}{\lambda}(1-p)\sin^2\theta\cos\theta\cos^2\phi$$

$$+\frac{2\pi\gamma p}{\lambda}\left(\frac{q+q^*}{qq^*}\right)\sin^2\theta\cos\theta\cos^2\phi+\frac{i\gamma p a_0}{2}(q-q^*)\sin^2\theta\cos\phi \tag{132}$$

$$+\frac{\pi a_0\gamma}{2}\sin^2\theta\cos^2\phi+\frac{6\pi^2 i(q^{*2}-q^2)}{\lambda^2(qq^*)^2}\gamma p\sin^2\theta\cos^2\theta\cos^2\phi$$

$$-\frac{4\pi^2}{\lambda^2}a_0 p\left(\frac{q+q^*}{qq^*}\right)\sin^2\theta\cos^2\theta\cos^2\phi+\frac{2\pi^2}{\lambda^2}\frac{a_0 i\gamma}{qq^*}(q^*-q)\sin^2\theta\cos^2\theta\cos^2\phi$$

$$+\frac{32i\pi^3}{\lambda^3(qq^*)^3}(q^3-q^{*3})\sin^2\theta\cos^3\theta\cos^2\phi$$

$$+\frac{48i\pi^3}{\lambda^3 qq^*}\left(\frac{1}{q}-\frac{1}{q^*}\right)\sin^2\theta\cos^2\theta\cos^2\phi.$$

If the notations used by Sommerfeld are adopted, then

$$a_0=a/Z\ ;\quad q=Z/a+i\kappa\ ;\quad \gamma=\alpha Z \tag{133}$$

and so

$$\begin{gathered} q+q^*=2Z/a\ ;\qquad q-q^*=2i\kappa\ ;\qquad qq^*=Z^2/a^2+\kappa^2\ ; \\ q^2-q^{*2}=4i\kappa Z/a\ ;\ q^2+q^{*2}=2(Z^2/a^2-\kappa^2)\ ;\ q^3-q^{*3}=2i\kappa(3Z^2/a^2-\kappa^2)\ ; \end{gathered} \tag{134}$$

Moreover, according to Eq. (55)

$$p=\frac{B}{A}=\left(\frac{E'-mc^2}{E'+mc^2}\right)^{1/2}=\frac{\kappa}{A^2}\cong\frac{\kappa h}{4\pi mc}=\frac{\alpha\kappa a}{2} \tag{135}$$

but $E'-mc^2$ is equal to the kinetic energy of the photoelectron, $E'\sim mc^2$ and therefore

$$p\cong\left(\frac{mv^2}{4mc^2}\right)^{1/2}=\frac{v}{2c}\,. \tag{136}$$

Substitution of these values into Eq. (132) leads

$$\begin{aligned} \phi\psi\sim&\sin^2\theta\cos^2\phi\left(1+p^2+\frac{\pi a\alpha}{\lambda}\right)+\sin^2\theta\cos\theta\cos^2\phi\left\{\frac{8\pi\kappa}{\lambda(Z^2/a^2+\kappa^2)}\right. \\ &\left.+\frac{2\pi\alpha Z^2}{\lambda(Z^2/a^2+\kappa^2)}\cdot\frac{p}{a}-\frac{2\pi\kappa\gamma^2}{\lambda(Z^2/a^2+\kappa^2)}-\frac{2\pi a\alpha}{\lambda}(1-p)\right\}+\sin^2\theta\cos^2\theta\cos^2\phi \\ &\cdot\left\{\frac{48\pi^2\kappa^2}{\lambda^2(Z^2/a^2+\kappa^2)^2}-\frac{8\pi^2}{\lambda^2(Z^2/a^2+\kappa^2)}+\frac{4\pi^2 a\alpha\kappa}{\lambda^2(Z^2/a^2+\kappa^2)}-\frac{24\pi^2 p a\alpha\kappa Z^2/a^2}{\lambda^2(Z^2/a^2+\kappa^2)^2}\right. \\ &\left.-\frac{8\pi^2 p}{\lambda^2(Z^2/a^2+\kappa^2)}\right\}+\sin^2\theta\cos^3\theta\cos^2\phi\left\{\frac{256\pi^3\kappa^3}{\lambda^3(Z^2/a^2+\kappa^2)^3}-\frac{96\pi^3\kappa}{\lambda^3(Z^2/a^2+\kappa^2)^2}\right\} \\ &+\frac{\pi^2a^2}{Z^2\lambda^2}-\frac{\pi a\alpha p}{\lambda}\cos\theta+\frac{a^2\alpha^2p^2}{4}\left(\frac{Z^2}{a^2}+\kappa^2\right)\cos^2\theta. \end{aligned} \tag{137}$$

According to Sommerfeld and to the Eqs. (47)

$$\kappa=\frac{2\pi mv}{h(1-v^2/c^2)^{1/2}}\,; \qquad a=\frac{h^2}{4\pi^2mc^2} \tag{138}$$

$$\frac{Z^2}{a^2}+\kappa^2=\frac{8\pi^2mv}{h} \tag{139}$$

furthermore

$$p^2\cong\epsilon/2mc^2=(h\nu-I_0)/2mc^2 \quad (I_0-\text{ionization potential}) \tag{140}$$

and

$$\pi a\alpha/\lambda=h\nu/2mc^2\,. \tag{141}$$

If these values are substituted into Eq. (137) then

$$\begin{aligned}\phi\psi=\sin^2\theta\cos^2\phi&\left(1+\frac{h\nu}{mc^2}-\frac{I_0}{2mc^2}\right)+\frac{2v}{c}\left(1-\frac{\alpha^2z^2}{8}+\frac{v^2}{c^2}+\frac{h\nu}{4mc^2}\right.\\&\left.-\frac{h\nu}{c^2mv}\right)\sin^2\theta\cos\theta\cos^2\phi+\frac{3v^2}{c^2}\left(1-\frac{h\nu}{3mv^2}\right)\sin^2\theta\cos^2\theta\cos^2\phi\\&+\frac{4v^3}{c^3}\left(1-\frac{3h\nu}{4mv^2}\right)\sin^2\theta\cos^3\theta\cos^2\phi+\frac{\pi^2a^2}{Z^2\lambda^2}-\frac{h\nu}{4mc^2}\cdot\frac{v}{c}\cos\theta\\&+\frac{h\nu}{8mc^2}\,\frac{v^2}{c^2}\cos^2\theta\,.\end{aligned} \tag{142}$$

The term $-\alpha^2Z^2/4$ in the parenthesis after $3v^2/c^2$ was omitted, because other terms of the same order have been also omitted for the present approximation.

If the right side of the Eq. (142) is divided by $1+h\nu/mc^2-I_0/2mc^2$ then to the same degree of approximation

$$\begin{aligned}\phi\psi=\sin^2\theta\cos^2\phi&\left\{1+\frac{2v}{c}\left(1-\frac{\alpha^2Z^2}{8}+\frac{I_0}{2mc^2}+\frac{v^2}{2c^2}-\frac{3h\nu}{4mc^2}-\frac{1}{2}\,\frac{h\nu}{cmv}\right)\cos\theta\right.\\&\left.+\frac{3v^2}{c^2}\left(1-\frac{h\nu}{3mv^2}\right)\cos^2\theta+\frac{4v^3}{c^3}\left(1-\frac{3h\nu}{4mv^2}\right)\cos^3\theta\right\}\\&+\frac{\pi^2a^2}{Z^2\lambda^2}-\frac{h\nu}{4mc^2}\,\frac{v}{c}\cos\theta+\frac{h\nu}{8mc^2}\,\frac{v^2}{c^2}\cos^2\theta\end{aligned} \tag{143}$$

On the basis of Eq. (143) one can calculate, as Sommerfeld has done, the angle of the cone surrounding the z axis inside of which half of the electrons are emitted. Then to Sommerfeld's degree of approximation

$$\theta=\pi/2-v/2c\,. \tag{144}$$

This result agrees with the elementary calculation of the basis of the quantum hypothesis.[17] Sommerfeld's result differs by the factor 9/5 before

[17] A. H. Compton, X-rays and Electrons, London, 1927, p. 240.

$-v/2c$ which is due, as can be seen by repeating his calculations, to the neglecting of the normalizing factors for the spherical harmonics. Thus, instead of the harmonics

$$P_k^m(\cos\theta) \tag{145}$$

in the formula (4) on the 210th page of the "Wellenmechanisches Ergänzungsband," the functions

$$\left[\frac{(k-m)!}{(k+m)!}\,\frac{2k+1}{2}\right]^{1/2} P_k^m(\cos\theta) \tag{146}$$

ought to be used, otherwise the formula (7) on the page 212 is not correct. The same remark applies to the result of Carrelli.

To calculate the angle θ with a higher degree of accuracy one can start from the equation given by Sommerfeld

$$\int_0^{2\pi}\int_0^{\theta}\phi\psi\,\sin\theta d\theta d\phi = \int_0^{2\pi}\int_0^{\pi}\phi\psi\,\sin\theta d\theta d\phi. \tag{147}$$

To simplify the notations the relation (143) can be written in the form

$$\phi\psi = \sin^2\theta\cos^2\phi(1+b\cos\theta+c\cos^2\theta+d\cos^3\theta)+A-B\cos\theta+C\cos^2\theta. \tag{148}$$

Eq. (147) leads then to

$$2\cos\theta+4A\cos\theta+b\cos^2\theta-\frac{2\cos^3\theta}{3}=\frac{b}{2}+\frac{d}{6}-2B. \tag{149}$$

If it is supposed that θ is equal to $\pi/2-x$, then from (149) it follows that

$$\sin x=\frac{b}{4}+\frac{d}{12}-B-\frac{5b^2}{192}-\frac{Ab}{2} \tag{150}$$

whence, on account of (143)

$$\sin x=\frac{v}{2c}\left(1-\frac{\alpha^2Z^2}{8}+\frac{I_0}{2mc^2}+\frac{3v^2}{4c^2}-\frac{7h\nu}{4mc^2}-\frac{1}{2}\,\frac{h\nu}{cmv}-\frac{2\pi^2a^2}{Z^2\lambda^2}\right). \tag{151}$$

If it is supposed that the photoelectrons are emitted from the K-level only, which conforms with the initial assumptions in this paper then

$$\frac{I_0}{2mc^2}=\frac{RhZ^2}{2mc^2}=\frac{\alpha^2Z^2}{4} \tag{152}$$

and so Eq. (151) can be written in the following form

$$\sin x=\frac{v}{2c}\left(1-\frac{5\alpha^2Z^2}{8}-\frac{h\nu}{4mc^2}-\frac{1}{2}\,\frac{h\nu}{cmv}-\frac{2\pi^2a^2}{Z^2\lambda^2}\right). \tag{153}$$

According to Birge[18] $\alpha=7.283\times10^{-3}$ and $h/mc=0.02428$A. If moreover the value of λ is given in Ångström units, then finally

[18] R. T. Birge, Phys. Rev. Suppl., July 1929.

$$\sin x=\frac{v}{2c}\left(1-3{,}53.10^{-5}Z^2-\frac{v}{4c}-\frac{0.006}{\lambda}-\frac{5.50}{Z^2\lambda^2}\right). \tag{154}$$

Eq. (154) shows that the increase of the frequency of the incident radiation causes a decrease of $\sin x$ from the value $v/2c$. However, this effect becomes appreciable only for very high frequencies such as correspond to very hard x-rays, and γ-rays. This does not apply to the last term in the brackets, namely $5.50/Z^2\lambda^2$, which becomes of importance even for ordinary x-rays in the case of low values of Z. Therefore for helium and especially for hydrogen the value of $\sin x$ should be markedly less than $v/2c$. For both these gases and for x-rays of the order of 1Å the coefficient A in Eq. (149) becomes of the order of unity and so instead of Eq. (159) it follows that

$$\sin x=\frac{b}{4(1+2A)}\left\{1+\frac{d}{36}-\frac{4B}{6}-\frac{b^2}{48}\frac{(5+12A)}{(1+2A)^3}\right\} \tag{155}$$

whence finally

$$\sin x=\frac{v}{2c(1+2A)}\left\{1-3.77\times10^{-5}Z^2-\frac{v}{4c}-\frac{0.002}{\lambda}-\frac{v^2}{12c^2}\frac{5+12A}{(1+2A)^3}\right\} \tag{156}$$

where

$$A=\frac{\pi^2a^2}{Z^2\lambda^2}=\frac{2.75}{Z^2\lambda^2}\,. \tag{157}$$

The formulas (154) and (156) do not agree with the results obtained recently by Williams, Nuttall and Barlow[19] but they represent fairly well the results of other authors.[20] However, the experimental methods used to find the spatial distribution of photoelectrons cannot as yet claim a high degree of accuracy and it seems therefore well to wait for a final decision till more experimental data are available.

It is to be noted that the angle of the maximum emission of photoelectrons does not coincide with the above computed $\theta=\pi/2-x$. This angle can be calculated from the formula

$$\frac{d}{d\theta}(\phi\psi)=0. \tag{158}$$

In the first approximation this leads to the value

$$\theta_1=\pi/2-v/c \tag{159}$$

which differs from the corresponding value of Sommerfeld

$$\theta_1=\pi/2-9v/5c \tag{159'}$$

by the disappearance of the factor 9/5.

[19] E. J. Williams, Nature, **121,** 134 (1928). E. J. Williams, J. M. Nuttall and H. S. Barlow, Proc. Roy. Soc. **121,** 611 (1928).

[20] A. Sommerfeld, l.c. p. 225, fig. 20.

In the second approximation it can be found that according to Eqs. (158) and (148)

$$\theta_1 = \pi/2 - x_1$$

where

$$\sin x_1 = \frac{b}{2} + \frac{cb}{2} - \frac{5b^3}{16} - \frac{B/\cos^2\phi}{2} \qquad (160)$$

or according to Eqs. (148) and (143)

$$\sin x_1 = \frac{v}{c}\left\{1 - \frac{11h\nu}{4mc^2} + \frac{5\alpha^2 Z^2}{8} + \frac{1}{2}\,\frac{h\nu}{cmv} - \frac{h\nu}{8mc^2}\,\frac{1}{\cos^2\phi}\right\}. \qquad (161)$$

Hence finally by using the formerly given values of h/mc and α

$$\sin x_1 = \frac{v}{c}\left(1 + 3{,}53.10^{-5}Z^2 - \frac{v}{4c} - \frac{0.067}{\lambda} - \frac{0.003}{\lambda\cos^2\phi}\right). \qquad (162)$$

It can be readily seen from this formula that for very hard x-rays the value of sin x_1 begins to be appreciably smaller than v/c, but for the same values of v and λ the values of sin x_1 increases with the increase of Z.

The independence of the maximum of photoelectric emission from the value of A can be readily understood with regard to the fact that Eq. (148), if coefficients B and C are neglected represents a superposition of an emission given by the term

$$\sin^2\theta\cos^2\phi(1 + b\cos\theta + c\cos^2\theta + d\cos^3\theta)$$

which shows a pronounced maximum and an emission independent from the direction in space, represented by the term A.

The values of the angles of maximum photoelectric emission which follow from the data of Loughridge[21] agree fairly well with the formula (162). This formula ceases to be valid for ϕ nearly equal $\pi/2$ or $3\pi/2$.

The author wishes to express his gratitudes to the International Education Board for the granting of a fellowship.

Note added during the proof. The average forward momentum of the photoelectrons can be calculated readily from the Eq. (148). It appears to be equal to $bmv/5$ or, if the ionization energy is neglected, so that

$$b = \frac{4h\nu}{c}/mv$$

equal to $0.8h\nu/c$. According to Williams (Proc. Roy. Soc. **121,** 611, 1928) an average momentum $0.8h\nu/c$ of photoelectrons in the direction of the x-ray beam corresponds to a constant momentum 5/4 $(0.8h\nu/c)$ in the direction of the x-ray beam, superimposed on the radial momenta of the photo-

[21] D. H. Loughridge, Phys. Rev. **30,** 488 (1927).

electrons distributed proportionally to $\sin^2\theta\cos^2\phi$. It follows that this additional component of momentum is equal to the momentum of the photon.

It is to be noted that all the results of this paper were obtained by neglecting the term $-i\delta\log r$ in the exponential of the formula (56). The value of δ is according to Eq. (57)

$$\delta=\frac{\gamma^2}{2}\left(\frac{A}{B}+\frac{B}{A}\right)=\gamma^2\frac{c}{v}\,. \tag{163}$$

The smaller the value of δ, the smaller the effect of its neglect. It follows that the results of this paper are more exact, the greater the velocity of the photoelectrons and the smaller the atomic number.

The calculations of this paper can be repeated taking δ into account, which causes the wave functions representing the photoelectrons to take the form

$$\psi\sim r^{-i\delta}e^{-i\kappa r}/r\,. \tag{164}$$

The calculations are easy but rather long; they lead to the result that to the first approximation

$$\phi\psi\sim\sin^2\theta\cos^2\phi\left\{1+\frac{2v}{c}\left(1+\frac{\delta Z}{2a\kappa}\right)\cos\theta\right\}. \tag{165}$$

It follows that for $\delta Z/2a\kappa\ll 1$ or $(v/c)^2\gg(\alpha Z)^3/2$ the terms with δ can be neglected and the formula (143) is then valid.

Thus for comparatively slow photoelectrons and high atomic numbers the formula (165) is to be applied instead of (143), whereas this latter formula is valid for high speed photoelectrons and low atomic numbers. Eq. (165) ceases to be valid for very slow photoelectrons, because the use of the asymptotic formula (164) is then not justified.

THE REFLECTION OF BEAMS OF THE ALKALI METALS FROM CRYSTALS

By John B. Taylor*
General Electric Company, Schenectady, N. Y.

(Received January 9, 1930)

Abstract

Beams of lithium, potassium, and caesium were reflected from crystals of sodium chloride and lithium fluoride, as a means of studying the wave nature of these atoms. Incident angles from 2° to 60° were investigated. Although one one-hundredth percent of specular reflection could have been detected, no trace of such a reflection or of diffraction was found. The measured angular distribution of reflected atoms followed closely the cosine law. Apparatus, and the detecting device depending on positive ion emission by which this sensitivity of measurement was obtained, are described.

THE reflection of a beam of atoms from a crystal or ruled grating has for some time been recognized as a means of investigating the wave nature of the atoms.[1] Recently the author has described a method of detection and intensity measurement of molecular beams.[2] This method has proved so reliable and sensitive that it gave opportunity for a very detailed study of the reflection of the alkali metals from crystals. This has been done, using the detector for measuring the angular distribution of the atoms reflected when a beam of alkali metal atoms is allowed to fall upon a crystal.

Reflection experiments have already been carried out for a few atoms. Knauer and Stern[3] have obtained specular reflection of helium and hydrogen molecules from sodium chloride and potassium chloride crystals. In addition they have measured distinct surface diffraction beams arising from the crossed grating. These occur, within the present limits of the experiment, at the angle calculated from the surface grating formula using the de Broglie wave-length, $\lambda = h/mv$, obtained from the velocity and mass of the helium atom. Johnson[4] has shown that hydrogen atoms are specularly reflected from sodium chloride. Kirschbaum[5] also reports experiments with hydrogen atoms. No evidence of diffraction was found in either case. Ellett, Olson, and Zahl[6] have obtained specular reflection of cadmium, mercury, arsenic, and antimony from sodium chloride crystals. Certain features of their results not in

* National Research Fellow, University of California, Berkeley, California.

[1] O. Stern, Zeits. f. Physik **39,** 762 (1926).

[2] J. B. Taylor, Zeits. f. Physik **57,** 242 (1929).

[3] F. Knauer and O. Stern, Zeits. f. Physik **53,** 779 (1929); O. Stern, Naturwiss. **21,** 391 (1929).

[4] T. H. Johnson, J. Frank. Inst. **206,** 301 (1928).

[5] H. Kirschbaum, Ann. d. Physik **2,** 213 (1929).

[6] A. Ellett and H. F. Olson, Phys. Rev. **31,** 643 (1928); Ellett and Zahl, Phys. Rev. **31,** 1122 (1928).

agreement with a surface grating action are yet to be explained. They also report a trial of reflection of sodium from sodium chloride. No regular reflection was observed.

In the present work, beams of lithium, potassium and caesium have been reflected from crystals of sodium chloride and lithium fluoride. The most probable de Broglie wave-lengths in question, at furnace temperatures of 900°, 500°, and 450°K respectively, vary from about 0.2×10^{-8} cm for lithium to 0.07×10^{-8} cm for caesium. No trace of specular reflection or diffraction has been found. On the contrary the intensity of reflection measured at various angles with the surface follows almost exactly the cosine law of Knudsen; i.e. all of the atoms are reflected diffusely from the point of incidence. One-tenth of one percent specular reflection could easily have been observed in the

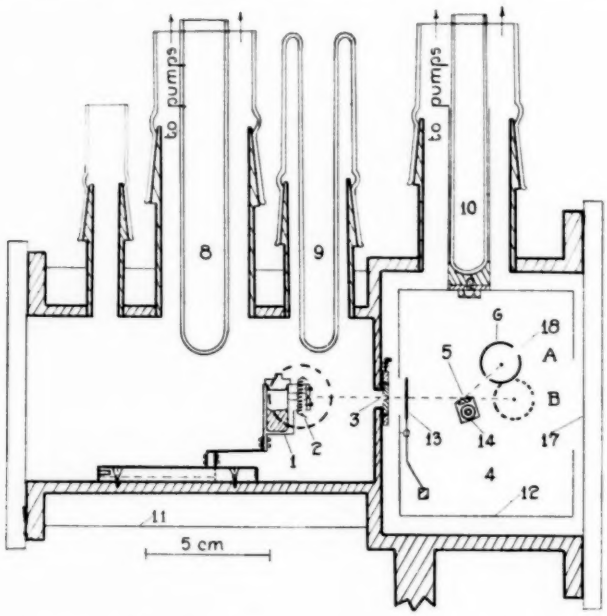

Fig. 1. Section of apparatus showing path of beam to crystal and detector.

present experiments. In some cases one one-hundredth of a percent could have been detected. In the other experiments mentioned the specular reflection has varied from almost one hundred percent[7] in the case of helium, to 10 to 20 percent in the case of cadmium, and one or two percent for atomic hydrogen.

Apparatus

The beam forming arrangement, furnace, slits, etc. are practically the same as have been described previously.[8] Figure 1 gives a schematic view

[7] Recent experiments of O. Stern about to be published, and as described to the author in private communication.

[8] J. B. Taylor, Zeits. f. Physik **52,** 846 (1929); **57,** 242 (1929).

of the situation. Atoms of the alkali metal evaporate through a fine slit in the steel oven (1) which is heated by radiation or by electron bombardment from the tungsten spiral (2). The beam is then formed by a second slit (3) and passes into the reflection chamber (4). Here it impinges on the crystal surface (5). The reflected atoms are received on the filament of the detector (6) which can be moved to intercept and measure the number of atoms leaving the crystal at any angle.

In the sketch the detector in position (*A*) observes the specular beam. The detector was a platinum cylinder eighteen×fifty mm with a coaxial pure tungsten filament 0.05 mm in diameter. The cylinder was held ten volts negative to the filament and at a temperature of about 1500°K. Every alkali metal atom striking the filament leaves as a positive ion.[9] Thus the positive ion current is at once a measure of the intensity of the beam or of the reflected atoms at the point. The detector is carried on the ground joint (7) Fig. 2, by

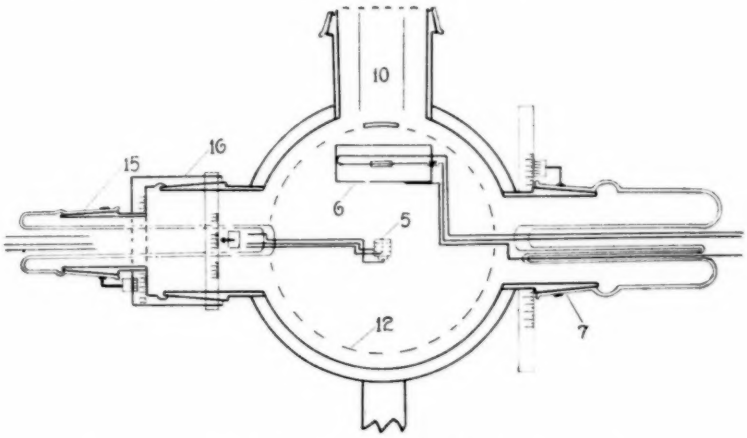

Fig. 2. End view of detecting chamber showing mounting and motions of crystal and detector.

which it may be moved to cover various angles of reflection. For lithium the detector filament was oxygen on tungsten.

The oven and crystal chambers were evacuated separately by two large Langmuir pumps. Liquid air traps (8), (9), (10), served to protect the chambers from grease vapors from the joints. The walls of the apparatus were held below room temperature by the water jacket (11). Added protection is given the detector and crystal by a sheet copper shield (12) cooled by liquid air from the trap (10). (13) is a shutter operated by action of a small magnet on an iron lever. It allowed interuption of the beam at any instant.

The crystal (5) is carried in the holder and heater (14). A tungsten spiral running through the body of the holder allows heating the crystal by radiation to at least 500°C. The holder is mounted on the ground joints (15) and (16) Fig. 2. (15) is eccentric in (16) so that by turning (16) the crystal can be

[9] I. Langmuir and K. H. Kingdon, Proc. Roy. Soc. **21,** 380 (1923).

raised into or lowered out of the path of the beam. By turning (15) the crystal is rotated on an axis through its surface and coaxial with the motion of the detector, to set the crystal at any incident angle with the beam.

Since the detector motion is coaxial with the crystal motion, the filament remains equidistant from the crystal at all angles and the positive ion currents require no correction for distance.

Graduations on the various joints permitted accurate readings of the angular settings.

Crystals used. Natural crystals of sodium chloride were used in a few experiments. Later to secure more perfect crystals, they were grown from the melt by the excellent method of Kyropolous.[10] Single crystals 3 to 5 cm in diameter were easily made in a few hours. Lithium fluoride was first purified by this method from an impure melt, and then crystalized from a melt of the pure product. The crystals were held at 2 to 300°K until ready for use. After cleaving they were immediately inserted in the apparatus and evacuation and heating begun at once.

During the reflection experiments the crystals were held at temperatures varying from room temperature to about 500°C. The elevated temperatures were to prevent if possible the momentary condensation or adsorption of alkali metal atoms on the crystal surface, and to insure a surface free from adsorbed gases.

The crystals used were 5 to 10 mm $\times$ 6 mm.

Procedure

The oven was loaded and the experiment begun as described[8] previously, with the addition of the crystal introduction. After five to eight hours pumping and heating of the crystal the oven was brought gradually to a temperature giving the desired beam intensity. This changing oven pressure could be readily followed by moving the detector into the path of the beam, (position *B* in Fig. 1), with the crystal lowered. In addition when the desired intensity was reached the detector filament was moved by 0.01 to 0.05 mm steps through the beam to measure its intensity from point to point. Thus in size and intensity the incident beam was accurately known. Fig. 3 gives examples of such measurements. The small displacements of the filament during this measurement were controlled by use of a traveling microscope with eyepiece micrometer. Through the glass window (17) and the detector opening (18), the filament could be seen as a bright line against the scale.

The width of the beams striking the crystal was changed in different trials from 0.05 mm to 1 mm. The maximum intensity in the undeflected beam at *B* was varied from 30 cm full galvanometer sensitivity to about 60 meters equivalent deflection. These latter were measured with galvanometer shunted to one-thirtieth of full sensitivity. The galvanometer had a full sensitivity of 4×10^{-11} amps. per mm.

Then by means of the joint (16) the crystal was raised into and parallel to the beam. This could be done very accurately by noting the decrease in gal-

[10] S. Kryopolous. Zeits. f. Anorg. Chemie **154,** 308 (1926).

vanometer deflection as the crystal intercepted half of the beam. Next with the shutter (13) closed the crystal was turned to whatever incident angle desired, the shutter opened and observations begun. Incident angles from 2° to 60° were investigated. By joint (7) the detector was moved around the crystal, the intensity of the reflected atoms at any angle being recorded immediately by a certain steady galvanometer deflection. In the neighborhood of the expected specular reflection the steps could be made in fractions of a degree and the whole region explored a number of times to remove any question as to the character of the reflection. Readings could also be made by setting the detector at a given angle and then rotating the crystal to investigate any preferred angles of reflection.

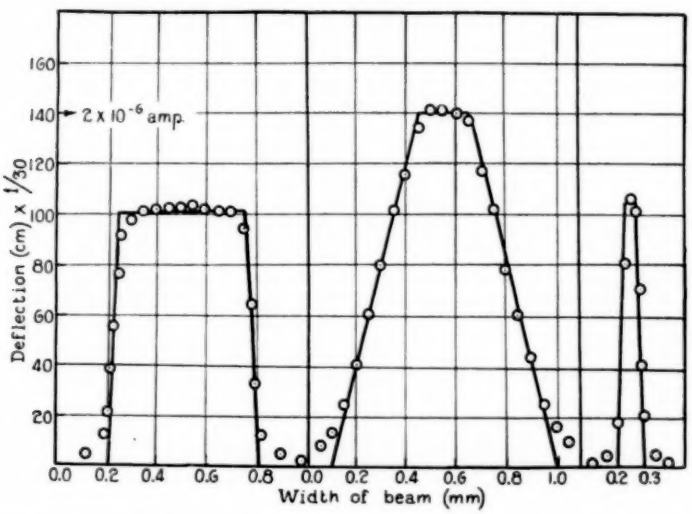

Fig. 3. Examples of intensity measurements of beams used. Solid lines are the geometrical beams constructed from the slit arrangements.

At any angle of reflection, if the shutter was closed the galvanometer deflection fell at once to zero.

At any time the crystal could be lowered and a check made on the constancy of the incident beam.

At the larger beam intensities one-tenth percent of specular reflection would have given 30 to 60 mm galvanometer deflection. However in no case was there the slightest indication of specular reflection.

Fig. 4 shows a reflection measurement with potassium from sodium chloride at an incident angle of 15°. The reflection from lithium fluoride and at other intensities of the main beam gave similar data.

An interesting critical temperature phenomenon was noted in the course of the experiments. If the crystal was allowed to cool, a temperature range was reached where the reflection at any angle fell very quickly practically to zero. This temperature where almost all the incident atoms were condensing on the crystal varied, as to be expected, with the incident beam intensity. It

is apparent that the combination of beam and detector offers a precise method of studying surface condensation and evaporation phenomena.

The experiments made so far on the reflections of atoms from crystals have led to no explanation of the efficiency of reflection. The great ease with which the alkali metal atoms are adsorbed on surfaces is believed to explain at least in part their failure to be specularly reflected or diffracted. To avoid this, the possibility is suggested of employing crystals which may be heated to

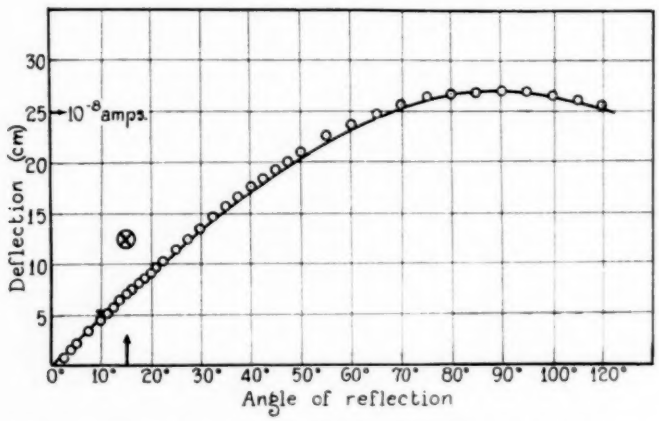

Fig. 4. Showing measured angular distribution of reflection (points) as compared to a cosine distribution (solid curve); the incident beam making an angle of 15° with crystal. Cross indicates intensity which would have been measured at 15° if one-tenth percent of the incident atoms had been specularly reflected.

still higher temperatures than in these experiments, or crystals on which the adsorbing forces are much smaller. However unless unusual conditions as to reflecting surface can be secured, it may not be possible to detect an appreciable specular reflection of the alkali metal atoms.

The writer wishes to express his appreciation of support from the National Research Council and to Professor G. N. Lewis for the facilities so kindly made available at the University of California.

THE EMISSION OF POSITIVE IONS FROM TUNGSTEN AND MOLYBDENUM

By Lloyd P. Smith
Department of Physics, Cornell University

(Received November 25, 1929)

Abstract

An examination of the positive ion emission from tungsten and molybdenum has been made in which it was sought to determine the following points: (1) The nature of the ions emitted at various temperatures; (2) the temperature variation of the positive ion current; (3) the theory of positive ion emission with regard to where and how the ions are formed; (4) the positive ion work function for these metals; (5) whether the work function, determined by experiment, checks with that calculated by a simple cyclic process involving the thermionic work function, the ionizing potential, and the latent heat of evaporation of the metal.

The mass spectrum for tungsten and molybdenum filaments taken at moderate temperatures (1700° to 2000°K) has shown that the emitted ions consist of sodium, the two isotopes of potassium, and aluminum. At high temperatures these impurities disappear and finally both tungsten and molybdenum filaments yield positive ions of their own metal. The latter confirm a report by Wahlin. The temperature variation of the positive ion current at high temperature yields a value of 6.55 volts for the positive ion work function of tungsten and 6.09 volts for that of molybdenum. These values disagree widely from the values 10.88 volts and 9.26 volts calculated from the simple cyclic process mentioned above. This suggests that the ions are formed as a by-product of an irreversible recrystallization of the metal. Theoretical considerations show that the ions are emitted from the metal and are not formed after a neutral atom evaporates.

UNTIL recently, it has been thought that any positive ion emission from metals was due entirely to ionized atoms of one or more impurities which existed in the metal. O. W. Richardson[1] has shown that most metals contain a very small amount of potassium which is driven out of the metal as the temperature is raised. He obtained rather erratic results from tungsten and did not give any data concerning molybdenum. His work was carried on for temperatures below 2,000°K. J. J. Thomson[2] investigated the positive ion emission from platinum by crossed electric and magnetic fields and found in addition to those of alkaline impurities, ions having an atomic weight of 27 which he concluded were ionized CO molecules. More recent work[3] has shown definitely that platinum contains potassium and sodium as impurities which are ionized and emitted at high temperatures.

During the summer of 1927 the author attempted to perfect a pliotron having a grid extremely well insulated. It was found during the course of this investigation that part of the electric leakage to the grid was due to positive

[1] O. W. Richardson. Emission of Electricity From Hot Bodies.
[2] J. J. Thomson, Camb. Phil. Proc. **15,** 64 (1908).
[3] Barton, Harnwell, and Kunsman, Phys. Rev. **27,** 739 (1926).

ions arising at the filament. These ions persisted even after the filament was flashed to some 3,000° and then well aged. An investigation of the nature of these high temperature ions and the variation of the positive ion current with temperature was undertaken. After the work was begun it was noted that Jenkins[4] had found that the tungsten cathode of a Coolidge x-ray tube was a source of positive ions. Mitra[5] carried on the investigation and obtained data on the temperature variation of the positive ion current using a commercial type of radio tube having a tungsten filament, but did not attempt to determine the positive ion work function. The author has given a preliminary report[6] on such a work function.

Mass Spectrograph

The apparatus for obtaining the mass spectrum of the ions is shown diagrammatically in Fig. 1. It consisted essentially of a copper tube A in the form of a half torus ring spun from sheet copper. The diameter of the cross section was approximately 2.5 cm. Caps having the slits S_1 and S_2 were placed over the ends. The slit S_1 was about 0.8 mm wide and 8 mm long. The slit

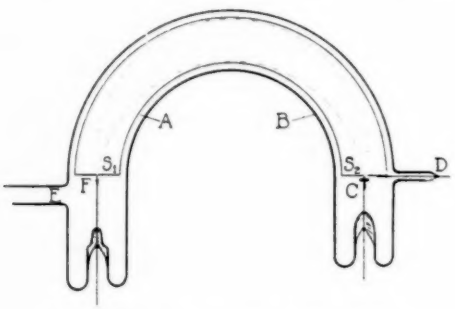

Fig. 1. Diagram of mass spectrograph.

S_2 was somewhat larger being about 3 mm wide and 1 cm long. A wire filament of the metal under investigation having a length of about 1.4 cm was placed at F, parallel to the slit S_1 and about 5 mm away from it. Ions passing through S_1 and bent by the magnetic field on an arc whose radius was 6.95 cm were focused at S_2. Those passing through S_2 were collected on the electrode C which was connected to a quadrant electrometer. The accelerating potential was applied between D and F. The copper tube together with the filament leads and collector leads were all sealed into a glass tube B which was exhausted at E. A pressure less than 10^{-6} cm of Hg was maintained. The tube was placed between poles of an electromagnet having pole pieces of large diameter. The field in the region occupied by the tube was found to be uniform and its intensity was determined by careful flip coil measurements.

In determining the mass spectrum, the field intensity was set at a given value and the accelerating potential was varied very slowly but continuously

[4] Jenkins, Phil. Mag. **47,** 1025 (1924).
[5] Mitra, Phil. Mag. **5,** 67 (1928).
[6] Smith, Phys. Rev. **33,** 279 (1929).

by a mechanical device. The presence of a particular ion was noted by a drift of the electrometer. When it began to drift, the rate of drift for various accelerating potentials was taken and from these data the voltage yielding the maximum rate of drift was obtained. The voltage across the filament was measured and one half of this drop was added to the voltage producing maximum drift to yield the true accelerating potential.

Nature of the Ions

From the accelerating potential corresponding to a given electrometer current, the atomic weight W was computed by means of the expression $W=(1/V)\ [RH/144.5]^2$ where R is the radius of the path traversed in cm, H is the field intensity in gauss, and V is the accelerating potential in volts. The electrometer current in arbitrary units was plotted against W to give a mass spectrogram. A typical mass spectrum for tungsten at moderate temperature is shown in Fig. 2. The peak at $W=23.1$ is due to sodium ($W=23.0$) and could

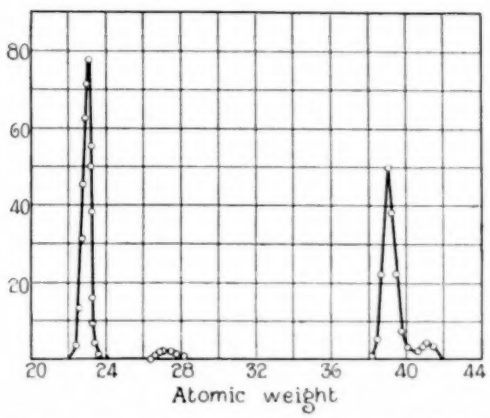

Fig. 2. Mass spectrum from tungsten at moderate temperatures (1600–2000°K).

be detected at a temperature of about 1700°. The peaks at $W=39$ and 41.1 were also present at this temperature. They are undoubtedly due to the two isotopes of potassium occurring at $W=39$ and 41. The only element falling in this region is calcium($W=40.07$). No evidence of calcium ions has been found and in fact it would be quite improbable that any appreciable amount of calcium would be ionized at these temperatures for its ionization potential is too high (6.09 volts). The peak occurring at $W=27.2$ did not show up until temperatures over about 2,000° were reached. This atomic weight compares well with aluminum ($W=27.0$), and since the ionizing potential of aluminum is 5.9 volts we would not expect to find it until a higher temperature is reached than would yield either potassium or sodium ions whose ionizing potentials are 4.3 and 5.1 volts respectively. As mentioned before, J. J. Thomson found ions of atomic weight 27 emitted from platinum and concluded that they were ions of CO molecules ($W=28$). It seems improbable that these were really positively ionized CO molecules because the ionizing potential of such molecules is of the order of 14 volts, much too high to have any ions of CO present

below the melting point of platinum. It therefore seems extremely likely that aluminum was present as an impurity.

Fig. 3 is the mass spectrum obtained from molybdenum. It shows the presence of the same impurities as existed in the tungsten. This spectrum does not show as high a resolution as the one for tungsten but this is doubtless due to the fact that it was obtained at a higher temperature and the voltage drop along the filament broadened the peaks. It is interesting to note that

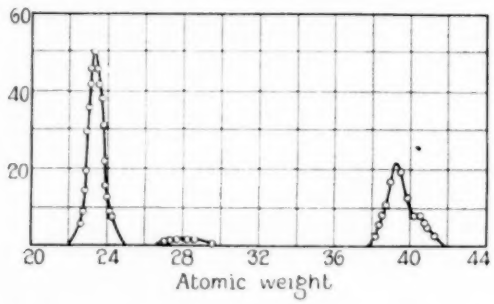

Fig. 3. Mass spectrum from molybdenum at moderate temperatures.

these impurities are present in extremely small amouts. A spectroscopic analysis was made on the samples of tungsten and no trace of the impurities here detected was found, which indicates that each was probably present in an amount less than 1 part in 100,000 and certainly less than 1 part in 10,000.

These ions which are emitted at moderate temperatures become less in number as time of heating increases and they can be gotten rid of quite

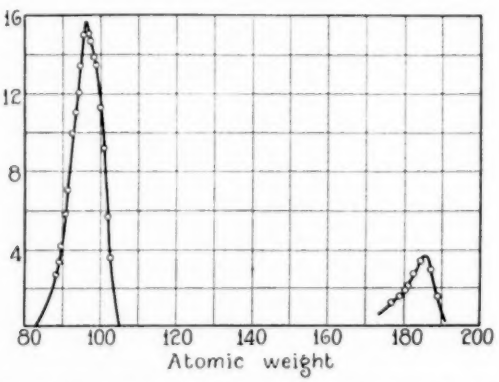

Fig. 4. Mass spectrum of molybdenum and tungsten at high temperatures.

rapidly if the filament is aged at higher temperatures. As the temperature is increased a point is found where no ions of impurities are emitted. On further increasing the temperature to about 2500° for tungsten and 2300° for molybdenum new ions are emitted. The spectrum curves for molybdenum and tungsten at these temperatures are plotted in Fig. 4. These spectra leave no doubt that the high temperature ions from tungsten found by Jenkins and the author are really tungsten ions, and that molybdenum also emits positive ions

of molybdenum. While this paper was being prepared Wahlin reported in a brief note[7] that he had found tungsten, molybdenum, tantalum, and rhodium to emit positive ions of their own metal. The results given here corroborate his results for tungsten and molybdenum.

No trace of doubly ionized atoms was found nor was there any evidence of ions which were singly charged but having a mass of two or more atoms of the material, although they were looked for. It appears that the ion of the metal is emitted as a singly ionized atom.

Variation of Emission with Temperature

To obtain the magnitude of the positive ion current for a given temperature, the form of tube shown in Fig. 5 was used. The current to the lower cylinder was measured. For tungsten, the temperature was determined from the current through a given sized filament as given by Langmuir and Jones.[8]

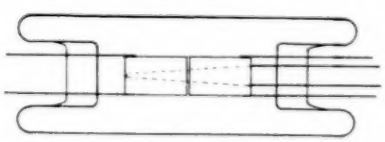

Fig. 5. Tube used to measure the positive ion current.

For molybdenum the temperature was determined from data kindly supplied by S. Dushman giving the watts per cm² as a function of the temperature. Volt-ampere characteristics of two hair pin filaments were taken. They had the same diameter but different lengths, and were electrically welded to identical lead wires. By a method of differences the cooling effect of the leads was eliminated and the temperature of the center of the longer filament was obtained as a function of the current through it.

The magnitude of the positive ion current from tungsten at a given temperature depends on the heat treatment through which the filament has passed. Furthermore there exists a decay with time which is slow after the filament has been allowed to age for a time and has been carried over the range

Table I. *Variation of positive ion current with temperature.*

Tungsten		Molybdenum	
Current per cm²	Temp. °K	Current per cm²	Temp. °K
5.39×10^{9}	2390	2.43×10^{9}	2300
9.71	2450	3.89	2340
18.3	2500	5.71	2375
25.1	2560	7.79	2400
62.6	2585	9.71	2420
79.2	2635	13.6	2460
113.	2670	17.3	2470
168.	2715	20.4	2490
276.	2760	24.3	2500
424.	2800	29.1	2520

[7] Wahlin, Phys. Rev. **34,** 164 (1929).

[8] Langmuir and Jones, General Electric Rev. p. 510, June 1927.

of temperatures to be used. Hence in the case of tungsten no final value of the current at a given temperature can be given. After a few hours aging at about 2300°, molybdenum seemed to give values that were reproducible. These values could be duplicated after aging for several hours more at 2300°. Table I shows data for tungsten and molybdenum obtained after some 5 hours aging.

Positive Ion "Work Function"

In determining electronic work functions it has been customary to make use of the usual electron emission formula

$$I = AT^2\epsilon^{-(\phi_-\epsilon/kT)}.$$

The work function ϕ_- is found by plotting $\log I - 2\log T$ against $1/T$ and determining the slope of the straight line thus found. This procedure however would be incorrect for determining the work function for positive ions because of the difference in the process involved in the evaporation of ions. We shall therefore deduce an expression which should be applicable for the evaporation of ions.

Following Bridgman[9] we take a neutral metal composed of n atoms at 0° absolute and raise its temperature to T and evaporate m ions reversibly at the equilibrium pressure. At this temperature we then have a positive ion gas, a negative surface charge, and the remaining neutral metal. Let the entropy of one atom in the condensed state be denoted by s_1, the entropy of one evaporated ion by s_2 and the entropy to be associated with the heat of surface charging produced by the evaporation of one ion by s_2'. The entropy before evaporation is then ns_1 and the entropy after the evaporation of m ions is $ms_2+ms_2'+(n-m)s_1$. Since the entropy after evaporation minus the entropy before evaporation must equal the change of entropy during evaporation we have,

$$(mL/T) = m(s_2+s_2')+(n-m)s_1-ns_1$$

where L is the latent heat of evaporation of one ion, the metal being isolated. This expression reduces to

$$(L/T) = s_2+s_2'-s_1. \tag{1}$$

Using essentially the same expressions for s_1, s_2 and s_2' as Bridgman, Eq. (1) becomes—

$$\frac{L}{T} = k\left[\frac{5}{2}+\log_\epsilon \frac{(2\pi M)^{3/2}k^{5/2}}{h^3}+\frac{5}{2}\log_\epsilon T-\log_\epsilon P\right] + \int_0^T \frac{C_{p\rho}}{T}dT - \int_0^T \frac{C_{pm}}{T}dT + s_\rho \tag{2}$$

where p is the equilibrium vapor pressure of the ion gas; M is the mass of one ion; C_{pm} is the heat capacity, at constant pressure, of an ion in the condensed

[9] Bridgman, Phys. Rev. **27**, 173 (1926).

state; $C_{p\rho}$ is the heat capacity associated with the surface heat of charging produced by the evaporation of one ion, and s_ρ is the entropy associated with the surface heat of charging at $T=0$.

The latent heat of evaporation may be expressed as a function of the temperature by the relation[9]

$$L_T = L_0 + (5/2)\ kT + \int_0^T C_{p\rho} dT - \int_0^T C_{pm}\ dT \tag{3}$$

Combining Eqs. (2) and (3) we have:

$$\log_e p = -\frac{L_0}{kT} + \frac{5}{2}\log_e T + \log_e \frac{(2\pi M)^{3/2} k^{5/2}}{h^3} + \frac{s_\rho}{k} + \frac{1}{k}\left[\int_0^T \frac{C_{p\rho}}{T} dT - \frac{1}{T}\int_0^T C_{p\rho} dT\right] - \frac{1}{k}\left[\int_0^T \frac{C_{pm}}{T} dT - \frac{1}{T}\int_0^T C_{pm} dT\right]$$

This reduces to

$$\log_e p = -\frac{L_0}{kT} + \frac{5}{2}\log_e T + \log_e \frac{(2\pi M)^{3/2} k^{5/2}}{h^3} + \frac{1}{k}\int_0^T \frac{dT}{T^2}\int_0^T C_{p\rho} dT + \frac{s_\rho}{k} - \frac{1}{k}\int_0^T \frac{dT}{T^2}\int_0^T C_{pm} dT. \tag{4}$$

Under equilibrium conditions just as many ions condense as are evaporated per second, hence we may take the rate at which ions strike the surface of the metal at the equilibrium pressure as the rate of evaporation. It may be shown that at the pressure p the number of ions striking unit area per sec is

$$n = p/(2\pi M kT)^{1/2}$$

where M is the mass of the atom concerned. If some of the ions striking the metal are not condensed but are reflected then the number emitted must be $n=(1-r)p/(2\pi MkT)^{1/2}$ where r is a reflection coefficient. The positive ion current will be given by

$$I = ne = \frac{pe(1-r)}{(2\pi M kT)^{1/2}}$$

or

$$\log_e p = \log I + \tfrac{1}{2}\log_e 2\pi MkT - \log_e e - \log(1-r). \tag{5}$$

Making use of (5), Eq. (4) becomes:

$$\log_e I = -\frac{L_0}{kT} + 2\log_e T + \log_e M + \log_e 2\pi k + \log_e \frac{k}{h^3} + \log_e e + \log_e (1-r) + \frac{1}{k}\int_0^T \frac{dT}{T^2}\int_0^T C_{p\rho} dT + \frac{s_\rho}{k} - \frac{1}{k}\int_0^T \frac{dT}{T^2}\int_0^T C_{pm} dT$$

or

$$\log_e I = -\frac{L_0}{kT} + 2\log_e T + \log_e M + \log_e \frac{2\pi k^2 e}{h^3} + \log_e (1-r) + \frac{1}{k}\int_0^T \frac{dT}{T^2}\int_0^T C_{p\rho}dT + \frac{s_\rho}{k} - \frac{1}{k}\int_0^T \frac{dT}{T^2}\int_0^T C_{pm}dT. \tag{6}$$

The integral containing C_{pm} has been evaluated[10] for tungsten and molybdenum. Making use of the evaluation for tungsten and changing to logarithms to the base ten, Eq. (6) becomes

$$\log_{10} I + 0.363\log_{10} T + 1.64\times 10^{-4}T = \frac{-\phi_{+0}e}{2.203kT} + \frac{1}{2.303k}\int_0^T \frac{dT}{T^2}\int_0^T C_{p\rho}dT + \frac{s_\rho}{2.303k} + \log_{10}(1-r) + 12.43. \tag{7}$$

Where $\phi_{+0} = L_0/e$ is the equivalent difference of potential through which an ion must be moved. The corresponding equation for molybdenum is,

$$\log_{10} I + 0.453\log_{10} T + 2.70\times 10^{-4}T = \frac{-\phi_{+0}e}{2.303kT} + \frac{1}{2.303k}\int_0^T \frac{dT}{T^2}\int_0^T C_{p\rho}dT + \frac{s_\rho}{2.303k} + \log_{10}(1-r) + 12.76. \tag{8}$$

If it were known how $C_{p\rho}$ varied with the temperature then the above equation would show exactly how the positive ion current varies with the temperature and the work function ϕ_{+0} could be found by putting all functions of T on the left hand side of the equation except the term containing ϕ_{+0} and plotting it against $1/T$. The slope of the straight line so obtained would yield ϕ_{+0}.

Langmuir and Tonks[11] have shown that the surface heat of charging for the removal of electrons from a surface is very small i.e., of the order of 0.04 volts, at 2270°. Although the fact that it is small does not mean that it cannot vary rapidly with the temperature, we shall for the present assume $C_{p\rho}=0$.

Fig. 6 shows the result of plotting the data for tungsten according to Eq. (7). Curve I is that obtained by plotting the data for tungsten given in Table I. The points lie very close to a straight line. Curve II was obtained after a sample of tungsten had aged some 30 hours and the rate of decay of the positive ion current had become very small. The point to be noticed is that even though a decay has taken place and the positive ion current has become smaller for a given temperature it has the same temperature variation as it had for considerably less aging, for the slopes of the lines I and II are the same. Curve III shows the result of plotting the data given by Mitra according to Eq. (7), As is evident, the curve so obtained has a slope almost identi-

[10] Jones, Langmuir and Mackay, Phys. Rev. **30,** 201 (1927).
[11] Langmuir and Tonks, Phys. Rev. **29,** 524 (1927).

cal to that of Curves I and II. The fact that it is displaced relative to the other lines does not yield any definite information because the area of emission used by him was not given. Since the slopes of these curves are the same the work function ϕ_{+0} is definitely determined. Eq. (7) represents each of the Curves I and II with suitable change in the constant term. A discussion concerning the value of the constant term will be given later.

As stated before, molybdenum after suitable aging gave reproducible results. The data given for Mo in Table I were plotted according to Eq. (8). Fig. 7 shows how well these data give a straight line thus determining a value for ϕ_{+0} for Mo.

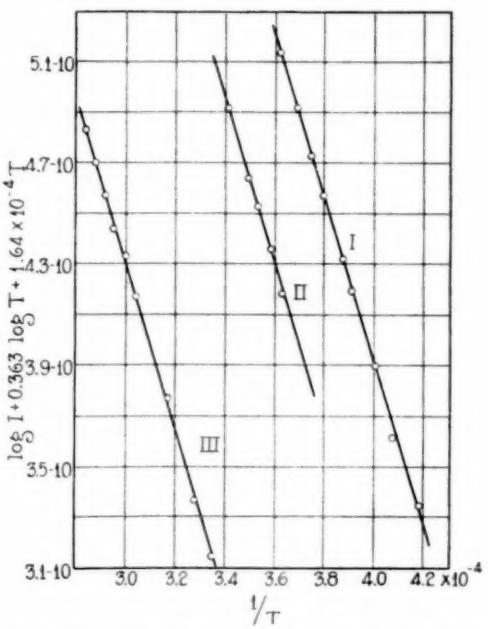

Fig. 6. Curves for determining the positive ion work function of tungsten.

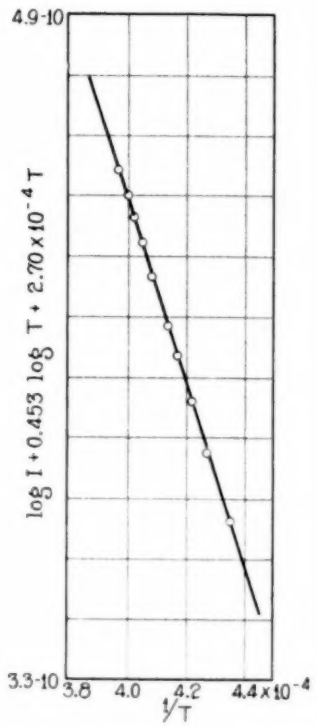

Fig. 7. Work function curve for molybdenum.

From Curve I, Fig. 6, ϕ_{+0} for tungsten is 6.55 volts, ϕ_{+0} determined from Curve II is 6.60 volts and from Mitra's data $\phi_{+0} = 6.55$ volts. It cannot be inferred that ϕ_{+0} is determined with an accuracy suggested by these figures for a slightly different line through the points yields a considerably different ϕ_{+0} as regards the third place, but 6.55 volts is undoubtedly a good representative value. The curve for molybdenum gives $\phi_{+0} = 6.09$ volts.

The constant term that must appear in Eq. (7) to represent the data plotted in Curve I, Fig. 6, is 6.51. If Curve II is considered to have the same slope as Curve I then the constant term for it is 6.28. From the curve for Mo it is found that the constant term of Eq. (8) must be 6.90.

Two serious difficulties now present themselves. The first is in regard to the constant terms just determined. Each of them is respectively much smaller than the numerical term appearing on the right side of Eqs. (7) and (8). On the assumption that the entropy associated with the surface heat of charging is zero, the constant 12.43 in Eq. (7) must be reduced to the value obtained (about 6.5) solely by the magnitude of the reflection coefficient r. To yield the proper constant, r would have to be so great that only 1 ion out of about 100,000 striking unit area would be condensed. It appears, however, that there is no quantitative evidence for such high values of r. For the evaporation of atoms, it has been found that satisfactory results are obtained when r has been assumed to be equal to or nearly zero, and even in thermionic emission r is probably not greater in order of magnitude than 0.5. Even if it had not been assumed that the entropy associated with the surface charge was zero, it is not likely that it would contribute a negative entropy constant term in Eqs. (7) and (8). Such a negative entropy would mean that heat would be developed when the metal surface became negatively charged and seems improbable. In fact evidence is presented later to indicate that heat is absorbed in the process of charging a metallic surface negatively.

The second difficulty seems more serious than the first. If we consider an inclosure in which molybdenum say is in equilibrium with its radiation at a given temperature T we may carry out the following cycle. Remove an electron and positive ion from the metal thus requiring an amount of work $\phi_{-T}+\phi_{+T}$ where ϕ_{-T} and ϕ_{+T} are the respective work functions at the temperature T, then allow the electron and ion to recombine thus producing a neutral atom and yielding an amount of energy corresponding to its ionizing potential V. Then let the atom condense on the metal thus yielding the heat of condensation. This is a reversible cycle and the sum of all the energy transfers should vanish thus:

$$\phi_{+T}+\phi_{-T}=V+U_T \tag{9}$$

where U_T is the heat of evaporation at the temperature T. Güntherschulze[12] has made use of such a cycle to compute ϕ_{+0} for those elements where the remaining data were available. With the ϕ_{+0} determined as above for molybdenum, all the terms of the cycle are known. U_T has been determined by Langmuir and Tonks,[11] V has been determined from the spectral series for molybdenum.[13] At zero degrees, $\phi_{-0}=4.42$ volts, $V=7.35$ volts, $U_0=6.33$ volts. We note then that

$$V+U_0=7.35+6.33=13.68$$

$$\phi_{+0}+\phi_{-0}=6.09+4.42=10.51$$

and that the cycle (9) *fails to close* by some 3.17 volts. Although the ionization potential for tungsten has not been determined it can be estimated as about 7.1 volts, and $U_0=8.31$ volts while $\phi_{-0}=4.53$. For tungsten we have

[12] Güntherschulze, Zeits. f. Physik **31,** 507 (1925).

[13] Compton and Mohler, Nat. Res. Council Bulletin No. **48,** 81.

$$V+U_0=7.1+8.31=15.41$$

$$\phi_{+0}+\phi_{-0}=6.55+4.53=11.08.$$

Again the cycle does not close by some 4.33 volts.

Since the value of ϕ_{+0} which has been determined depends so greatly on the theoretical equation used, and the effect of a possible surface heat of charging and its variation with temperature, a check was made by computing the values occurring in Eq. (9) at a given temperature. In order to do this the Clausius-Clapeyron equation,

$$L_T=T(V-v_0)(dp/dT) \tag{10}$$

was used, where L_T is the heat of evaporation at the temperature T, V the volume of the vapor, v_0 the volume of the metal and p is the vapor pressure. Neglecting v_0 and setting $V=kT/p$ we have

$$L_T=\frac{kT^2}{p}\frac{dp}{dT}=kT^2\frac{d(\log_e p)}{dT}. \tag{11}$$

We may express p in terms of the positive ion current by the relation (5), obtaining:

$$\log p=\log\left\{\frac{\beta}{1-r}IT^{1/2}\right\} \tag{12}$$

where β is a constant. If r does not depend on T then Eq. (11) becomes:

$$L_T=kT^2\frac{d}{dT}(\log_e IT^{1/2}).$$

This gives L_T in terms of the positive ion current measured and the temperature, and does not depend on any assumptions made concerning the surface heat of charging. Changing to logarithms to the base 10 and expressing L_T in terms of volts we have:

$$\phi_{+T}=1.987\times10^{-4}T^2\frac{d}{dT}(\log_{10} IT^{1/2}). \tag{13}$$

The values of $\log_{10}IT^{1/2}$ were plotted against T for molybdenum and the slope of this curve was determined at 2350°K. Using this slope, ϕ_+ at 2350° was found to be 5.43 volts.

The electron work function ϕ_- at 2350° was computed from Eq. (3) assuming that the specific heat of the electrons in the condensed state was zero. It's value was found to be 4.92 volts. The value of U at 2350° was also computed by means of Eq. (3) in which the integral, $\int_0^T C_{pm}\,dT$ for Mo was obtained from the work of Jones, Langmuir, and Mackay.[10] At $T=2350°$, U was found to be 5.41 volts. It is readily seen that if these values are substituted in the cycle (9) it still *fails to close* by some 2.45 volts. The failure of the cycle to close is, therefore, not due principally to our lack of knowledge concerning the surface heat of charging.

Under the assumption that $C_{p\rho}$ equals zero Eq. (3) assumes the form

$$L_T = L_0 + \frac{5}{2}kT - \int_0^T C_{pm}dT. \tag{14}$$

The value of $\int_0^T C_{pm}dT$ for Mo was determined as stated above. Converting L_T to volts, Eq. (14) becomes,

$$\phi_{+T} = \phi_{+0} - 2.71\times10^{-4}T - 5.37\times10^{-8}T^2 + 0.019. \tag{15}$$

If $C_{p\rho}$ is really zero then Eq. (15) should yield the same value of ϕ_+ at 2350° as Eq. (13). Using the value of ϕ_{+0} already determined (6.09), ϕ_{+T} from Eq. (15) at 2350° is 5.17 volts as compared with 5.43 volts determined from Eq. (13). The difference between these two values represents a contribution due to surface charging, thus indicating that heat is absorbed in the process. By combining Eqs. (13) and (3) it would be possible to determine an empirical value for the $\int_0^T C_{p\rho}\,dT$ which in turn would modify the equation used to determine ϕ_{+0} and therefore yield a slightly different value for ϕ_{+0}. It does not seem desirable to do this until the theoretical form of $C_{p\rho}$ is determined because the empirical relation could be expressed in several different forms which have no obvious theoretical significance.

It should be noted that ϕ_{+T} as expressed in Eq. (13) is independent of the reflection coefficient as a result of the *assumption* that r was independent of T. It is not at all unreasonable to suppose that r varies somewhat with the temperature but it would have to vary with *extreme* rapidity to yield a value of ϕ_{+0} which would satisfy the energy cycle (9). Such an extreme variation in r is not found in the evaporation of neutral atoms or electrons and therefore may be regarded as untenable in the case of ionic evaporation. It is therefore apparent that in Eqs. (7) and (8) there are no terms missing which change violently with the temperature and thus yield a value of ϕ_{+0} sufficiently large to close the energy cycle (9).

Possible Effects of the Filament Surface

It is well known that the condition of the filament surface affects the electron emission very greatly. The ordinary thermionic work function of a filament can be varied within wide limits by allowing a monatomic layer of foreign atoms to deposit on its surface. Such a layer of thorium on tungsten reduces the work function from 4.53 volts to 2.69 volts. On the other hand a layer of oxygen on tungsten increases it to 9.2 volts. Since the positive ion work function is related to the electron work function by Eq. (9) it follows that impurities on the surface would effect the positive ion work function materially. It could be supposed for example that the positive ions were really coming from small patches of the filament which were coated with oxygen atoms. For a tungsten filament coated with oxygen $\phi_{-0} = 9.22$ volts. Using this value of ϕ_- in Eq. (9), ϕ_{+0} comes out to be 6.2 volts which agrees fairly well with the value 6.55 volts determined by experiment.

If surface contamination is the cause of the discrepancy between the work function determined experimentally and that calculated from the cycle, it

is difficult to see how it could be due to oxygen. In the first place, as far as the writer is aware, it is impossible to keep oxygen atoms on the surface of tungsten at temperatures above 2300° or 2400°. In order to be sure that oxygen was not playing any part in the positive ion emission, a small amount of oxygen was admitted while the tungsten was emitting positive ions but the ion current was not affected until sufficient oxygen was admitted sensibly to cool the filament. A small amount of argon was admitted in the same way but the only effect was to decrease the ion current if an excessive amount was admitted. Argon is chemically inactive and its only action was probably a cooling of the filament.

It might be supposed that the surface of the filament was rough and jagged when looked at through a microscope and that the ions were being emitted from these microscopic points in the same way as electrons are emitted from cold metals. In the latter phenomenon, however, the electrons are emitted from the points because the field strength is extremely high at the point. In the case of positive ions however the voltage applied between the collector and filament was never greater than 150 volts and Mitra has shown that the ion current saturates very well thus making the correction for the Schottky effect very small. Furthermore tungsten undergoes a recrystallization at about 2800°K and filaments that have been made rough by ion bombardment can be made smooth again by raising the temperature above 2800°K. No extraordinary behavior of the ion current was noted in the neighborhood of this temperature.

Recombination at the Filament Surface

If an appreciable amount of recombination took place at the surface of the filament, then it would be possible that the positive ion current as measured would not correspond to the actual rate of emission. The rate of recombination would be a function of the temperature and would modify the ion current in such a way that the measured ion current would not yield the true work function. The order of magnitude of this rate can be calculated from the Thomson theory of recombination. Such a calculation shows that at 2500°K the fraction of the ion current actually emitted which would be removed by recombination is $6.5 \times 10.^{-7}$ It is therefore seen that recombination does not measurably influence the measurement of the positive ion current.

Probable Ionization of Atoms after Evaporation

One may reasonably ask whether the ions might not be formed from atoms after they evaporated. Ions certainly exist in the vapor of metal in equilibrium with the metal itself, if the temperature is high enough even though the metal emits electrons but no ions. The concentration of positive ions in such a vapor may be obtained from Saha's ionization equation, and some idea of the rate of formation of ions in such a vapor may be obtained by calculating the number of collisions which occur with sufficient energy to ionize, and the number formed by the action of radiation from the hot metal. Such calculations have been made by the writer with the result that the maxi-

mum rate of formation of ions from neutral atoms in the vapor is entirely negligible compared to the ion currents measured.

Photoelectrons from the Collecting Electrode

The effect of radiation from the filament in producing photoelectrons from the collecting electrodes which would thereby influence the ion current measured has been investigated in several ways. In the first place Jenkins applied a magnetic field at right angles to the ion current in his Coolidge x-ray tube which was of sufficient strength to prevent electrons leaving the cathode from arriving at the target when a positive potential was applied to it equal to the negative potential used to collect the ions. This had no effect on the ion current which could be true only if heavy ions alone were conducting the current. Similar magnetic experiments performed by the writer produced no effect on the ion current. Collecting electrodes of different metals were used but they produced no changes in the ion current or the variation of it with temperature. The photoelectric effect does not therefore account for a measurable part of the current observed.

Possibility of an Apparent Work Function

It appears then that positive ions of the metal are actually emitted from the metal and the amount of heat required to emit them is less than the amount deduced from cycle (9) the latter of which should be the true heat required. It seems necessary in order to overcome this discrepancy to assume that the value of ϕ_+ obtained from cycle (9) is the true work function for positive ions while the value ϕ_+ determined from the positive ion current is an apparent work function, just as it was necessary to assume in the Sommerfeld[14] theory of the Richardson effect that the true electron work function is W_a, and the value ϕ_{-0} determined by actual measurement is only apparent. In the Sommerfeld theory

$$\phi_{-0} = W_a - W_i$$

Where W_a is the true work required to remove an electron from the metal and W_i is the maximum energy which the electrons already have in the metal due to their high velocities acquired as a result of the velocity distribution law of the Fermi Statistics. It should be pointed out that W_a should not replace ϕ_- in cycle (9) because ϕ_- actually represents the work required to remove an electron which already has the energy W_i. The term W_i occurs implicitly in cycle (9) in the heat of condensation term U, since in condensing the atoms together to form the metal, part of the heat U must have been used up in giving the free electrons the energy W_i.

In the case of positive ions, the degeneracy condition which gave the electrons their high internal energy W_i, is not fulfilled due to their large mass, and their internal energy is the relatively small amount given by classical theory. Hence the question concerning a W_i for ions does not arise. However if it is to be assumed that ϕ_{+0} is an apparent work function then there must

[14] Sommerfeld, Zeits. f. Physik **47,** 27 (1928).

exist a source of energy of an amount ψ, which is not included in one of the terms in Eq. (9) and the magnitude of which is equal to that required to close the cycle (9). Such an amount of energy could not be supplied through the agency of a force field tending to repel the ion from the metal since such energy would be implicitly included in the work function ϕ_+.

It may be that tungsten and molybdenum slowly recrystallize in an irreversible manner at high temperatures yielding the necessary energy ψ to emit an ion. The ions would thus be emitted as a secondary effect. In all probability some electrons and atoms would be emitted as a result of the recrystallization but the number thus emitted would be small compared with the number actually emitted per second per cm^2 and would not therefore measurably effect the heat of evaporation of atoms or the electron work function. This may readily be seen by noting that at 2500°K, 3.52×10^{16} atoms of Mo evaporate per sec per cm^2 while only 1.53×10^{11} ions are emitted.

It must be concluded from the foregoing investigation that some, if not all, hot metals emit positive ions of their own metal as well as neutral atoms and electrons. The analysis made above shows that the mechanism of emission of electricity from hot metals is not clearly understood especially as regards the emission of positive ions, for, unlike the evaporation of electrons and neutral atoms, the evaporation of ions is not strictly represented by an equation based upon thermodynamical arguments under equilibrium conditions.

The writer wishes at this time to express his appreciation of the constant help he has received from Professor R. C. Gibbs under whose direction this work was carried out, of the valuable suggestions received from Professor E. H. Kennard and of help given from time to time by other members of the Cornell faculty interested in this work.

ON THE EARLY STAGES OF ELECTRIC SPARKS

By Ernest O. Lawrence and Frank G. Dunnington
University of California

(Received January 3, 1930)

Abstract

With the Kerr-cell electro-optical shutter of Abraham-Lemoine and Beams, phenomena in the early stages of sparks between electrodes of Zn, Cd and Mg have been studied. It was found that, during $50(10^{-8})$ sec after beginning of the sparks, the spark doublet lines $3d_{1,2}-4f_{1,2}$ of Zn have widths of 45A, while the corresponding lines of Cd and Mg are about 30A in width. The luminosity of the metallic vapors of Zn, Cd and Mg was observed to spread from the electrodes with speeds of $2.1(10^5)$ cms/sec, $1.5(10^5)$ cms/sec, and $1.2(10^5)$ cms/sec, respectively. Photographs of the early stages of single sparks with exposure times as short as $4(10^{-8})$ sec were obtained. The snapshots showed that during these short intervals of time after beginning of a spark the discharge is confined to a filament having a cross-section at the anode of $5(10^{-4})$ cm^2 which broadens out to four times this size at the cathode. From the circuit constants and these dimensions of the discharge it was accordingly estimated that the discharge current density attained the magnitude of $1.7(10^6)$ amps/cm^2. The asymmetry of the photographed images of the sparks disappeared when the exposure times were extended to include a complete cycle of the discharge, thereby proving the satisfactory operation of the shutter.

Assuming that the broadening of the lines to be due to the Stark effect of inter-ionic fields and with the aid of existing data on the Stark effect behavior of the lines, it was calculated that the average inter-ionic field was 10^6 volts/cm. This result in turn implies that the average separation of the ions was $3.8(10^{-7})$ cm and therefore that 1/3 of the molecules in the path of the discharge were ionized. Approximately the same degree of ionization follows from the assumption that 1/2 of the discharge current is carried by the positive ions moving towards the cathode with the observed velocity of $2.1(10^5)$ cms/sec.

Four more or less independent methods of estimating the temperature of the early periods of the spark from the present observations lead to values of the order of magnitude of 10,000°K which point to thermal ionization as a prominent feature of such discharges.

Introduction

ELECTRIC sparks have been studied extensively for a long time and yet much remains to be understood concerning the physical process involved. One of the great remaining mysteries[1] centers around the observations of Pedersen,[2] Rogowoski,[3] Torok,[4] Beams,[5] Peek,[6] Burawoy[7] and others that sparks sometimes break down in time intervals of about 10^{-8} sec after ap-

[1] Loeb has proposed a solution of the difficulty, Science **69,** 509 (1929).
[2] Pedersen, Ann. d. Physik **71,** 317 (1923).
[3] Rogowski, Archiv. f. Electrotech. **16,** 496 (1926).
[4] Torok, Jour. A. I. E. E. **47,** 177 (1928).
[5] Beams, Jour. Frank. Inst. **216,** 809 (1928).
[6] Peek, A. I. E. E. Trans. **34,** 2, 1857 (1915).
[7] Burawoy, Archiv. f. Electrotech. **26,** 14 (1926).

plication of electric fields. Their work and the work of Lawrence and Beams[8] made it clear, moreover, that during such short time intervals the voltage across a spark gap drops from its initial high value to low values characteristic of arcs. Thus, the interesting high voltage processes which distinguish a spark from an arc occur during such short intervals of time that they are not easily susceptible to experimental observation.

However, several experimental methods have been developed which have contributed valuable information of the above mentioned sort. Pedersen[2] used Lichtenberg figures to measure spark lags, Rogowski[3] developed a high speed cathode ray oscillograph and studied time variations of potential across spark gaps, Torok,[4] Peek[6] and others used surge or transient voltages of very short duration in their studies of sparks, and Anderson and Smith[9] devised a revolving mirror camera and obtained interesting information on the early phenomena occurring during the "explosion" of wires. The adaptation by Beams[10] of the electro-optical shutter of Abraham and Lemoine[11] to the studies of the relative time of appearance of spectrum lines in spark discharges has perhaps pointed to one of the best ways to the attack of the problem of the early stages of sparks, because the Kerr cell optical shutter makes it possible to view sparks during the desired short intervals of time.

The present paper is concerned with such an experimental study in which, for example, snapshots of single sparks with exposure times as short as $4(10^{-8})$ sec. have been obtained, which show interesting features of the early state of affairs in the discharge.

Apparatus

The apparatus (Fig. 1) consisted essentially of a spark gap *SG*, with condenser *C* in parallel, connected across a source of high voltage *T*, and an electro-optical shutter placed in the optical path between the spark gap and the light recording device at *P*. The latter was either a spectrograph or a camera. When the spectrograph was used, the source of high voltage was

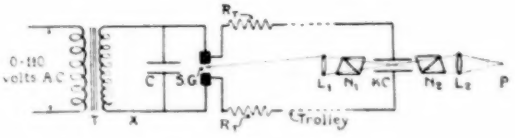

Fig. 1. Experimental arrangement.

simply a 25,000 volt 1 KW transformer which supplied a 60 cycle voltage of any value up to its maximum. When the camera was used a high voltage kenotron (KM−1) rectifying tube was inserted at *X* together with a resistance of about 500,000 ohms. The electrodes of the spark gap made of Zn, Cd or Mg were shaped so that the spark jumped between two parallel faces

[8] Lawrence and Beams, Phys. Rev. **32,** 478 (1928).
[9] Anderson and Smith, Astrophys. J. **64,** 295 (1926).
[10] Beams, Phys. Rev. **28,** 475 (1926).
[11] Abraham and Lemoine, Comp. Rend. **130,** 245 (1900).

6 mm apart. The dimensions of these faces were, when using the spectrograph 3×6 mm (the short dimension being perpendicular to the optical path), and when using the camera, 3×3 mm. The spectrograph was a Hilger constant deviation type having a dispersion of about 36A per millimeter at 4900A. The camera consisted of a plate holder and bellows to exclude light, no lenses other than L_1 and L_2 being necessary.

The electro-optical shutter which was the heart of the apparatus was essentially the same as that described by Beams,[10] but with certain minor though important modifications. A Kerr cell consisting of parallel plates 9.5 cm long, 1.2 cm wide and 0.5 cm apart immersed in carbon bisulphide and situated between crossed Nicol prisms N_1 and N_2 was attached to the terminals of the spark gap by wires of variable length. This system operated as an optical shutter controlled by electrical means in the following manner. With no voltage on the Kerr cell, the carbon bisulphide was not doubly refracting and hence light could not pass through the crossed Nicols. Upon application of a potential across the cell the liquid became doubly refracting and a fraction of the light was passed, within a limited range of voltages the amount of light passed being proportional to the fourth power of the voltage. Now since the voltage which was impressed across the gap and condenser was also impressed across the Kerr cell, by the time the voltage had built up to a value sufficient to cause a breakdown of the gap the shutter was open. When the gap broke down the voltage across it dropped to a relatively small value in a time interval at least not greater than 10^{-8} sec. A resulting discharge wave was propagated along the wires to the Kerr cell causing a lowering of the voltage across the plates at a time after the spark breakdown approximately equal to the length of wire in one lead from *SG* to *KC* divided by the velocity of light. At about the same time that this discharge wave started from the gap, light from the spark began to be emitted and traveled towards the Kerr cell system. A part of the light which reached the cell before the wave was transmitted, while all of the light reaching the shutter thereafter was rejected. Thus it was possible to observe the light from the spark from its beginning up to any desired time of cut off determined by the lengths of the trolley leads. The times of cut off in the present experiments ranged from practically zero to 50 (10^{-8}) sec. after beginning of the spark.

The modifications in the electro-optical shutter had to do with the control of oscillations. It is obvious that if oscillations should exist in the Kerr cell circuit after the voltage is supposedly reduced to a low value, light from later periods of the spark would be transmitted, thereby producing spurious results. Because previous work has been questioned[12] on this basis, it is believed worthwhile to give some of the details and show proof that the shutter operated in the manner outlined above. The methods used to control the oscillations in the trolley circuit were as follows

(1) *Reduction of coupling between the condenser-spark gap circuit and the trolley-Kerr cell circuit to a minimum.* Upon breakdown of the gap, the dis-

[12] Gaviola, Phys. Rev. **33**, 1023 (1929).

charge of the condenser C through the gap is oscillatory. If the coupling between this condenser-spark gap circuit (hereinafter referred to as the condenser circuit) and the spark-gap-trolley-Kerr cell circuit (hereinafter referred to as the trolley circuit) were appreciable, forced oscillations would be produced in the latter. With this in mind the length of path in common between the two circuits was reduced to a minimum by taking off the leads to the trolley circuit by taps in the electrodes about a millimeter back from the sparking surfaces. The coupling was further reduced by taking off these leads to the trolley in a plane at right angles to the condenser circuit.

(2) *Maintaining the fundamental wave-length of the condenser circuit always considerably under that of the trolley circuit.* The trolley circuit consisting of distributed inductance and capacity has a fundamental oscillatory period of its own. It is obvious that even though the coupling were small, the effect in the trolley circuit of oscillations in the condenser circuit would be much greater at or near resonance. To avoid the effect of harmonics as well as that of the fundamental oscillations of the condenser circuit, its wave-length was adjusted so as to be considerably less than that of the trolley circuit. The wave-length of the condenser circuit was calculated and checked by a wavemeter. That of the trolley circuit was obtained by comparison with the condenser circuit by resonance in the following manner. The trolley leads to the gap were disconnected and joined together and the plane of the leads was turned so as to increase the mutual inductance of the circuits. For every set of condenser circuit constants that gave a wave-length within the range of that of the trolley circuit, a position of the trolley could be found that allowed light to pass. Approximate calculations showed that such resonance between the circuits involved fundamentals and not harmonics of the condenser circuit.

(3) *Damping of the oscillations in the trolley circuit.* Even though the trolley circuit were free of all outside disturbances, the charge stored by its distributed capacity previous to a breakdown of the spark would oscillate upon the shorting of the gap by the spark. If these oscillations were critically damped by the insertion of sufficient resistance R_t, the rate of fall of voltage across the Kerr cell would thereby be greatly diminished. However, this impasse to arranging the circuit so that the shutter closes with great rapidity free of appreciable oscillations is only apparent. The intensity of the light passed by the shutter is proportional to the fourth power of the voltage. Hence were the amplitude of the voltage on the first reversal only damped to a value one half the original voltage, the light passed per unit time would be only a sixteenth that at the original voltage. Thus, since the delay in the voltage-drop caused by damping is small until the region of critical resistance is reached, it is possible to damp the oscillations sufficiently without appreciably delaying the closing-time of the shutter. Exact calculations being difficult, the best value for the damping resistance was found experimentally by finding the value which gave the smallest observed distance of migration of the metallic vapor out from the electrodes (see results). The value found was 500 ohms (250 ohms distributed over each lead from spark gap to Kerr cell).

Oscillations were apparent when using resistances considerably below this value. Increasing the damping resistance produced little effect until values of over 1000 ohms were reached when the slowing down of the rate of closing of the shutter became observable

That the shutter was effectively closing at times close to those calculated from the wire path was definitely proved by the direct photographs of the spark (see results). When the time of cut off was made equal to or less than that of a half cycle of the condenser circuit, the pictures obtained were assymmetric relative to the cathode and anode, the images of the discharge being narrower and more intense near the latter electrode. This experimental observation constitutes indisputable evidence that the shutter operated in the manner outlined above.

The Experiments

The initial experiments were concerned with observations of spectra emitted during early stages of the spark. An image of a portion of the spark near one electrode was projected through the optical shutter and was focused lengthwise on the slit of the spectrograph and photographs of the spark spectra of Zn, Cd and Mg were obtained with the shutter closing at various times after the beginning of the sparks. In order to obtain sufficient blackening of the photographic plates it was necessary to expose for from 3 to 10 minutes. Since 120 sparks occurred per sec. the photographs represent the integrated spectra of the beginning of a large number of sparks. The general features of the results were the same for the three metals studied and therefore only the data on Zn are here exhibited. Fig. 2h shows the spectrum of the Zn spark obtained with the Nicol prisms uncrossed, being consequently the ordinarily observed spark spectrum. The Zn spark doublet 4912–24A and the arc lines 4680A, 4722A and 4811A together with several air lines are prominent. 2a exhibits the spectrum observed with the shutter closing 19 (10^{-8}) sec after the beginning of the spark—a spectrum which bears little resemblance to 2h. As the experiments of Schuster-Hemsalech[13], Beams[10] and others have shown, the metallic lines of the spark are absent in its early stages, the spectrum being that of air with a strong continuous background. Taking into account the dependence on wave-length of the photographic sensitivity of the plate and the absorption in the optical system it is estimated that the maximum intensity of the continuous spectrum occurred well below 4600A. It is of particular significance to note the extreme diffuseness of the air lines during this early period of the spark which is attributed to the Stark effect of the inter-ionic fields

Fig. 2b shows the spectrum photographed with the shutter closing 27 (10^{-8}) sec after the beginning of the spark. In this photograph, as in all the others, light which produced the lower ends of the spectrum lines came from the region of the spark adjacent to one of the electrodes and the length of the lines represents about 2 mm of the gap. The continuous background at this later time appears definitely to be most intense near the electrodes.

[13] Schuster and Hemsalech, Phil. Trans. **193A,** 189 (1900).

This photograph indicates also that the position of maximum intensity of the continuous spectrum shifts to a slightly longer wave-length at this later time. This photograph also shows the first appearance of the Zn metallic spark doublet 4912–24A as a very diffuse region of luminosity near the electrodes. The broadening of the lines is more easily seen in 3g which is

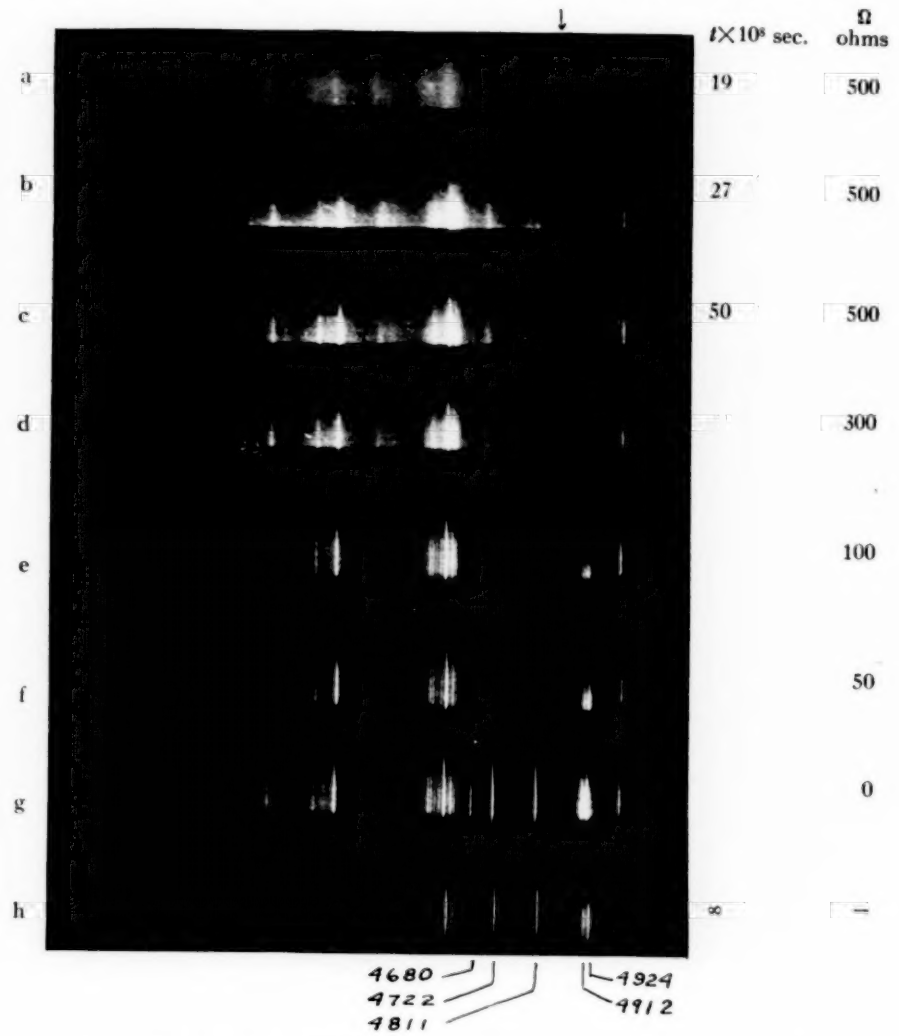

Fig. 2. Photographs of spectra emitted during various intervals of time after beginning of sparks between Zn electrodes in air.

a magnified section of 2c. It was estimated from these observations that each of *the spark lines during this early period of the discharge were broadened symmetrically to a total width of 45A*. The widths of the corresponding lines of Cd and Mg were observed to be somewhat less—approximately 30A.

Fig. 2c shows that at the later time of 50 (10^{-8}) sec after the beginning of the spark, the metallic spark lines were emitted at a greater distance from

the electrodes. This observation gives at once a measure of the average velocity of migration of the metallic ions away from the electrode surfaces. From several such observations it is found that *during the first 27 (10^{-8}) sec the average velocity of migration of the metallic ions away from the electrode surface is 2.1 (10^{5}) cms per sec.* The corresponding observed velocities for Cd and Mg ions were 1.2×10^{5} cm/sec and 1.5×10^{5} cm/sec respectively. Due to photographic difficulties, these values however are much less accurate than that for Zn.

The above mentioned spectra were taken with a distributed resistance in series with the Kerr cell of 500 ohms. Reducing this resistance to 300 ohms produced no perceptible change—as shown by the spectrum 2d which was taken under the same conditions as 2c excepting that the resistance was reduced to the lower value. On reducing the resistance to 100 ohms, 50 ohms and practically zero, however, a marked effect resulted as shown by Fig. 2e, f and g. From the fact that the luminosity of the spark lines extended further from the electrodes in the latter cases and that even the arc lines were in evidence, it is concluded that the oscillations were of sufficient magnitude to reopen the shutter at a later time. Careful examination showed that the operation of the shutter was sensibly independent of the damping resistance over the range 300 to 1000 ohms. Inserting resistance in excess of 1000 ohms over damped the discharge of the Kerr cell to such an extent that its effective time of closing was perceptibly delayed. Though it was not possible to make an accurate estimate, a calculation from the dimensions of the circuit agreed with the above values as being the right order of magnitude to damp the oscillations to the extent desired.

Our photographs fail to show the metallic arc lines at all, during 50 (10^{-8}) sec after beginning of the spark, a result not in agreement with the observations of Beams[10] and Locher.[14] A faint haze of luminosity near the electrode of wave-length near 4811A shown in 2c might easily have been thought to be due to the Zn arc line 4811A. However, measurements shew that it is nearer 4817.5A. The origin of this line is uncertain at the present time as there are no well known Zn or air lines of this wave-length.

The photographs 2a, b, c, show a diffuse air line near 4865A (indicated by arrow) which occurs only in these very early periods of the discharge. 2a shows it extending practically across the spectrogram while in 2b and 2c it is confined successively nearer the lower edge. As will be evident in the discussion, very intense ionization and accompanying high temperature exists in the early period of the spark and it is probable that this line therefore is due to an ionized constituent of the air. There are many examples in the literature of lines which appear only under such conditions.[15]

For the purpose of measuring the cross-section of the discharge during its early development in order to obtain an estimate of the current density, direct snapshots of the spark of the requisite short exposures were attempted. A kenotron and a one-half megohm resistance inserted in series with the

[14] Locher, J.O.S.A. and R.S.I. **17,** 91 (1928).

[15] Handbuch der Physik **21,** p. 434.

condenser made it possible to apply known differences of potential across the spark gap resulting in single sparks. Images of the spark projected through the Kerr cell and focused on a photographic plate are shown in Fig. 3. The polarity indicated in all the photographs is that of the first half cycle. 3a is a series of single sparks taken with the Nicol prisms uncrossed (with the

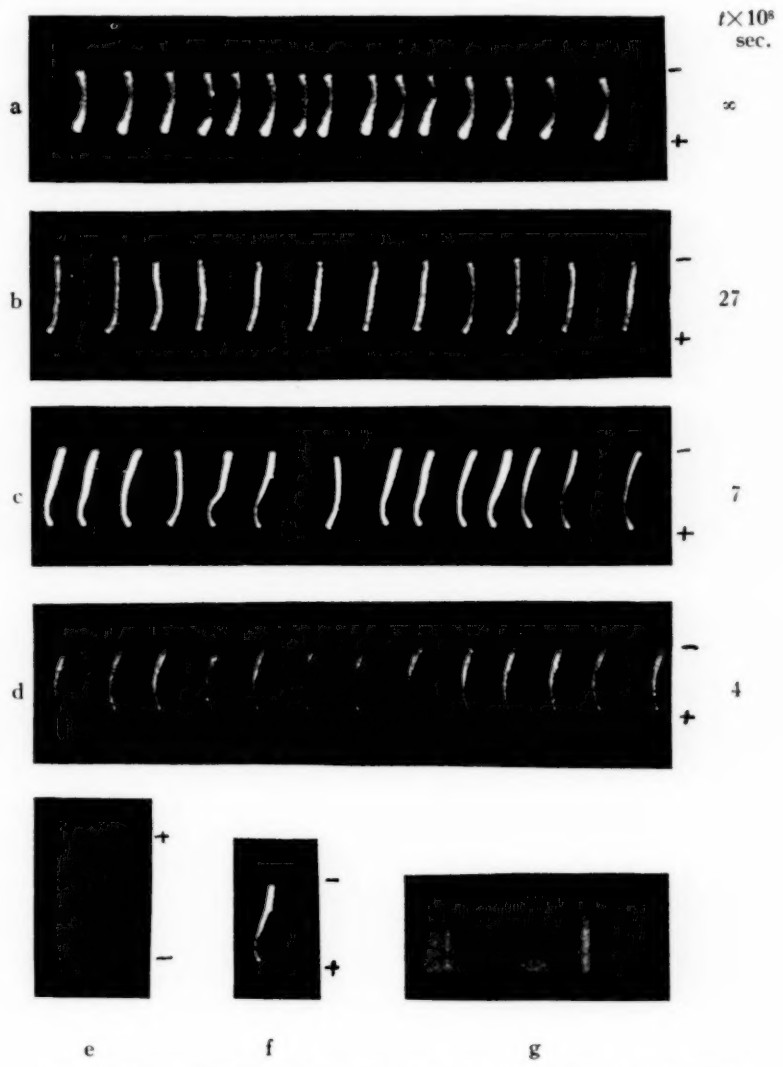

Fig. 3. Photographs of the early stages of sparks between Zn electrodes.

shutter continuously open) and therefore represent images of completed sparks. 3d shows the spark during the first 4 (10^{-8}) sec of its existence. To obtain these photographs it was necessary to have a condenser capacity of 0.004 mf in order to maintain the oscillations in the spark circuit out of resonance with the Kerr cell circuit. It is seen that *the discharge is confined*

to a very narrow filament near the anode which widens out towards the cathode. Measurement of the plates showed that *the average diameter of the discharge at the anode was 0.25 mm and at the cathode 0.5 mm.* Since the period of oscillation of the spark was 26 (10^{-8}) sec, these photographs represent the form of the discharge during the earlier part of the first half cycle. Changing the condenser capacity to 0.008 mf, the photographs of 3c were obtained with the shutter closing 7 (10^{-8}) sec after the breakdown of the potential across the gap. In this instance the period of oscillation was 36 (10^{-8}) cm and consequently these are pictures of approximately the first quarter cycle of the discharge. The dissymmetry of the discharge is still evident, though not as marked as in the shorter exposures,—the average diameter of the discharge at the anode being 0.45 mm and at the cathode 0.5 mm. Another interesting feature of these photographs is the presence of *a very bright spot of luminosity close to the anode*, indicating an intensity of light there greatly in excess of that of the central section of the filament. 3b was obtained with the shutter closing at 27 (10^{-8}) sec. In this instance the shutter closed after the setting in of the second half cycle, as the period of oscillation remained at 36 (10^{-8}) sec. As was to be expected, this photograph shows a more nearly symmetrical filament with minute intense spots of light as both electrodes, that at the cathode being less intense than the one at the anode because the cut off occurred at about the middle of the second half cycle. The average diameter of the filaments is 0.5 mm. It is perhaps not amiss to emphasize again that *these observations of the asymmetry of the discharge during the first half cycle are indisputable evidences that the electro-optical shutter functioned in the manner outlined above and that oscillations were of inappreciable magnitudes.*

Thus during the period of 23 (10^{-8}) sec between the closing of the shutter for groups d and b, the cross-section of the discharge at the anode was observed to vary from 4.9 (10^{-4},) sq cms to 1.9 (10^{-3}) cm^2 and since during these periods the average discharge currents (estimated from the circuit constants) were 800 and 1100 amps respectively, *the average current density varied from 1.7 (10^6) amps per cm^2 to 5.8(10^5) amps per $cm.^2$* These enormous current densities produced the great brilliance of the spark which made possible the short exposure photographs of the present experiments.

The path of breakdown of the sparks usually were along the lines of force. When the electrode surfaces were flat with sharp edges the sparks jumped from edge to edge along the curved lines shown in many of the photographs. When the edges were rounded off the sparks jumped between the middle of the electrode surfaces along the straighter lines of force in that region. However, interesting exceptions have been observed during the first 30 (10^{-8}) sec of the spark as shown in Fig. 3, e and f. 3f shows a sharp spur protruding from the main filament of the discharge of the sort that might arise from an ion path initiated by a high velocity particle. The spur is bent away from the anode and luminosity is seen to extend outside the main discharge from the spur to the cathode, as though positive ions formed along the path of the spur produced additional luminosity during their

passage to the cathode. 3e shows a case where the spark took two simultaneous paths, the bifurcation suggesting that the spark breakdown was initiated at the cathode. Examples of bifurcation at the anode and also in the middle of the gap, however, have been observed.

Discussion

There can be little doubt that large broadening of spectrum lines produced by high current densities is due to the Stark effect of inter-ionic fields.[16] The width of the spark doublets of Mg, Cd and Zn observed in the early stages of the spark therefore can serve as a measure of the average ionic fields, and in turn, the average number of ions per cc in the discharge. Such an estimate requires an independent knowledge of the Stark effect behavior of the lines. Now the spark lines in question result from transitions between the hydrogen like energy levels $3d_{1,2}$ and $4f_{1,2}$ and indeed are very similar to the corresponding line 4686A of ionized helium. It is therefore to be expected that the metallic spark lines should exhibit a Stark effect closely resembling the observed Stark effect of the corresponding He line. Several experimental measures of the Stark effect of the He line in question have been made, the most recent being that of Foster[17] who finds that the maximum displacement of the components from the undisplaced position is about 2.4A per 100,000 volts/cm field. The results of Nagaoka and Sugiura[18] show that the corresponding line 4811A of Mg is broadened to a width of about 2A on each side of the undisplaced position in an average field of 116,000 volts/cm, a fact which supports the expectation that the corresponding lines of He, Zn, Cd and Mg should exhibit nearly the same Stark effect. From the total width of 45A observed in the present experiments then it can be concluded with considerable confidence that *the average ionic field during the early stage of the Zn sparks here studied was approximately 10^6 volts per cm.*

From this value for the average ionic field and the inverse square law it follows that the average separation of the ions was approximately 3.8 (10^{-7}) cm and therefore that the total number of ions and electrons was about 1.8 (10^{19}) per cc. *Thus, about 33 percent of the molecules in the path of the discharge were ionized.* Anderson and Smith[9] have found an equally great degree of ionization during the early stages of the "explosion" of wires.

The present experimental data lead to a second and independent estimate of the ionic density. The average velocity of migration of the metallic spark luminosity, and therefore presumably of the positive ions away from the anode was observed. Assuming that the positive ions moved towards the cathode with this speed and carried one-half the discharge current, it follows that there were necessarily present about 0.82 (10^{19}) positive ions per cc. Thus, this second estimate indicating 30 percent ionization is in excellent agreement with the first.

[16] An excellent resume of the subject of the broadening of spectrum lines is to be found in volume 21 of the "Handbuch der Physik."

[17] Foster, Astrophys. Jour. **62,** 229 (1925).

[18] Nagaoka and Sugiura, Jap. Jour. of Phys. **3,** 46 (1924).

The objection might be raised perhaps that, because of the far greater mobility of the electrons, they carry most of the current of the discharge and consequently it is not valid to assume that half the current is carried by the positive ions. Loeb[1] states, for example, that the electrons have about 1000 times the mobility of the positive ions. However, such estimates are made with the assumption that the density of the ions is small compared to the density of the neutral molecules, a state of affairs existing in low current-density discharges. The above results make it clear that in the early stages of sparks because of the high degree of ionization a pumping action of the ions produces a general flow of both ions and neutral molecules resulting thereby in a greater mobility of the ions than calculated in the usual manner. Moreover, a simple calculation shows that the high current density of the discharge produced a magnetic field as great as 20,000 Gauss which exerted a great influence on the trajectories of the electrons. Thus, if the velocity of the electrons were 10^8 cms/sec perpendicular to the magnetic field, it is calculated that the magnetic field caused them to travel in curved paths with radii of curvature 3 (10^{-4},) cm. The effect of the magnetic field was consequently to increase greatly the paths traversed by the electrons in passing from cathode to anode, thereby producing a great reduction of their general drift velocity (mobility). Space charge effects played an unknown though probably important part also in keeping the electron current and the positive ion current at the same order of magnitude.

Several independent estimates of the temperature may be made as follows.

(1). From the degree of ionization the effective temperature of the discharge can be calculated after the manner of Saha.[19] We have the reaction-isochore

$$\log \frac{x^2}{1-x^2} P = -\frac{5050 V_i}{T} + 2.5 \log T - 6.69.$$

where x is the fractional number of the atoms ionized, P is the pressure in atmospheres, V_i is the ionization potential in volts and T is the absolute temperature. Taking for x the here-observed value 1/3, for V_i 9.3 volts, the ionization potential of Zn, and for P, 10 atmospheres, there results for the temperature of the discharge the value of 13,500°K. A higher assumed value for V_i corresponding to ionization of O or N would lead to a correspondingly higher estimate of the temperature. However, the observations were taken in the proximity of the electrode where the metallic vapor predominated. From the observed spreading of the filament of the discharge during the course of time, from the work of Anderson and Smith on exploded wires, and from other considerations, it appears that the assumed pressure is right in order of magnitude.

(2). It is also possible to make a rough estimate of the temperature of the discharge from knowledge of the rate of dissipation of energy in the spark. Professor J. W. Beams has kindly let us see some of his revolving mirror

[19] Saha, Proc. Roy. Soc. **A99,** 135 (1921).

photographs of sparks in advance of publication from which we deduce that the sparks we worked with had a duration of the order of magnitude of 10^{-5} sec, and therefore that about one one-hundredth of the energy of the discharge was dissipated in the spark during the first 10^{-7} sec. Knowing in addition the capacity of the condenser, the voltage at breakdown, the specific heat of the, and the volume of the gas heated, an elementary calculation leads to 5000°K as the temperature of the discharge. This estimate is somewhat lower than that resulting from Saha's equation, a fact that is to be accounted for by the assumption that only 1/100 of the energy stored in the condenser is dissipated in 10^{-7} sec. Beams has shown in his revolving mirror photographs that the first cycle of the spark discharge has a period about 1.5 times longer than the period of later oscillations and therefore that the resistance and rate of energy dissipation is greater at the beginning of the spark. This fact was also taken into account in estimating the current density in the above calculations.

(3). As has been pointed out above, the high degree of ionization produced a general flow of ions and neutral molecules to such an extent that the observed velocity of migrations of the ions probably also measured the average velocity of the molecules. An estimate of the temperature then follows from

$$(3/2)kT=(1/2)mv^2$$

where k is Boltzman's constant, T is the temperature, m is the mass of a Zn atom and v is the observed velocity. Such an estimate yields a temperature of 10,900°K.

(4). Finally, an estimate of the temperature may be made from the intensity distribution in the continuous spectrum of the discharge. From the observation that the intensity was a maximum well below 4600A, it is concluded that the discharge temperature was considerably above 6200°K. This value is least reliable of all because many sources of error in estimating light intensities were not carefully investigated.

Thus, four more or less independent estimates of the temperature of the sparks obtained from the data of the present experimental study agree in indicating that it is of the order of magnitude of 10,000°K. This result points to thermal ionization as the main process in the early stages of sparks as has been suggested by Slepian.[20]

[20] Slepian, Phys. Rev. **31,** 1123 (1928).

A NEW REGULARITY IN THE LIST OF EXISTING NUCLEI

By Henry A. Barton
Department of Physics, Cornell University

(Received January 13, 1930)

Abstract

In the absence of a theory of nuclear constitution, a search for regularities in the list of existing nuclear types is of value. Aston's data form a fairly complete list up to atomic number 61. Previous investigations disclosed evidence of several types of regularity. A new type has been observed in which most of the known nuclei in the range studied fall into three clusters, each characterized by a two dimensional symmetry. More specifically, when the nuclei are plotted as points whose ordinates and abscissas indicate the number of protons and electrons respectively in their constition, there exists for each cluster a center (P, E) such that if there is a nuclear type $(P-X, E-Y)$ there is, in general, also a symmetrical type $(P+X, E+Y)$. A consideration of the relatively few departures from this rule within the clusters leads to a list of *predicted isotopes* as yet undiscovered. A possible physical interpretation of the new type of regularity is tentatively suggested. The considerations advanced apparently do not apply to a number of points scattered through the regions between the clusters.

Introduction

THERE is no comprehensive theory of the structure of atomic nuclei. The present position is one in which it is very desirable to examine the available data in search of empirical laws with which to simplify the statement of what is known. The list of nuclei embracing all known isotopes of all elements which actually exist, in contra-distinction to those conceivable nuclei which do not, presents a fruitful field for such a scrutiny. Any rule or regularity of occurrence which can be found will facilitate the development of a satisfactory theory. Beck[1] has pointed out that Aston's work has now furnished a body of excellent data[2] covering nearly all elements up to atomic number 61. A knowledge of the isotopes of many elements heavier than this is as yet lacking so that the data do not have the completeness which is necessary, or at least most desirable, when it is a question of the existence or non-existence of each possible nucleus. Only that part of the list of elements which lies below atomic number 61 is considered in the present paper. For such a list presented in significant tabular form the reader is referred to Beck's papers.

The considerations which Beck advances lead to valuable rules in addition to those already noted by others.[3] The work of Harkins,[4] based on evidence

[1] G. Beck, Zeits. f. Physik **47,** 407 (1928); **50,** 548 (1928).

[2] F. W. Aston, Phil. Mag. **49,** 1191 (1925); Proc. Roy. Soc. **A115,** 487 (1927), p. 509.

[3] A summary of speculations about nuclear constitution and structure is given by E. N. da C. Andrade, "The Structure of the Atom," Chap. VII.

[4] W. D. Harkins, Science **70,** 433 and 463 (1929). Zeits. f. Physik **50,** 97 (1928). Also many earlier papers references to which are made in the two cited.

concerning the relative abundance[5] of the elements in the earths crust and in meteorites, has been particularly fruitful in establishing rules governing the existence and stability of nucleur types. The kinds of regularity pointed out by these and other authors deal with the numbers of α-particles, protons, and electrons in the nuclei. For example, the fact that mass increments of four units together with charge increments of two units occur frequently in almost any sort of classification gives strong evidence of the existence of

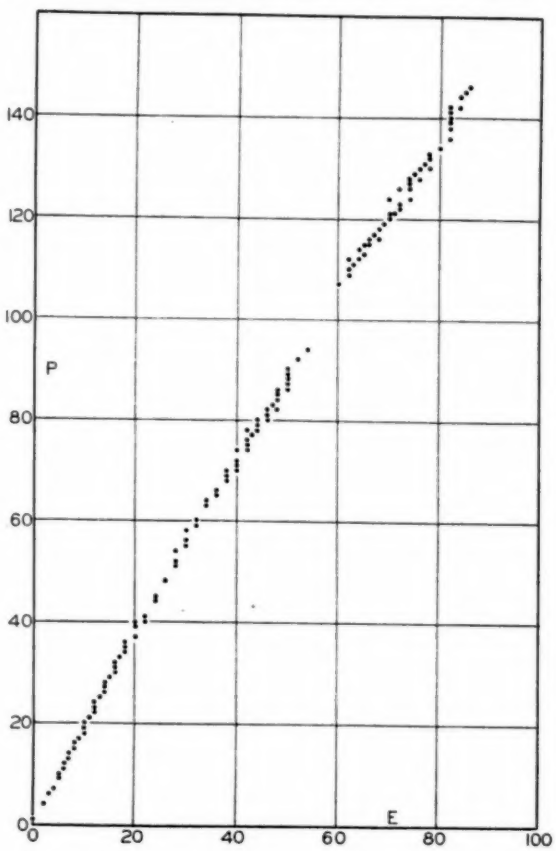

Fig. 1. Constitution of all known nuclear types in the range of elements below atomic number 61.

nuclei which differ from one another merely in the number of integral α-particles they contain. Other rules are, for example, the tendency for the number of nuclear electrons to be even, the limitation to two isotopes in the cases of elements of odd number, etc.

A New Type of Regularity

The writer has recently observed an altogether different type of regularity which does not seem to be described in the literature. It appears when a

[5] F. W. Clark, "The Data of Geochemistry," Bulletins **491** (1911) and **616** (1915), U. S. Dept. of the Interior. "Evolution and Disintegration of Matter," U. S. Geol. Surv., Prof Paper **132-D** (1924). W. D. Harkins, J. Am. Chem. Soc. **39,** 856 (1917).

suitable chart is made of the constitution of the existing nuclei. Fig. 1 is such a chart in which a point is plotted for each nucleus opposite the ordinate P representing the number of protons it contains and the abscissa E representing the number of electrons it contains. P, the number of protons,is approximately equal to the atomic mass. E stands for *all* of the nuclear electrons whether constituting α-particles or not, so the atomic number, or nuclear charge, Z, is equal to $P-E$. The chart was compiled from Aston's data.

It is evident even on this small scale chart that there are three clusters of points separated by regions of relatively low density, i.e., where the ratio of the number of actual to conceivable nuclei is relatively small. The clusters themselves are individually of interest. A superficial examination of a small

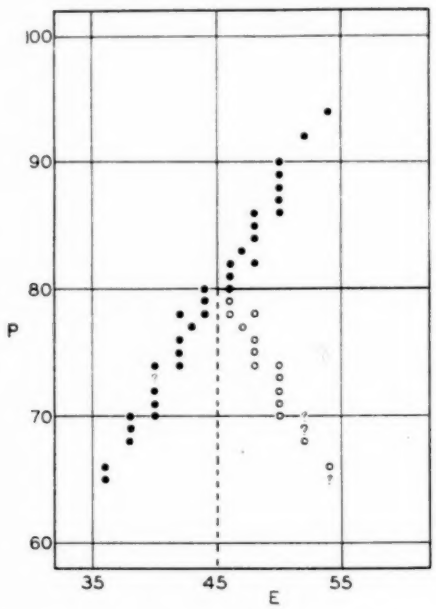

Fig. 2. Enlargement of the middle portion of the chart in Fig. 1 to show the two-dimensional symmetry of the cluster. (Cluster II.)

chart such as Fig. 1 gives little basis for specifying the limits or centers of the clusters. On a larger scale, however, it is apparent that in each group there exists a regularity in the form of a two dimensional symmetry about a definite point near the center of gravity of the clusters. For example, Fig. 2 shows the region of Fig. 1 occupied by the middle cluster. The solid dots are the same as those of Fig. 1. The circles show the positions occupied by the dots in the upper right quadrant if that quadrant is rotated 180° around the axis of symmetry $P=80$. The extent of the symmetry can now be estimated at a glance. In this cluster, evidently centered at $(P, E)=(80, 45)$, the symmetry is perfect except that in the cases of four out of the thirty-two points plotted, the symmetrically located positions are vacant. Such vacant positions are indicated by question marks.

Similar charts of the clusters in the regions of heavier and lighter elements respectively are shown in Figs. 3 and 4. In the cluster made up of heavier elements, it is noteworthy that the symmetry, centering at (124,72) consists largely of two long diagonal lines of points. One of these, starting at (124, 74), runs one way to (112,62), and the other starting at (124, 70), runs the other way to (136,82). The one represents the isotopes of tin and the other the isotopes of xenon. Although two positions are vacant in the case of xenon, the end positions of the two lines are symmetrical, and in each case, the outer end is followed by several points in a vertical row.

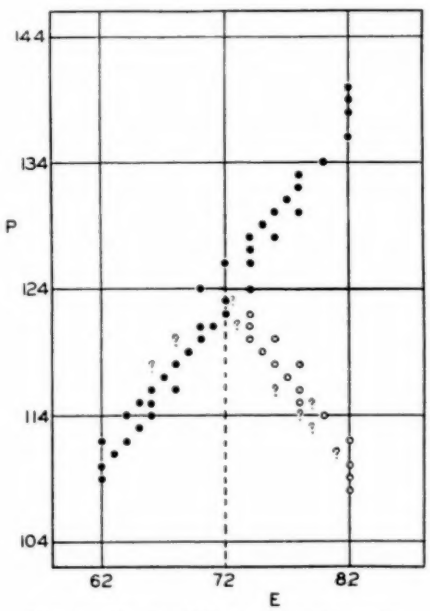

Fig. 3. Cluster III; heavier elements.

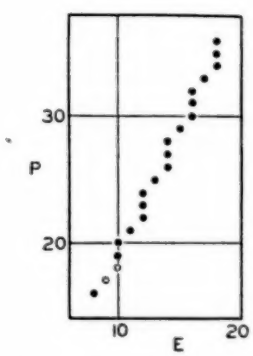

Fig. 4. Cluster I; lighter elements.

The cluster in the region of lighter elements presents so simple a type of symmetry that the center cannot be located without ambiguity. The point (25,13) would serve as well as (27,14). The discovery of the new oxygen isotopes[6] (shown by circles) would tend to shift one's estimate of the "center of gravity" of the cluster downward.[7]

Aston has recently published the result of some further experiments with the mass spectrograph.[8,9] These must be considered now in so far as they

[6] W. F. Giauque and H. L. Johnson, Nature **123,** 318 and 831 (1929). J. Am. Chem. Soc. **51,** 1436 (1929).

[7] It is interesting to note that the new oxygen isotopes are nuclei which would have been predicted by extrapolation of the obvious step-like regularity of the cluster.

[8] F. W. Aston, Nature **120,** 224 (1927); **122,** 167 and 345 (1928).

[9] The writer was not aware of these when he published a preliminary notice. (Phys. Rev. **34,** 1228 (1929)). He wishes to take this opportunity of also acknowledging his error in including in that notice a nuclear type (80+11, 45+7) which has not been shown to exist. Beck has postulated its existence on fairly firm grounds. However, the writer wishes to confine himself to Aston's experimental data with the addition of the isotopes 17 and 18 of oxygen, 15

affect the symmetry of the clusters. New isotopes of lead, mercury, germanium and zinc are announced. It is not of interest for the present purpose to add the corresponding points to Fig. 1. In fact, lead and mercury are above the range of elements investigated. The isotopes of germanium and zinc alter only Cluster II. To bring Fig. 2 up to date it would be necessary to add points corresponding to the additional isotopes of germanium and zinc, namely (73, 75, 76, 71 and 77) and (67 and 65) respectively. The previously known isotopes were of course already plotted in Fig. 2. None of the new points falls into a position symmetrical with one already existing. The symmetry of this cluster is thereby considerably impaired although strong evidence of the tendency remains.

Aston states[8] that it is impossible to exclude the possibility that the mass spectrum lines representing some of these isotopes really represent hydrides of the previously known isotopes. Germanium is known to be like carbon in its tendency to form unstable hydrogen compounds, so it would be expected that such hydrides would appear in the discharge tube in the same way as CH, CH_2, etc. appeared when compounds of carbon were present. The symmetry considerations would be helped if this were found to be the case. On the other hand, it may be that here is an example of the danger of working with only partially gathered data. The relative abundance of the new isotopes is obviously very small since they escaped discovery in Aston's previous study of germanium. It is possible that symmetrical nuclear types of the same order of abundance (very faint isotopes of strontium) may yet be found to restore a high degree of symmetry to the cluster. It is because of these reservations that the cluster has been plotted without, rather than with, the new data.

Discussion

The boundaries of the three clusters as represented in Figs. 2, 3, and 4 are of course, arbitrarily chosen. However, it can be said that there is good evidence of symmetry just inside these boundaries and little of such evidence just outside. There remain, then, the regions below and between the clusters in which fall the points of a number of very common nuclei, among them hydrogen, helium, carbon, calcium, and iron. In these regions no evidence of symmetry has been discovered, so that no claim for applicability over the whole list of natural elements can be made for the type of regularity described in this paper.

Alternative points of view may be taken with regard to the departures from perfect symmetry within the clusters. The vacant positions may be vacant only through lack of data. On the other hand, the existing points symmetrical to these vacant positions may represent nuclei not properly belonging to the cluster in some sense which we do not now know how to define. The first alternative may at least be adopted tentatively. On this

---

of nitrogen, and 13 of carbon discovered through the band spectra of compounds of these elements. See Ref. 6; also A. S. King and R. T. Birge, Nature **124,** 127 (1929); Phys. Rev. **34,** 376, 379 (1929); S. M. Naudé, Phys. Rev. **34,** 1498 (1929).

basis it is predicted that the question marks in Figs. 2 and 3 represent isotopes which should still be found, perhaps in very small quantity. A list of the isotopes so predicted is given in Table 1.

TABLE I

P, E	Z	Element	Remarks
		(*Cluster II*)	
73,40	33	As	Note 1
90,52	38	Sr	
91,52	39	Y	Note 1
95,54	41	Nb	Note 2
		(*Cluster III*)	
108,62	46	Pd	
118,66	52	Te	
120,68	52	Te	
125,72	53	I	Note 1
127,73	54	Xe	
133,79	54	Xe	
132,76	56	Ba	
134,78	56	Ba	
135,79	56	Ba	Note 3
137,81	56	Ba	

Note 1. Gives this odd element two isotopes at usual mass interval of two units.

Note 2. Isotopic constitution entirely unknown. Atomic weight of 93.1 would suggest strongly the two isotopes 93 and 95 following the rule for odd elements referred to in Note 1.

Note 3. Atomic weight of 137.37 indicates existence of some isotopes lower than the known 138.

At the foot of the table are some notes as to independent reasons for expecting these isotopes to exist or not to exist in the several cases.

The additional isotopes of germanium and zinc, to which reference has already been made, would demand, on the basis of symmetry, the isotopes 83, 84, 85, 87 and 89 of strontium and 93 and 95 of zirconium.

Even if complete data do not make the symmetry perfect, it is nevertheless a strongly marked tendency and calls for explanation. There is probably not sufficient basis as yet for the serious advancement of a theory. As a point for discussion, however, the suggestion which follows is not out of order.

Consider, for example, the middle cluster whose center is at the point (P_2, E_2) representing a conceivable nucleus consisting of 80 protons and 45 electrons. That this nucleus apparently does not exist is a matter of no concern. Suppose that at an early stage in the evolution of the matter from which terrestrial matter was drawn, there were formed fairly abundantly nuclei of constitution ($2P_2$, $2E_2$), i.e., (160, 90) containing just twice as many protons and electrons as the center of the symmetrical cluster. Such a nucleus has not been found to exist in the earth's crust and may hypothetically be regarded as unstable. Suppose there to be a tendency on the part of this nuclear type to break into just two nearly (but not precisely) equal parts. The products of any one such event would be $(80+X, 45+Y)$ and, since the second part is postulated to contain the rest of the nuclear matter, $(80-X, 45-Y)$. Obviously there would thus come into existence always two nuclei symmetrically located X, Y and $-X$, $-Y$ units respectively from the sym-

metry center (80, 45). The possible values X, Y would presumably be governed by nuclear forces of cohesion. That is, like a crystal, the nucleus might have particular surfaces of division more probable than others.

To explain the three observed clusters, three transitory parent nuclear types must be postulated. They would have the constitutions: a) (248, 144) representing an element a little beyond uranium and, therefore, almost certainly unstable; b) (160, 90) falling near the upper region of the rare earths; and c) possibly (54, 28) the lesser isotope of iron, or (50, 26) an unknown isotope of chromium.

Nothing has thus far been said about the relative abundance of the nuclear types. On the basis of the suggestion that symmetrical nuclei are natal twins, the observed symmetry of existence would be expected to extend itself to a like symmetry of abundance. Roughly speaking this is not found to be the case. A test of such a consideration is difficult when the elements involved are different chemically. It is possible, however, to observe whether the course of abundance of the isotopes of tin corresponds symmetrically to that of the isotopes of the symmetrically located element xenon. Aston places the tin isotopes in the order 120, 118, 116, 124, 119, 117, 122, 121, 112, 114, 115. A comparison of the symmetrical order for xenon with the observed order of that element is given below:

Expected from symm.	128, 130, 132, 124, 129, 131, 126, 127, 136, 134, 133
Found by Aston	129, 132, 131, 134, 136, 128, 130, 126, 124

It may well be the case that an initial symmetry of abundance has ceased to exist on account of differences in the stability of the several nuclear types, and only the symmetry of existence remains as a relic of the originating process.

Before concluding, it should be acknowledged that the suggestion outlined may be entirely supplanted by an assumption of inherent symmetry in the rules giverning the stability of the nuclei. Probably no more explicit statement in this vein may be made for the present.

BLACK BODIES IN THE EXTREME INFRA-RED

By C. Hawley Cartwright
California Institute, Pasadena

(Received December 30, 1929)

Abstract

Absorbing power of various materials of wave-lengths greater than 50μ.—For blackening a receiver of a thermocouple for radiation for obtaining pure rotation band spectra, it is desirable to use a material that is an efficient absorber of the extreme infra-red but a poor absorber of radiation of shorter wave-lengths. The absorbing power of 25 materials were tested for radiation of wave-lengths near 4μ and greater than 50μ. Of all the materials tested, white lead, litharge, red phosphorus, powdered glass, copper sulphide, and celestite were found the best for covering a receiver to absorb the extreme infa-red radiation. The 25 materials were tested by painting them on a receiver of a thermocouple which was exposed to extreme infra-red radiation. The same receiver and thermocouple were used throughout the experiment. A D'Arsonval type galvanometer was improved by using a quartz suspension and replacing each conducting lead with silver leaf or gold plated silver ribbon 1μ thick wound in a spiral.

Glass as a source of extreme infra-red radiation.—Hot glass made a good source of extreme infra-red radiation when used with a cold thin glass shutter.

Introduction

While working with thermocouples and radiometers in the extreme infra-red, it was found that nothing was known quantitatively of the absorbing qualities of the materials used for blackening the receiver. Since the efficiency of the receiver depends on its absorbing power, it was fundamentally important to know the relative merits of the various materials suitable for blackening a receiver. Twenty-five such materials were selected and comparisons made of their respective absorbing powers for both extreme and near infra-red radiation. It was desired to find a material that was black for infra-red radiation of wave-length greater than 50μ and a poor absorber of shorter radiation and especially adapted for coating a thermocouple or radiometer. Some materials that had no practical usefulness were also tested to see if any were exceptional absorbers of the extreme infra-red.

The experimental difficulties encountered in working with radiation of longer wave-length than 50μ is due mostly to the very small amount of energy available in that region and the interference of the large amount of shorter radiation. Various means are used to filter out the shorter radiation. A black body at 1000°K radiates 57 percent of its energy between 2μ and 5μ[1] and only 0.08 percent of its energy in wave-lengths greater than 50μ. Increasing the temperature to 2000°K increases the energy between 2μ and 5μ 12-fold while radiation of 70μ is only increased $2\frac{1}{2}$ times; the proportion is less favorable at 3000°K.

[1] L. L. Holladay, J.O.S.A. **17**, 333 (1928).

The small amount of energy available makes it desirable to use a material that is an efficient absorber of long waves; also, it would be desirable if the material were a poor absorber of the near infra-red. The desirability of a material depends on the type of receiving apparatus. For thermocouples, the material should be a good heat conductor, so that it will quickly heat the metal receiver. For radiometers, it is better to use a poor heat conductor so that the back side of the vane will be cool; also, it is better to have a high temperature gradient.[2,3]

A material that absorbs the extreme infra-red well could be used as a source, if the temperature is not too high to alter the physical or chemical state of the material, so that Kirchoff's law would no longer apply. Here, too, it would be an advantage to use a material that is a poor absorber of the short infra-red.

The Experimental Arrangement

The apparatus was essentially that used by most investigators of pure rotation band spectra with regard to the method of isolating the long wavelengths. Fig. 1 shows schematically the apparatus. The source of radiation

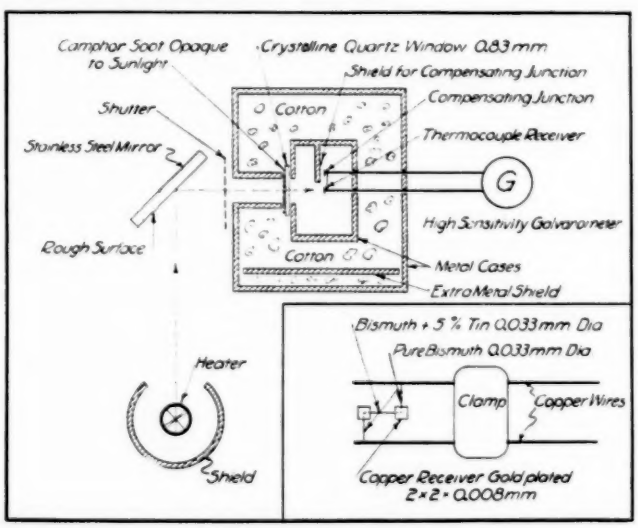

Fig. 1. Apparatus.

consisted of an electric heater painted with ground glass in tartaric acid and sugar. The temperature was held constant at 1000°K. The radiation was reflected from a stainless steel mirror that had been ground rough with emery. The average depth of the pits was about 8μ and since the reflection was at 45°, the effective depth was about 6μ. A crystalline window 0.83 mm thick was sooted with camphor smoke, so that it was opaque to sunlight. The thermocouple was a balanced type and was shielded from stray radiation and conduction. The wires were 0.033 mm in diameter and had a high ther-

[2] G. Hettner, Zeits. f. Physik **47**, 499 (1928).
[3] Paul S. Epstein, Zeits. f. Physik **54**, 537 (1929).

moelectric power. The receivers were gold plated copper 2 mm by 2mm and 0.008 mm thick. The receivers were waxed to the thermojunctions. Two shutters, one of metal and one of microscope cover glass 0.014 mm thick were used separately and in combination. The galvanometer had a sensitivity of 11 mm microvolt when critically damped. It was found desirable to rebuild the galvanometer in order to get more reliable measurements. The silver ribbon suspension was replaced by a quartz fiber and the conducting leads were each made from a narrow strip of silver leaf. The galvanometer with this arrangement was much improved for there was practically no zero shift even for deflections of two feet at a meter scale distance. Another advantage of this arrangement was that the silver leaf damped out forced vibrations due to earth tremors. A more rugged and simple construction, suggested by Mr.

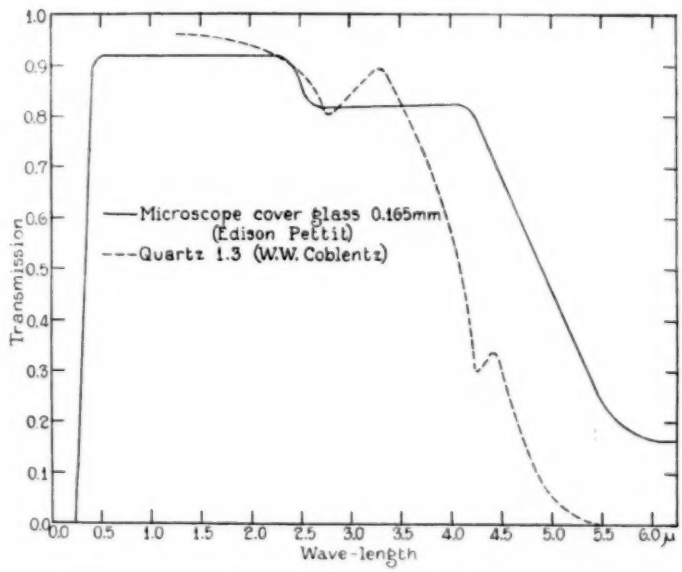

Fig. 2. Transmission of quartz and thin glass, 0–6.2μ.

Julius Pearson, consisted of making each conducting lead of a gold plated silver ribbon rolled to 1μ thickness and wound into a flat spiral.

Fig. 2[4,5] shows the transmission curve for quartz and a microscope cover glass. The quartz becomes opaque at 5μ but transmits wave-lengths greater than 50μ except for a narrow absorption band at 78μ. The microscope cover glass remains opaque to long wave-lengths.

Four groups of readings were taken, using (1) the metal shutter to exclude all radiation, (2) the glass shutter to exclude all of the extreme infra-red but only a small fraction of the near infra-red, (3) the glass shutter always in and moving the metal shutter to find the effect of the near infra-red, and (4) the metal shutter again to see if conditions had remained constant during the

[4] Edison Pettit, Astrophys. J. **61,** 163 (1926).
[5] W. W. Coblentz, B. S. Bull. **2–3,** 462 (1906).

experiment. Designating by V the energy below 5μ that is received by the thermocouple without any shutter, I the energy above 50μ under the same conditions, and k the fraction of energy below 5μ either reflected or absorbed by the glass shutter, the four groups become:

$$(1),\ V+I; \quad (2),\ kV+I; \quad (3),\ (I-k)V; \quad (4),\ V+I.$$

(2) and (4) are redundant but are useful as a check and for taking averages. Thus: $(2)-(1)=(3)$ and $(2)+(3)=(1)=(4)$.

The value of k can be seen from Fig. 2 to be between 0.15 and 0.20. The value of k was determined experimentally by using an additional window of microscope cover glass 0.008 mm thick, and using the metal shutter to find V and the glass shutter to find kV. The value of k was found to be 0.18. This value depends on the particular apparatus and in a small way on the material used to blacken the receiver.

The table shows the relative blackness or absorbing power of the different materials tested.

TABLE I. *Absorbing power of various materials.*

Substance	Radiation absorbed for $\lambda<5\mu$ V	Radiation absorbed for $\lambda>50\mu$ I	I/V	Substance	Radiation absorbed for $\lambda<5\mu$ V	Radiation absorbed for $\lambda>50\mu$ I	I/V
1. Litharge	10.8	4.3	.40	14. Copper sulphate crystals from solution	15.0	4.1	.27
2. Ground Glass	11.9	4.7	.40	15. Wellsbach mantle material	8.9	3.1	.35
3. Powdered Glass	11.7	5.0	.43	16. Platinum Black	18.2	4.4	.24
4. White Lead 2 Pb $CO_3 \cdot Pb(OH)_2$	14.9	4.9	.33	17. Tartaric Acid and Sugar	16.0	3.9	.24
5. White Lead in lacquer	14.3	4.4	.31	18. Talc $H_2MgSi_4O_{12}$	12.5	3.8	.30
6. Red Phosphorus	18.3	5.0	.27	19. Water glass	12.1	3.7	.31
7. Red Phosphorus from a match box	17.7	5.1	.29	20. Tellurium, powdered	19.2	3.3	.17
8. Celestite, powdered $SrSO_4$	14.7	4.6	.31	21. India Ink	18.8	3.8	.20
9. Brucite, powdered $Mg(OH)_2$	11.4	4.2	.37	22. Lacquer	8.6	3.0	.35
10. Angelsite, powdered $PbSO_4$	14.2	4.2	.30	23. Castor Oil	8.8	2.8	.32
11. Copper Sulphide	17.1	5.2	.30	24. Glycerine	11.2	3.1	.28
12. Copper Oxide	13.8	4.4	.32	25. Turpentine	8.1	0.2	.02
13. Silver Sulphide	12.8	4.4	.34	26. Clean Receiver	2.9	0.2	.07

Some of the materials were selected because they were transparent to near infra-red, some because they had been used by investigators of the extreme infra-red. The powdered materials were painted on the receiver by mixing them with one part turpentine and five parts alcohol. After a material was tested, the receiver was carefully cleaned and painted with another material. Care was taken to replace the thermocouple in the apparatus in the same place each time. The absorbing materials were painted with uniform thickness on the receiver and in each case the thickness of the coat was about 0.01 mm as estimated under a microscope.

Water glass was very unsuitable for a delicate thermocouple for it caused the heavy receiver used here to curl. The glue mixed with the red phosphorus taken from a match box also caused the receiver to curl.

Item 25 in the table shows that turpentine did not absorb the long waves. To determine whether they were reflected or transmitted by the turpentine, a receiver painted with white lead in lacquer was covered with turpentine. The far infra-red was absorbed equally well which showed that turpentine is transparent to long wave-lengths.

The absorbing power of a receiver depends on the thickness of the absorbing material. A copper receiver tarnished with H_2S, so that it appeared quite black was about 50 percent efficient in the near infra-red and only 25 percent efficient in the extreme infra-red, compared with a 0.01 mm coat of copper sulphide painted on the receiver. The physical state of the receiver affects its absorbing power. A receiver, electroplated rapidly with copper, so that the surface was rough, absorbed the far infra-red well; it had a ratio of $I/V=0.28$. A heavy coat of platinum black electroplated on a receiver had the same absorption as if it were painted on the receiver.

The transmission of crystalline quartz, hard rubber, and a cellulose paper used for wrapping candy was also tested to compare their merits as window material. The cellulose paper is very strong and gas tight. The same apparatus was used and the radiation made to shine through the sample being tested. The following table shows the percentage of radiation transmitted by the three samples, used as extra windows:

Material	*V*	*I*	*I/V*
Cellulose paper, 0.033 mm	47%	37%	0.79
Crystalline quartz, 0.83 mm	70	23	0.33
Hard Rubber, 1.2 mm	11	6	0.55
Without an extra window	100	100	0.30

The reflection of the far infra-red from a glass surface was tested by replacing the rough mirror by a piece of plate glass. The ratio of the number of waves reflected from the plate glass to the number reflected from the rough steel mirror was 31 percent.

Conclusion

It is to be noticed that the absorptive power of the materials tested was an integrated effect extending over the entire far infra-red.

Litharge, powdered glass, white lead, copper sulphide, celestite, and red phosphorus were the best absorbers of radiation longer than 50μ.

The physical state of the receiver determined its efficiency. A very thin coat of the absorbing material in most cases was an inefficient absorber of the extreme infra-red waves. A very poor absorbing material such as copper or platinum will absorb if the surface is sufficiently rough.

For radiometers, the absorbing material is better when mixed with turpentine and alcohol and painted on the vanes. Very delicate fly-wing radiometers were made in this manner, weighing only 0.04 mg. The vanes were double and a sputtered mica mirror was used.

For thermocouples, absorbing material is better if it is mixed with lacquer. The thermocouples must be in vacuum to be steady; in some cases an increase of 60 times the sensitivity was obtained by evacuation.

The high absorption in glass of the extreme infra-red and its low absorption of the near infra-red suggested its use as a source. Such a source was made by covering with glass two platinum wires that were separated 4 mm. The wires were heated by an electric current and the hot portion of glass between the two wires served as a source of extreme infra-red radiation. This source was tested in a vacuum spectrometer[6] and found to be satsifactory.

A convenient method of filtering out the near infra-red is to grind the windows with emery so that the pits are about 4μ deep. The apparatus can be aligned with visible light by covering the rough surface with turpentine.

Although a tarnished metal surface is not an efficient absorber of the extreme infra-red, it may be desirable to sacrifice efficiency for the extra speed with which the thermocouple will come to thermal equilibrium,—particularly if the readings are recorded photographically. The receiver of a thermocouple can be improved by pressing it against the surface of a file to make the surface rough. A thermocouple with tarnished silver receivers reached equilibrium in one second. White lead is especially desirable for blackening a receiver for it is white to visible light and allows almost perfect alignment of the apparatus.

[6] Badger and Cartwright, Phys. Rev. **33**, 696 (1929).

PELTIER AND THOMSON EFFECTS FOR BISMUTH CRYSTALS

By H. D. Fagan and T. R. D. Collins
Physics Laboratory, University of Iowa

(Received November 20, 1929)

Abstract

The Peltier and Thomson effects are directly measured (the former against copper) in single crystal rods almost covering the entire orientation range. For the first effect the Voigt-Thomson symmetry relation is definitely not substantiated, while for the latter the data do not provide an adequate test, though it appears likely that there is a deviation here also.

The following values are found: at a temperature of 27°C, $\pi(\parallel \text{vs.} \perp) = 13.8$, $\pi(45° \text{vs.} \perp) = 8.6$ microvolts; at a temperature of 48.5°C, $\sigma_\parallel - \sigma_\perp = 43$, $\sigma_{45} - \sigma_\perp = 26.5$ microvolts/°C. These values are all in fair agreement with values deduced from thermal e.m.f. temperature data of the writers and of previous observers.

Introduction

Bridgman[1] and Boydston[2] have recently measured the thermal e.m.f of bismuth crystals of various orientations[3] against a reference metal. From these results are deduced by the usual thermodynamic relations, values of the Peltier e.m.f. between the reference metal and a crystal of any orientation or between two crystals of different orientations; likewise the differences in the Thomson coefficients for the two parts of the above combination are deduced. In the investigation described below the Peltier e.m.f. against copper and the Thomson coefficient of bismuth crystals, covering most of the possible orientation range, were measured directly. Two sets of crystals were used, the first for measurement of Peltier coefficient, the other for all the other measurements, which included determination of specific resistance, mean thermoelectric power (between 0° and 100°C) against both copper and constantan, and the Thomson effect. From such data it should be possible to test the validity of the Voigt-Thomson symmetry relation for the directly observed Peltier e.m.f. and Thomson coefficient and to make comparison with the indirectly determined values of these same quantities.

Apparatus and Experimental Method

The method for determining the Peltier e.m.f. is essentially that of Câswell,[4] or Barker.[5] The two thermo-junctions (Cu-Bi and Bi-Cu) are isolated

[1] P. W. Bridgman, (a) Proc. Amer. Acad. of A. and S. **61,** 101 (1926); (b) Proc. Amer Acad. of A. and S. **63,** 351 (1929).

[2] R. W. Boydston, Phys. Rev. **30,** 911 (1927); also gives reference to earlier work.

[3] Orientation is used as usual to define the angle between the length of the specimen and the principal crystallographic axis, which for bismuth is perpendicular to the plane of best cleavage.

[4] A. E. Caswell, Phys. Rev. **33,** 379 (1911).

[5] H. C. Barker, Phys. Rev. **31,** 321 (1910).

from each other by placing them in separate Dewar flasks each containing the same amount of calorimetric fluid, a heating coil, a stirrer, and a copper-constantan thermocouple. See Fig. 1 (a). Current from the battery B_2 may be passed in either direction around the Bi-Cu circuit. The purpose of the heating coils is made clear below. By obvious manipulations of switches S_1 and S_2 it is possible to read the temperature in either flask, or to detect a very minute difference in temperature between the flasks. The heating coils, L and R, are wound of No. 36 constantan wire on thin mica sheets, while the leads, which go through the surface of the liquid and through holes in the flask covers, are of No. 2 constantan. The calorimetric fluid is "Finol," a light oil of low specific heat and high mobility. The amount contained in each

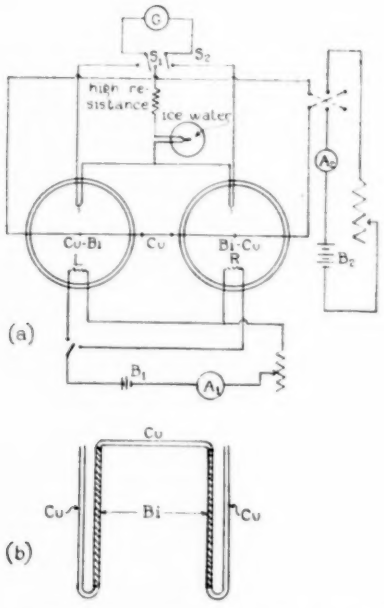

Fig. 1. Diagram of apparatus and electrical connections.

flask is about 150 cc. Stirring is done by glass propellors (not shown in Fig. 1) running at the rate of about 1 r.p.s.

The construction of the two bismuth copper junctions, in which the effect is measured, is apparent from the vertical section shown in Fig. 1(b). The two bismuth portions are parts of one crystal rod cut in two. The two ends adjacent to the cut are used to form the two Bi-Cu junctions in the flasks. The copper is No. 6 wire of commercial grade. The bismuth-copper connections are made without solder by fusing the bismuth directly to the copper, using zinc chloride as a flux. To take a reading a known constant current is sent in one direction through the bismuth-copper circuit. Heat is absorbed at the junction where current passes from bismuth to copper. To compensate for this loss of heat (and for the generation of heat at the other junction) current is passed through the appropriate heating coil. This current is con-

tinually so regulated that the flasks show no temperature difference. In about an hour no further adjustment is necessary. The reading of A_1 is then recorded. The current in the main (bismuth-copper) circuit is then reversed, but kept at the previous value, and the procedure above repeated. Caswell has shown that in this case the Peltier e.m.f. is given in volts by

$$\pi = \frac{i_R^2 R + i_L^2 L}{4I}$$

in which i_R, i_L = current (amperes) in right and left heaters, respectively; R, L = resistance (ohms) of right and left heaters respectively; I = current (amperes) in main circuit. This relation is valid provided the following conditions are satisfied.

1. The heat capacities of the two flasks and their contents are the same. This condition was met by making the two as nearly identical as possible.

2. The rate of loss of heat from each flask must be approximately the same. This was tested from time to time during the investigation and found to be satisfactory.

3. The temperature difference between the flasks and their surroundings must be small. The oil in the flasks never exceeded 2°C above room temperature at the end of any run.

For measuring the Thomson coefficient the method of Nettleton,[6] as modified by Ware,[7] was used. Measurements of the same specimen made on Ware's apparatus and the writers' agree well. The resistance of each crystal with one end at about 0° and the other at about 100°C is a necessary datum for determining the Thomson coefficient, and from it the specific resistance (at 48.5°C) can be computed. To do this the average cross section of a crystal is found from its measured mass and length, and assumed density (9.78 gm/cm^3). The crystals were from 6 to 10 cm long and from 5 to 10 mm^2 cross sectional area.

With the temperature gradient established along a crystal the thermal e.m.f. was measured with a potentiometer. The reference metal is copper, since the ends of the specimen were fused or soldered to copper blocks. Dividing this e.m.f. by the temperature difference gives the mean thermoelectric power. This is approximately the thermoelectric power at the mean temperature, 48.5°C. The thermoelectric power against constantan was measured in a similar fashion.

The two sets of bismuth crystals were grown by drawing them from a crucible full of molten bismuth. This method and the apparatus have been described by Linder.[8] The modifications in the procedure mentioned by Boydston and by Hoyem[9] and Tyndall were also followed. The crystals of

[6] H. R. Nettleton, Proc. Lond. Phys. Soc. **29,** 59 (1916–17).

[7] In connection with unpublished work in this laboratory by L. A. Ware on the Thomson Effect in zinc crystals.

[8] E. G. Linder, Phys. Rev. **29,** 554 (1927).

[9] R. W. Boydston, Phys. Rev. **30,** 911 (1927); A. G. Hoyem and E. P. T. Tyndall, Phys. Rev. **33,** 81 (1929).

one set (for Peltier Effect) were 30 cm long and from 2.5 to 3.0 mm in diameter. The others have been described above. The material used was Mallinckrodt C. P. bismuth with the following analysis:[10]

Zn 0.01%	Cu 0.00%	Fe 0.00%
Pb 0.00%	As 0.000%	Ag 0.04%

Results and Discussion

Measurements of Peltier e.m.f. against copper were made on fourteen single crystals ranging in orientation from 16° to 90°. For a majority of the crystals five readings were taken. For two, however, six readings were taken, while for three crystals, only four were taken. The arithmetic mean of all the readings on one specimen is the adopted value. The results are shown graphically in Fig. 2, in which the observed Peltier e.m.f. in millivolts is plotted

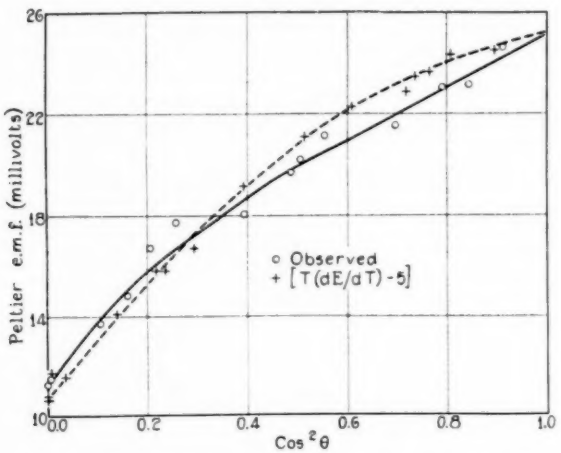

Fig. 2. Peltier e.m.f. as function of orientation angle.

(circles) against the square of the cosine of the orientation angle. By substituting in $\pi = Te$, in which $T = 300°$A and e is the mean thermoelectric power (at 48.5°C) against copper,* previously mentioned, it is possible to obtain values of the Peltier e.m.f. Values obtained in this way are plotted (as crosses) in the same figure. Before plotting, each value has been arbitrarily reduced by 5 millivolts, since any constant difference between the two sets of data can readily be ascribed to the use of different samples of reference metals (a copper block in one case and a copper wire in the other). These two curves are probably in agreement within experimental error. Such plots should yield straight lines to satisfy the Voigt-Thomson symmetry relation.

[10] The bismuth used by Boydston had this same stated analysis. The omission of Ag 0.04% is due to an oversight on his part. It seems certain, however, that the content of Ag in the crystals used in this investigation must be much less than 0.04%. This point is considered later.

* The value of e at 27°C should be used, of course, but it was not determined and probably does not differ much from the value at 48.5°C.

It is obvious that the experimental relation is not linear in either case. Moreover Bridgman[11] finds a very similar deviation from linearity for the thermoelectric power (as a function of $\cos^2\theta$) of bismuth crystals against copper, and therefore for the indirectly determined Peltier e.m.f.

TABLE I. *Peltier e.m.f. (millivolts) at 27°C.*

Junction	Directly * observed	$T(dE/dT)$*	$T(dE/dT)$* (Bridgman)	$T(dE/dT)$**	$T(dE/dT)$** (Boydston)
M–Bi_0	25.1	30.2	32.2	18.2	20.2
M–Bi_{45}	19.9	25.6	25.9	13.1	11.6
M–Bi_{90}	11.3	15.7	17.2	3.3	3.0
Bi_0–Bi_{90}	13.8	14.5	15.1	14.9	17.2
Bi_{45}–Bi_{90}	8.6	9.9	8.7	9.8	8.6

* Reference metal, M, copper.
** Reference metal, M, constantan.

Table I presents a comparison of previous work with the present, the subscript for Bi being the value of θ. The data in the second and third columns are obtained from the two curves in Fig. 2. To compute Bridgman's values use is made of his empirical formulas[12] for thermal e.m.f. as a function of temperature. The fifth column is obtained from a plot of the observations on thermoelectric power against constantan, previously mentioned. By interpolation in Boydston's Fig. 3 the thermoelectric power (against constantan) is found for 27°C, and from this the values in the last column are easily computed. All the results in this table are found to be in fair agreement, when allowance is made for the fact that in the upper 3 rows of data a different reference metal (or different specimen of the same metal) was used. In the lower two rows the results are typical of bismuth alone and an absolute comparison is allowable. It will be seen that the directly observed values are lower than those computed from $\pi = TdE/dT$. The agreement with this relation is, however, probably as good as is usually obtained. There seems little doubt that the deviation from the Voigt-Thomson symmetry relation is real for the Peltier effect in these crystals. Boydston finds no deviation (at 27°C) and one must conclude that the bismuth used by Boydston differed from ours in spite of having the same stated analysis

The specific resistance at 48.5°C is plotted in Fig. 3 against $\cos^2\theta$. The line drawn represents Bridgman's latest results, changed to 48.5° C, however, assuming a temperature coefficient of resistivity of 0.0044. With the exception of four points, the results are satisfactory and indicate that the crystals are not badly strained and that the bismuth is very pure, since both strains and impurities seem to affect the specific resistance seriously.[13] The three high points may be ascribed to slight accidental strains occurring during growth or in the subsequent handling of the crystals. This seems probable also because crystals of intermediate orientations are very easily deformed.

[11] Reference 1, (b),
[12] Reference 1, (b), p. 383.
[13] See discussion by Bridgman, reference 1, (b) pp. 386–389.

Ware has shown for zinc crystals that a deformation which is large enough to raise the specific resistance has a negligible effect on the Thomson coefficient. It might be expected, therefore, that the group of crystals of Fig. 3 would give consistent and satisfactory results for the Thomson coefficient. This is,

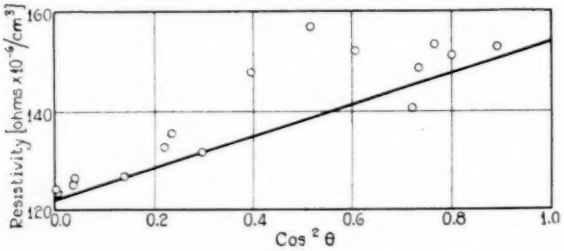

Fig. 3. Specific resistance as function of orientation angle.

however, not the case as is evident on reference to Fig. 4, particularly for orientations less than about 50°. These data, moreover, do not provide an adequate test of the Voigt-Thomson symmetry relation. In spite of this an attempt has been made to draw a smooth curve through the observations. Assuming that -8.5 microvolts/°C is a reasonably certain value for $\sigma_\perp$ (i.e. for $\theta=90°$), it is possible to make comparison with Bridgman's latest data. The values of σ for $\theta=45°$ and $\theta=0°$ for a temperature of 48.5°C have

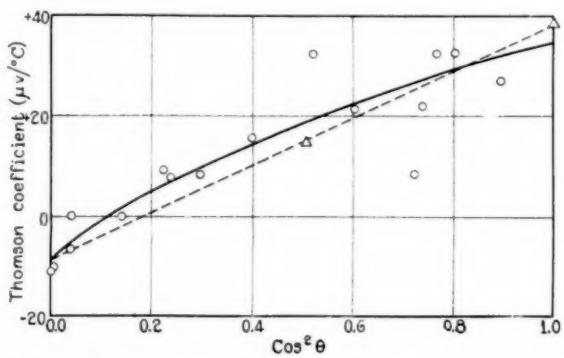

Fig. 4. Thomson coefficient as function of orientation angle.

been computed from formulas deduced by Bridgman[14] from his thermal e.m.f data. These values are plotted as triangles in Fig. 5. Our curve gives $(\sigma_\perp-\sigma_\parallel)=43$ microvolts °C at 48.5°C, dependent on a very uncertain extrapolation to $\cos^2\theta=1$. Boydston's data give $(\sigma_\perp-\sigma_\parallel)=57.5$, and Bridgman's, 48. At 43.5°C Caswell[15] finds 58 microvolts/°C for polycrystalline bismuth, a value considerably in excess of what might be expected from the above stated values for crystals. Laws[16] finds a much lower value, 10 microvolts/°C.

[14] Reference 1, (b) pp. 384, 385.
[15] Caswell, Phys. Rev. **12,** 235 (1918).
[16] Laws, Phil. Mag. [6] **7,** 560 (1904).

It seems certain, from the investigations of the two writers just mentioned, that a small admixture of tin raises the Thomson coefficient to a very great extent. It therefore seemed desirable to make an analysis of the bismuth. This was done spectroscopically using the spark spectrum and the general procedure of Meggers, Kiess, and Stimson.[17] A small quartz spectrograph was used the dispersion of which was such that the length of spectrum between 3400 and 2600A was 1.5 cm. About 120 spectrograms were taken of three crystals[18] with normal, low, and high Thomson coefficients, respectively, as judged from the curve of Fig. 4. Between exposures a two millimeter piece was clipped from each of the two portions of the crystal between which the spark occurred. All of the spectrograms, except one, were identical and indicated a material of high purity. A very faint and diffuse line which might be the "raie ultime" of silver (3281A) was present in all the spectrograms. No trace of 3383A, another very sensitive silver line, was found. Moreover, comparison of these spectrograms with others taken in this laboratory of bismuth known to contain far less than 0.04 percent Ag, has led to the conclusion that the silver content is much lower than the figure stated in the analysis. Certainly the crystals examined showed no difference from each other and no detectable inhomogeneity in composition between different parts of the same crystal. In the one exceptional case mentioned above one of the electrodes consisted of a portion (one end) which had been accidentally fused and was probably contaminated with solder. Several lead and tin lines were easily identified in this spectrogram.

In conclusion the writers wish to express their thanks to Prof. E. P. T. Tyndall for suggesting this work and for his advice and interest during its prosecution.

[17] Meggers, Kiess and Stimson, Sci. Pap. Bur. Stand. **18,** 235 (1922–23).

[18] $\text{Cos}^2\theta = .894$, $\sigma = 27$; $\cos^2\theta = .517$, $\sigma = 32.4$; $\cos^2\theta = .719$, $\sigma = 8.5$.

SHATTER OSCILLATIONS, THEIR NATURE AND THEORY*

By E. H. Kennard
Cornell University

(Received December 30, 1929)

Abstract

Shatter oscillations are an apparently novel type in which the pressure sinks periodically to the minimum value which the liquid can sustain, the liquid mass becoming then porous or "shattered"; they tend to be much slower but more powerful than purely elastic vibrations and the wave-form is very different, pressure impulses alternating with long intervals of quiet. An experimental case is described and the general theory of such oscillations is developed. Further experiments are needed.

An Experiment

SEVERAL years ago the writer was privileged to witness some interesting experiments upon liquid oscillations in the plant of the Goulds Pumps Company at Seneca Falls, N. Y., which were of an astonishing and apparently little-known type. It is the purpose of this paper to describe them briefly, together with the theory proposed by the author, in the hope that some physicist may be induced to make a detailed study of the phenomena and so to find out whether the theory is correct and adquate.

In the most interesting experiment a pipe 31 m long and full of water was connected at one end to a tank which contained a considerable mass of water and over it air at a pressure of about 4 atmospheres (the pressure of the atmosphere included). At the other end of the pipe was a small pump with its

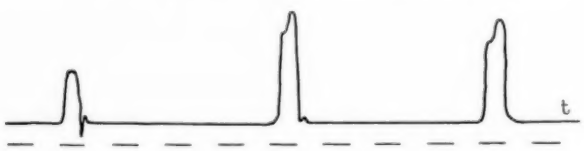

Fig. 1. Indicator record showing pressure distribution.

discharge valve removed and its suction valve blocked shut, so that it served merely to "fan" the water with an approximately simple-harmonic motion. A recording gauge recorded the pressure of the water in the pipe at a point near the pump.

Under the circumstances one might expect the water column to oscillate like a "closed organ pipe" (i.e. open only at the tank end, where the pressure must have been sensibly constant); the speed of sound in water in such a pipe being about 1360 m per sec, the fundamental period should be around 0.091 sec. Nothing of the sort was observed. At suitable pump speeds oscillations

*Part of this paper was read before the National Academy of Sciences; an abstract of this part appears in Science, **70**, 618 (1929).

did occur, and of enormous amplitude, but they were much slower than the slowest possible elastic oscillation, and the distribution of pressure was of the remarkable type shown in Fig. 1, which is copied from one of the actual indicator cards. Isolated "humps" of pressure appeared at intervals, in the figure one every 0.7 second, separated by long quiet intervals during which the pressure seemed to be about zero (certainly below atmospheric); the humps always occurred during discharge strokes of the pump (which are shown by horizontal lines in the diagram, four per oscillation in that case). The maximum pressure was usually around 25–30 atmospheres but in one case it rose to 75 atmospheres before the gaskets blew out of the pump and stopped the experiment.

Now the direction in which to look for an explanation of this phenomenon seems obvious enough. In an ordinary elastic oscillation a compression is followed by an equal rarefaction, but water cannot withstand a tension of 20–30 atmospheres; under special conditions tensions up to 5 atmospheres have been observed, but in practice, according to what appears to be the opinion of engineers, the pressure never sinks below zero (i.e. one atmosphere below atmospheric)—at all events no appreciably lower pressures were ever observed in these experiments, although the indicator was often capable of showing them.

We have, then, a case, apparently new in hydrodynamical theory, of large-amplitude oscillations in a liquid whose pressure cannot sink below a certain critical pressure, p_0. It was at first naively supposed that under these circumstances large gaps might form in the liquid mass; for instance, in the present case, that the column might break loose from the pump and retreat several feet down the pipe. But a little reflection shows that this cannot happen when the minimum pressure is really quite definite. For in order to form such a gap the layer of liquid on one side or the other of it must at some time experience an acceleration directed away from the incipient gap, and, since by hypothesis the pressure is p_0 in the gap and cannot become less than this in the liquid, no force producing such an acceleration can be developed by pressure differences in the liquid (although it could arise, of course, from gravity in a non-horizontal column, and large gaps could then form). For theoretical purposes the stituation might be idealized satisfactorily by assuming that when the pressure sinks to p_0 the elasticity drops discontinuously to zero. What happens in practice, however, must be that the liquid mass does break, at many closely spaced points, in consequence of local inhomogeneities of composition or of state and under the action of cohesive forces, so that the liquid becomes full of small crevices or, as we shall call it, "shattered." We shall study this process a little more closely.

Theory of Shattering in a Liquid Column

The point at which the pressure first sinks to the minimum value, p_0, must be one where, momentarily,

$$\frac{\partial p}{\partial t}<0, \quad \frac{\partial u}{\partial x}=-\frac{1}{\epsilon}\frac{\partial p}{\partial t}>0, \tag{1}$$

in which p = pressure, t = time, ϵ = elasticity, u = particle velocity, x = distance along the column. Continuity being assumed, p will then proceed to reach p_0 at neighboring points and a shattered region will form in which $p = p_0$ and is thus uniform, so that $\partial u/\partial t = 0$. In this region, according to (1), $\partial u/\partial x > 0$ (see also below, after Eq. (2)); the liquid will therefore expand at a constant rate through enlargement of the crevices so long as the shattered condition persists. The boundaries of the region, which we shall call "shatter-fronts," advance thru the liquid with a speed V which can easily be calculated. During an interval dt let the shatter-front advance positively a distance Vdt from a point P to P'; then at the beginning of dt the pressure was p_0 at P and $p_0 + (Vdt)\,\partial p/\partial x$ at P', whereas at the end of dt it has risen at P' by an amount, actually negative, $(\partial p/\partial t)\,dt$ and has now become p_0; thus $(Vdt)\,\partial p/\partial x + (\partial p/\partial t)dt = 0$ and

$$V = -\frac{\partial p}{\partial t}\Big/\frac{\partial p}{\partial x} = \epsilon\frac{\partial u}{\partial x}\Big/\frac{\partial p}{\partial x}. \tag{2}$$

A second and rather peculiar condition for the propagation of the shatter-front arises from the condition that the liquid must be left behind it in an expanding condition (or at least not in a contracting one, since then the pressure would immediately rise above p_0 again). In the same notation, at the beginning of dt let the particle velocities at P and P' resp. be u and $u + (Vdt)\,\partial u/\partial x$; then at the end of dt the velocity is still u at P (because of the uniformity of pressure), but at P' it has changed by $(\partial u/\partial t)dt$. The condition stated then requires that the final velocity at P' shall exceed that at P, or that $u + (Vdt)\,\partial u/\partial x + (\partial u/\partial t)\,dt \geqq u$; and, since $\partial u/\partial t = -(1/\rho)\,\partial p/\partial x$ where ρ is the density and the speed of sound is $c = (\epsilon/\rho)^{1/2}$, we have by (2):

$$k^2\left(\frac{\partial u}{\partial x}\right)^2 \geqq \left(\frac{\partial p}{\partial x}\right)^2, \quad V^2 \geqq c^2, \tag{3}$$

where $k = (\epsilon\rho)^{1/2}$. It follows that the shatter-front moves with a speed above that of sound; its progress therefore depends upon conditions in the liquid due to other causes than what may be going on in the shattered region.

In its advance the shatter-front may eventually come to a point where the first of Eqs. (3) is no longer satisfied. It will then turn into a "reconsolidating front" and immediately start back in the opposite direction, for the higher pressures in the adjacent unbroken region will accelerate the liquid toward the shattered region. As the reconsolidating front reaches each point in the shattered region, the crevices suddenly close up and the liquid already present undergoes an impulsive acceleration and compression which give to it both the particle velocity u and the pressure p that obtain on the unbroken side of the advancing front. For convenience let us resolve conditions in the unbroken column as usual into two wave-trains moving in opposite directions; let the unbroken column lie on the left, toward $-x$, and let u_1, p_1 be particle velocity and pressure in the wave-train moving positively and u_2, p_2 the corresponding quantities in the other wave-train. Then by the usual laws for elastic waves

$p_1 = ku_1$, $p_2 = -ku_2$, and at the front $p = p_1 + p_2$, $u = u_1 + u_2$. Here u_1, p_1, referring to the "incident" waves, are determined by conditions to the left and can be regarded as known, while u_2 and p_2 can be regarded as referring to waves "reflected" from the boundary of the shattered region and are to be found. Let U = velocity of advance of the reconsolidating front and in the shattered region let u_s = particle velocity and f = degree of shattering or fraction of the space that is empty of liquid, both taken at a point just ahead of the advancing front. Then in time dt the front sweeps over a section PP' of length Udt; during this time the liquid flowing in at P, of volume udt per unit of cross-section, must fill up not only the crevice-space $fUdt$ but also the space $(1-f)$ Udt $(p-p_0)/\epsilon$ emptied through compression of the liquid already in the section PP' and the space emptied by the outflow past P' of a volume $u_s dt$ of the shattered column. Hence

$$u = \left[f + (1-f)\frac{p-p_0}{\epsilon} \right] U + u_s . \tag{4}$$

(We assume u/U small so that terms in u^2 or u/U can be neglected, as in the ordinary theory of sound.) During the same interval dt the difference in pressure at the ends of the section PP' must impart to the liquid already in it the additional momentum acquired as its velocity changes impulsively from u_s to u; whence,

$$p - p_0 = \rho U(1-f)(u-u_s) . \tag{5}$$

From these two equations we find:

$$(p-p_0)^2 + \frac{\epsilon f}{1-f}(p-p_0) = k^2(u-u_s)^2 , \tag{6}$$

$$\frac{1}{U^2} = \frac{1-f}{c^2}\left[1 - f + \frac{\epsilon f}{p-p_0} \right] = \frac{1}{c^2}\left[1 + f^2 + f\left(\epsilon \frac{1-f}{p-p_0} - 2 \right) \right] . \tag{7}$$

Equation (6) expresses the "boundary condition" that must hold under these conditions at the junction of shattered and unbroken regions. Eq. (7) gives U, and shows, among other things, that $U < c$ under the conditions assumed, since $\epsilon/(p-p_0)$ will be many times greater than 2.

The reconsolidating front in its turn will diasppear upon meeting either a similar front moving in the opposite direction or an obstruction, with resulting final elimination of the shattered region (as a third alternative, of course, it might also be overtaken and destroyed by a fresh shatter-front). When two reconsolidating fronts meet, with pressure and particle velocity p, u in the one moving positively and approaching from the left and p', u' in the other one, then at the point of meeting these quantities will change impulsively to certain values p_m, u_m. Let us resolve the motion on each side into positive and negative wave-trains, with respective pressures $p_1 = (p+ku)/2$, $p_2 = (p-ku)/2$ on the left, and $p_1' = (p'+ku')/2$, $p_2' = (p'-ku')/2$ on the right. Then, after the two fronts meet, these wave-trains advance as usual and by

their superposition determine subsequent conditions in the liquid; after the lapse of a very short time the trains will overlap a little at the point of meeting and will produce there the following values:

$$p_m = p_1 + p_2' = \frac{1}{2}(p+p') + \frac{k}{2}(u-u'),\ u_m = \frac{p_1}{k} - \frac{p_2'}{k} = \frac{1}{2}(u+u') + \frac{1}{2k}(p-p') \quad (8)$$

The case in which the reconsolidation front is stopped by an obstruction, such as the closed end of the pipe, can be handled by putting $u_m = 0$ in the last equations and eliminating p' and u'; this gives the usual impact formula:

$$p_m = p + ku. \quad (9)$$

The extension of the theory just developed to the three-dimensional case is easy, but for completeness we shall sketch it. The boundary of the shattered region is in this case a closed surface which may move either as a shatter-front or as a reconsolidating front, or in part as one and in part as the other; the theory developed above will apply provided we take the x-axis along the normal to the surface, with the single exception that we must also take account of expansion due to the component of particle velocity tangential to the surface. The tangential acceleration vanishes because over the surface $p = p_0$ and is constant. One finds thus as the conditions for the advance of a shatter-front, in the unbroken liquid just ahead of it:

$$\operatorname{div} u > 0,\ k^2(\operatorname{div} u)^2 = \left(\frac{\partial p}{\partial n}\right)^2, \quad (1'), (3')$$

n denoting distance along the normal to the front (which is also the direction of ∇p), and for V, the speed of advance of the front along its normal:

$$V = -\frac{\partial p}{\partial t}\Big/\frac{\partial p}{\partial n} = \epsilon(\operatorname{div} u)\Big/\frac{\partial p}{\partial n};\quad V^2 \geqq c^2. \quad (2'), (3'')$$

When the boundary starts back through the shattered region as a reconsolidating front, we have as boundary conditions for the determination of p and u in the unbroken liquid,

$$(p-p_0)^2 + \frac{\epsilon f}{1-f}(p-p_0) = k^2(u_n - u_{sn})^2, \quad (6')$$

in exact analogy with (6), n denoting the component normal to the front, and also, owing to the absence of pressure gradient over the front,

$$u_t = u_{st}, \quad (6'')$$

the t denoting the vector component tangential to the front. These equations are equivalent to three scalar ones and suffice to determine the reflected wave in terms of the variables describing the incident waves and the conditions in the shattered region. The value of U, the speed of advance of the front along its normal, is given as before by Eq. (7).

Explanation of the Experiment

In the light of these theoretical developments the course of the oscillation described at the beginning of the article is believed to be as follows. The enormous gradient implied by the momentary high pressure at the pump sets the water into rapid motion toward the tank; this phase should last about $0.091/4 = 0.023$ sec. Then as the pressure sinks to p_0 a shatter-front sweeps quickly along the pipe and a considerable section of the column becomes shattered and remains so, the crevices widening steadily, for a considerable time. Some photographs of the column taken thru a short glass section of the pipe seemed to confirm the prediction of the theory as to its condition during this phase. Finally, as the reconsolidating front arrives at the pump and the now rapidly moving column is brought to rest, a "water-hammer" results and the high hump of pressure is thereby restored.

Unfortunately the mathematical discontinuity in the equations seems to preclude obtaining any simple solution as an illustrative case. The best method of attack seems to be to start with an assumed hump of pressure and determine the motion of the liquid by approximate methods of calculation. It seems most profitable, however, for such a calculation, rather laborious at best, to be undertaken in conjunction with a repetition of the experiment in which simultaneous pressure records are obtained at several points along the pipe, in order to obtain a complete check on the theory. No projected experiment of this sort is known to the writer at the present moment.

LETTERS TO THE EDITOR

Prompt publication of brief reports of important discoveries in physics may be secured by addressing them to this department. Closing dates for this department are, for the first issue of the month, the twenty-eighth of the preceding month; for the second issue, the thirteenth of the month. The Board of Editors does not hold itself responsible for the opinions expressed by the correspondents.

Atomic Stability as Related to Nuclear Spin

As is well known, the stability of an ordinary atom nucleus is very great. For example almost head-on collisions between α-particles with velocities greater than $0.055c$ (ten thousand miles per second) with nitrogen or argon nuclei, commonly do not disrupt the nucleus, though it is true that in certain collisions the α-particle adds itself to a nitrogen nucleus and a proton is emitted at high speed. Such a high stability in a body of high positive charge does not seem probable on the basis of electrostatic forces alone, so the existence of powerful forces (partly magnetic) associated with spin and other types of quantized momenta, may be assumed. In the extra-nuclear atom, magnetic moments are associated with both orbital and with spin angular momentum, and the stability is greatest when the resultant of each of these sets of momenta is zero, or if $L=0$ and $S=0$.

The problem may be approached from the standpoint of known nuclear relations. In 1917 the writer assumed the electrons in nuclei to be associated in pairs (J. Am. Chem. Soc. **39**, 859 (1917), Phys. Rev. **15**, 73 (1920)), and it was also shown (Phil. Mag. **43**, 305 (1921)) that in almost all atoms the total number of electrons (the electronic number) is even. In addition the number of protons is in general found to be even. Such pairing suggests the relation of antiparallel spins.

It has been shown (loc. cit.) that all atomic species fall into four classes, if oddness and evenness in the number (N) of nuclear electrons, and the number (P) of protons is used as the basis of the classification. The general stability of the atoms of each class is represented by the abundance in the meteorites, in which the abundance follows very general relations, and on earth, where segregation has been more effective. See table at bottom of page. The numbers in parentheses represent later work in which species of smaller abundance have been detected.

Both the abundance and the number of known species are very much higher for class 1 than for the other classes. In fact the abundance in the meteorites for this class is 19 times that for all of the other three classes. For this class alone the known values of the quantum number i, which represents the resultant angular momentum ($ih/2\pi$), are all equal to zero, while for all of the other three classes all of the known values are greater than zero.

In class 1 the nuclear spins (in units $h/2\pi$) have been found to be zero for helium, carbon 12, oxygen 16, and for those isotopes of zinc and of cadmium which belong to class 1 (have even isotopic number). In class 2 the known values are: Li >0; F, 1/2; Na $\geqq 5/2$; Cl, 5/2; La, 5/2; Pr, 5/2; Cs >0; I, large; Tl, 1/2;

Class	N	P	Z	Meteorites	Earth	Number species	Nuclear spin number	Examples
1	Even	Even	Even	95.4	87.4	71 (73)	0	O^{16}, C, He, Cd (even isotopes)
2	Even	Odd	Odd	2.1	10.8	33	1/2 to 9/2	F, La, Bi
3	Odd	Odd	Even	2.5	1.8	18 (25)	1/2	Cd (odd isotopes)
4	Odd	Even	Odd	0.0	0.0	3	1	N^{14}

and Bi, 9/2. In class 3 the odd isotopes of cadmium are supposed by Schüler and Bruck to exhibit a value of 1/2.

Class 4 represents the most unstable of all nuclei, since only three species of this type are thus far known, and all of these have only a minute abundance. The only one of these for which the spin is known is nitrogen 14, for which the spin is 1.

Unfortunately, the interpretation of the nuclear spin in terms of intra-nuclear spins, and possibly of other intra-nuclear momenta, is uncertain, though the present values seem to indicate that only the proton spins are apparent. This seems peculiar in view of the fact that the pairing of the electrons is more apparent than that of the protons. It may be possible that the nucleus is too densely packed to allow an electron spin, but it is also possible that the present apparent absence of electron spins is fictitious.

It may be assumed that one important factor in nuclear stability is to be found in the relations of the intra-nuclear spins, and also of any other types of angular momentum. Since these relations are unknown it has seemed important to show that all known data indicate that: *In general high nuclear stability is associated with zero nuclear angular momentum (zero spin)*. The relations of the atomic species indicate that the limits of stability are related to other quantities, and are a function of the relation between Z and N/P, and of some other variables.

WILLIAM D. HARKINS

University of Chicago,
January 28, 1930.

The Unified Field Theory and Schwarzschild's Solution: A Reply

I have read with a great deal of interest Mr. Salkover's criticism (Phys. Rev. **35**, 209 (1930)) of my paper on Einstein's unified field theory and the Schwarzschild solution (Proc. Nat. Acad. **15**, 784 (1929)). I agree with Mr. Salkover that the expression for the electromagnetic potential which I used in my paper for the calculation of the tensor $V_{\beta\gamma}{}^{\alpha}$ was not correctly copied from the previous paper by Wiener and myself there referred to (Proc. Nat. Acad. **15**, 802 (1929): communicated in May, 1929). The expression given in the latter paper of course agrees with that calculated by Mr. Salkover, and also with the value of the tensor $\Lambda_{\mu\nu}{}^{\sigma}$ reported in my paper. This mistake, while vitiating my results on the Schwarzschild solution, in no way affects our previously announced conclusions, in particular the non-existence in the unified theory of an electrostatic field with spherical symmetry.

M. S. VALLARTA

Massachusetts Institute of Technology,
Cambridge, Mass.,
February 3, 1930.

Scattering of Light in Sodium Vapor

An artificial chromosphere was constructed in the following manner: Sodium vapor was admitted into a cylindrical glass shell, like the region between the walls of an unsilvered Dewar flask, and a filament was inserted along the axis of the cylinder. The filament is considered to be the photosphere, and the sodium vapor shell the chromosphere. When a spectroscope was directed through the shell of vapor, at right angles to the axis, at the continuous background furnished by the filament, the "Fraunhöfer" lines were observed. When the shell was lowered so only the upper part of the cylinder was in front of the slit, resonance radiation was seen, corresponding to the flash spectrum. It was observed that the D lines appeared in absorption *at lower vapor densities than those for which they appeared in emission.*

This is in accord with the work of J. Q. Stewart and the author, (Astrophys. J. January, 1930). The reason for this is not understood. It is probably not due to quenching of resonance radiation by the hydrogen present in the sodium, since kinetic theory calculations indicate that it is necessary to assume effective collision radii of order 10^{-4} cm before a collision frequency is obtained comparable to the unloading time of the $2P$ state of sodium; though the work of Mannkopf (Zeits. f. Physik **36**, 315 (1926)) leaves some doubt on this point. Since in the experiments of R. W. Wood (Physical Optics, Pp. 575 et seq.) the vapor density was not

accurately known, his experiments cannot given an answer to this problem. While in the present experiment feeble resonance radiation may have been lost through experimental difficulties, such as reflections from the glass surfaces, yet the result is what one would expect on the assumption that pure scattering is not the only process at work in the production of the cores of "absorption" lines, whereas scattering alone produces the edges. Further evidences for this assumption are discussed in the paper referred to above. It would be interesting to know whether resonance radiation has even been observed at as low vapor densities as to produce just observable absorption.

S. A. KORFF

Palmer Physical Laboratory,
Princeton University,
January 28, 1930.

The Heat of Dissociation of Oxygen

In a recently written paper on the heat of dissociation of carbon monoxide, the writer has pointed out that the energy of the $^1D_2$ level in the oxygen atom is 1.3 volts. This value agrees well with the one given recently in Nature by McLennan and Crawford. Since the heat of dissociation of oxygen can be calculated from band spectrum data if the energy of the ^1D level is known, it is proposed here to point out the source of this new value for the ^1D level. The resulting heat of dissociation is equal to 5.7 volts and it lies between the limits set by Professor Birge in his Faraday symposium paper.

In the above mentioned paper, reasons were advanced for the correctness of a linear extrapolation of the vibrational levels associated with the F level of CO. Such an extrapolation yields a value of 2.5 volts for the total energy of the products of dissociation from this level. At the time that the paper was written, the writer was not aware of the fact that Fowler and Selwyn had determined the energy of the $^1D_2$ carbon atom. Consequently the value of 1.3 volts for the energy of the $^1D_2$ oxygen atom, proposed by McLennan and Crawford, was used to predict a value of 1.2 volts for the energy of the $^1D_2$ carbon atom. This however is exactly equal to the value found by Fowler and Selwyn, so that the above work is really independent evidence that the energy of the ^1D oxygen atom is 1.3 volts.

The new value of the heat of dissociation of oxygen follows immediately from the theoretical prediction that the products of dissociation from the B level of oxygen are a normal oxygen atom and one in the ^1D level. This has already been used by both Herzberg and Birge in their discussions regarding the heat of dissociation of oxygen. Since that total energy in the B level is known exactly and is equal to 7.0 volts, it follows that the heat of dissociation of oxygen is 5.7 volts. It is believed that, in view of the nature of both the present evidence and that of McLennan and Crawford, this low value for the heat of dissociation is correct to within 0.1 volt.

JOSEPH KAPLAN

University of California at Los Angeles,
February 2, 1930.

A Remark on Hyperfine Structure

An error which has crept into the literature of the theory of hyperfine structure might easily cause misunderstanding and indeed in some places has already led to incorrect deductions.

The problem is to determine what is the direction of the magnetic field produced at the nucleus by a spinning electron in its orbit. For large values of l the classical theory will give the correct result and elementary considerations show, that the magnetic field has the opposite direction of the mechanical moment l. The field produced by the spin is parallel to the spin-vector s, but for large values of l may be neglected. This result means that a spinning proton will be in its most stable state when its mechanical moment i is opposite to j, from which follows that the produced hyperfine splitting will be "regular," the lowest level having the smallest total resultant f.[1]

It is obvious that the orbital picture can

[1] For the complete classical expression and its quantum mechanical equivalent see L. Pauling and S. Goudsmit, The Structure of Line Spectra, Chapter XI, McGraw-Hill, to appear soon.

not be used for an s state, where $l=0$. Here one should use a model that comes nearer to the results of the quantum mechanics. An s state is then a spherically symmetric charge distribution and the spin may be represented by a current distribution within this charge distribution. The result is that the magnetic field at the nucleus is now *opposite* to the spin direction, in complete agreement with the quantum mechanics calculations of Fermi (Nature **125,** 16, 1930). One thus also expects "regular" hyperfine structure if protons interact with an s electron. (For details, especially in more complicated configurations, see S. Goudsmit and R. F. Bacher, Phys. Rev. **34,** 1501, 1929).

Jackson (Proc. Roy. Soc. **A121,** 432, 1928) in his paper on the hyperfine structure of caesium used incorrect results for both s and p states. He assumes his fine structures to be all inverted, which causes his deductions about the nuclear moment of caesium being $\frac{1}{2}$ to be quite uncertain. Also Hargreaves (Proc. Roy. Soc. **A124,** 568, 1929) in his paper dealing with the quantum mechanics treatment of the interaction between nuclear magnetism and the electron orbit, seems to have adopted this incorrect result when he compares his expressions with the results obtained by Jackson. It must be mentioned here that the derivations of Hargreaves clearly show that the minus sign entering in his final formula must be an accidental error.

Finally the same error occurs in the important papers of White (Phys. Rev. Dec. 1929 and Feb. 1930) and causes his deductions about the origin of the nuclear magnetism to be incorrect.

Actually "inverted" fine structure[2] occurs in Cd and probably in Li an explanation of which can not yet be given with certainty.

I hope that this letter will prevent further spreading of this unfortunate mistake.

S. GOUDSMIT

Department of Physics,
University of Michigan,
February 12, 1930.

[2] "Inverted" means here when the fine structure appears as if it were due to a negative particle in the nucleus. Certain fine structures are inverted because of complications in the electron configurations. (See S. Goudsmit and R. F. Bacher, l.c.)

Doublets in the Vibration Spectrum of Cyclohexane

Infra-red and visible absorption spectra and Raman scattered spectra have shown that the C-H bands of organic compounds are often made up of more than one component. In particular the spectrum of cyclohexane is of interest. The writer has already shown that the second, fifth, sixth and seventh members of the C-H anharmonic series* of this liquid are doublets of comparable intensities. By means of the Raman effect the fundamental band has also been shown to be a doublet by Petrikaln and Hochberg, Ganesan and Venkateswaran, and Daure. The writer has thus far failed to resolve the third and fourth members, probably largely because of the relatively great widths of the component lines. In attempting to resolve the third band a recording quartz spectrograph with a slit width equivalent to 0.006μ was used, but only a single broad band was obtained. A Hilger El spectrograph with neocyanine stained plates was employed when trying to resolve the 0.93μ band. This band occurs in the region of the spectrum for which the plate is relatively insensitive. Considerable halation resulted from an overexposure of the 0.85–0.90μ region for which the plate is very sensitive. Even when the intensity of the spectrum in this region was cut down by placing a cell of neocyanine solution before the slit of the spectrograph, the broad region of absorption near 0.93μ could not be resolved into a doublet. Although no precise measurement could be made upon the center of the band it seems certain that it has a somewhat lower value than 0.93μ which had been previously determined thermally.

In spite of the inability to separate the components of these two bands, the frequency separations of the remaining five are sufficient to permit us to arrive at some interesting conclusions. In the table are shown the wavelength values λ, λ', their frequencies ν, ν', the doublet separations $\delta\nu$, the first differences in the frequencies of the members of the separate series $\Delta\nu$, $\Delta\nu'$, and the second differences $\Delta'\nu$, $\Delta'\nu'$. Since it has been necessary to

* Although the term series is used here, we are in reality dealing with an n' progression according to the general theory of band spectra.

assume reasonable data for the doublet structure of the third and fourth bands these have been bracketed in the table.

TABLE I.

n	λ	λ'	ν	ν'	$\delta\nu$	$\Delta\nu$	$\Delta\nu'$	$\Delta'\nu$	$\Delta'\nu'$
1	3.50μ	3.40μ	2860cm^{-1}	2940 cm^{-1}	80cm^{-1}	2860cm^{-1}	—	2940cm^{-1}	—
2	1.77	1.74	5650	5750	100	2790	70cm^{-1}	2810	130cm^{-1}
3	*[1.21]	[1.19]	[8270]	[8400]	[130]	2620	170	2650	160
4	*[0.930]	[0.917]	[10750]	[10900]	[150]	2480	140	2500	150
5	0.763	0.753	13100	13280	180	2350	130	2380	120
6	0.653	0.644	15300	15520	220	2200	150	2240	140
7	0.575	0.567	17390	17640	250	2090	110	2120	120

* 1.20 ± 0.01 and 0.93 ± 0.01 are the values observed thermally for these unresolved bands.

Since the $\delta\nu$ values are not the same for all of the bands the two broad components cannot be regarded as P and R branches of single bands.

Within the limits of certainty of the $\delta\nu$ values we may conclude that there is a linear relation between these values and n. From this we conclude that the coefficients of n differ in the two anharmonic formulas which relate ν and ν' independently to n. Furthermore, it can be seen that $\delta\nu$ will not extrapolate to zero when n equals zero, and from this fact we conclude that a constant term must appear in one or both of the equations. An inspection of the $\Delta\nu'$ and $\Delta'\nu'$ columns of the table indicates that the equation for the components of higher frequency requires no constant term. We are led therefore to the remarkable conclusion that a subtractive constant term must be included in the equation relating the lower frequency components to n. We have then $\nu_n' = a'n - bn^2$; $\nu_n = -c + an - bn^2$; $\delta\nu = c + (a'-a)n$. It is impossible to say whether there is any small change in the b coefficient.

The writer has already pointed out an instance in the case of ammonia in solution in which an additive constant must be included in the formula which relates a set of anharmonic overtones to their fundamental. (Jl. Franklin Inst. **208,** 507 (1929). A paper further supporting this interpretation has been submitted for publication). In that instance it was assumed that the constant term is a measure of the energy which goes to change the molecule to a form with slightly greater potential energy. In the present instance we are forced to conclude that a drop in the potential energy of the vibrator which yields the ν_n frequencies supplies the additional energy which the quantum lacks to produce the vibration. The behavior of the molecule in this respect is in a way similar to its behavior when producing an anti-Stokes line in a Raman spectrum. In the latter instance however the energy which the molecule gives up as it drops to a lower quantized level goes to increase the magnitude of the scattered quantum.

The data of the table cannot be used to decide whether we are dealing with a single kind of C-H vibrator which shifts at times to a lesser value of the restoring force, or with two distinct types of C-H vibrators. The writer however still inclines to his previous viewpoint that vibrations of one of the hydrogen atoms bonded to each carbon atom contribute to one component of the doublet series whereas vibrations of the second hydrogen atom contribute to the other component.

JOSEPH W. ELLIS

Physics Department,
University of California at Los Angeles,
February 4, 1930.

Secondary Emission from Metals by Impact of Metastable Atoms and Positive Ions

In studying the positive column of the noble gases, using plane sounding electrodes, some phenomena were observed, which could not be explained by the theory proposed by Langmuir[1] and applied by himself and Mott Smith[2] to the mercury arc. The simplest interpretation of the observed discrepancies, was to assume a secondary electron emission

[1] Langmuir, G. E. Rev. **26,** 731 (1923).
[2] Langmuir and Mott Smith, G. E. Rev., **27,** 449, etc. (1924).

from a negatively charged plane electrode, amounting to from 40 to 50% of the measured current. This value was obtained by comparing the measured current i_m and the current i_c, calculated from the observed thickness of the space-charge layer with the usual equations.[3] We have succeeded in proving directly that there is an electron emission from the electrode of that magnitude, and that it is principally due to impact of metastable atoms on the collecting electrode.

A plane circular collecting electrode (Ni) with a guard-ring was placed in the positive column of a neon discharge ($p=0.02$ mm) with hot cathode. At the center of the metal disk was a small hole, and behind this a Faraday box. The arrangement was such that the box was practically completely shielded from the radiation in the discharge. It was thought that a comparison of the ion current coming through the hole with the apparent ion current density on the central disk would give a measure of the secondary electron emission from the latter. Indeed, the chance for a secondary electron liberated in the Faraday box to get out is so small, that the current recorded at the box was supposed to be a pure positive ion current, provided the plate is sufficiently negative with respect to the gas (-125v) to keep out all electrons coming from the discharge. The experimental results were much more complicated than expected. Using different arrangements of potentials we proved that neutral particles, diffusing out of the main discharge through the gap between disk and guard-ring, caused a considerable electron emission from the metal parts behind the collector. This suggested that the secondary emission referred to above was due principally to the action of metastable atoms on the collector.[4]

More quantitative results were obtained in the same tube with another arrangement. Opposite to the plane collector with the guard ring, mentioned above, was a small hollow cylindrical one, whose axis was perpendicular to the plane collector. The near end, covered with Ni gauze, was exposed to the discharge, the sides and other end being shielded by glass. This cylinder was movable in the direction of its axis, i.e., perpendicular to the surface of the disk collector. Suppose the cylinder at a potential $V_c=-125$v with respect to the gas; it is then collecting a certain positive ion current i_c. The potential of the plate, V_p, originally -75v with respect to the gas, is now made more negative and the variation of i_c is studied as a function of V_p. As long as the plate is positive with respect to the cylinder, no secondary electrons from the plate can reach the latter, since in falling through the positive space charge layer on the disk they can only acquire an energy corresponding to V_p. When the potential of the plate reaches V_c, the ion current i_c shows a decrease due to incoming electrons originating in the space charge sheath on the plate. The mean free path of the electrons with a velocity corresponding to V_p depends on the degree of ionization and can be determined experimentally in each case by varying the distance between the cylinder and the plate, all other conditions remaining the same. Knowing the electron mean free path and the secondary electron current at a given distance, the secondary emission from the plate can be computed and is found to be from 40 to 50% of the total current i_p.

When the current voltage curve of the secondary electrons is differentiated, a velocity distribution curve is obtained which shows that most of the electrons have at least an energy corresponding to V_p; it follows that they must be liberated at the plate or at a very small distance from it. In addition to the energy, acquired in falling through the space charge sheath, they possess energies of a few volts which are probably initial energies of emission. Some velocity distribution curves show that there are also electrons produced in the sheath at some distance from the plate, but only in small numbers. The interpretation proposed earlier[5] that the electrons are principally due to photoelectric ionization in the sheath has to be given up. The experiments are continued with an improved apparatus to study the influence of different factors on the secondary emission.

W. Uyterhoeven
M. C. Harrington
Palmer Physical Laboratory,
Princeton, N. J.,
February 10, 1930.

[3] Uyterhoeven, Phys. Rev. **31**, 931 (1928); Proc. Nat. Ac. Sc. **15**, 32 (1929).

[4] Oliphant, Proc. Roy. Soc. **A124**, 228, 1929.

[5] Morse and Uyterhoeven, Phys. Rev. **31**, 827 (1928); see also de Groot Naturwiss. **17**, 13 (1929).

Predictions of Manganese Hyperfine Structure

In a recent letter to the Physical Review H. E. White (Phys. Rev., **35**, 208, 1930) announces that he has obtained an analysis of the hyperfine structure of the manganese arc spectrum. His letter contains the results for three levels and mentions that he has been able to analyze many more.

With the aid of the theoretical considerations given in a previous paper (S. Goudsmit and R. F. Bacher, Phys. Rev. **34**, 150, 1929) it is possible to predict the hyperfine structure for a number of manganese levels from the few data given by White. Here follow the predictions for the separation factors[1] and the total separations:

$3d^6\,4s\,{}^6D$	$J=4\frac{1}{2}$	$A=0.0139$	$\nu\Delta=0.384$[2]
	$3\frac{1}{2}$	.015	.29
	$2\frac{1}{2}$	.016	.25
	$1\frac{1}{2}$	.022	.19
	$\frac{1}{2}$	.058	.17
^4D	$3\frac{1}{2}$	$-.011$	$-.21$
	$2\frac{1}{2}$	$-.009$	$-.14$
	$1\frac{1}{2}$	$-.005$	$-.05$
	$\frac{1}{2}$	$+.025$	$+.08$
$3d^5\,4s\,5s\,{}^8S$	$3\frac{1}{2}$	.020	.40
^6S	$2\frac{1}{2}$	.022	.33

These predictions are based on the following assumptions and will, therefore, be correct only if the assumptions are.

(a). The $3d$ electrons give no appreciable contribution to the fine structure. The fact mentioned by White, that the $3d^5 4s^2\,{}^6S$ level shows no ne structure does not prove that the contribution of the $3d$ electrons will be small in all other configurations too, though it is probable.

(b). The addition of the $4s$ electron does not affect the *resultant* spin of the already present $3d$ electrons. This means that in the expression for A,

$$A = a\cdot(s/S)\cos(s,S)\cdot(g-1),$$

$(s/S)\cos(s,S)$ is equal to $+1/5$ for the ^6D and $-1/5$ for the ^4D. This is verified by the formulas for the multiplet separations themselves (S. Goudsmit and C. J. Humphreys, Phys. Rev. **31**, 960, 1928) in which this same cosine occurs.

The contribution of the $5s$ electron is estimated to be about one tenth of that of the $4s$ electron.

The contribution of a p electron is of a more complicated type and general expressions which I obtained for it can only be applied to a few simple cases. For two electrons, one being in an s state, the complete expression for A becomes:[3]

$$A = a\frac{1}{2}(g-1)+b\Big[(2-g)+\frac{l(l+1)}{2(l-1/2)(l+3/2)}\Big\{\frac{1}{2}(g-1)-3(2-g)\Gamma/2L(L+1)\Big\}\Big].$$

The hyperfine structures in Tl II (J. C. McLennan, A. B. McLay, and F. M. Crawford, Proc. Roy. Soc. **A125**, 570, 1929) and in Cd (H. Schüler and H. Brück, Zeits. f. Physik **56**, 291, 1929) are not yet known with enough accuracy to test the second part of this formula.

S. Goudsmit

Department of Physics,
University of Michigan,
February 12, 1930.

[1] The separation factor A is the proportionality constant which one obtains if one applies the interval rule to the splitting up of the level. It is only then strictly a constant when the interval rule holds. The validity of the vector model and of the interval rule for hyperfine structure was for the first time pointed out with certainty in the bismuth spectrum (E. Back and S. Goudsmit, Zeits. f. Physik **43**, 321, 1927) it formed in fact the basis for the analysis of its hyperfine structure and the determination of the nuclear moment, later confirmed by the Zeeman effect.

[2] Value given by White.

[3] The constants a and b measure the interaction energy of the nucleus with the s electron and the p electron respectively. Unpublished calculations of H. Casimir give for b in a hydrogenic case

$$b = R\alpha^2 Z^3 g(i)/n^3 l(l+\tfrac{1}{2})(l+1)$$

in which $g(i)$ is the Landé g-value for the nucleus and thus expected to be of the order 1/1840.